Integrative Systematic Structuring of the Widespread Psammophiid Snakes (Psammophiidae): A Multi-evidence Species Delineation Approach

Submitted in partial fulfilment of the requirements for the degree

DOCTOR OF PHILOSOPHY

in the Faculty of Science

at Rhodes University

Department of Zoology and Entomology

by

Chad Keates

May 2021

Supervisor: Dr Shelley Edwards

Co-supervisor: Werner Conradie

Summary

Species form the foundations upon which we build our understanding of the natural world. Although a focus of much scientific attention, our understanding of species is stunted by the intrinsic 'fuzziness' of boundaries within nature. Due to the complexity of the evolutionary process, coupled with an ever-changing abiotic landscape, species are hard to delineate, even at the best of times. Whilst various species concepts and sophisticated delimitation methods have helped scientists tease apart species, many species complexes persist. This is because taxonomy is a discrete ordering system imposed upon the continuous and intercalated structure of life.

To improve our understanding of a wide-ranging family of snakes, I investigated the taxonomy and evolutionary structuring within Psammophiidae using both molecular and morphological approaches, employing phylogenetic, phylogeographic, and morphometric analyses on the group. The systematic complexity of the family (as evidenced by past research) coupled with the group's widespread distribution and ecological importance, made the taxon an ideal candidate for a broad-sweeping multi-level systematic analysis using multiple species delimitation methods. Additionally, in this thesis I attempted to build on the ground-breaking work of Christopher Kelly by addressing several knowledge gaps identified within the family, and in so doing, produce the most thorough evolutionary and taxonomic study of Psammophiidae possible.

Given the taxonomic uncertainty associated with the family, Chapter Two used a representative sampling from every available species (near complete taxon sampling approach) in the family. The chapter used both standard and time-calibrated phylogenetic modelling and distance/threshold-based species delimitation, to elucidate the finer-level structuring within the family. Geometric morphometrics was used to determine whether there were diagnosable differences in head structure between the different genera. The final phylogenetic tree incorporated 320 samples, representing the most comprehensive phylogenetic reconstruction of the family to date. By using a near-complete taxon sampling approach, I was able to resolve previously unsupported relationships within the family whilst also identifying several novel instances of an under- and over-appreciation of species diversity within the family. Geometric morphometrics also identified clear distinctions between genera based on head shape (head width and 'beakedness'). This chapter showcased the importance of complete taxon sampling and robust methodology for species delimitation and the deleterious effect of species concepts when implemented in isolation.

In Chapter Three, I narrowed the scope of the study to focus on the genus level. *Psammophylax* (Fitzinger 1843) is an abundant, yet poorly studied genus of grass snakes, endemic to Africa. The generalist nature of the genus and wide-spanning distributions of the constituent species has given rise to several subspecies and a poor understanding of the taxonomic structuring within the genus. The overlapping distributions (sympatry) of many of *Psammophylax* species, coupled with the potential for cryptic speciation via mechanisms such as convergent evolution, made the group the ideal candidate for a broad-sweeping systematic study (as evidenced in Chapter Two). By applying the suite of analyses used in Chapter Two to the generic level, we aimed to determine the effectiveness of a multi-evidence species delineation approach when tackling systematic problems at lower taxonomic levels. A genetic phylogeny of six of the seven species was estimated using multiple phylogenetic and distance/ threshold-based species delimitation methods. To support the molecular analyses, we conducted morphological analyses on the body (traditional morphology) and head (geometric morphometrics) separately. Phylogenetic analyses recovered a similar topology to past studies, but with better resolution and node support. I found substantial genetic structuring within the genus, supported by significantly different head shapes between *Ps. a. acutus* and other *Psammophylax* species. *Psammophylax a. acutus* was recovered as sister to its congeners, and sequence divergence values and morphometrics supported its recognition as a new genus. Increased sampling in East Africa (Tanzania, Kenya, and Ethiopia) revealed that *Psammophylax multisquamis* is polyphyletic, necessitating the description of a new, morphologically cryptic, species from northern Tanzania. The distribution of *Ps. multisquamis sensu stricto* is likely restricted to Kenya and Ethiopia. Within this chapter, taxon-specific phylogenetic analyses yielded stronger intrageneric support as compared to Chapter Two, allowing for more defensible conclusions about taxonomical amendments. Geometric morphometrics proved similarly useful (as compared to Chapter Two) in teasing apart genera within the family but lacked the robustness to delineate species within *Psammophylax* with confidence, highlighting the apparent convergence of form within the genus.

In Chapter Four, I investigated the evolutionary structuring within the Southern African endemic *Psammophylax rhombeatus.* The structural and environmental heterogeneity within the region has given rise to many morphological forms distributed throughout the country, with previous studies neglecting the associated molecular significance of these forms. Irrespective of their small sample sizes, both Chapter Two and Three identified substantial phylogenetic structuring within the species, making *Ps. rhombeatus* the ideal candidate for a multi-faceted systematic review, using a combination of phylogenetics, geometric morphometrics and, for the first time in this species, phylogeographic analyses. By investigating a single species, in detail, I was able to assess the effectiveness of the methodologies implemented in previous

chapters on systematic sorting using the multi-evidence species delineation approach. Phylogenetic and haplotype analysis retrieved four well-supported clades: southeast South Africa (SESA), southwest South Africa (SWSA), north-eastern South Africa (NESA) and western South Africa (WSA). Although not variable enough to warrant taxonomic re-evaluation, the clades represented important genetic hotspots, with relatively high intraspecific genetic divergence values separating them, irrespective of the small geographic distances separating populations. This is likely a product of the taxon's habitat-generalist lifestyle, enabling them to bypass vicariant barriers that might otherwise cause speciation in less versatile species. The clades are also geographically distinct, with little overlap, indicating previous vicariance, a finding that is supported by the split of *Ps. rhombeatus* from *Ps. ocellatus* in the mid-Pliocene, followed by the diversification of *Ps. rhombeatus* into four clades throughout the Pleistocene. The genetic structuring observed in *Ps. rhombeatus* may be a product of population expansion following ancient refugial isolation (potentially Last Glacial Maximum [LGM]). The molecular distinctiveness of the clades was not replicated in the morphological component of this chapter, with neither dorsal nor lateral geometric morphometric analyses of head shape showing any discernible distinctiveness based on geography. Whilst head shape has not been shown to be an effective delineator of evolutionary units at the species level (within this taxon), body colour, scalation, and snout-vent length has been linked to morphotypes within the species based on the work of Broadley (1966). These morphological groupings are loosely attributable to the molecular clades identified in the phylogenetic analyses, highlighting the complex interplay of genetic and morphological characteristics in the process of speciation, and their representation in systematic accounts.

This thesis represents the most thorough evolutionary and systematic study of the family currently possible. In addition to identifying and describing both a new genus and species, this thesis also highlighted several instances of an over- and under-appreciation of species diversity within Psammophiidae. By applying a multi-evidence species delineation approach to this thesis, I show the intricacy of the evolutionary process (at various taxonomic levels) and showcase the ease to which species boundaries can be confounded when species concepts are implemented in isolation. These findings also highlighted the importance of sample size, sample range, species delimitation method on the outcome of taxonomic analyses, and their interpretation. Lastly, this thesis addressed the knowledge gaps left by Christopher Kelly's PhD work and investigated the findings of recent papers that attempted to do the same. Whilst this study answers the questions of old, the taxon-intensive focus revealed several new knowledge gaps within the family, highlighting how much we know about snake systematics, and furthermore, how much we still need to learn about evolutionary structuring.

Table of Contents

Preface

Funding

The research in this thesis was funded by the National Research Fund (NRF; grant number TTK160602167413) and the Foundational Biodiversity Information Programme (FBIP; grant number FBIS160602167430). The National Geographic Okavango Wilderness Project (National Geographic Society grant number EC0715–15) also funded various trips to Angola, attended by Werner Conradie and myself, that resulted in the acquisition of genetic material, crucial to the completion of this thesis. Although not directly linked to this thesis, novel samples from the Democratic Republic of Congo were acquired by Eli Greenbaum during several expeditions funded by a National Geographic Research and Exploration Grant (no. 8556-08), UTEP, and a grant from the National Science Foundation (DEB-1145459).

Ethics and Permissions

A collecting permit was obtained from the Department of Economic Development, Environmental Affairs and Tourism (DEDEAT), Eastern Cape Province, which allowed us to utilise genetic samples from field-caught specimens (permit number: CRO 72/17CR). Ethical clearance that allowed us to handle and excise tissue samples from wild-caught snakes was obtained from Rhodes University (Protocol number: RU-DZE-2017–03–003) and Port Elizabeth Museum (Ethics clearance no.: 2013–01 and 2017–2). Permits for fieldwork in Democratic Republic of Congo were provided by the Centre de Recherche en Sciences Naturelles and the Institut Congolais pour la Conservation de la Nature. Permits for fieldwork in Kenya (Christopher Kelly) were provided by the Kenya Wildlife Service (KWS) and the National Museums of Kenya. Permits for collection in Tanzania (Christopher Kelly) were provided by the Tanzania Commission for Science and Technology (COSTECH) and the Director of Wildlife. Permits for collection in Malawi (Christopher Kelly) were facilitated by the Forestry Research Institute of Malawi. Angolan material was collected and exported under the following export permits: 31/GGPCC/2016, 89/INBAC.MINAMB/2017 and 002/GGPTBOK/18.

Disclaimer

The main chapters of this thesis have been prepared as stand-alone manuscripts. Sections of the methods may seem redundant, but in the interest of being clear and thorough, several sections have been repeated to reduce confusion.

Acknowledgments

First and foremost, I would like to thank my supervisors for their constant and ever-present support. I have been privileged in my time as a postgraduate to have been exposed to two phenomenal scientists and people in the form of my supervisors. Their numerous skills and attributes have strengthened me both as a herpetologist and a molecular biologist.

To my supervisor Dr Shelley Edwards, thank you for you for exposing me to molecular biology, thank you for your guidance in and out of the laboratory, and thank you for guiding me through the intricacies of young professional life. Your kindness, patience and passion for both science and teaching has played a huge part in my life and has moulded me into the scientist that I am today.

To my co-supervisor Werner Conradie, thank you for believing in me and trusting me with big projects, thank you for exposing me to the wonderful world of herpetology, and thank you for all the help in and out of the museum. Your passion and talent for both herpetology and taxonomy is unrivalled and has not only improved my skills but has broadened my horizons as a reptile and amphibian lover.

Thank you to Rhodes University for playing host to my amazing journey from student to postgraduate to professional scientist. Your phenomenal staff, facilities, and academic program have enabled me to achieve so much more than I have ever dreamed possible. Thank you as well for the funding, both direct and indirect, that facilitated my studies and allowed me to achieve my goals as a young scientist.

Thank you to Professor Froneman, the academic staff, and all the great academics that I have met along the way. Through your wisdom I have learned so much, and the university and the students are lucky to have you. Your expertise and passion are unrivalled, and I am honestly proud to say that I share a building with everyone that makes zoology and entomology such a force in South African science.

Molecular biology owes much of its thanks to the people and the institutions that collect tissue samples. For this reason, I would like to thank the South African National Biodiversity Institute (SANBI, Kirstenbosch), Port Elizabeth Museum (Port Elizabeth) and the McGregor Museum (Kimberley) for the generous donations of samples for my PhD. I would also like to thank the following individuals: Pedro Vaz Pinto, Ninda Baptista, Ryan van Huyssteen, Bryan Maritz, Luke and Ursula Verbught, Courtney Robert Hundermark, Cara Marie Trivella, Darren Pietersen, Alexander Rebelo, Rian Stander, Tyrone James Ping, Paul Rabiega, Beryl Wilson, Luke Kemp, Megan Kim Reid, Theo Busschau, Gary Kyle Nicolau, Andries Cilliers, Dave Maguire, Christopher Hobkirk, and the late Bill Branch. I would like to give specific thanks to Christopher Kelly for affording me a large selection of samples and sequences that were integral to the completion of this thesis. My thesis builds on the phenomenal work of Christopher, and without both his sampling and his insights, I believe this thesis would not have been as thorough.

Various expeditions were undertaken to secure the sampling seen in this thesis. For this reason, I would like to thank Luke Kemp, Cara Marie Trivella, Anthony Evlambiou and Bruce Roestof for assisting me in targeted trips in and around the country. Whilst not attended by myself, expeditions to Angola and Democratic Republic of Congo resulted in the acquisition of several samples crucial to my thesis. The herpetological components of these trips were headed by Werner Conradie and Eli Greenbaum, respectively. I would thus like to thank both them and their various assistants (refer to acknowledgments section in Keates *et al.* 2019) for their profound contribution to my thesis.

I would also like to thank Shiela Broadley (Natural History Museum of Zimbabwe, Bulawayo) who kindly made available Donald Broadley's data and Danny Meirte (Royal Museum for Central Africa, Tervuren) for confirming the type locality of *Ps. tritaeniatus subniger.* The Field Museum of Natural History (FMNH), American Museum of Natural History (AMNH), Natural History Museum of Los Angeles County (LACM) and Museum of Comparative Zoology (MCZ) are also thanked for providing photographs of preserved specimens for morphological analysis. I would also like to thank Luke Kemp for hand-drawn illustrations of the different species of *Psammophylax,* and both Gareth Nuttall-Smith and Megan Kim Reid for rendering maps. Lastly, I would like to thank Gerald Dunger, Christopher Kelly, Stephen Spawls, Tyrone James Ping, and Luke and Ursula Verbugt for contributing photographs for use in my figures.

This PhD was by no means a walk in the park and whilst I would like to say I was a testament to positivity throughout the experience, this would not be true. For this reason, I would like to thank my partner Megan Kim Reid. Whether it was rendering maps, reading through drafts, or just making tea, your positivity was ever-present. Thank you for picking me up when I fell down and thank you for believing in me when I could not. Your patience, kindness, and love were instrumental to the completion of my thesis.

I would also like to thank my family, my friends and more specifically my mother, father and brother. Whilst this was not the path I originally set out upon, your encouragement and belief in me stayed the same. Thank you, Mom and Dad, for equipping me with the skills and the lessons necessary to see this through. Whether it was financial backing or emotional support, you guys have always been there, and for that I can never thank you enough. This thesis is as much a testament to my hard work as it is to your parenting skills. Lastly, I would like to dedicate this thesis to my late grandfather, Kenneth John Keates. Whilst you could not see me finish this, I would like you to know that my passion for wildlife stemmed from you. Through our trips to Walter Sisulu Botanical Gardens and Pilanesberg Nature Reserve, you showed me the wonder that is the natural world. I only hope that I can use this degree to leave the natural world better than I found it, and in doing so, protect what you held so dear for all the Keates's to come.

List of Figures

Chapter Two

Appendices

List of Tables

Chapter Two

Chapter Three

Chapter Four

Appendices

Chapter One: General Introduction

Overview

Since its inception over 160 years ago, the theory of evolution and the mechanisms that drive evolutionary change have been among the most defining aspects of biology (Darwin, 1859). The biological field has grown through the development of novel methodologies and ambitious theories. The mechanisms of diversification have also shifted and expanded through time to account for the enormity of the biotic diversity found on Earth. Boundaries in nature are highly structured, incredibly complex, and for a lack of a better word, 'fuzzy'. Taxonomy is our attempt to classify and order nature into understandable groupings, so that meaningful science can follow. Unfortunately, taxonomy is a binary ordering system, imposed upon a continuous, chaotic natural system (Hey, 2001; Zachos, 2016). Whilst grey areas of divergence at the lower levels of taxonomy confound species delimitation, they also serve as evidence for the evolutionary process, because without this 'fuzziness', evolutionary theory would not make sense.

Novel research has shown that evolution and the process of adaptive evolution, whereby genetic and morphological traits evolve at similar rates to create distinctive units in response to competition and habitat heterogeneity, is no longer the only way of distinguishing species (Burns *et al.*, 2002; Darwin, 1859; Rainey & Travisano, 1998). Non-adaptive evolution can disproportionately favour genetic variation over morphological variation, and convergent evolution can lead to species acquiring similar morphologies when exposed to similar ecological conditions (Gittenberger, 2004; Losos, 2011). Discordance between phenotypic and genotypic traits can confound conventional taxonomists (Morphological Species Concept), resulting in over-estimation of species diversity because of rapid morphological divergence and phenotypic plasticity (Cureton & Broughton, 2014; Zhao *et al.*, 2018) or under-estimation of species diversity because of cryptic speciation and morphological stasis (Bromham *et al.*, 2002; Renoult *et al.*, 2009; Torres-Pérez *et al.*, 2009).

This variable effect is the result of evolution being a highly complex mechanism that affects different taxa in contrasting ways depending on a varying suite of biotic and abiotic factors. Species delimitation is problematic and no single method has been shown to work equally well across all taxa (Sites & Marshall, 2004). The intricacy of the evolutionary mechanisms involved in speciation are further bolstered by the complexity of the environment in which speciation takes place, making Africa one of the most interesting continents to study from an evolutionary perspective.

Africa is a mega-continent, and one of the largest landmasses on the planet. The size of Africa, coupled with its position straddling the equator, has resulted in a large variety of habitats spread across the continent (Critical Ecosystem Partnership Fund, 2020; Tolley *et al.*, 2016). Increased habitat heterogeneity results in higher-levels of diversity and endemism (Bazzaz, 1975; Tews *et al.*, 2004), with Africa being host to eight of the 36 biodiversity hotspots worldwide (Critical Ecosystem Partnership Fund, 2020).

Herpetological diversity in Africa is amongst the highest on Earth because of the increased niche availability associated with the structural complexity of the continent (Tolley *et al.*, 2016; Uetz *et al.*, 2020). Reptiles and amphibians are generally smaller and ecologically pliable in comparison to their mammalian and avian counterparts, allowing them to utilise and diversify into smaller microhabitats. There are currently more than 1600 species of reptiles in Africa and this number is ever-growing (Tolley *et al.*, 2016; Uetz *et al.*, 2020). Irrespective of the large diversity and abundance that Africa harbours, the continent is considered understudied (Böhm *et al.*, 2013; Tolley *et al.*, 2016) and furthermore misrepresented because much of the past herpetological research is morpho-centric and potentially taxonomically incorrect (Adalsteinsson *et al.*, 2009; Böhm *et al.*, 2013).

Since the turn of the twenty-first century, snake systematics has been the subject of much research because genetic analysis has become increasingly more accessible. The higher-level relationships of Caenophidia (advanced snakes) were rigorously examined (Kelly *et al.*, 2003; Vidal *et al.*, 2007; Vidal & Hedges, 2002) and as time passed, smaller taxonomic groups were studied in more detail, leading to improved taxonomy and a better understanding of the processes that have led to the diversification of extant snakes. Lawson *et al.* (2005) investigated the superfamily Colubroidea and Kelly *et al.* (2009) investigated the superfamily Elapoidea, both using molecular phylogenies, thus improving our understanding of the higher-level systematics over time (Figueroa *et al.*, 2016; Pyron *et al.*, 2013; Zaher *et al.*, 2019).

Psammophiidae is a diverse family of snakes that is relatively well-represented in the literature, with various taxonomic and systematic papers underpinning their current nomenclature (Boulenger, 1896; Broadley, 1966, 1977; Hughes, 1999; Keates *et al.*, 2019; Kelly *et al.*, 2008; Loveridge, 1940; Portillo *et al.*, 2018; Ruane *et al.*, 2018; Taft, 2018; Trape *et al.*, 2019; Zaher *et al.*, 2019). Barring this, the group remains troublesome both because of its previous morpho-centric taxonomical assignments and because it is ecologically, phenotypically, behaviourally, and genetically complex (Kelly *et al.*, 2008). Whilst Kelly (2005) resolved many taxonomical uncertainties within the group, his work identified seven glaring gaps in our knowledge of the family, several of which are yet to be addressed. The group is wide-ranging and ecologically diverse, with fossorial, arboreal, and terrestrial lifestyles being

represented (Portillo *et al.*, 2018; Spawls *et al.*, 2018). Many constituent species are also wide-ranging, and thus overlap with geographically and morphologically similar congeners, complicating systematic sorting and assignment.

Cryptic speciation, rapid morphological divergence, and morphological stasis are among a few mechanisms proposed to explain the development of the species within this group, making them the ideal candidate taxa for a broad-sweeping multi-faceted analysis to determine adequately the evolutionary mechanisms that drive speciation in the group (Kelly *et al.*, 2008; Ruane *et al.*, 2018; Taft, 2018). The use of multiple delimitation approaches together with other lines of evidence (morphology, ecology, behaviour, geography, historical biogeography) allows for more defensible conclusions than any one method in isolation.

Variation

Adaptive and non-adaptive radiations result in speciation and increased biodiversity. Whilst both echo the importance of environmental factors on the expression of morphotypes, they differ in the evolutionary avenues via which these taxa develop their genotypes and associated phenotypes. Adaptive radiations encompass the more mainstream understanding of evolutionary processes given their role in the speciation of charismatic taxa, such as cichlid fish (Kornfield & Smith, 2000), Caribbean *Anolis* lizards (Pinto *et al.*, 2008) and Darwin's finches (Burns *et al.*, 2002). Contrasting resources and competition select for ecological specialisation resulting in adaptive phenotypic change and lastly rapid lineage diversification (Schluter, 2000). Adaptive radiations can be associated with sympatric speciation because of competition for limited resources within a connected population, resulting in multiple species occupying the same environment, yet exploiting contrasting ecological niches.

Unlike allopatric speciation, which hinges on vicariance and genetic drift to facilitate speciation, sympatric speciation is facilitated by natural selection given the lack of barriers to gene flow (Foote, 2018). Whilst Darwin advocated for the evolutionary power of natural selection (sympatric speciation) within the evolutionary landscape, the revolutionary work of Mayr (1963) showed the enormous influence of geography (allopatric speciation) on promoting speciation (Via, 2001). Given this, examples of sympatric speciation remain rare as a taxon must be acted on by extreme circumstances to escape the homogenising effects of gene flow in an open system, devoid of vicariance (Via, 2001).

Although sympatric speciation is hard to measure, adaptive evolution may be useful in explaining the co-existence of multiple Psammophiidae species within several parts of Africa. *Psammophylax*, *Psammophis*, *Dipsina* and *Rhamphiophis*, for example, can all be found in

Namibia, in the same environment, given their utilisation of contrasting lifestyles and the exploitation of different resources (Branch, 1998).

Extreme adaptive phenotypic diversification can also result in rapid morphological diversification and multiple distinct phenotypic forms with little associated genetic differentiation using traditional neutral markers (Bickford *et al.*, 2007; Mayr, 1942). This can confound conventional taxonomists, causing them to conflate species numbers through over-estimation of species diversity (Bickford *et al.*, 2007; Mayr, 1942). Rapid morphological divergence can result from strong divergent natural selection, through interspecific competition for limited resources (Funk *et al.*, 2006).

The *Psammophis 'leightoni* complex' is a prime example of the effect of rapid morphological divergence and ecological specialisation on the phenotype and genotype of problematic taxa (Taft, 2018). Broadley (2002) split [1]*P. leightoni* into three species, namely *P. leightoni*, *P. namibensis* and *P. trinasalis*, based on geographic (disjunct populations) and morphological (pattern) grounds. Whilst all three species share overlapping scale counts and similar snout-vent lengths, they contrast in colouration and patterns, making identification possible (in most cases) using the Morphological Species Concept (Broadley, 2002). The reasoning for this split was based on assumed allopatric speciation (Broadley, 2002). Taft *et al.* (2018) found limited genetic difference between all three species, corroborating the findings of Kelly *et al.* (2008), with the biggest genetic differences existing between the most geographically distant samples, in the former study. The superficial morphological differences between the populations are thus likely an adaption to contrasting environmental and interspecific factors. Support for these findings are found in the morphological similarity of southern *P. namibensis* and northern *P. leightoni* given the similar environmental selective pressures they are exposed to (Taft, 2018).

Alternatively, non-adaptive radiations produce genetically distinguishable populations with little to no morphological or ecological differentiation, enabling them to utilise the same resources as their competitors. Non-adaptive radiations are likely the product of allopatric speciation as species that occupy the same ecological niche could not, or should not, be able co-exist (Armstrong & Mcgehee, 1980; McKane *et al.*, 2002).

Past vicariant events can thus dissect populations permanently or temporarily, resulting in rapid genetic diversification, with little ecological and morphological diversification, creating cryptic taxa. Similar habitats necessitate similar ecologies promoting stabilising selection, which can disproportionately favour genetic differentiation and cause the

[1] Explanation of symbols: *R—Rhamphiophis*, *Rh—Rhagerhis*, *Ma—Malpolon*, *M—Mimophis*, *H—Hemirhagerrhis*, *Ps—Psammophylax*, *D—Dipsina*, *P—Psammophis.*

reduction/elimination of morphological variance, potentially leading to morphologically static cladogenesis (Renoult *et al.*, 2009; Torres-Pérez *et al.*, 2009). Habitat fragmentation can often lead to allopatric speciation via mechanisms such as the founder effect, genetic drift, and convergence. This can affect an animal's genotype, mate recognition mechanism(s) (both intrinsic and extrinsic), and various other properties with little to no effect on the morphology of the animal (Bickford *et al.*, 2007). Irrespective of the evolutionary mechanism of evolution, it forms similar taxonomical conundrums for Morphological Species Concept advocators (Bickford *et al.*, 2007).

Mimophis mahafalensis is a widespread morphologically polymorphic psammophiid with three separate colour and pattern combinations being found within the species (uniform grey, striped, and zig-zag) (Ruane *et al.*, 2018). Domergue (1969) and Glaw and Vences (1994, 2007) suggested that these polymorphisms may be linked to sex (males–zig-zag, females–uniform grey) whilst It is also postulated that the striped pattern is representative of *M. m. madagascariensis* on the central Madagascan plateau (Glaw & Vences, 1994; Gunther, 1868). Ruane *et al.* (2018) recovered cryptic speciation within the northern populations and described these animals as a separate species, *M. occultus* (Ruane *et al.*, 2018). Interestingly all three colour forms are found in both species irrespective of geography and sex, meaning that previous morpho-centric assertions were misguided as the distinction between the two species was entirely genetic (Ruane *et al.*, 2018). The interplay between non- and adaptive radiations may be responsible for the various species complexes found within Psammophiidae (Branch *et al.*, 2019; Broadley, 2002; Kelly *et al.*, 2008; Trape *et al.*, 2019) due to the antagonistic effects of evolutionary mechanisms, such as cryptic speciation and rapid morphological divergence, and the interpretation of these mechanisms by conventional taxonomists in the absence of a multidisciplinary framework.

Species Concepts

The concept of 'species' is amongst the most fundamental tenets of biology, an integral part of our understanding of the living world, and yet the definition of the concept of species remains controversial. Speciation results in the creation of new species through the irreversible separation of two population lineages through time, but the mechanisms that underpin speciation events are numerous, intercalated, and often complex to tease apart (Zachos, 2016). Unfortunately, species are ephemeral and the concept itself is abstract, given the enormous plasticity of the evolutionary process (De Queiroz, 2005, 2007; Sites & Marshall, 2004).

The complexity of the species problem is well-illustrated by the difference between T (taxonomical) and E (evolutionary) species (Endler, 1989; Ghiselin, 2001; Williams, 1992). Taxonomical species refer to subjective taxa named by taxonomists whilst E species refer to objective entities in the natural world, borne out of the evolutionary process (Zachos, 2016). T species are approximations of E species, with taxonomists identifying and delimiting natural taxa based on their perception of what a species level is (Zachos, 2016). Due to the complexity of the evolutionary process, and the 'fuzziness' associated with the lines between species, it is rare to find a T species that is very clearly an E species. For this reason, taxonomy is filled with misidentifications due to the misunderstanding of E species. Whilst geographically isolated, homogeneous genetic populations do exist in nature, albeit infrequently, as most E species are hard to delineate. Furthermore, T species are very easy to erect and a single divergent molecular sequence can be enough to warrant the description of a new species. Whether or not the divergent sequence truly reflects an E species is irrelevant when compared to a taxonomist's own opinion of what constitutes a species. Species pluralism (non-overlapping species concepts) combined with contrasting nomenclature codes confounds the recognition of E species. In essence, T species should be a hypothesis of E species (Baum, 1998; Hey *et al.*, 2003). Species concepts can be further complicated by the time scale attached to their recognition, as they can be viewed as synchronic (horizontal) or diachronic (vertical). Synchronic species would take the form of a single slice through time (time-limited dimension) whilst diachronic species can be viewed as entities existing through time (time-extended dimension) (Zachos, 2016).

The complexity of the species problem has led to many sub-groups of biologists advocating for different species concepts and denouncing others, causing an enormous amount of confusion when delineating new species, and evaluating the validity of established ones. Currently, there are approximately 32 species concepts, with a whole suite of alternate definitions, further compounding the confusion (De Queiroz, 2007; Mayden, 1997; Zachos, 2016). The problem with species concepts is that most of them are at least partially incompatible with one another, resulting in different conclusions concerning boundaries and numbers of species (De Queiroz, 2005). The defining properties underpinning individual species concepts, represent thresholds that, once crossed, signal the process of speciation, but these can occur at different times, independent of the properties of other species concepts resulting in the recognition of contrasting numbers of species (De Queiroz, 2005). Species concepts are not to be confused with 'species delimitation', the process of determining the species boundaries and number of species from empirical data (De Queiroz, 2005, 2007; Hey, 2001). The species concept problem, therefore, hampers species delimitation by presenting confounding criteria by which to separate evolutionary units. All species concepts are based

on biological realities, and are therefore not applicable to all taxa, so 'Reductio ad absurdum' views on species concepts is counter-productive because all concepts have their failings, and to focus on them is detrimental to the process of species delimitation (Zachos, 2016).

The key to reconciling the contrasting criteria is to identify the common thread linking all species concepts, and that is that all species are, primarily, separately evolving lineages with secondary species identification criteria (Zachos, 2016). This central tenet of species description underpins both the Evolutionary Species Concept (ESC) (Mayden, 1997, 1999, 2002; Wiley & Mayden, 2000) and the General/Unified Species Concept (GSC/USC) (De Queiroz, 1998, 1999, 2005, 2007). The Evolutionary Species Concept, termed by Mayden (1997), requires only that speciation and evolution are natural processes involving unique and cohesive lineages with their own evolutionary fate. The General/Unified Species Concept states that species are segments of population-level evolutionary lineages, evolving separately to other segments. Whilst the jargon differs between the ESC and USC, they are considered synonymous by Mayden (2013) as both concepts accept the inoperability of the primary concept, and the need to supplement taxonomic assertions with secondary species concepts. For the interest of time and simplicity, only the Unified Species Concept (USC) will be discussed hereafter.

According to the USC, a lineage is a population extended through time (diachronic) whilst a population is a cross-section through a lineage (synchronic) (Zachos, 2016). Therefore, under the USC, and for the purpose of this thesis, a species can be referred to as a collection of separately evolving metapopulation lineages, or more specifically, segments of lineages (De Queiroz, 2005, 2007; Zachos, 2016). A metapopulation refers to an inclusive population, comprised of multiple sub-populations (De Queiroz, 2005, 2007). If viewed on a continuum, a species would preside at the higher-level, and would be separated from demes and family groups, units of organisation, found at the lower end of the population-level continuum (De Queiroz, 2007). In essence, species give rise to other species and thus represent one segment of a species-level lineage. Whilst congruent in terms of the primary property (separating evolving metapopulations), most species concepts have contrasting secondary criteria. In addition to being separate evolving metapopulations, a species must be intrinsically/extrinsically reproductively isolated (Biological Species Concept), occupy a different ecological niche (Ecological Species Concept), be phenetically distinguishable (Phenetic Species Concept) or be monophyletic (Phylogenetic Species Concept) (De Queiroz, 2007). The reason that secondary species' criteria lead to incompatible species concepts is because they arise at different times during the process of speciation. The evolutionary process is highly complex and can affect organismal characteristics in a multitude of ways.

The change in these characteristics lead to the acquisition of different properties in species lineages, ultimately resulting in divergence and speciation (De Queiroz, 2007).

For example, following a selection event, a lineage begins to diverge, it becomes phenetically distinctive, develops contrasting physiology, and becomes unrecognisable to prospective mates, both intrinsically and extrinsically. Through time, the lineage develops a distinctive ecology, ultimately resulting in the evolution of a monophyletic taxon. Evolution is, however, complex and highly variable. Speciation can result from mutation, natural selection, migration, and/or genetic drift, and can affect multiple characters across various levels of organismal biology (De Queiroz, 2007). Hence, the secondary species characteristics do not evolve at the same time or in the same order (De Queiroz, 2007).

Pigliucci (2003) proposed the Family Resemblance Concept (Cluster Concept) as a better representation of the ‘concept of species’ given his perceived failings within the application of the Unified Species Concept (Metapopulation Lineage Concept). Based on Wittgenstein's (1953) family resemblance groups, species should be treated as polythetic groups and/or cluster groups given that the species’ category cannot be defined using a finite set of necessary and sufficient properties (Hull, 1965; Needham, 1975). Much like the word ‘game’ cannot be defined, due to its variety of uses (soccer, sailing, paintball, poker, wildlife), the concept of species is much the same (De Queiroz, 2005). No number of finite properties can separate ‘species’ from everything that is not a ‘species’. Utilising the Cluster Concept, a species is a cluster of overlapping sets of shared properties (De Queiroz, 2005; Hull, 1965).

Whilst Pigliucci (2003) viewed the Unified Species Concept (and by extension the Evolutionary Species Concept) as flawed, both proposals can be viewed as synergistic given that they answer two separate aspects of the species problem (De Queiroz, 2005). Firstly, the USC answers the question of, “what properties must a metapopulation lineage possess to be considered a species?”. The metapopulation lineage concept answers this question by creating the unified/general concept of species by elucidating the central tenet of species and by removing the alternative and partially incompatible definitions of the species category (De Queiroz, 2005). Secondly, the Cluster Concept answers the question of “what phenomena are responsible for the existence of species?” by allowing different phenomena or sets of phenomena to be responsible for speciation in different cases (De Queiroz, 2005).

To navigate this biological conundrum, it is important to acknowledge the difference between the theoretical concept of species (species as segments of separately evolving metapopulation lineages) and the practical application of species delimitation (lines of evidence) (De Queiroz, 2005, 2007). Both the Metapopulation Lineage Concept and the Cluster Concept answer conceptual questions, whilst the third question, “how do we recognise

species in practice?", is methodological and thus requires a methodological answer. There are multiple methods that can be utilised to answer the third question (Sites & Marshall, 2003, 2004), these will be discussed in deatil in the following section. The implementation and use of different methodologies and data types has contributed to the 'species' problem because they are based on lines of evidence for the properties (different species concepts) previously treated as necessary to support speciation (De Queiroz, 2005). This is because previous theorists have confounded the conceptual and methodological problems, thereby blurring the line between the concept of species and the criteria and methods used to recognise species (De Queiroz, 2005).

Because species are conceptualised as segments of separately evolving metapopulations, the secondary characteristics can be viewed as support for speciation. The presence of any secondary characteristic can thus be evidence for lineage separation, and the lack of any secondary property does not constitute evidence against lineage separation (De Queiroz, 2007). This is a revolutionary way of looking at systematics and taxonomy because it removes the ambiguity and contention from the application of species concepts (by different factions of biologists) through the acceptance of the central tenet that species are, in essence, segments of separating evolving metapopulation lineages. Furthermore, metapopulation lineages can be interpreted using the Cluster Concept that can be supported by the diverse suite of methodologies and data types available to modern taxonomists (De Queiroz, 2005).

Whilst the acceptance of the USC supports the acceptance of a lack of structure in nature, it also represents a step towards a more holistic interpretation of evolutionary biology. Whilst some may argue that the lack of systematic prerequisites may hamper correct classification because any line of evidence can be misleading if interpreted incorrectly, it also serves as an invitation to taxonomists to shed the concept of 'tick box' taxonomy in favour of a more rigorous multi-faceted, cross-disciplinary, evidence-based taxonomy.

Species Delimitation

Unlike species concepts that are theoretical, species delimitation is a methodological question, with multiple applications. These include estimating genetic and geographical distances, phylogenetic analysis, phenetic clustering, and the use of coalescent theory (De Queiroz, 2005). There are also a wide range of data that can be analysed, from morphological and physiological, to geographical and ecological through to behavioural and genetic data (De Queiroz, 2005, 2007).

Whilst currently more integrative (Padial *et al.*, 2010), the process of delimiting species has changed drastically since the creation of the binomial nomenclature system by Carolus Linnaeus in the tenth edition of his book 'Systema Naturae' in 1758 (Hillis, 2019). Naturalists of the early-to-mid 1800's attempted to organise the natural world without the evolutionary understanding that underpins biology today (Hillis, 2019). Following the publication of, 'On the Origin of Species', by Darwin (1859), evolutionary theory and phylogeny became an important component of species delimitation (Hillis, 2019). As time passed, new methods for delimiting species were developed faster, with large advances in statistical analysis of geographic variation and morphology in the early 1900's (Ruthven, 1908; Hillis, 2019). In the late 1900's, genetics became available, ushering in a new era for species delimitation (Hillis, 2019). Whilst originally met with contention by conventional taxonomists, it has since become an integral part of systematics (Hillis, 2019). With each new methodology the process of species delimitation has improved through the acquisition of novel insights and information. It is however important to note that each method has its own caveats, and without an understanding of them, species delimitation becomes problematic (Hillis, 2019). The consideration of multiple lines of evidence thus provides the best basis for accurate species delimitation.

Within the field of molecular biology, both single locus and multilocus species delimitation can be used to delineate species. Single locus species delimitation is more common because it is simpler and cheaper (Dellicour & Flot, 2018). Single locus species delimitation falls into several broad categories, each with varying levels of effectiveness depending on the context. These include distance-based methods such as DNA barcoding, barcode gap discovery and ABGD analysis (Puillandre *et al*., 2012); tree-based methods such as generalised mixed yule-coalescent (GMYC) (Zhang *et al.*, 2013) and Poisson tree process (PTP) (Pons *et al.*, 2006) and lastly allele-sharing based methods such as haplowebs (Flot *et al.*, 2010). Within each category there are various implementations such as the Bayesian implementation of GMYC (Reid & Carstens, 2012) and the Bayesian implementation of PTP (Zhang *et al.*, 2013). For each category of single locus species delimitation analysis there exists optimal conditions. Unfortunately, this 'sweet spot' differs between and within each category of analysis making a one-size-fit-all approach virtually impossible (Dellicour & Flot, 2015). This is because the study taxon and its associated sampling pattern/ speciation rate/ species richness/ mutation rate/ effective population size have variable effects on different types of analyses (Dellicour & Flot, 2018). One benefit of this is that if multiple methods yield the same result, the answer is likely correct (Dellicour & Flot, 2018). The use of all three categories of single locus species delimitation together is only possible with nuclear, diploid markers (Dellicour & Flot, 2018). Because of this, haplowebs are not feasible in many studies

given the sheer abundance of mitochondrial, haploid datasets on online repositories like Genbank.

Multilocus species delimitation however navigates several of the caveats presented by single locus species delimitation by using multiple unlinked loci when delimiting species. This method affords a more robust dataset to the question, and according to the findings of Dupuis *et al.*, (2012), produces more accurate estimates of species when compared to single locus methods. Multilocus species delimitation is however hampered by an increased computational requirement, especially with larger datasets (Dellicour & Flot, 2018). Additionally, when conducting species delimitation analyses, one is limited by the availability of closely related, comparative material from online molecular repositories (Dellicour & Flot, 2018). This is especially true of African herpetology, with much of our knowledge of the systematics of snakes built on (predominately) mitochondrial datasets (Rato *et al.*, 2006; Kelly *et al*., 2008). Because multiple mitochondrial genes are linked together on the same molecule, they can be viewed as a single locus. Without a substantial financial input to sequence existing material in a multiplicity of loci, multilocus species delimitation is just not possible with many existing datasets currently. Given these limitations, single locus species delimitation, remains a valuable, yet cost effective method of investigating species diversity.

Study Animals

Psammophiidae is a large, species-rich family of snakes comprising of 55 species in eight genera, and includes the sand snakes, grass snakes (including 'skaapstekers'), and their relatives (Branch *et al.*, 2019; Kelly *et al.*, 2008; Trape *et al.*, 2019). The family is widely-distributed in Africa and Madagascar, stretching into southern Europe, the Middle East, and Asia, as far south-east as Java (Branch *et al.*, 2019; Kelly *et al.*, 2008). These snakes can be considered generalists, being found in almost every biome from deserts and savanna through grassland, fynbos, and woodland (Bates *et al.*, 2014; Branch, 1998; Kelly *et al.*, 2008; Spawls *et al.*, 2018). Most species are terrestrial diurnal hunters, with the exception of some species (e.g., *Hemirhagerrhis* spp.), that actively seek out small vertebrates in open habitats, thus making them ecologically important (Bates *et al.*, 2014; Branch, 1998; Loveridge, 1940). Most of these species are oviparous and *Psammophylax rhombeatus*, a southern African endemic, is among only a handful of snakes in Africa to display clutch-guarding (Broadley, 1990; Marais, 2004). Psammophiid venom is considered mild and harmless to humans, as no serious envenomation has ever been recorded (Weinstein *et al.*, 2013; Ineich *et al.*, 2021), besides speculation that bites from *Malpolon* have hospitalised people in Spain. Although generally widespread, some species, such as *Psammophis leightoni*, have restricted distributions within

fragmented habitats, meaning that conservation is a priority for this species and several other range-restricted psammophiids (Bates *et al.*, 2014; Branch *et al.*, 2019).

The monophyly of the Psammophiidae group has been supported by numerous phylogenetic studies (Cadle, 1994; Figueroa *et al.*, 2016; Kelly *et al.*, 2008, 2011; Nagy *et al.*, 2003; Pyron *et al.*, 2013; Vidal & Hedges, 2002; Zaher *et al.*, 2019). Although originally a member of Lamprophiidae, Psammophiidae (previously Psammophiinae) was recently raised to family level based on the findings of Zaher *et al.* (2019). The large family of African snakes can now be found within the superfamily Elapoidea (Zaher *et al.*, 2019). Whilst our understanding of Psammophiidae has improved drastically in the past few decades, the family is far from understood, with improved taxon sampling producing several new taxonomical amendments in the past three years (Branch et al., 2019; Ruane et al., 2018; Trape et al., 2019).

Motivation

Species form the backbone of biological science with many metrics such as 'species richness' and 'species diversity' being dependent upon our understanding of species and their presence. Our understanding is, however, flawed because species pluralism coupled with contrasting systematic methodologies creates a vastly different interpretation of species diversity. Ultimately, where you draw the species line is important and in many cases is the breaking point underpinning species problems (Zachos, 2016).

Africa, and particularly central Africa, is considered poorly studied (Böhm *et al.*, 2013; Tolley *et al.*, 2016). Understudied regions are critical focal points for increased research because they have the potential to harbour misunderstood and under-represented species diversity. In addition to one in five of the world's reptiles being data-deficient, 20% of the world's reptiles are threatened with extinction, with species in Africa being particularly susceptible because of the compounded data deficiency being localised in central Africa (Böhm *et al.*, 2013). The genetically-orientated research of late has, however, had much success because molecular studies of previously studied taxa have shown multiple cryptic species that were missed by morphological taxonomists (e.g., Adalsteinsson *et al.*, 2009; Nagy *et al.*, 2012; Oliver *et al.*, 2009; Ruane *et al.*, 2018)

Elapoidea is a large, diverse superfamily of caenophidians, which up until recently was poorly understood (Zaher *et al.*, 2019). Although recent phylogenetic work has helped clarify many aspects of Elapoidea systematics (Broadley *et al.*, 2018; Greenbaum *et al.*, 2015; Kelly *et al.*, 2011; Portillo *et al.*, 2018; Ruane *et al.*, 2018; Vidal *et al.*, 2008), there is still little known

about many of its constituent families. Psammophiidae is a prime example of this and whilst many species in the group have received detailed attention in past studies (Branch *et al.*, 2019; Broadley, 1977, 2002; Kelly *et al.*, 2008; Ruane *et al.*, 2018; Trape *et al.*, 2019), many genera remain poorly sampled and taxonomically misrepresented and/or misunderstood. The taxonomical uncertainty involving the Asiatic *Psammophis* is further compounded by the complete lack of molecular evidence for all but two of the Asiatic species. The genera: *Dipsina*, *Psammophylax, Hemirhagerrhis*, and *Rhamphiophis* are phylogenetically under-represented in the literature (Kelly *et al.*, 2008; Pyron *et al.*, 2013; Vidal *et al.*, 2008), and the inclusion of more samples from a wider range of localities may uncover cryptic diversity missed by morpho-centric studies.

Psammophiidae are important in ecosystems, prey-predator relationships, and food web structure (Gaston, 2010). Climate change and anthropogenic expansion and alteration remain at the forefront of threats to reptiles, but before we can understand their effects we need to understand the taxonomy, the systematics, and what constitutes a species (Trombulak *et al.* 2004; Dawson, Jackson, and House, 2011). Common snakes may be able to adapt better, but if these species' retain cryptic taxa, it would be detrimental to their conservation to refer to them as continuous taxa with high intraspecies diversity (Hewitt, 2004a; Nowak *et al.*, 2008). Widespread species may contain a larger number of evolutionary lineages, potentially exposing them to localised threats across their ranges (Taylor *et al.*, 2013).

With extinction rates currently 1000 times the rate of normal background extinction rates, conservation will be tantamount to the survival and sustainability of Africa's reptilian diversity (Böhm *et al.*, 2013; Tolley *et al.*, 2016). Without over-looking distribution and ecology, the importance of systematics cannot be stressed enough, because without an understanding of species and the boundaries between different taxa, conservation becomes virtually impossible. Giving a species a name not only affords it protection but also gives it value for future studies (Scott & Rines, 1975). Taxonomy works in collaboration with conservation and should inform decisions within the wildlife management sector. With climate change and anthropogenic expansion, habitable environment is bound to contract, putting pressure on species' density and diversity. Psammophiidae is characterised by many widespread, morphologically divergent, and cryptic taxa, and without an understanding of the species boundaries and geographical distribution, it may shroud their incorporation into the conservation framework (Brito, 2010).

The implementation of molecular biology within the herpetological world has resulted in the resolution of many species complexes across a multitude of systematic levels. The effectiveness of phylogenetic analysis in resolving problematic taxonomy within

Psammophiidae cannot be overstated. However, taxonomic amendments based on neutral molecular markers neglects ecological and adaptive significance. The diagnosability version of the Phylogenetic Species Concept thus has the potential to introduce triviality into the systematic process when evolutionary history is ignored in favour of single base-pair differences (Zachos, 2016). This can result in an inflated biodiversity, but with little associated biological and ecological relevance. According to Agapow *et al.* (2004), taxonomy of this variety has resulted in an increase of species numbers of 48.7% across all taxa. Over-estimations of species diversity can ultimately lead to conservation problems, a devaluing of diversity, more supposedly threatened species, and in some cases, increased poaching and trophy hunting (Zachos, 2016).

In addition to resolving problematic taxonomy, and facilitating best conservation practice, this thesis represents an opportunity to investigate the more theoretical aspects of evolutionary biology using a robust and variable taxon. Psammophiidae is the ideal study group because it contains ecologically and morphologically diverse taxa from a wide suite of habitats. This is demonstrated by past studies (Kelly *et al.*, 2008; Segniagbeto *et al.*, 2011; Taft, 2018; Trape *et al.*, 2019) that showed a high degree of evolutionary structuring. The interplay between ecological specialisation and geographical isolation amongst the different species of the family allows us to assess the effect of both convergent and divergent evolution on taxonomical classification. Using a molecular and morphological framework, both the striking similarity and difference of the species across the family can be investigated for potential cryptic diversity and rapid morphological divergence. Both of thave been responsible for confounding taxonomists in the past. The combination of morphology and molecular taxonomy thus offers the best means of delimiting species in the absence of a one size fits all delimitation approach (Bickford *et al.*, 2007; De Queiroz, 2007; Sites & Marshall, 2004).

Ultimately, the concept of species is an ephemeral thing filled with complexity through the intricacy of the evolutionary process. To delineate species using any one method is like trying to understand a puzzle with only one piece. Although there exist multiple species concepts, some have more bearing on the process of speciation than others, especially in certain taxa. For example, mate recognition, both intrinsic and extrinsic, may be a small piece of the puzzle, but when coupled with the morphological and phylogenetic species concept, makes the picture clearer, enabling clearer decisions when deciphering the puzzle and describing the bigger picture.

Aims

The main research aim was to elucidate the most accurate taxonomic arrangement of the Psammophiidae family using a multidisciplinary systematic approach, incorporating both morphological and molecular information to tackle the question of species and species concepts. The thesis has been partitioned into sections based on taxonomical rank with the family, genus, and species level being investigated sequentially, to determine the most effective methodology for delineating taxa of contrasting sizes and complexity, using the frameworks stipulated by the Unified Species Concept. This thesis also aimed to address several knowledge gaps (*Psammophylax* taxonomy; the '*acutus*' problem; cryptic speciation in *Mimophis*; the '*leightoni* complex'; the '*sibilans* complex'; taxon sampling; disparity between node dates) identified in Psammophiidae (Kelly, 2005), whilst also investigating the validity of the results from several recent studies that attempted to do the same.

Chapter Two: Systematic Study of the Psammophiidae family

All available species of Psammophiidae were sourced to build the most comprehensive phylogenetic tree of the family possible. The chapter builds on past research and aims to enrich our molecular understanding of the group through the utilisation of a wider, more representative dataset (as compared to past studies) and novel molecular techniques. The study was supplemented with geometric morphometrics to determine whether there were diagnosable differences in head structure between the different genera. Family-level studies are important because they address problematic taxonomy borne out of taxon-specific studies, undertaken by different scientists with contrasting conceptualisations of 'species', using different species delimitation methods. By addressing all the species available in one study, using the same techniques, I aim to produce more defensible conclusions about species boundaries, to enable better taxonomical sorting going forward.

Chapter Three: Taxonomic Re-evaluation of Psammophylax

Psammophylax species were sampled from throughout their ranges and investigated using both the Phylogenetic and Morphological Species concepts. *Psammophylax* is characterised by the presence of several morphologically similar, sympatric species. Molecular analysis of a limited number of *Psammophylax* in Chapter Two revealed previously unappreciated species diversity in the genus. By broadening the dataset, and incorporating all members of the genus, this chapter aimed to elucidate the most accurate taxonomic structuring of the genus using phylogenetics, geometric morphometrics, and standard morphology.

Chapter Four: Phylogeographic Study of Psammophylax rhombeatus

Psammophylax rhombeatus was sampled from throughout its range and investigated using phylogenetic, phylogeographic and morphometric analyses. In both Chapters Two and Three, *Ps. rhombeatus* displayed high levels of intraspecific diversity irrespective of its smaller distributional extent. The aim of Chapter Four was thus to determine whether the implementation of taxon-specific phylogenetics and geometric morphometrics could identify cryptic diversity in the species. The specificity of the dataset (single species) allowed me to test the effectiveness of the contrasting methodologies, used in the previous chapters, at the species and population level. Population genetics and population-specific morphological analysis were thus utilised to help tease apart intra-specific variation within *Psammophylax rhombeatus.*

Chapter Two: Evolutionary Structuring within Psammophiidae

Introduction

Overview

Psammophiidae is a large family of snakes within the superfamily Elapoidea, made up of approximately 55 species and eight genera (Branch *et al.*, 2019; Kelly *et al.*, 2008; Trape *et al.*, 2019; Wallach *et al.*, 2014; Zaher *et al.*, 2019). Distributed throughout Africa, Madagascar, southern Europe, and south-central Asia, it is a widespread family of snakes. Their wide distribution coupled with their high abundance and associated ecological and socio-political importance have made them the focus of multiple studies in recent years (Branch *et al.*, 2019; Gonçalves *et al.*, 2018; Kelly *et al.*, 2008; Ruane *et al.*, 2018; Trape *et al.*, 2019).

Taxonomy

The Psammophiidae family has been the subject of much taxonomic confusion, since work started on it in the late 1800s (Boulenger, 1896; Broadley, 1966, 1977; Hughes, 1999; Loveridge, 1940). In a “tentative arrangement of African Colubridae”, Bogert (1940) placed in his Group XVI the genera *Cerastes* (= *Psammophylax*), *Dromophis* (since synonymized with *Psammophis*), *Hemirhagerrhis, Malpolon, Psammophis* and *Rhamphiophis* (subsequently split with the revival of the monotypic genus *Dipsina* for *D. multimaculata*) (Branch *et al.*, 2019). The taxonomical shift was based largely on dentition and vertebral characteristics with a particular emphasis on hemipenal structure, with psammophiids sharing thin, short hemipenes with reduced ornamentation (Bogert, 1940), a finding supported by most morphological studies since then (Bourgeois, 1968; Broadley, 1990; Dowling & Duellman, 1978; Zaher, 1999). The revision of Bourgeois (1968), whilst investigating cranial anatomy, placed the genera in Psammophiinae, within the Colubridae family.

Whilst crucial to our understanding of the higher-level relationships of the group, conventional (morpho-centric) taxonomy has proven ill-equipped to deal with many generalist, co-occurring taxa. Evolutionary mechanisms such as convergent evolution and rapid morphological divergence confound conventional systematics, resulting in incorrect taxonomic conclusions. Molecular biology has been successful in remedying this limitation and has improved our understanding of the lower-level taxonomy of the group (Branch *et al.*, 2019; Gonçalves *et al.*, 2018; Ruane *et al.*, 2018; Trape *et al.*, 2019). The monophyly of the family has been supported by numerous phylogenetic studies with evidence from immunological data (Cadle, 1994), mitochondrial DNA datasets (Gravlund, 2001; Kelly *et al.*, 2003; Nagy *et al.*,

2003; Vidal & Hedges, 2002) and mitochondrial + nuclear DNA datasets (Branch *et al.*, 2019; Gonçalves *et al.*, 2018; Kelly *et al.*, 2008, 2009, 2011; Pyron *et al.*, 2013; Vidal *et al.*, 2007; Zaher *et al.*, 2019). Up until the work of Zaher *et al.* (2019), the group was considered a subfamily within Lamprophiidae, but novel sampling and sophisticated phylogenetics have resulted in the elevation of the group to family level.

The currently recognised genera of Psammophiidae are: *Dipsina* Jan, 1863; *Hemirhagerrhis* Boettger, 1893; *Malpolon* Fitzinger, 1826; *Mimophis* Grandidier, 1867; *Psammophis* Fitzinger, 1826; *Psammophylax* (Fitzinger, 1843); *Rhamphiophis* Peters, 1854 and *Rhagerhis* Peters, 1862. *Psammodynastes* (Günther, 1858 [Elapoidea *incertae sedis*]), a genus of Asiatic grass snakes, was placed in Psammophiinae *fide* Figueroa *et al.* (2016), but this genus has bifurcate, heavily-adorned hemipenes (Zaher, 1999). This contrasts with the synapomorphy of the simple, unadorned hemipenes found in the other psammophiids. Additionally, Zaher *et al.* (2019) recovered *Psammodynastes* within the synonymy of Pseudaspididae, with ambiguous support. For this reason, we exclude *Psammodynastes* from Psammophiidae.

Dipsina is a monotypic genus found in southwestern Africa. The type species of this genus is *Coronella multimaculata* Smith, 1847 in 1838–1849 (= *Dipsina multimaculata*). It is a small terrestrial snake with a sharp nose that it uses for digging in soft sand (Marais, 2004; Wallach *et al.*, 2014). Previous assignments of the genus placed it within *Rhamphiophis* but it was subsequently resurrected as a separate genus based on cranial osteology (Broadley, 1983).

Hemirhagerrhis is a small genus of arboreal snakes (except for *H. viperina*, which is rupiculous), comprising four species (Branch *et al.*, 2019; Wallach *et al.*, 2014). The group is distributed throughout central and eastern Africa and the type species of the genus is *Hemirhagerrhis kelleri* Boettger, 1893. Members of the genus are the only strictly arboreal snakes in Psammophiidae.

Malpolon is a small, widespread genus of terrestrial snakes found in southern Europe, southwestern Asia, and northern Africa. The type species of the genus is *Coluber monspessulanus* Hermann, 1804 (= *Malpolon monspessulanus*). The genus has a chequered taxonomical past with different studies recognising contrasting numbers of taxa. The genus is currently comprised of two species, *Malpolon monspessulanus* and *Malpolon insignitus*. The latter species was once considered a subspecies of *Ma. monspessulanus*, but was subsequently elevated to species level (Carranza *et al.*, 2006). Whilst *Malpolon fuscus* was considered a full species by Wallach *et al.* (2014), recent findings suggest that the Grecian endemic is a subspecies of *Ma. insignitus* (Carranza *et al.*, 2006). The taxon is referred to as

Ma. i. fuscus in this study. *Malpolon monspessulanus* contains a subspecies called *Malpolon m. saharalanticus*, found in southern parts of Morocco (Geniez *et al.*, 2006; Mangiacotti *et al.*, 2014).

Mimophis is a widespread terrestrial genus endemic to Madagascar, absent only from the humid eastern parts of the country. The type species is *Psammophis mahafalensis* Grandidier, 1867 (= *Mimophis mahafalensis*). The genus was considered monotypic, but recent work resulted in the acknowledgement of a novel cryptic species, *Mimophis occultus*, restricted to the northern section of Madagascar (Ruane *et al.*, 2018).

Psammophis is the largest genus within the family with 35 currently recognised species and multiple species complexes. It is also the most widespread with species being found from the southern tip of Africa through to the northern reaches of southern Asia, and as far south as Indonesia and Java. The type species is *Coluber sibilans* Linnaeus, 1758 (= *Psammophis sibilans*). Whilst recent work has resolved many taxonomic discrepancies, the group remains problematic given the large number of species complexes within the genus (Branch *et al.*, 2019; Gonçalves *et al.*, 2018; Kelly *et al.*, 2008; Trape *et al.*, 2019). Kelly *et al.* (2008) synonymised *Dromophis* with *Psammophis* based on strong molecular evidence. Within *Psammophis* exists a group of Asiatic whip snakes' (plus southern African endemic, *P. crucifer*), referred to as '*Taphrometopon'.* The genus was first termed by Brandt (1838), with the type species of the proposed genus being *T. lineloatus* (= *P. lineolatus*) Originally described The proposed genus comprises six species with three of them, *P. indochinensis*, *P. longifrons* and *P. leithi*, yet to be sequenced. Irrespective of this, the group has been retrieved as well-structured and distinctive from the rest of *Psammophis* in past phylogenies (Figueroa *et al.*, 2016; Kelly *et al.*, 2008; Zaher *et al.*, 2019).

Psammophylax is a genus of terrestrial grass snakes restricted to eastern and southern Africa (Branch, 1998; Spawls *et al.*, 2018. The type species is *Coluber rhombeatus* Linnaeus, 1758 (= *Psammophylax rhombeatus*). With the elevation of *Ps. ocellatus* to species level (Branch *et al.*, 2019), the genus now consists of five species, most of which are relatively widespread and ecologically plastic. Based on the findings of Kelly *et al.* (2008), *Psammophylax a. acutus* (previously *Rhamphiophis*) was transferred to *Psammophylax* based on shared monophyly with the group. The taxonomical validity of *Ps. togoensis* (previously a subspecies of *Ps. acutus*) requires attention given that it was elevated to species level (Segniagbeto *et al.*, 2011) based on minor morphological variation, in the absence of phylogenetic testing.

Rhagerhis is a monotypic genus distributed throughout the Middle East and northern Africa. The type species of the genus is *Coluber moilensis* Reuss, 1834 (= *Rhagerhis*

moilensis). *Rhagerhis moilensis* has a complex taxonomic past and has been moved from *Scutophis* (Schlüter, 2006), to *Malpolon* (Trape & Mane, 2006), back to *Scutophis* (Padial, 2006), back to *Malpolon* (Largen & Spawls, 2010), into *Rhagerhis* (Böhme & de Pury, 2011) and back to *Malpolon* (Figueroa *et al.*, 2016). *Rhagerhis* was synonymised with *Malpolon* based on the findings of Figueroa *et al.* (2016), but given the erroneous placement of *R. oxyrhynchus* in the same phylogeny, doubt is cast on the polyphyletic placement of *Rhagerhis*. Unfortunately, most recent phylogenies (Pyron *et al.*, 2013; Zaher *et al.*, 2019), that focused on Psammophiidae, omitted representatives of *Ma. insignitus*, leaving the aged findings of Carranza *et al.* (2006) as the only published support for the distinctiveness *of Rhagerhis*. Given the contentious and unsupported relationships found within Figueroa *et al.* (2016), *Rhagerhis* will be used in this study to determine its validity as a taxonomical unit.

Rhamphiophis is a small genus of large-bodied, semi-fossorial snakes. As they all had a beak, *Ps. a. acutus* was also considered a member of *Rhamphiophis,* prior to the rearrangements of Kelly *et al.* (2008). The type species of the genus is *Rhamphiophis rostratus* Peters, 1854. Restricted to sub-Saharan Africa, this group contains four recognised species: *R. rostratus*, *R. oxyrhynchus, R. rubropunctatus* and *R. maradiensis*. Recently, *Rhamphiophis maradiensis* (Chirio & Ineich, 1991) was called into question with Trape and Mane (2006) suggesting that the species description resulted from a misidentified *Rh. moilensis*. Based on variable head patterning and ventral scale counts, Chippaux and Jackson (2019) suggested that the species is indeed valid. Whilst unavailable for phylogenetic testing in this study, the species is henceforth considered valid, pending further investigation.

Ecology & Conservation

Whilst our understanding of Psammophiidae was improved drastically by the molecular-centric findings of recent studies (Figueroa *et al.*, 2016; Kelly *et al.*, 2008; Zaher *et al.*, 2019), the family is far from understood, with improved taxon sampling producing two novel species in the past three years (Ruane *et al.*, 2018; Trape *et al.*, 2019). The family is characterised by many widespread, abundant, and morphologically cryptic taxa, and without an understanding of the species boundaries and geographical distribution, it may shroud their incorporation into conservation, ecological, and socio-political frameworks (Brito, 2010).

Barring Madagascar, the distribution of many of the species overlap, and because of this, the family is characterised by the co-occurrence of several morphologically similar species, performing similar ecological roles. There is thus a tendency, by scientists and citizens alike, to under-appreciate species diversity, and by association the ecological importance of the taxon, because of a perceived misunderstanding of their taxonomy. Robust systematic analysis can remedy this and help inform best conservation practice through the

correct recognition of diversity and their associated ecological roles. This is especially important for species such as *Psammophis leightoni,* which occur in increasingly more fragmented habitats caused by anthropogenic expansions and the persistent protraction of natural habitat (Bates *et al.*, 2014; Branch *et al.*, 2019; Taft, 2018).

Premise of This Chapter

This study builds on the tremendous PhD (Kelly, 2005) and subsequent publication of Christopher Kelly (Kelly *et al.*, 2008), which for the first time unpacked, in detail, the molecular structuring within Psammophiidae. Whilst Christopher Kelly's work on the family helped clarify many aspects of the taxonomy within the group, it also highlighted several glaring gaps in our understanding of the group, several of which have been addressed in past publications (Branch *et al.*, 2019; Gonçalves *et al.*, 2018; Ruane *et al.*, 2018; Taft, 2018; Trape *et al.*, 2019). A more comprehensive taxon sampling regime in Madagascar and western Africa revealed cryptic diversity in *Mimophis* and *Psammophis*, respectively (Ruane *et al.*, 2018; Trape *et al.*, 2019). Whilst in Taft (2018), increased sampling also revealed an over-appreciation of species diversity in the southern African *'leightoni* complex'. Lastly, the increased sampling in west and northern Africa has facilitated a better understanding of evolutionary history and taxonomy of Psammophiidae. All these findings coupled with the datasets to which these findings are attributed, enable me to address the biggest knowledge gap left by Kelly's thesis (Kelly, 2005): the sampling bias.

Although most species were incorporated in Kelly *et al.* (2008), there was a disproportionate number of east African samples, a result of targeted field work in the region. This sampling bias resulted in a disparity in phylogenetic node ages between his subfamily (previously Psammophiinae) and family level analyses. By incorporating both Christopher Kelly's original dataset, the taxon-specific datasets from the recent studies above, and newly sequenced material, this study will be afforded the largest molecular dataset of the family ever assembled.

To support the molecular component, geometric morphometrics analysis will be used on the dorsal and lateral head shapes of the different genera. Whilst most genera are morphologically similar diurnal terrestrials with a similar foraging strategy, individuals from *Hemirhagerrhis, Rhamphiophis,* and *Dipsina* exhibit widely contrasting head shapes and foraging strategies. In Mangiacotti *et al.* (2018), geometric morphometrics on the dorsal view of the head was successful in teasing apart subtle differences in head structure between species of *Malpolon*. By utilising this method in this study, the aim is to determine whether the genera of Psammophiidae can be separated using head structure and whether animals with similar head shapes show similar phylogenetic relationships.

The overall aim of the study is to elucidate the most accurate taxonomical structuring of Psammophiidae using a combination of both standard and time-calibrated phylogenetics, distance and threshold-based species delimitation and geometric morphometrics. By using a multi-evidence species delimitation approach (motivated by the USC), this study allows us to produce more defensible conclusions when accessing systematic structuring within one of the most taxonomically problematic snake families in Africa.

Methods

Genetic Sampling

The phylogeny of Psammophiidae was estimated using genetic information from 320 individuals. Most of the dataset comprised of accessioned samples from Genbank (https://www.ncbi.nlm.nih.gov/genbank/; Table S2.1). To avoid sampling bias, a relatively equal number of samples was selected from the full distributional range of each species, with more widely distributed species warranting larger representation in the study. Molecular markers used were selected based on their availability in online data repositories and their effectiveness in resolving phylogenies in past studies. To address the sampling bias of past studies, a more distribution-representative sampling from several taxa (e.g. *P. crucifer, P trigrammus, P. leopardinus, R. rostratus, D. multimaculata, Hemirhagerrhis viperina*) was utilised in this study. The study also incorporated two novel, never-before-sequenced species (*Hemirhagerrhis nototaenia, Psammophis zambiensis*), and several unidentified psammophiids. Due to the logistical constraints, arising from the outbreak of the Covid-19 viral pandemic in 2020, samples of *P. leithi* and *P. longifrons* were unavailable for this study. These samples will be incorporated into the resulting paper, but in an effort to resolve the relationship between Asiatic and African *Psammophis* in this study, two additional samples of *P. lineolatus* have been incorporated into this study, thereby doubling the amount of Asian psammophiids used in Kelly *et al.* (2008). Barring the Asiatic whip snakes, the only other species missing from this study were *P. pulcher* and *Malpolon m. saharalanticus*, from East African and southern Morocco, respectively. Newly sequenced tissue samples were obtained from Port Elizabeth Museum (PEM, Port Elizabeth), and from scientists situated throughout Africa. Tail tips (live specimens) and liver or muscle tissues (preserved specimens) were preserved in ~95% ethanol.

Genetic Laboratory Protocols

A standard salt extraction method was used to isolate Genomic DNA (Bruford *et al.*, 1992) from tissues with the use of lysis (Buffer ATL; Qiagen) and elution (Buffer AE; Qiagen) buffers.

Standard PCR procedures were utilised to amplify three partial mitochondrial genes (cytochrome b [cytb], 16S ribosomal ribonucleic acid [16S] and NADH-dehydrogenase subunit 4 [ND4]) and one partial nuclear gene (oocyte maturation factor [c-mos]). PCR amplification was carried out using the primer pairs listed in Table 2.1. Amplification of the selected genes was carried out using 20–50 ng/µl extracted genomic DNA. Each amplification was conducted with a PCR mixture to the total volume of 25 µl containing 12.5 µl TopTaq Mastermix (Qiagen; containing 10x PCR buffer, 1.5 mM $MgCl_2$, 0.2 mM dNTPs, and 0.75 U Taq polymerase) or 12.5 µl iTaq SYBR Green Supermix 2x Mastermix (Bio-rad Laboratories inc.), 2 µl forward primer (10 µM), 2 µl reverse primer (10 µM), and 8.5 µl of the genomic DNA and de-nucleated water combined. The cycling profile for gene amplification was as follows: initial denaturing step at 94 °C for 5 min, followed by 35–40 cycles of 94 °C for 30 s, 48–56°C for 45 s, and 72 °C for 45 s, with a final extension at 72 °C for 8 min (Table 2.1). The prepared PCR products were sent to Macrogen Corp. in Amsterdam, Netherlands or Stellenbosch University in Western Cape, South Africa, for sequencing (after purification) with the forward primers only.

Table 2.1: Primers and PCR protocols used to the generate sequences for the study.

Gene	Primer	Source	Annealing Temp (°C)	Cycles
16S	L2510: 5'—CGCCTGTTTATCAAAAACAT—3'	Palumbi (1996)	50—52	35
	R1478: 5'—TGACTGCAGAGGGTGACGGGCGGTGTGT—3'			
cytb	WWF: 5'—AAAYCAYCGTTGTWATTCAACTAC—3'	Whiting, Bauer, & Sites (2003)	50—52	35
	Cytb-R2: 5'—GGGTGRAAKGGRATTTTATC—3'			
ND4 + LeutRNA	ND4: 5'—TGACTACCAAAAGCTCATGTAGAAGC—3'	Arèvalo, Davis, & Sites (1994)	52—56	35
	LeutRNA: 5'—CATTACTTTTACTTG GATTTGCACCA—3'			
c-mos	S77: 5'—CAT GGACTGGGATCAGTTATG—3'	Slowinski & Lawson (2002)	48—52	35—40
	S78: 5'—CCTTGGGTGTGATTTTCT CACCT—3'			

**Sequences of Rag2 were acquired solely from GenBank and were not sequenced in this study.*

Sequence Alignment and Gene Partition Congruence Testing

All novel sequence trace files were checked using BioEdit Sequence Alignment Editor v.7.2.5 (Hall, 1999) and aligned, along with GenBank sequences, using MUSCLE v.3.7 (Edgar, 2004), implemented in CIPRES Science Gateway XSEDE online resource (http://www.phylo.org;

Miller *et al.* 2010). Aligned sequences were formatted and checked for errors using MEGA v.6.0 (Tamura *et al.*, 2013) and trimmed. The region representing LeutRNA was split from the genetic region of ND4 and omitted from the study given its lack of representation in most samples acquired from Genbank. Gene alignments were used to construct separate Maximum Likelihood (ML) gene trees in MEGA v.6.0 (Tamura *et al.*, 2013) using the GTR+G+I nucleotide substitution model and 100 bootstrap replicates. Congruence between each gene tree pair was tested using Congruence Index (I_{cong}; http://max2.ese.u-psud.fr/icong/index.help.html; Vienne, Giraud and Martin, 2007). All gene-tree combinations were found to be congruent and four datasets were created.

Datasets

To facilitate molecular best practice, different datasets were put together using specific genes, partition schemes, and models of evolution for different analyses. By doing this, I was able to optimize each analysis and ensure that the phylogenetic modelling was as robust as possible.

Dataset 2.1 was used to infer the phylogenetic structuring within the family and comprised of 325 samples (including outgroups), from all eight genera (Table S2.1). Samples were chosen with the intention of capturing the full distribution of each species, to ensure objective taxon sampling, across all species' ranges, with several closely related members of Elapoidea (Table S2.1) being used to root the tree. *Dataset 2.1* used the following genes: 16S (110 sequences [sq], 424 base pairs [bp]); cytb (301 sq, 1101 bp); ND4 (280 sq, 666 bp); c-mos (139 sq, 579 bp); Rag2 (30 sq, 714 bp).

Dataset 2.2 was used for the time-calibrated phylogeny (Table S2.1). The dataset utilised a representative sampling (two to four samples) from each genus of the family, plus representatives from several outgroup taxa from Serpentes, to calibrate the analysis (Table S2.1). The 16S and Rag2 alignments were omitted from the dataset given the lack of comparable material in the outgroup taxa. *Dataset 2.2* used the following genes: cytb (129 sq, 1101 bp); ND4 (119 sq, 666 bp); c-mos (86 sq, 579 bp).

Dataset 2.3 was used for single locus species delimitation, using the ND4 gene (188 sq, 666 bp), and comprised of all available samples for *Psammophis* (Table S2.1). The dataset omitted sequences with more than 10% missing data or identical sequences and outgroup taxa (Table S2.1).

Dataset 2.4 was used for pairwise distance analysis of the genera within Psammophiidae. The dataset utilised all available cytb (271 sq, 630 bp) and ND4 (254 sq, 666 bp) sequences that did not exceed 10% missing data (Table S2.1). The molecular markers and models of evolution utilised in each dataset can be found in Table 2.2.

Models of Evolution and Partition Scheme

All gene alignments were tested for saturation using DAMBE v.6.4.67 (Xia, 2013). The protein-coding genes (cytb, ND4, c-mos, Rag2) were checked for stop codons to ensure they started on the correct reading frame and analysed according to codon position. No saturation was found, enabling the use of gene-partitioned datasets (where necessary). *Dataset 2.1* utilised a codon partition scheme (codon positions partitioned separately) as it produced better supported topologies using both the Bayesian Inference (BI) and Maximum Likelihood (ML) algorithm. The BEAST algorithm, however, retrieved stronger support using a gene-partitioned dataset (genes partitioned separately) hence gene-partitioning was used in *Datasets 2.2* and *2.3*.

The best partition schemes and best-fitting models of molecular evolution were selected using PartitionFinder 2 (Lanfear *et al.*, 2016) with the following settings: BIC model selection criterion, BEAST models, linked branches and all partition schemes searched (Table 2.2). Due to the size of *Dataset 2.1* (323 samples, 5 genes), the greedy search method was used to speed up the process. For BEAST analysis (*Datasets 2.2* and *2.3*), the gene partitions were run through jModelTest 2 (Darriba *et al.*, 2012; Guindon & Gascuel, 2003) to determine the optimal gamma shape and invariant site values for the partitions selected by PartitionFinder 2.

Table 2.2: Best-fit partitioning schemes and models of evolution for each dataset, according to PartitionFinder 2, with number of sites per partition. Numbers following genes in the subset partition column refer to codon position. NA = Not Applicable.

Dataset	Initial Partition	Subset Partition	Best Model*	Number of Sites
2.1	codon	16S, cytb_1, ND4_1	TVM (GTR)+I+G	1013
		cytb_2, ND4_2	HKY+I+G	589
		cytb_3, ND4_3	GTR+I+G	589
		Rag2_1, Rag2_2, c-mos_1, c-mos_2	HKY+I+G	862
		c-mos_3, Rag2_3	HKY+G	431
2.2	gene	cytb, ND4	GTR+I+G	1767
		c-mos	HKY+G	579
2.3	gene	ND4	GTR+I+G	666
2.4	NA	cytb	NA	630
		ND4	NA	666

***MrBayes does not support many of the models implemented in BEAST. In these cases, the best alternative implemented in MrBayes was used. These models are shown in brackets.*

Phylogenetic Tree

Dataset 2.1 was used to infer the phylogenetic structuring within the family using BI and ML (Table 2.2, S2.1). Bayesian Inference was carried out using MrBayes v.3.2.2 (Ronquist *et al.* 2012) implemented on the CIPRES Science Gateway. Four parallel runs of 20 million generations (MCMC analysis) were performed, with trees being sampled every 1000 generations, using uniform priors. BEAGLE was not used as it produced anomalous topologies. The number of generations discarded as burn-in was determined using Tracer v.1.5 (Rambaut & Drummond, 2009). The effective sample size (ESS) was found to be above 200 for all parameters with all runs reaching convergence, indicating that a burn-in of 10% was adequate. Maximum Likelihood analysis was conducted using the GTRGAMMA model in RAXML-HPC v.8.2.12 (Stamatakis, 2014) on the CIPRES Science Gateway. A random starting tree and the rapid bootstrapping method was used. One thousand bootstraps were run, and all other parameters were set to default. All BI and ML trees were viewed and edited in FigTree v.1.4.2 (Rambaut, 2014).

Time-calibrated Phylogeny

Dataset 2.2 was used in a time-calibrated phylogeny of Psammophiidae (Table 2.2, S2.1). A gene-partitioned input file was created in BEAUti v2.6.2. (Bouckaert *et al.*, 2019; Drummond & Rambaut, 2007) using the following settings: linked trees, unlinked clock models, and unlinked site models. A relaxed lognormal clock model with a Yule prior was used, along with a calibration scheme similar to the one in Portillo *et al.* (2018). The tree was constrained with four primary calibration points from Head *et al.* (2016). These were the split between Caenophidia and Booidea (72.1–66 MYA), split between *Acrochordus* + *Xenodermatidae* and Colubroidea (50.5–72.1 MYA), the divergence of Colubridae and Elapoidea (31–30.8 MYA) and the split between Crotalinae and Viperinae (23.8–20 MYA). All calibrations were constrained with lognormal MRCA priors and set as monophyletic. Means of the age estimates were given in real space and the standard deviations were calculated by working out the standard deviations of the log-transformed range of the fossil calibrations. Three independent analyses of 50 000 000 generations, sampling every 5000, were run through BEAST v.2.6.3 (Bouckaert *et al.*, 2019; Drummond & Rambaut, 2007; Suchard & Rambaut, 2009) on the CIPRES Science Gateway. The independent runs were combined in LogCombiner v.2.6.2 (Bouckaert *et al.*, 2019; Drummond & Rambaut, 2007) and a maximum clade credibility tree using mean heights, with a burn-in of 10%, was created in TreeAnnotator v.2.6.2 (Bouckaert *et al.*, 2019; Drummond & Rambaut, 2007). The effective sample size (ESS) was found to be above 200 in Tracer v.1.5 and the final trees were viewed and edited in FigTree v.1.4.2.

Species Delimitation of Psammophis

Based on the findings from the initial phylogenetic tree, *Psammophis* was investigated using species delimitation analyses to determine whether the genus harbours unappreciated species diversity. Barring *Psammophylax*, the other genera in Psammophiidae lacked robust-enough sampling to warrant further investigation. Given the lack of comparable sequences of *Psammophis* on Genbank, the gene with the largest representation (ND4) was used in single locus species delimitation. Bayesian implementation of the Generalized Mixed Yule Coalescent (bGMYC), Automatic Barcode Discovery (ABGD) and Poisson Tree Processes (PTP) were used to determine whether the topological structuring and novel sequences from previous phylogenies constitute separate species.

Firstly, an ND4 FASTA alignment was created using the sequences from *Dataset 2.3* (Table 2.2, S2.1). The alignment was uploaded onto the ABGD web interface (abgd web (mnhn.fr), web version 10 January 2021) where ABGD infers hypotheses about putative species through the creation of a barcode gap separating intra- and interspecies pairwise distances. The following settings were used: standard p-distance metrics, minimum barcode gap width (1.0), intraspecific divergence minima (0.001) and maxima (0.1). For bPTP and bGMYC, phylogenetic tree creation was carried out using BEAST v.2.6.3. A gene-partitioned file (Table 2.2) was input into BEAUti v.2.6.2 using the following settings: linked trees, unlinked clock models, and unlinked site models, with a relaxed lognormal clock and a Yule prior. The reduced length of the alignments in *Dataset 2.3* resulted in erroneous topologies, and thus the tree was rooted with *P. condanarus* + *P. lineolatus* + *P. crucifer* to ensure that the tree topology remained consistent with prior analyses. Three independent analyses of 50 000 000 generations, sampling every 5000, were run through BEAST v.2.6.3. The independent runs were combined in LogCombiner v.2.6.2 and a maximum clade credibility tree, with a burn-in of 10% was created in TreeAnnotator v.2.6.2. The effective sample size (ESS) was found to be above 200 in Tracer v.1.5 and the final trees were viewed and edited in FigTree v.1.4.2.

The final maximum clade credibility tree was analysed using the package bGMYC v.1.0.2 in R studio v.1.1.442 (R Core Team, 2016; Reid & Carstens, 2012). A traditional GMYC aims to determine when the branching rates within a calibrated tree shift from a Yule to coalescent process, and the Bayesian implementation of the model incorporates more flexibility into the model through the integration of MCMC. The tree was subjected to 50 000 MCMC steps, a burn-in of 40 000 steps, and sampling every 100 steps. Bayesian implementation of the PTP model was conducted via the bPTP server (http://species.h-its.org/ptp/; Zhang *et al.*, 2013) on the same gene-partitioned maximum clade credibility tree. Unlike bGMYC, that examines time, bPTP differentiates speciation processes among species

from the diversification processes within species by examining the substitutions between nodes. The results from all three threshold analyses were overlaid on the maximum clade credibility tree from TreeAnnotator v.2.6.2.

Pairwise Distance Analysis

Pairwise distance analysis of Psammophiidae was carried out using *Dataset 2.4*. Pairwise distance matrices were created for cytb and ND4, using MEGA X v.10.1.7 (Kumar *et al.*, 2018) using the following settings: standard uncorrected p-distance model, uniform rates, pairwise deletion, and 500 bootstraps. The samples were tabulated and grouped according to generic affiliation to test the validity of the genera within the family.

Geometric Morphometrics

Geometric morphometric analyses of the external views of the head were implemented to investigate the head shape of genera of Psammophiidae, using representative species (2–14 individuals per genus, totalling 62 individuals). Dorsal and lateral photographs of the heads of specimens were obtained from the Port Elizabeth Museum (PEM) (Table S2.2). The following taxa were selected as representatives for each genus: *Psammophis mossambicus*, *Rhamphiophis rostratus*, *Psammophylax variabilis, Hemirhagerrhis kelleri and Dipsina multimaculata. Psammophis crucifer* was incorporated to test the taxonomic validity of the proposed *'Taphrometopon' genus.* Due to the inaccessibility of various museum collections during covid-19, representatives of *Malpolon, Rhagerhis* and *Mimophis* were not available for this study[2]. Because of this, geometric morphometrics in this study have been restricted to genera found in sub-Saharan Africa.

[2] Representatives of these genera will, however, be incorporated into the resulting paper.

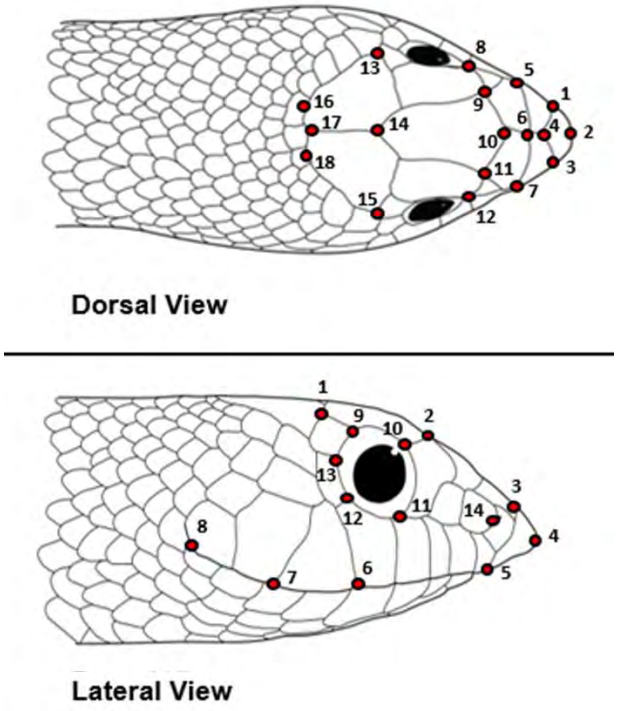

Figure 2.1: The placement of landmarks on photographs of dorsal and lateral aspects of the head for geometric morphometric analysis.

The dorsal and lateral profiles of the heads (all right-hand-side) were photographed on grid paper (1 cm x 1 cm) with a digital camera (Canon 600D [resolution 18.0 MP] and Canon 6D, [resolution 20.2 MP]), using a 100 mm macro lens. Homologous landmarks were placed and digitised on the two views of the heads (Fig. 2.1) (TpsUtil v.1.26, Rohlf, 2004b; TpsDig2 v.2.32, Rohlf, 2004a). A Generalized Procrustes Analysis (GPA; Rohlf and Slice, 1990; Rohlf, 1999) was performed, during which the landmark configurations were resized, translated and rotated (aligned by principal axis). A covariance matrix was estimated using the symmetrical (dorsal view dataset) or the asymmetrical (lateral view dataset) components. A principal components analysis (PCA) was performed on the covariance matrix to identify which portions of the heads showed the most variation between genera (MorphoJ v.1.06d; Klingenberg, 2011). Significant differences between genera and species with respect to principal components (PC) axes' scores were investigated using RStudio v.1.0.136 (R Core Team, 2016), applying the following tests: Analyses of Variance (ANOVAs; package: 'stats', functions: 'anova' and 'lm') and Tukey's Honest Significant Difference (HSD) post-hoc test (package: 'agricolae', function: 'HSD.test', group = F).

Results

Generic Phylogenetic Structuring

There were four supported clades recovered within the family: Clade A–Rhamphiophis + *Rhagerhis* + *Malpolon*; Clade B–*Hemirhagerrhis* + *Mimophis* + *Psammophylax*; Clade C–*Dipsina*; Clade D–*Psammophis* (Fig. 2.2). In the BI phylogeny, Clade A was recovered as sister to Clade B + C + D, and Clade B was recovered as sister to Clade C + D. In ML phylogeny, the only supported intergeneric relationship was the sister relationship between Clade A and Clade B + C + D. Unlike the BI phylogeny, the sister relationship between Clade B and Clade C + D was not supported. This lack of support at the deeper nodes appears to be due to the difficulty in placing *Dipsina* in the tree.

Within Clade A (in both phylogenies)*, Rhagerhis* + *Malpolon* was retrieved as sister to *Rhamphiophis* with *Malpolon* forming a sister relationship with *Rhagerhis*. Within Clade B, the sister relationship between *Hemirhagerrhis* + *Mimophis* and *Psammophylax* was supported by both algorithms.

The validity and structure of the postulated '*Taphrometopon*' genus was explored in the box below the main part of the figure (Fig. 2.2). The sister relationship between '*Taphrometopon'* and *Psammophis* was only supported by the BI algorithm, with '*T. crucifer'* forming a supported sister relationship with the rest of '*Taphrometopon'*. In the ML phylogeny, '*T. crucifer'* was retrieved as sister to '*Taphrometopon'* + *Psammophis* (supported). In ML, the sister relationship between *Psammophis* and *'Taphrometopon'* (excluding *'T. crucifer'),* was not supported. The monophyly of '*T. crucifer'* + rest of '*Taphrometopon'* + *Psammophis* was supported by both algorithms.

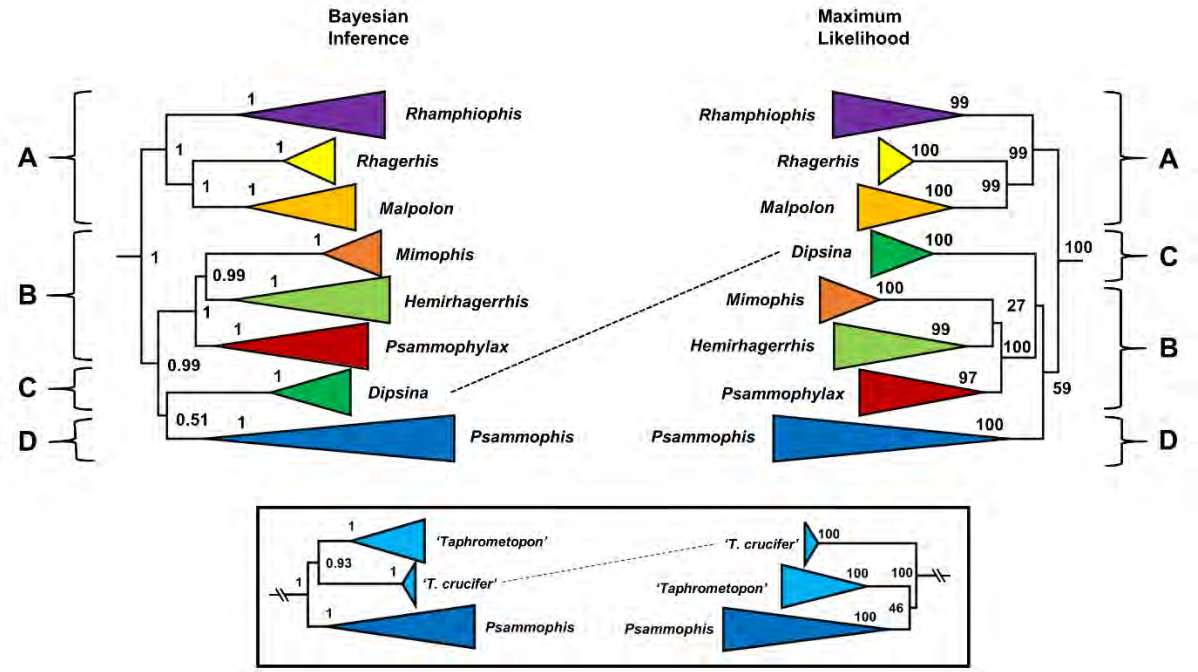

Figure 2.2: Bayesian Inference (BI) and Maximum Likelihood (ML) trees derived from *Dataset 2.1*, with the species grouped into genera. BI posterior probabilities ≥ 0.90 and ML bootstrap values ≥ 75% were considered supported. Dotted lines indicate differential placement of genera between molecular algorithms. Inserted box shows the relationship between *Psammophis* and the proposed genus '*Taphrometopon*'.

Genera of Psammophiidae were separated by pairwise distances that ranged from 13.25–17.70% and 14.02–18.14% in cytb and ND4, respectively (Table 2.3). Intergeneric variation was similar with an average of 16.18 ± 1.05% and 16.38 ± 1.09%, separating the genera of the family in cytb and ND4, respectively.

Species Phylogenetic Structuring

The combined BI and ML tree, from *Dataset 2.1*, consisted of 325 samples (including outgroup taxa), with representatives from every described genus of the family (Fig. 2.3). *Rhamphiophis* was retrieved as monophyletic with strong support for each species within the genus. Both molecular algorithms retrieved support for a sister relationship between *R. rostratus* and *R. rubropunctatus* + *R. oxyrhynchus.* The newly sequenced *R. rostratus* samples yielded limited structure in the tree, indicating gene flow, either presently or recently, between distant populations. Relationships within and among both *Malpolon* and *Rhagerhis* were supported with both phylogenetic algorithms supporting the sister relationship between both species of *Malpolon*. The sub-specific status of *Ma. i. insignitus* and *Ma. i. fuscus* is, however, questionable given the recovery of several *Ma. i. fuscus* samples within *Ma. i. insignitus*, rendering *Ma. i. fuscus* paraphyletic.

Table 2.3: Sequence divergences (uncorrected pairwise distance values) separating the genera of Psammophiidae using cytochrome b (cytb) and NADH dehydrogenase subunit 4 (ND4) (*Dataset 2.4*). Numbers in the diagonal (in bold) denote intrageneric divergences, numbers below the diagonal denote intergeneric divergences and numbers above the diagonal denote the standard error of the intergeneric divergences. Not Available: NA.

	cytb								
		1	2	3	4	5	6	7	8
1	*Dipsina*	**5.95**	1.26	1.25	1.32	1.11	1.25	1.40	1.25
2	*Hemirhagerrhis*	16.84	**9.92**	1.19	1.09	1.05	1.12	1.23	1.28
3	*Malpolon*	16.87	15.91	**9.89**	1.31	1.12	1.17	1.26	1.23
4	*Mimophis*	16.42	14.24	16.38	**3.59**	1.11	1.21	1.44	1.36
5	*Psammophis*	16.73	17.22	16.59	16.92	**12.72**	1.15	1.17	1.10
6	*Psammophylax*	16.45	14.96	16.10	15.24	17.70	**8.60**	1.27	1.31
7	*Rhagerhis*	16.04	14.95	13.25	15.33	15.86	15.33	**NA**	1.38
8	*Rhamphiophis*	16.51	17.00	16.14	17.43	17.44	17.60	15.73	**7.90**
	ND4								
1	*Dipsina*	**5.62**	1.14	1.08	1.26	1.08	1.10	1.32	1.36
2	*Hemirhagerrhis*	17.03	**9.77**	1.10	1.17	1.03	1.02	1.24	1.25
3	*Malpolon*	15.16	16.00	**10.15**	1.20	1.07	1.08	1.20	1.19
4	*Mimophis*	16.71	16.03	16.61	**4.15**	1.11	1.15	1.40	1.35
5	*Psammophis*	17.23	17.17	16.73	17.17	**13.23**	1.04	1.11	1.09
6	*Psammophylax*	16.16	15.33	15.19	15.99	17.49	**8.96**	1.27	1.23
7	*Rhagerhis*	17.16	16.19	14.02	16.63	16.51	15.92	**NA**	1.27
8	*Rhamphiophis*	17.98	17.79	14.76	18.14	16.83	17.01	13.83	**5.27**

There are strong phylogenetic relationships within *Dipsina* with the newly sequenced samples highlighting structure within the genus. Although CKD26 and KF330 form a supported relationship, indicating a potential South African clade, the Namaqualand sample (TM 84514) forms a sister relationship with a sample from central Namibia (WB2), indicating gene flow, either recently or presently, between these two populations. *Hemirhagerrhis* formed a monophyletic taxon with strong support for all the species within the genus. Barring this, the intrageneric relationships remain relatively unresolved irrespective of the larger taxon-sampling afforded to this study. Whilst both molecular algorithms supported the sister relationship between *H. viperina* and *H. hildebrandtii* + *H. nototaenia* + *H. kelleri,* only BI supported the sister relationship between *H. hildebrandtii* and *H. nototaenia* + *H. kelleri*. Novel sampling from Angola resulted in increased structuring within *H. viperina*, with a supported relationship between itself and west African samples. Although not supported by either BI or ML, *H. kelleri* was recovered as its closest relative. *Hemirhagerrhis nototaenia* was sequenced and phylogenetically placed for the first time. The two samples of this species are relatively genetically disparate, with long branch-lengths between them, similar to and often exceeding species level splits within other genera (such as *Psammophylax*).

Both ML and BI inference supported the sister relationship between *Hemirhagerrhis* and *Mimophis* with only BI recognising *M. occultus* and *M*. *mahafalensis* as sister taxa. Maximum Likelihood supported a sister relationship between an *M. occultus* sample (23) and the rest of the genus. The intra- and intergeneric structuring was shallow throughout the genus. *Psammophylax* was recovered as sister to *Mimophis* + *Hemirhagerrhis*. *Psammophylax a. acutus* was recovered as sister to the rest of Psammophylax, with long branches separating it from the rest of the genus. *Psammophylax multisquamis* was also recovered as polyphyletic, with Tanzanian *Ps. multisquamis* being recovered as sister to all *Psammophylax* (excluding *Ps. a. acutus*). These results coupled with substantial structuring throughout the rest of the genus indicates potential cryptic speciation and unappreciated taxonomical diversity within the genus. The taxonomy of *Psammophylax* will not be discussed here in further detail, as the genus is the focus of detailed systematic analysis in Chapters Three and Four.

The final monophyletic group comprises the genus *Psammophis,* which is divided into eight main clades. Within Clade 1*,* the Asiatic species (*P. condanarus* and *P. lineolatus,* assignable to *'Taphrometopon'*) show a strong sister relationship with long branch lengths separating them. Whilst both molecular algorithms show differential support for the distinctiveness of *P. crucifer*, relative to the rest of the clade, relationships within *P. crucifer* were well-supported, but with shallow structuring across the range of the species.

Within Clade 2, *P. trigrammus* was recovered as sister to the rest of the clade with novel sampling within the species producing shallow structuring. *Psammophis ansorgii* + *Psammophis jallae* formed an unsupported clade sister to *P. notostictus* + *P. leightoni* + *P. namibensis* + *P. trinasalis*. The relationship between *P. jallae* + *P. ansorgii* and the rest of Clade 2 was only supported by BI. *Psammophis notostictus* was characterised by the presence of a potential cryptic species from Angola, with strong support and long branch lengths separating ANG0257 from the rest of *P. notostictus*. The rest of *P. notostictus* was characterised by relatively shallow structuring. Within the *'leightoni* complex', Namibian *P. namibensis* was retrieved as sister to *P. trinasalis* + *P. leightoni* + South African *P. namibensis*, rendering *P. namibensis* polyphyletic. Although not supported by either BI or ML, *P. trinasalis* was retrieved as sister to South African *P. namibensis* + *P. leightoni*, with *P. leightoni* forming a clade lumped within South African *P. namibensis*.

Clade 3 which comprised of only *P. angolensis,* was well-supported with strong sub-structuring and shallow divergences separating distantly distributed samples. Clade 4 + 5 + 6 + 7 + 8 were retrieved as sister to Clade 3. Bayesian Inference recovered *P. p. trivirigatus* as sister to *P. elegans*, with shallow divergences being observed in both species. Although

unsupported by either BI or ML, *P. praeornatus* (originally *Dromophis*) was recovered as sister to *P. p. trivirigatus* + *P. elegans*, once again with shallow divergences. *Psammophis schokari* + *P. aegyptius* were recovered sister to the rest of Clade 4, with BI + ML retrieving the northern *Psammophis* as sister species. Within Clade 4, *P. schokari* was the most structured species, whilst *P. aegyptius* displayed comparably shallow structuring, akin to that of the rest of the clade, irrespective of its sister relationship with *P. schokari*. Clade 5, which consists of *P. biseriatus*, *P. tanganicus* and one unidentified sample (TP28431) from Somalia, was retrieved as sister to Clade 6 + 7 + 8 by BI. Within Clade 5, strong support and short branch lengths characterized the clade. The Somalian sample, retrieved as sister to *P. tanganicus* may thus represent unappreciated species diversity, given the relatively shallow divergences observed with the rest of *P. tanganicus*.

Clade 6 consisted of *P. lineatus* (originally *Dromophis*) and the newly sequenced *P. zambiensis*. Whilst *P. zambiensis* lacked structure, *P. lineatus* was characterized by the presence of two clearly defined, and well-supported clades. Clade 7 + 8 were retrieved as sister to Clade 6. Within Clade 7, the placement of *P. leopardinus*, sister to the rest of the clade, was supported by both BI and ML. *Psammophis* cf*. occidentalis* was recovered as sister to *P. brevirostris*, with relatively shallow structuring within both species. Within Clade 7, *P. phillipsi* was recovered as sister to *P. mossambicus* and two supported clades were identified within *P. phillipsi*, with the Togoan individuals forming a clade sister to the rest of the species. The sister relationship between *P.* cf. *occidentalis* + *P. brevirostris* and *P. phillipsi* + *P. mossambicus* was only supported by BI. *Psammophis mossambicus* represents the most sampled species in this phylogeny with over 31 samples from throughout the range of the species. Whilst the species exhibits supported sub-structuring, many of the divergences are shallow with short distances separating distantly distributed samples.

Clade 8 bears the least resolution of all the clades investigated in this phylogeny. Within Clade 8, there are three major subclades (Clade 8A, 8B, 8C). Clade 8A was made up of *P. sibilans* + *P. sudanensis.* Samples identified as *P. sudanensis* were recovered within the within the *P. sibilans* clade*,* with a clade made up of only Ethiopian *P. sibilans* being recovered sister to *P. sudanensis* and the rest of the *P. sibilans* samples (MBUR08588, BEV T.4799, AUZC R.143973, AUZC R.143972). Clade 8A was recovered as sister to Clade 8B + 8C with support from both BI and ML. Clade 8B was made up of *P.* cf*. sudanensis*, *P. subtaeniatus* + *P. orientalis,* with *P. subtaeniatus* forming a supported relationship with *P.* cf*. sudanensis* + *P. orientalis.* Whilst neither BI or ML supported the sister relationship between *P.* cf*. sudanensis* and *P. orientalis,* all three species were supported with the novel sampling afforded to *P. subtaenatius* revealing a South African clade, sister to the rest of *P. subtaeniatus*. Within *P.* cf. *sudanensis*, two supported clades were also identified, but these clades were not based

on geographic relatedness, indicating an abundance of gene flow in the area, or a recent divergence. Within *P. orientalis,* structuring was relatively shallow, except for a sample from Udzungwa National Park, that formed a sister relationship with the rest of *P. orientalis*. Clade 8C was comprised of *P. rukwae* + *P. afroccidentalis*, and was recovered as sister to Clade 8B (unsupported). The sister relationship between *P. rukwae* and *P. afroccidentalis* was recovered by BI and ML, with both algorithms also recognising two supported clades within *P. afroccidentalis*. The clades identified within *P. afroccidentalis* were attributable to geography with one clade residing in West Africa and the other in central/western Africa. *Psammophis rukwae* was characterised by relatively shallow structuring, with exception to a single sample (BK10620) from Kenya that formed a branch sister to the rest of the species.

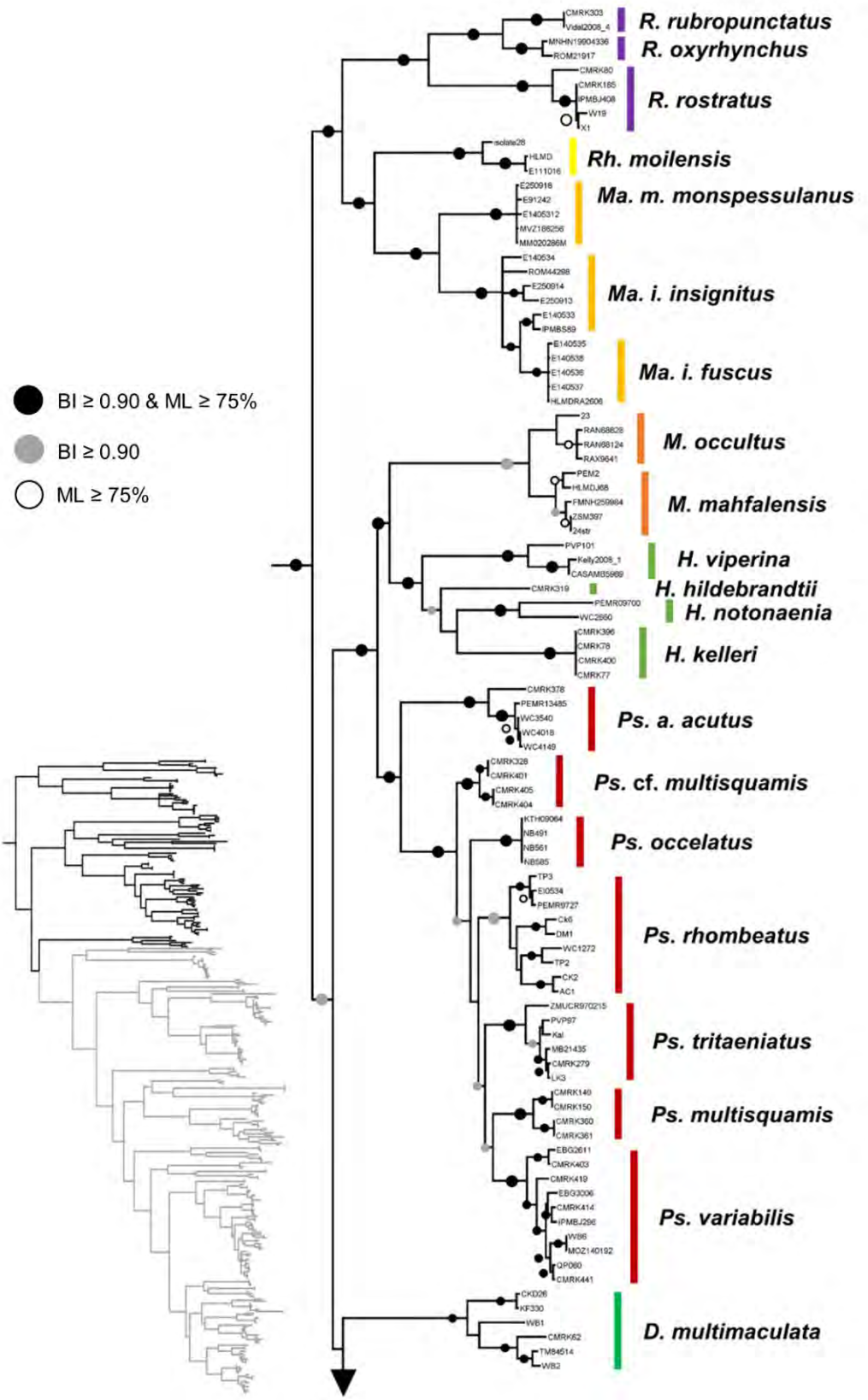

Figure 2.3**:** Bayesian Inference tree (BI) derived from *Dataset 2.1* with Maximum Likelihood (ML) support overlaid, showing the relationships of the genera and species of Psammophiidae. Size of circles at nodes bear no meaning. Colours indicate separate genera and match that of Fig. 2.2. Numbers next to the *Psammophis* genus indicate main clades. *R—Rhamphiophis, Rh—Rhagerhis, Ma—Malpolon, M—Mimophis, H—hemirhagerrhis, Ps—Psammophylax, D—Dipsina, P—Psammophis.*

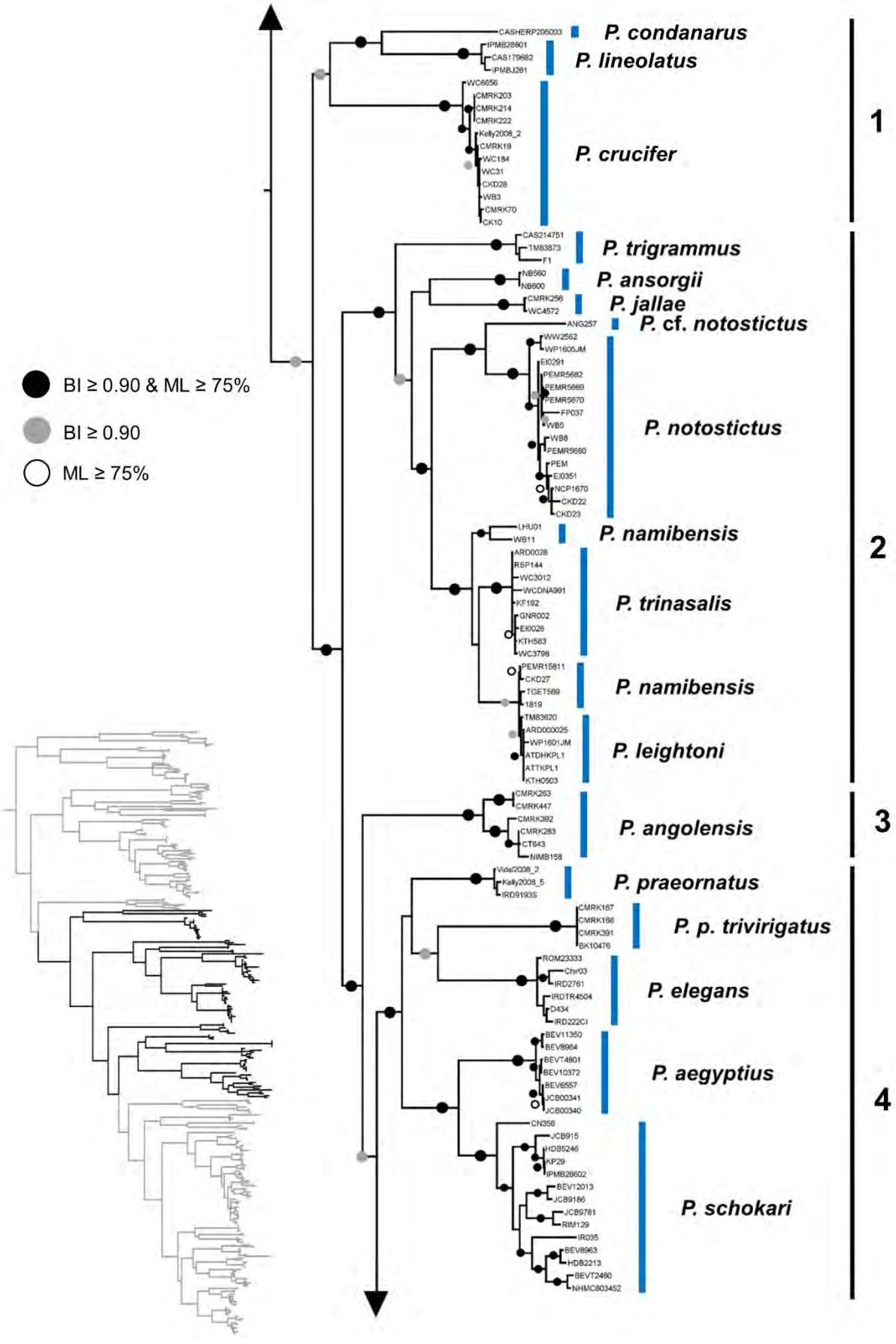

Figure 2.3: Continued.

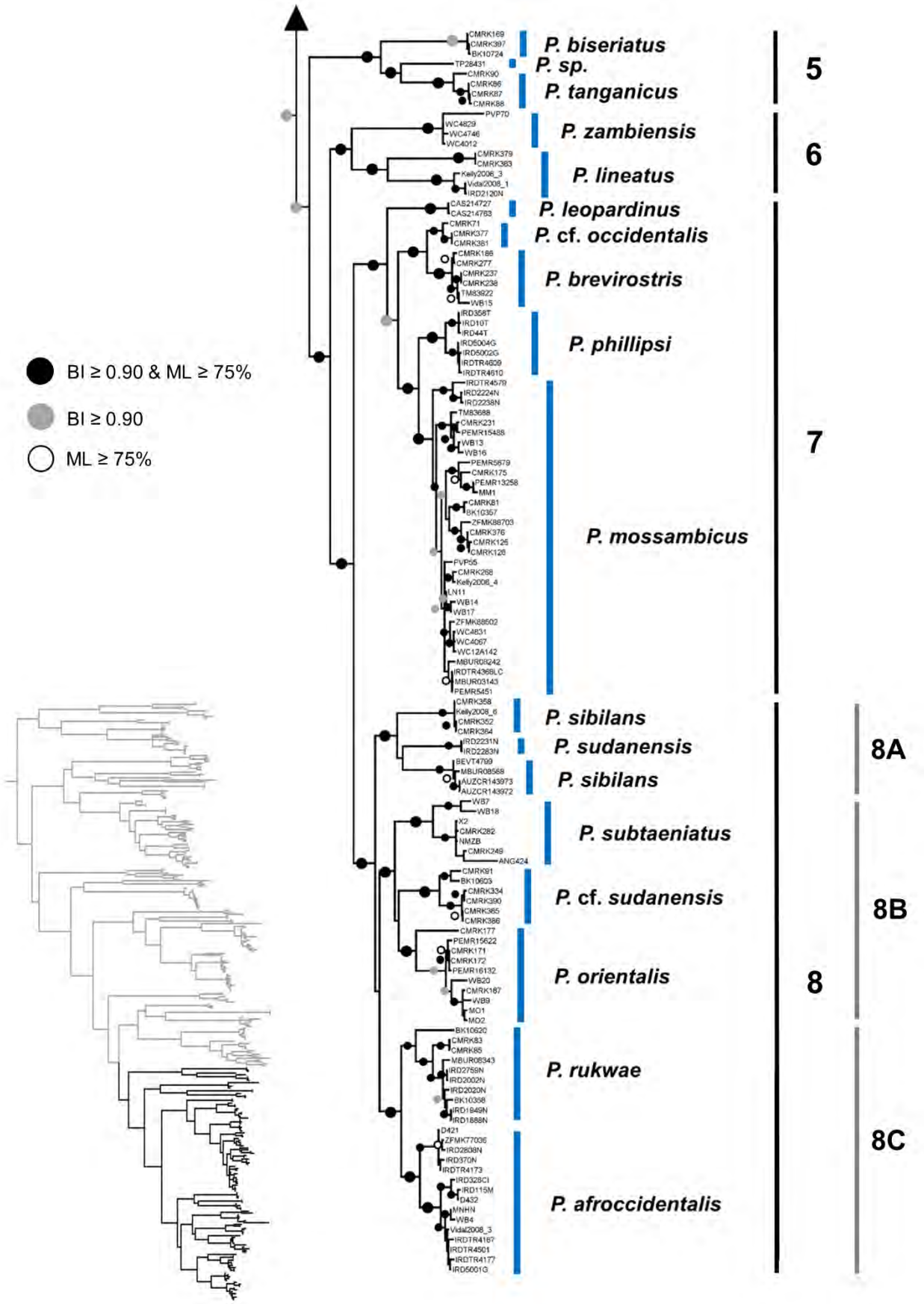

Figure 2.3: Continued.

Time-calibrated Phylogeny

The time-calibrated (BEAST BI) tree (Fig. 2.4) from *Dataset 2.2* incorporated a representative sampling from every available species of Psammophiidae, and yielded strong support, akin to that of phylogenetic tree (BI and ML) employed in (Fig. 2.3). The intergeneric relationships were similar but several of the intrageneric relationships differed between Fig. 2.3 and Fig. 2.4. For the interest of brevity, only the supported differences between the two phylogenies will be listed hereafter.

In the time-calibrated BEAST BI tree, *R. rubropunctatus* was recovered as sister to *R. oxyrhynchus* + *R. rostratus*. Within *Hemirhagerrhis*, *H. kelleri* was retrieved as sister to *H. nototaenia* + *H. hildebrandtii.* Within *Mimophis*, a single sample (23) of the newly described *M. occultus* was recovered as sister to all other members of the genus, identical to the findings of the ML phylogeny (Fig. 2.3). Within *Psammophis*, *P. trinasalis* was recovered as sister to *P. namibensis* + *P. leightoni* and Namibian *P. namibensis* was recovered as sister to South African *P. namibensis* + *P. leightoni*. Within *Psammophis*, *P. sudanensis* was recovered as sister to *P. sibilans* and *P.* cf. *sudanensis* was recovered as sister to *P. orientalis* + *P. subtaeniatus*.

Psammophiidae was recovered as separating from the superfamily Elapoidea in the late Oligocene/early Miocene, ~24.87 MYA (23.10–26.74 95% Highest Posterior Density [HPD]). This was followed by the divergence of the family in the early Miocene with the splitting of *Rhamphiophis* + *Rhagerhis* + *Malpolon* from the rest of Psammophiidae, ~17.97 MYA (16.16–19.97 HPD). In the early to mid-Miocene, ~17 MYA (15.34–19.13 HPD), *Dipsina* + *Hemirhagerrhis* + *Mimophis* + *Psammophyla*x split from *Psammophis*.

The finer intra- and intergeneric temporal structuring can be found in Table 2.4. All currently described genera originated during the Miocene and apart from the species of *Psammophylax* (barring *Ps. acutus*), *Mimophis*, *P. tanganicus*, the unidentified sample from Somalia (TP28431), the '*leightoni* complex', and the '[3]*sibilans* complex', all species within Psammophiidae also arose during the Miocene (Table 2.4). The only species-level splits retrieved during the Pleistocene occurred between South African *P. namibensis* and *P. leightoni*, *P. brevirostris* and *P.* cf. *occidentalis* and lastly, *P. mossambicus* and *P. phillipsi* (Table 2.4).

[3] The '*sibilans* complex' consists of: *P. leopardinus, P.* cf. *occidentalis, P. brevirostris, P. phillipsi, P. mossambicus, P. mossambicus, P. sibilans, P. sudanensis, P. subtaeniatus, P.* cf. *sudanensis, P. orientalis, P. rukwae* and *P. afroccidentalis.*

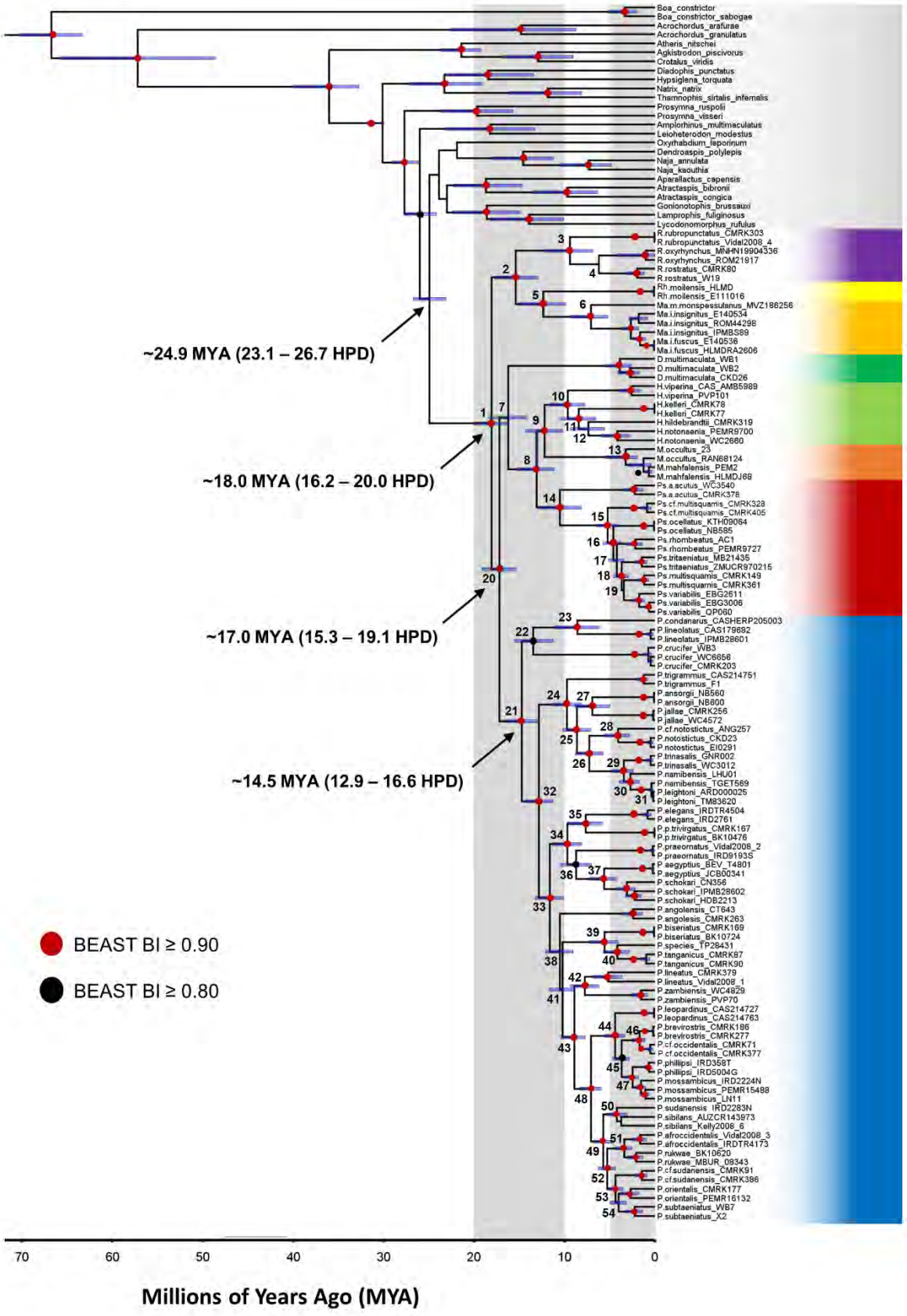

Figure 2.4: Time-calibrated BEAST BI phylogeny of Psammophiidae derived from *Dataset 2.2*. Blue horizontal bars reflect the 95% Highest Posterior Distributions of node ages (HPD). Colours on the right match the generic colours in Figs 2.2 and 2.3. Node circle sizes and grey bars bear no meaning.

Table 2.4**:** Mean node age and 95% highest posterior densities (HPD) of node ages for major divergences within Psammophiidae. Supported nodes: BEAST BI ≥ 90%. The node labels correspond to those in Fig. 2.4. Shade of colour corresponds with geological time-period: light–Miocene, medium–Pliocene, dark–Pleistocene.

Node	Event	Support (BEAST BI)	95% HPD of node ages (MYA)	Mean age (MYA)
1	Split between *Rhamphiophis/Malpolon/Rhagerhis* and the rest of *Psammophiidae*	Yes	16.2–20.0	18.0
2	Split between *Rhamphiophis* and *Malpolon/Rhagerhis*	Yes	13.0–17.7	15.3
3	Split between *R. rubropunctatus* and *R. oxyrhynchus/R. rostratus*	Yes	6.8–12.2	9.3
4	Split between *R. oxyrhynchus* and *R. rostratus*	No	1.8–10.1	6.0
5	Split between *Rhagerhis* and *Malpolon*	Yes	9.8–15.0	12.3
6	Split between *Ma. monspessulanus* and *Ma. insignitus*	Yes	5.1–9.3	7.1
7	Split between *Dipsina* and *Hemirhagerrhis/Mimophis/Psammophylax*	No	14.2–18.4	16.1
8	Split between *Hemirhagerrhis/Mimophis* and *Psammophylax*	Yes	11.1–15.3	12.9
9	Split between *Hemirhagerrhis* and *Mimophis*	Yes	10.2–14.3	12.1
10	Split between *H. viperina* and *H. kelleri/H. hildebrandtii/H. nototaenia*	Yes	7.7–11.7	9.5
11	Split between *H. kelleri* and *H. hildebrandtii/H. nototaenia*	Yes	6.5–10.4	8.3
12	Split between *H. hildebrandtii* and *H. nototaenia*	No	5.5–9.3	7.3
13	Split between *M. occultus* and *M. mahafalensis*	Yes	1.9–5.5	3.4
14	Split between *Ps. acutus* and *the rest of Psammophylax*	Yes	8.1–12.9	10.4
15	Split between *Ps. cf. multisquamis* and *Ps. ocellatus/Ps. rhombeatus/Ps. tritaeniatus/Ps. multisquamis/Ps. variabilis*	Yes	4.1–6.5	5.2
16	Split between *Ps. ocellatus* and *Ps. rhombeatus/Ps. Tritaeniatus/Ps. multisquamis/Ps. variabilis*	Yes	3.6–5.7	4.5
17	Split between *Ps. Rrhombeatus* and *Ps. tritaeniatus/Ps. multisquamis/Ps. variabilis*	No	3.4–5.1	4.2

18	Split between *Ps. tritaeniatus* and *Ps. multisquamis/Ps. variabilis*	Yes	2.9–4.6	3.6
19	Split between *Ps. multisquamis* and *Ps. variabilis*	No	2.7–4.3	3.4
20	Split between *Dipsina/Hemirhagerrhis/Mimophis/Psammophylax* and *Psammophis*	Yes	15.3–19.1	17.0
21	Split between P. *condanarus/P. lineolatus* and *P. crucifer* from the rest of *Psammophis*	Yes	12.9–16.6	14.5
22	Split between P. *condanarus/P. lineolatus* and *P. crucifer*	No	11.2–15.5	13.3
23	Split between P. *condanarus* and *P. lineolatus*	Yes	6.1–11.1	8.5
24	Split between *P. trigrammus* and *P. ansorgii/P. jallae/P. notostictus/P. trinasalis/P. namibensis/P. leightoni*	Yes	8.1–11.4	9.6
25	Split between *P. ansorgii/P. jallae* and *P. notostictus/P. trinasalis/P. namibensis/P. leightoni*	Yes	7.1–10.2	8.5
26	Split between *P. notostictus* and *P. trinasalis/P. namibensis/P. leightoni*	Yes	5.7–8.8	7.1
27	Split between *P. ansorgii* and *P. jallae*	Yes	5.0–8.9	6.8
28	Split between *P. cf. notostictus* and *P. notostictus*	Yes	2.8–5.6	4.1
29	Split between *P. trinasalis* and *P. namibensis/P. leightoni*	Yes	2.4–4.7	3.4
30	Split between Namibian *P. namibensis* and *P. namibensis/P. leightoni*	Yes	1.7–3.9	2.7
31	Split between South African *P. namibensis* and *P. leightoni*	Yes	0.2–0.6	0.4
32	Split between *P. trigrammus/P. ansorgii/P. jallae/P. notostictus/P. trinasalis/P. namibensis/P. leightoni* and *relatives*	Yes	11.3–14.3	12.7
33	Split between *P. elegans/P. p. trivirigatus/P. praeornatus/P. aegyptius/P. schokari* and *relatives*	Yes	10.1–13.2	11.5
34	Split between *P. elegans/P. p. trivirigatus* and *P. praeornatus/P. aegyptius/P. schokari*	Yes	8.0–11.3	9.6
35	Split between *P. elegans* and *P. p. trivirigatus*	Yes	5.8–9.7	7.6

36	Split between *P. praeornatus* and *P. aegyptius/P. schokari*	No	7.0–10.4	8.6
37	Split between *P. aegyptius* and *P. schokari*	Yes	4.2–7.2	5.6
38	Split between *P. angolensis* and *relatives*	No	9.0–12.1	10.4
39	Split between *P. biseriatus* and *P. species/P. tanganicus*	Yes	4.0–7.2	5.5
40	Split between *P. species* and *P. tanganicus*	Yes	2.8–5.7	4.1
41	Split between *P. biseriatus/P. species/P. tanganicus* and *relatives*	No	8.8–11.7	10.1
42	Split between *P. lineatus* and *P. zambiensis*	Yes	6.2–9.3	7.7
43	Split between *P. lineatus/P. zambiensis* and *relatives*	Yes	7.7–10.3	8.8
44	Split between *P. leopardinus* and *P. brevirostris/P. cf. occidentalis/P. phillipsi/P. mossambicus*	Yes	3.3–5.6	4.4
45	Split between *P. brevirostris/P.* cf. *occidentalis* and *P. phillipsi/P. mossambicus*	No	2.8–4.6	3.6
46	Split between *P. brevirostris* and *P. cf. occidentalis*	Yes	1.1–2.5	1.7
47	Split between *P. phillipsi* and *P. mossambicus*	Yes	1.8–3.3	2.5
48	Split between *P. leopardinus/P. brevirostris/P. cf. occidentalis/P. phillipsi/P. mossambicus* and *relatives*	Yes	5.9–8.3	7.0
49	Split between *P. sudanensis/P. sibilans* and *P. afroccidentalis/P. rukwae/P. cf. sudanensis/P. orientalis/P. subtaeniatus*	Yes	4.7–6.8	5.6
50	Split between *P. sudanensis* and *P. sibilans*	Yes	3.0–5.4	4.1
51	Split between *P. afroccidentalis* and *P. rukwae*	Yes	2.5–4.4	3.3
52	Split between *P. afroccidentalis/P. rukwae* and *P. cf. sudanensis/P. orientalis/P. subtaeniatus*	Yes	4.4–6.3	5.2
53	Split between *P. cf. sudanensis* and *P. orientalis/P. subtaeniatus*	Yes	3.5–5.3	4.3
54	Split between *P. orientalis* and *P. subtaeniatus*	No	3.1–5.0	4.0

Species Delimitation in Psammophis

The ND4 BEAST phylogeny (Fig. 2.5) created using *Dataset 2.3* utilised 188 samples from every species of *Psammophis* available and yielded strong support akin to that of Fig. 2.3 and Fig. 2.4. Like the BEAST BI tree (Fig. 2.4), *P. trinasalis* was recovered as sister to the '*leightoni* complex'. *Psammophis angolensis* and *P. praeornatus* remain problematic, with their placements being unsupported. Lastly, the ND4 BEAST tree retrieved similar intrageneric relationships and stronger nodal support for individuals belonging to the '*sibilans* complex'.

Species delimitation employed across *Psammophis* produced contrasting results depending on the method utilised. The bGMYC outputs were interpreted using two threshold values (bGMYC 1: $p \geq 0.95$; bGMYC 2: $p \geq 0.50$). ABGD yielded the most conservative results with thresholds 1 and 2 yielding 44 and 45 species, respectively. bGMYC identified similar numbers of putative taxa with thresholds bGMYC 1 and bGMYC 2 of the analysis yielding 50 and 58 species, respectively. The most sensitive methods employed were PTP and bPTP, recognising 75 and 76 species, respectively. The high number of putative taxa identified by the last two methods are likely representative of intraspecies diversity across populations. This casts doubt on the efficacy of Poisson Tree Processes (and its Bayesian implementation).

Inferences about cryptic taxa are problematic amid contrasting results. For this reason, putative taxa identified by every species delimitation method will be considered worthy of discussion. Across all analyses, *P.* cf. *sudanensis, P.* cf. *notostictus* (ANG257) and the unidentified Somalian sample (TP28431) were recognised as potential species. Other novel taxa include: four *P. schokari*, one *P. lineatus*, one *P. sibilans*, one *P. orientalis*, one *P. angolensis,* one *P. subtaeniatus* and one *P. rukwae*. All except the bGMYC 1, recognised an additional putative species within *P. zambiensis*. Whilst all the analyses employed ratified most of the existing taxonomy, no single delimitation method ratified the existence of South African *P. namibensis*, with every method lumping it with *P. leightoni*. Additionally, neither threshold of the ABGD analysis separated *P. brevirostris* and *P.* cf. *occidentalis.*

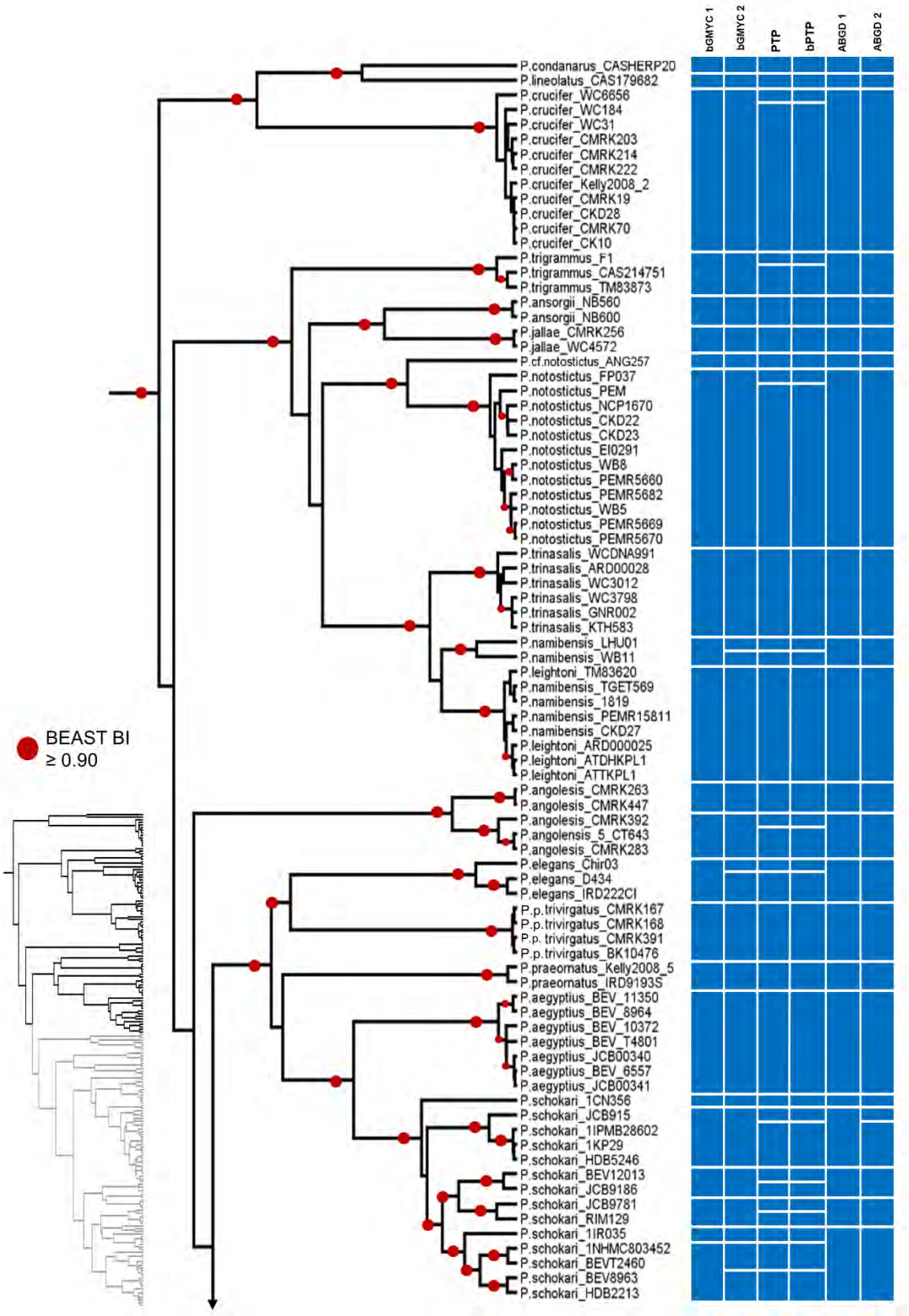

Figure 2.5**:** Bayesian Inference Beast BI phylogeny of *Psammophis* derived from *Dataset 2.3*. Vertical bars denote different species delimitation methods and horizontal white bars show the putative species based on the varying analyses. Size of red node circles bear no meaning. bGMYC 1: ≥ 0.95; bGMYC 2: ≥ 0.50; ABGD 1: prior maximal distance = 0.021544; ABGD 2: prior maximal distance = 0.012915.

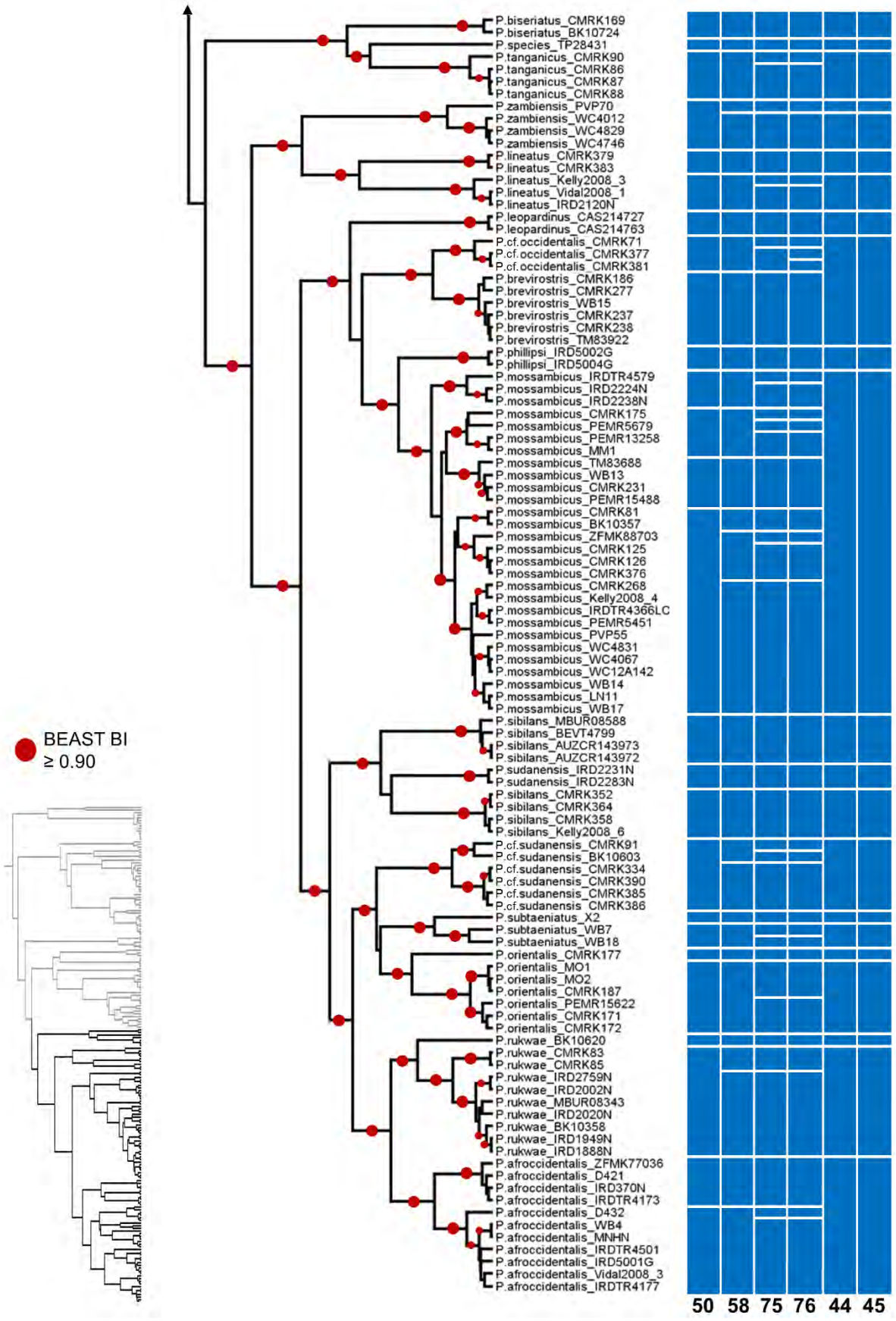

Figure 2.5: Continued.

Geometric Morphometric Analyses

On the dorsal view, the first PC (DC-PC1) axis contrasted head width, parietal scale anterio-posterior length and mid-snout length, accounting for 61.86% of total variation, whereas DC-PC2 contrasted the length of the mid-head region (frontal scale), the length of the parietal scales, and the length and width of the rostral scales, accounting for 15.87% of the variation (Fig. 2.6). DC-PC3 contributed only 6.17% of total variation, and contrasted the width of the parietal scales, the mid-snout region, and the width of the rostral scale (Fig. 2.6).

The first lateral PC axis (LC-PC1) contrasted height of the head, length of the nose and width of the upper labials describing 53.62% of total variation (Fig. 2.7). LC-PC2 described 15.76% of variation, and contrasted head length, nose length and upper labial width (behind the eye) (Fig. 2.7). LC-PC3 described only 7.32% of the variation and contrasted the length of the posterior part of the upper lip (back upper labials) (Fig. 2.7).

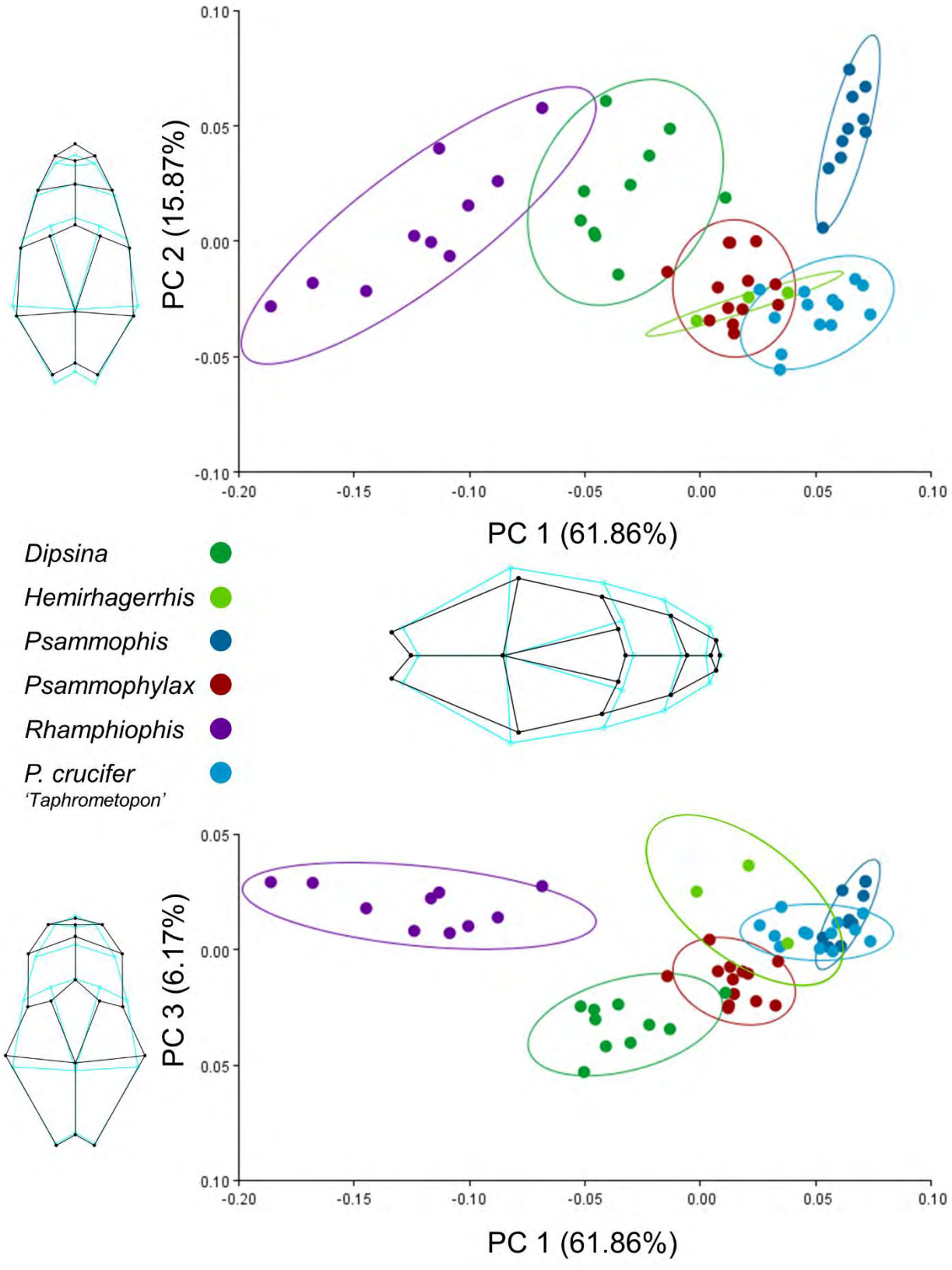

Figure 2.6: Geometric morphometric analyses of the dorsal view of the heads of the six genera of Psammophiidae (see inset key for colours). Wireframe diagrams to the left and below the scatterplots of the principal component scores for the first three PC axes, represent the shape changes of each axis. The wireframes showcase the warping of the positive sides of the axes (black lines) from the mean configuration (cyan lines).

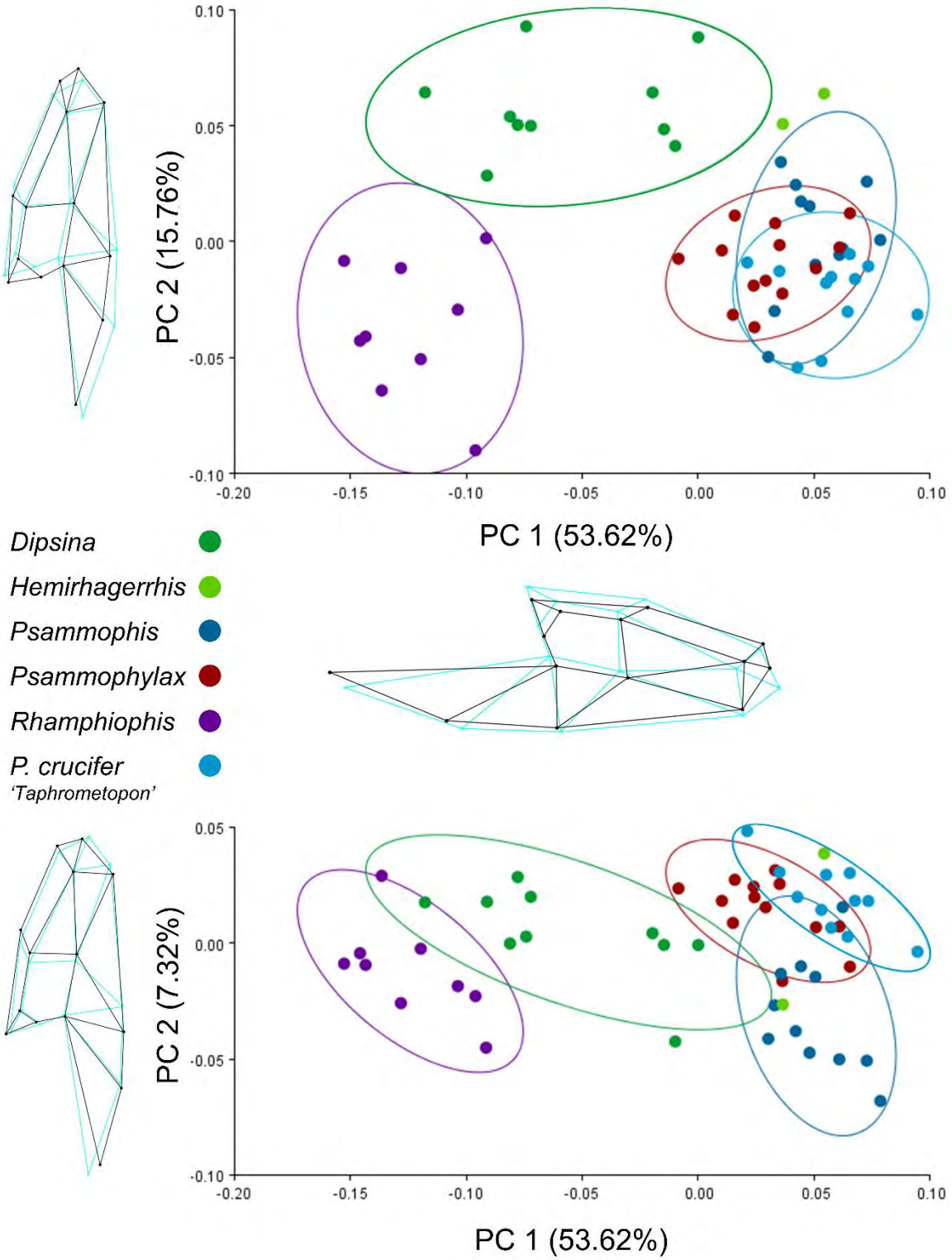

Figure 2.7: Geometric morphometric analyses of the lateral view of the heads of the six genera of Psammophiidae (see inset key for colours). Wireframe diagrams to the left and below the scatterplots of the principal component scores for the first three PC axes, represent the shape changes of each axis. The wireframes showcase the warping of the positive sides of the axes (black lines) from the mean configuration (cyan lines).

Discussion

This study has incorporated representative sampling from past studies and, with the addition of newly sequenced samples (this study), has produced a well-supported phylogenetic reconstruction of the family. It has built on the work of Kelly (2005) using a robust and comprehensive sampling regime from recently published species- and genus-specific molecular studies (Branch *et al.*, 2019; Gonçalves *et al.*, 2018; Ruane *et al.*, 2018; Taft, 2018; Trape *et al.*, 2019). Geometric morphometrics provided evolutionary context for several of the genus level molecular relationships observed in both this study and past studies.

Intergeneric Structuring

Whilst both BI and ML (Figs 2.2 and 2.3) produced similar topologies, some of the intergeneric relationships among Psammophiidae differed from those of past papers. Other than Figueroa *et al.* (2016), all past studies (Kelly *et al.*, 2008; Pyron *et al.*, 2013; Vidal *et al.*, 2007; Zaher *et al.*, 2019) retrieved *Rhamphiophis* as a monophyletic taxon, sister to *Malpolon* + *Rhagerhis*, with support. Whilst Figueroa *et al.* (2016) retrieved *R. oxyrhynchus* as sister to *Psammodynastes*, this is likely an error as the cytb sequence associated with ROM 21917 was closely related to an unnamed *Psammodynastes* sample from Genbank, whilst the ND4 and c-mos sequences associated with the same sample were similar to *Rhamphiophis* and other members of the family.

Rhagerhis moilensis has had a chequered taxonomic past, with the generic placement of the species shifting several times in the last few years (Chippaux & Jackson, 2019). Whilst Figueroa *et al.* (2016) retrieved *Ma. insignitus* as sister to *Ma. monspessulanus* + *R. moilensis*, phylogenetic structuring in this study supported the validity of *Rhagerhis* as a monotypic genus. Additionally, the split of *Rhagerhis* from *Malpolon* was estimated at ~12.27 MYA, whilst the split between *Mimophis* + *Hemirhagerrhis* and *Psammophylax* and the split of *Mimophis* from *Hemirhagerrhis* was estimated at ~12.90 MYA and ~12.06 MYA, respectively. These findings, coupled with the average intergeneric pairwise distances (cytb: 15.21 ± 0.94% and 15.75 ± 1.30% respectively) separating *Rhagerhis* from its congeners, support the validity of the genus. Based on the findings of this study, and with the support of Carranza *et al.* (2006), it is recommended that *Rhagerhis* be retained as a monotypic genus.

Dipsina was recovered as sister to *Psammophis* in most recent papers (Figueroa *et al.*, 2016; Kelly *et al.*, 2008; Zaher *et al.*, 2019) and in the BI phylogeny (Figs 2.2 and 2.3), whilst in the ML phylogeny (Figs 2.2 and 2.3), the BEAST phylogeny (Fig. 2.4) and Vidal *et al.* (2008), *Dipsina* was recovered as sister to *Mimophis* + *Hemirhagerrhis* + *Psammophylax*. Pyron *et al.* (2013) differed from everything else and recovered *Dipsina* as sister to *Mimophis*.

Between this study and all the aforementioned papers, no analysis retrieved a supported relationship between *Dipsina* and its congeners, rendering its placement within the family unresolved, irrespective of the larger dataset afforded to this species in the current study. From a morphological perspective, whilst the validity of the genus is unquestionable, its past placement within *Rhamphiophis* coupled with the morphometric results of this study that showed a morphological similarity between *Rhamphiophis* and *Dipsina,* based on head girth and length, provides evidence for convergence of form within the family. The presence of beaked snakes (ie. *Rhamphiophis*, *Dipsina, Ps. acutus*) in independent clades provides interesting grounds for further study to determine whether shared ancestry, or convergence of form, are responsible for the enlarged rostral scale ('beak') found within several different genera of the family.

Barring Pyron *et al.* (2013), recent studies (Figueroa *et al.*, 2016; Kelly *et al.*, 2008; Zaher *et al.*, 2019) retrieved *Mimophis* as sister to *Hemirhagerrhis*. Whilst these studies lacked support, both the BI + ML (Fig. 2.2) and BEAST (Fig. 2.4) phylogenies implemented in this study retrieved support for the sister relationship, building on the partial support of Kelly *et al.* (2008). Whilst genetically distinctive, *Hemirhagerrhis* remains morphologically conservative. In the morphometric component of this study, *Hemirhagerrhis* was the least morphologically distinguishable (Figs 2.6 and 2.7) of all the genera in sub-Saharan Africa. This is in stark contrast to the semi-fossorial genera (*Rhamphiophis* and *Dipsina*) that could be distinguished easily from the rest of the group both visually and statistically (Table S2.3). These results, coupled with the overlapping morphological traits (Broadley, 1997) within the genus, can be explained partly by the findings of Harrington *et al.* (2018) that arboreal snakes have a more constrained morphological evolution, with a tendency towards narrow bodies, and arboreal-orientated camouflage ('bark matching'). Given that both *Rhamphiophis* and *Dipsina* exhibit wide, pointed heads, it makes sense that *Hemirhagerrhis* would exhibit slender, rounded heads, similar to the rest of the family (more conservative morphology), to enable them to navigate their heterogeneous surrounds.

Unlike the sister relationship between *Mimophis* and *Hemirhagerrhis*, the sister relationship between *Psammophylax* and *Mimophis* + *Hemirhagerrhis,* and the placement of *Rhamphiophis acutus* within the synonymy of *Psammophylax* was supported by both this study and past studies (Figueroa *et al.*, 2016; Kelly *et al.*, 2008; Zaher *et al.*, 2019). Whilst the placement of *P. crucifer* (discussed later) varies between this study and past research (Kelly *et al.*, 2008; Zaher *et al.*, 2019), the recovery of *Psammophis* as sister to all other members of the genus was supported by all past research (Figueroa *et al.*, 2016; Kelly *et al.*, 2008; Pyron *et al.*, 2013; Vidal *et al.*, 2008; Zaher *et al.*, 2019).

Whilst BI (Figs. 2.2 and 2.3) supported the sister relationship between *P. crucifer* and *P. condanarus* + *P. lineolatus* in this study, the BEAST time-calibrated phylogeny (Fig. 2.4) did not find support. Several past studies (Figueroa *et al.*, 2016; Pyron *et al.*, 2013; Vidal *et al.*, 2007) also retrieved similar topological structuring to both BI and BEAST algorithms, but with no support. Like the ML phylogeny (Figs. 2.2 and 2.3) from this study, Kelly *et al.* (2008) and Zaher *et al.* (2019) retrieved *P. crucifer* as sister to the Asiatic (*P. lineolatus* and *P. condanarus*) + African *Psammophis*, with strong support across both studies, using multiple molecular algorithms. These results coupled with the geographical isolation of *P. crucifer* (Southern African endemic) from all other members of the genus (Asian endemics), supports the topological structuring observed in these papers and in the ML phylogeny (Figs. 2.2 and 2.3) (Broadley, 2002; Wallach *et al.*, 2014). *Psammophis leithi, P. longifrons* and *P. indochinensis* are yet to be sequenced and pending their inclusion in a robust phylogenetic tree, the validity of *Taphrometopon* remains uncertain. The inclusion of the full complement of Asiatic psammophiid snakes may also clarify the relationship between *P. crucifer* and the rest of the genus. Whilst future research may recover *Taphrometopon* as valid incomplete taxon sampling coupled with a lack of substantial support for the genus necessitates the continued use of *Psammophis* for both African and Asian whip snakes, and the synonymisation of *Taphrometopon* with *Psammophis*, pending more robust support.

Intergeneric pairwise distances were also consistent across the family with cytb and ND4 retrieving similar average pairwise differences, with very little difference between the lowest and highest average pairwise distances between genera, across both genes (Table 2.3). These findings support the taxonomic status of all the currently described genera, even though the placement of certain species (i.e., *P. crucifer and Ps. a. acutus*) within their respective genera remains unresolved.

Origin of the Family Psammophiidae

The various analyses employed in this study retrieved Psammophiidae as monophyletic, supporting all previous molecular-orientated studies of the taxon (Figueroa *et al.*, 2016; Kelly *et al.*, 2008; Vidal *et al.*, 2008; Zaher *et al.*, 2019). Time-calibrated phylogenies are highly subjective and vary depending on the calibration points and number of samples. The work of Kelly (2005) retrieved the split of Psammophiidae from the rest of the Elapoidea, during the late Cretaceous (~68 MYA), with the radiation of the family occurring during the mid-Miocene (~48 MYA). These findings were amended in Kelly *et al.* (2009), with the origin and the radiation of the family being retrieved during the mid/late-Eocene (~38 MYA) and the early Miocene (~22 MYA), respectively. The findings of the Kelly *et al.* (2009) have since been corroborated by Zaher *et al.* (2019) and in this study, with similar time-calibrations being

retrieved. In Zaher *et al.* (2019), the origin and radiation of the family were dated during the mid-Oligocene (~30 MYA) and early Miocene (~20 MYA), respectively. In this study, the origin and radiation of the family were retrieved during the late-Oligocene (~25 MYA) and the early/mid-Miocene (~18 MYA), respectively. Whilst the origin of the family remains elusive (mid Eocene–late Oligocene), based on the varying results of Kelly *et al.* (2009), Zaher *et al.* (2019) and this study, the radiation of the group is better understood with only a four million year gap separating the dated nodes of the three studies. Findings of past papers and the results of this study place the radiation of the group between 18 and 22 million years ago. These results coupled with the ancestral state reconstructions from (Kelly, 2005) and subsequent publication (Kelly *et al.*, 2009), indicate that either the southern savannahs or north eastern parts of Africa were the likely theatre of radiation for the family during the early/mid-Miocene.

Intrageneric Structuring

Past studies that incorporated *R. rostratus, R. rubropunctatus and R. oxyrhynchus* lacked intrageneric support whilst results for this study showed support for contrasting topologies. This is likely a product of differential taxon and gene sampling between studies, and within this study, with only two individuals available for both *R. oxyrhynchus* and *R. rubropuncatus*. Irrespective of the newly sequenced *R. rostratus* samples afforded to this study, the Tanzanian clade (CMRK80) remains the most divergent within the range, similar to the findings of Kelly *et al.* (2008). The limited genetic structure, coupled with shallow divergences within this study, irrespective of the wide distributional sampling afforded to this species, indicates gene flow, either presently or recently, between distant populations. Pending the discovery of relict populations of the species, it is unlikely that *R. rostratus* harbours unappreciated species diversity enough to warrant taxonomic re-evaluation.

Except for Figueroa *et al.* (2016), all previous studies retrieved *Malpolon* as a monophyletic taxon, corroborating the phylogenetic findings of this study. Whilst most of the aforementioned snake phylogenetic studies included *Ma. monspessulanus* and *Ma. insignitus,* the only study, besides this study, to include both subspecies of *Ma. insignitus* was Carranza *et al.* (2006). This study found similar phylogenetic structuring within *Malpolon,* retrieving *Ma. monspessulanus* as sister to *Ma. i. insignitus* + *Ma. i. fuscus* (Carranza *et al.*, 2006). The BEAST time-calibrated phylogeny (Fig. 2.4) retrieved the split between the two subspecies during the early Pleistocene, rendering the divergence incredibly young. This coupled with the finding in both this study and Carranza *et al.* (2006) that *Ma. i. fuscus* formed a clade within *Ma. i. insignitus* supports the synonymy of the Grecian endemic with *Ma. insignitus* (Carranza *et al.*, 2006; Uetz *et al.*, 2020; Wallach *et al.*, 2014). Whilst not included in this study, *Ma.*

monspessulanus comprises an enigmatic subspecies termed *M. m. saharatlanticus*. The species' taxonomic rank cannot be investigated because of a lack of genetic material, but according to more recent publications (Geniez *et al.*, 2006; Mangiacotti *et al.*, 2014), Carranza *et al.* (2006) may have sequenced the subspecies unknowingly in their paper. The sample (E14053.2) which originated from Essaouria, SW Morocco (Fig. 1; Carranza *et al.* 2006), may represent the northern limit of the distribution of *M. m. saharatlanticus* and given the sample's distinction from the rest of *Ma. monspessulanus* in Carranza *et al.* (2006), it may warrant future investigation.

Within *Dipsina*, the presence of supported clades, comprised of geographically disparate samples indicates an abundance of gene flow, probably historically, between South African and Namibian populations. Unless samples have been incorrectly geo-located, biogeographical barriers do not appear to influence phylogenetic diversity within the species. Additionally, the low intraspecies divergences (cytb: ~5.95%; ND4: 5.62% intraspecies pairwise distance) between samples in this study indicate a lack of unappreciated diversity within the genus. Unless samples from novel, geographically isolated populations are incorporated into a phylogenetic framework, it is unlikely that *Dipsina* will warrant taxonomic re-evaluation.

Barring Figueroa *et al.* (2016), every past study and the analysis from this study retrieved *H. viperina* as sister to the rest of *Hemirhagerrhis*. Given the absence of *H. nototaenia* from all past phylogenies, *H. hildebrandtii* + *H. kelleri* were recovered as sister taxa, with strong support. The inclusion of *H. nototaenia* in this study has resulted in contrasting topologies between the phylogenetic tree (BI and ML) (Fig. 2.3) and the BEAST BI phylogeny (Fig. 2.4). Whilst the phylogenetic tree (Fig. 2.3) supported the sister relationship between *H. hildebrandtii* and *H. kelleri* + *H. nototaenia*, the BEAST BI phylogeny (Fig. 2.4) supported a sister relationship between *H. kelleri* and *H. nototaenia* + *H. hildebrandtii*. These results confound our ability to resolve the intrageneric structuring within *Hemirhagerrhis* as both provide support for different interspecific relationships. Within *Hemirhagerrhis*, the novel sampling afforded to *H. viperina* and *H. nototaenia*, revealed strong sub-structuring, with the latter species exhibiting relatively long branch lengths between samples. Given the relatively large distribution of *H. nototaenia*, when compared to the rest of the genus, coupled with the arboreal lifestyle of the genus (Branch, 1998; Broadley, 1997), and reliance on wooded environments, it is unsurprising that geography has an effect on phylogenetic structuring. Whether or not this represents intra- or interspecies diversity, is debateable given the poor dataset available for the genus at present. Based on findings of both the morphological and molecular components, it is hypothesised that *Hemirhagerrhis* diversity would be strongly influenced by cryptic speciation and morphological stasis. The genus is thus a priority for

molecular orientated work, especially in the more widespread and potentially allopatric *H. nototaenia*.

Originally identified in Kelly *et al.* (2008), the monotypic *Mimophis* genus from Madagascar was hypothesised to harbour unappreciated species diversity. These findings were corroborated by Ruane *et al.* (2018) with the description of *M. occultus* from northern Madagascar. Findings from the phylogenetic component of this study however retrieved shallow structuring within *Mimophis*, with only the BI phylogeny (Fig. 2.3) retrieving similar topological structuring to Ruane *et al.* (2018). In both the ML (Fig. 2.3) and BEAST (Fig. 2.4) phylogenies a single sample of *M. occultus* (23) was recovered as sister to the rest of the genus, which may be explained by the lack of comparable data in this study. The novel sampling afforded to this study by Ruane *et al.* (2018) lacked comparable mitochondrial data, and thus the weakly resolved nodes in the phylogenies (Fig. 2.3, 2.4) may be a product of the lack of comparable mitochondrial material. The differential support between the BI + ML (Fig. 2.3) and BEAST time-calibrated phylogeny (Fig. 2.4) highlight the effect of differential taxon sampling on molecular results. Whilst Fig. 2.3 incorporated more samples, and more genes, it also had a lot of missing data, resulting in a lack of support in the under-sampled taxon. In Fig. 2.4, the inclusion of RAN68124 (in an attempt to ensure broad geographical sampling) may have confounded the phylogenetic resolution of the genus due to the availability of only nuclear markers for that sample. It is important to be aware of this when describing the results from molecular analysis as these problems can affect how species diversity is interpreted. Whilst likely a product of differential taxon sampling, the variable support may be a product of the novelty of the divergence between *M. occultus* and *M. mahafalensis*, with the BEAST BI phylogeny (Fig. 2.3) recovering the divergence of the genus during the late Pliocene (~3.2 MYA), making it one of the youngest species in Psammophiidae (Table 2.4). Interestingly *M. occultus* is considered cryptic as both itself and *M. mahafalensis* exhibit three identical polymorphisms, independent of genetics and geography. This highlights the complexity of the family and the importance of methodical and rigorous interpretation when inferring species boundaries, in the absence of well-delineated morphological characters.

Psammophylax was retrieved as monophyletic both in this study and past studies (Figueroa *et al.*, 2016; Kelly *et al.*, 2008; Zaher *et al.*, 2019). Vastly improved taxon sampling, as compared to past studies, through the inclusion of newly sequenced localities and species resulted in novel structuring in the genus. Notable findings include the large molecular distances separating *Ps. a. acutus* from the rest of *Psammophylax,* and the retrieval of *Ps. multisquamis* as polyphyletic. Albeit highly structured, intrageneric support remains lacking in the phylogenetic tree and so increased taxon sampling and genus-specific methodologies were utilised in Chapters Three and Four to elucidate the most accurate systematic structuring

within the genus. In the interest of brevity, *Psammophylax* will not be discussed further here as the genus is discussed in detail in forthcoming chapters.

Phylogenetic structuring within *Psammophis* has long been the subject of interest in the scientific world with multiple papers dedicated to the resolution of the taxonomically complex genus (Branch *et al.*, 2019; Broadley, 2002; Gonçalves *et al.*, 2018; Hughes, 1999; Kelly *et al.*, 2008; Rato *et al.*, 2015; Taft, 2018; Trape *et al.*, 2019). While the phylogenetic structuring in this study differs somewhat from the results of Kelly *et al.* (2008), the topological structuring was consistent with the more recent publications (Figueroa *et al.*, 2016; Zaher *et al.*, 2019).

Given the lack of sampling available for the Asiatic *Psammophis*, the lack of structuring observed in both this study and past studies (Figueroa *et al.*, 2016; Kelly *et al.*, 2008; Pyron *et al.*, 2013; Vidal *et al.*, 2008; Zaher *et al.*, 2019) is likely a product of incomplete taxon sampling. In *P. crucifer*, the shallow structuring coupled with the lack of phylogenetic diversity within southern Africa, means the species likely does not harbour any unappreciated diversity, especially since this study endevoured to capture the complete distribution of the species through comprehensive taxon sampling.

The assignment of *Psammophis trigrammus* was similar to past studies (Figueroa *et al.*, 2016; Kelly *et al.*, 2008; Zaher *et al.*, 2019) with the novel sampling afforded to this study producing shallow structuring. Whilst unsupported in this study, Branch *et al.* (2019) recovered a supported sister relationship between *P. ansorgii* and *P. jallae*. The inclusion of *P. ansorgii*, coupled with an additional *P. jallae* sample in this study, likely resolved the previous unsupported relationship between *P. jallae and P. notostictus* in Kelly *et al.* (2008), and more recently Figueroa *et al.* (2016). Much like past studies, *P. notostictus* was retrieved with shallow structuring irrespective of the large distribution, and wide range of biomes across which the species is found. Increased sampling, however, retreved a potential novel species from southwestern Angola, that separated from the rest of *P. notostictus* approximately four million years ago. The species delimitation results coupled with the recent description of several new snakes from Angola (Conradie *et al.*, 2020; Hallermann *et al.*, 2020), make this animal an ideal candidate for further investigation.

Past research lacked the sampling necessary to tackle the '*leightoni* complex' but the recent MSc thesis of Taft (2018) shed light on the taxonomy of the group through the acquisition of never-before-sequenced *P. trinasalis* samples, and a more complete taxon sampling for *P. leightoni* and *P. namibensis*. The phylogenetic results of his study recovered Namibian *P. namibensis* as sister to *P. trinasalis* + South African *P. namibensis* + *P. leightoni*, with South African *P. namibensis* being lumped within *P. leightoni*. These results were

replicated identically in the BI + ML phylogeny (Fig. 2.3) and similarly by the BEAST time-calibrated phylogeny (Fig. 2.4). The recommendation of Taft (2018) was that *P. trinasalis* and *P. namibensis* be sunk into the synonymy of *P. leightoni* based on shallow structuring and the results of species delimitation. Whilst the species delimitation methods employed in this study lumped South African *P. namibensis* and *P. leightoni*, they did recognise the *P. trinasalis* and Namibian *P. namibensis* as separate species, thereby conflicting with the results of Taft (2018), in spite of using the same sequences. Whilst Taft (2018) utilised a combined dataset (mitochondrial + nuclear genes), with all available samples, we omitted all identical sequences and removed nuclear genes from all species delimitation methods in this study. Identical sequences can produce zero branch lengths, whilst mitochondrial DNA evolves much faster than nuclear DNA (Brown *et al.*, 1979; Busschau, 2019; Vawter & Brown, 1986). Therefore, the use of identical sequences and both mitochondrial and nuclear DNA may produce erroneous branch lengths and confound results, especially when species delimitation is based on threshold criteria, as is the case with the methods employed in this study and Taft (2018). Whilst the differing results are negligible, their presence highlights the variability of molecular results when implementing phylogenetic analyses, using different genes, samples, and models of evolution. Within this study, the findings from the species delimitation analysis (Fig. 2.5) coupled with the split of South African *P. namibensis* from *P. leightoni,* approximately 0.4 million years ago (Table 2.4) would suggest that South African *P. namibensis* be synonymised with *P. leightoni,* leaving Namibian *P. namibensis* and *P. trinasalis* as valid species. Based on the findings from this chapter, a conservative systematic approach would support the synonymisation of South African *P. namibensis* with *P. leightoni*, and the continued recognition of *P. trinasalis* and *P. namibensis* as separate species. Given that *P. namibensis* is described from Harus, Uri-Hauchab mountains, Namibia (Broadley (2002), the amendment would only require that samples identified as South African *P. namibenis* be assigned to *P. leightoni*, and the distribution of *P. namibensis* be restricted to Nambia. More genetic material from Namibia is however needed to determine whether the phylogenetic differences between southern and northern *P. namibensis* are the product of incomplete taxon sampling. Whilst the results from this thesis offer a contrasting viewpoint to Taft (2018), it must however be noted that the systematic analyses employed in Taft (2018) were more robust, with both distribution modeling and morphology factoring into the systematic assessment.. For this reason, no formalised systematic recommendation will be made on the findings from this thesis. In regards to Taft's (2018) taxonomical recommendation, albeit contentious to morphological taxonomists that utilise the labile characteristics proposed by Broadley (2002), it is more in line with the Unified Species Concept (De Queiroz, 2005, 2007), as it recognises the three species as interconnected populations, with high intraspecific diversity. Ultimately, synonymisation of the '*leightoni* complex' would result in more clearly defined geographical limits and morphological

characteristics that could be used to better distinguish closely related congeners, such as *P. trigrammus* and *P. notostictus* from the '*leightoni* complex' (Broadley, 2002).

Whilst the placement of *P. angolensis* was unsupported in the BEAST phylogeny (Fig. 2.4), most past papers (Figueroa *et al.*, 2016; Kelly *et al.*, 2008; Pyron *et al.*, 2013; Zaher *et al.*, 2019) retrieved the same topological relationship as the phylogenetic tree (Fig. 2.3) in the BI + ML phylogeny and both Figueroa *et al.* (2016) and Pyron *et al.* (2013) lending support to the topology. Based on these findings *P. angolensis* can be confidently placed sister to Clade 4 + 5 + 6 + 7 + 8. *Psammophis angolensis* was well-structured with two supported clades, one comprised of Botswanian samples, and the other clade comprised of the remaining samples from Zambia, Tanzania, Democratic Republic of the Congo and South Africa. Whilst the substructuring is likely an artefact of incomplete taxon sampling given the absence of intermediate localities, increased sampling across the full extent of the species may produce interesting phylogeographic results given the large distribution of *P. angolensis.*

Kelly *et al.* (2008) retrieved Clade 4 as a polytomy, with the inclusion of *P. aegyptius* in latter studies resolving the relationship (Gonçalves *et al.*, 2018; Zaher *et al.*, 2019). Whilst the sister relationship between *P. schokari* and *P. aegyptius* is supported by this study and past papers (Figueroa *et al.*, 2016; Gonçalves *et al.*, 2018; Zaher *et al.*, 2019), the intrageneric relationships between *P. elegans, P. praeornatus* and *P. p. trivirigatus* remain unresolved with differential placements (Figueroa *et al.*, 2016; Zaher *et al.*, 2019). Gonçalves *et al.* (2018) retrieved support for a sister relationship between *P. p. trivirigatus* and *P. aegyptius* + *P. schokari* but given the omission of *P. elegans* and *P. praeornatus* from the dataset, this relationship is likely an artefact of incomplete taxon sampling. Irrespective of the weak support between species, the presence of *P. praeornatus* within the group ratifies the findings of Kelly *et al.* (2008), and supports the synonymisation of *Dromophis* with *Psammophis*. Barring *P. schokari*, all species within Clade 4 exhibited shallow structuring and did not contain any unappreciated species diversity. This is likely a product of adhoc sampling in *P. praeornatus, P. p. trivirigatus* and *P. elegans*, as can be seen by the distribution of samples in Table S2.1. *Psammophis aegyptius,* however, was the focus of a broad phylogeographic study that sourced samples from different parts of its range. The shallow structuring and lack of recognised novel taxa in the species delimitation analysis mean there is likely no unappreciated species diversity within the species. *Psammophis schokari,* however, contained a large amount of sub-structuring with deep divergences. Species delimitation analyses identified five putative species within *P. schokari*. Whilst Gonçalves *et al.* (2018) did not utilise sophisticated species delimitation, the structuring was similarly identified using pairwise distance matrices in their paper. Given the large geographic range of the species, it is likely that the analyses employed in this study, which utilises thresholds, has confounded

intra- and interspecies diversity given the comparably lower intraspecies diversity present within the endemic, range-restricted species farther south (Kelly *et al.*, 2008; Trape *et al.*, 2019). Given the lack of substantial morphological differentiation (Gonçalves *et al.*, 2018) between the populations of *P. schokari*, it is postulated that the clades identified here, like in the '*leightoni* complex', represent deeply divergent populations of a single species.

Clade 5 was retrieved similarly to recent studies (Figueroa *et al.*, 2016; Kelly *et al.*, 2008; Pyron *et al.*, 2013; Trape *et al.*, 2019; Zaher *et al.*, 2019), with support for a sister relationship between *P. tangancius* and *P. biseriatus*. The unidentified *Psammophis* (TP8431) was retrieved as sister to *P. tanganicus* (Figueroa *et al.*, 2016; Trape *et al.*, 2019) with the findings from this study and Trape *et al.* (2019) supporting the relationship. The sample was also retrieved as a potential new species by the species delimitation analyses employed in this study. Based on these combined findings, the unidentified sample may not be an unrecognised species but rather a representative of the highly elusive and enigmatic East African endemic, *P. pulcher*. The sample was recovered from Somalia (type locality of *P. pulcher* = Webi Shebeli, western Somaliland), and was recovered as sister to *P. biseriatus* and *P. tanganicus*, both of which are sympatric with *P. pulcher*, and similarly restricted to eastern Africa (Spawls *et al.*, 2018; Wallach *et al.*, 2014). While these findings are not conclusive, prior to 2011, this species was only known from four specimens collected upon initial discovery in 1894 (Steehouder, 2020). It is thus possible that the sample (TP8431), originally published in Vidal *et al.* (2008), was never identified as *P. pulcher* because of its absence from modern literature, given the lack of findings for 100 years prior to its most recent capture (Steehouder, 2020). Whether it is a new species, or an unidentified *P. pulcher*, increased sampling in north-eastern Africa is required for the taxonomical assignment of this animal.

The placement of *P. lineatus* was ratified by past research with most studies supporting the relationship between itself and its congeners (Figueroa *et al.*, 2016; Kelly *et al.*, 2008; Trape *et al.*, 2019; Zaher *et al.*, 2019). Increased sampling in Angola prior to this study made the acquisition and phylogenetic analysis of *P. zambiensis* possible for the first time. *Psammophis zambiensis* was recovered as sister to *P. lineatus* with strong support in both the BI + ML (Fig. 2.3) and BEAST BI phylogeny (Fig. 2.4). Previously confused with *P. leopardinus* (Hughes & Wade, 2002; Trape *et al.*, 2019; Uetz *et al.*, 2020), *P. zambiensis* was retrieved in a completely different clade. These findings highlight the importance of molecular biology in untangling complex taxonomical relationships among morphologically similar taxa.

The species composition and placement of Clade 7 (Fig. 2.3) as sister to Clade 8 was ratified by this study and most past publications (Figueroa *et al.*, 2016; Kelly *et al.*, 2008; Vidal

et al., 2008; Zaher *et al.*, 2019). The only study to retrieve the clade differently was Pyron *et al.* (2013) and this was likely a product of incomplete taxon sampling. Whilst the clade was unresolved in Kelly *et al.* (2008), results from the BI + ML phylogeny (Fig. 2.3), BEAST phylogeny (Fig. 2.4), and more recent publications (Figueroa *et al.*, 2016; Trape *et al.*, 2019), recovered *P. leopardinus* as sister to the rest of the clade, with strong support. Zaher *et al.* (2019) recovered *P. leopardinus* as sister to *P. brevirostris*, but this is likely erroneous given the weak support. Apart from Trape *et al.* (2019) and the unpublished work of Taft (2018), most studies omitted at least one member of the clade, making it hard to draw conclusions about the taxonomical validity of species within this enigmatic group. Both Taft (2018) and Trape *et al.* (2019) support the findings of this study, retrieving *P. brevirostris* and *P.* cf. *occidentalis* as sister species. Whilst both the findings of this study and Trape *et al.* (2019) retrieved *P. phillipsi* and *P. mossambicus* as sister species, Taft (2018) retrieved *P. phillipsi* nested within *P. mossambicus*. The findings of Taft (2018) are likely erroneous as the Gabonese *P. phillipsi* sample (PEM R5451) did not group with *P. phillipsi* material from Togo and Guinea (Trape *et al.*, 2019), but rather with *P. mossambicus* material from Gabon. This relationship was retrieved similarly in Kelly *et al.* (2008), meaning the sample is likely a misidentified *P. mossambicus*.

Psammophis mossambicus was the most well-sampled species in this study, with the recent work of Trape *et al.* (2019) affording many novel samples to this study. Whilst this study utilised a representative sampling of *P. mossambicus*, phylogenetic analysis retrieved similar results to Trape *et al.* (2019), with divergent colour and patterns morphs, within western and central African populations of *P. mossambicus* turning up very little molecular variance. Much like *Mimophis*, the '*leightoni* complex' and *P. crucifer*, colour and patterning have little bearing on speciation, highlighting the effect of phenotypic divergence on systematic structuring (Taft, 2018; Trape *et al.*, 2019).

Hughes and Wade (2004) previously resurrected *P. occidentalis* from the synonymy of *P. phillipsi* based on morphological grounds. Samples consistent with the distribution (Gabon and DRC) and morphology (scale colour pattern) of *P. occidentalis* were analysed in Trape *et al.* (2019) and in this study, retrieving the same results. The samples were recovered within the synonymy of *P. mossambicus*, corroborating the assertions of Branch (1998) and Broadley (2002) that *P. occidentalis* is a junior synonym of *P. mossambicus*. Based on these findings the samples identified in this study and Kelly *et al.* (2008), as *P.* cf. *occidentalis* are incorrectly identified as they form a sister relationship with *P. brevirostris*. Trape *et al.* (2019) postulated that these samples may constitute misidentified *P. zambiensis*, but given the retrieval of *P. zambiensis*, in this study, sister to *P. lineatus*, this is not plausible. *Psammophis* cf. *occidentalis* is either an undescribed species or a diverse population of *P. brevirostris*. Based

on the findings of the species delimitation analysis (Fig. 2.5) and 'recent' divergence time (~1.7 MYA) (Table 2.4), it is postulated that the samples attributed to *P.* cf. *occidentalis* in this study, and many past publications, represent a diverse clade of *P. brevirostris*. These findings extend the distribution of *P. brevirostris* north into Zambia and Burundi.

The placement and resolution of *P. sudanensis* has been a protracted problem with most recent papers (Figueroa *et al.*, 2016; Kelly *et al.*, 2008; Zaher *et al.*, 2019) recovering the species within the same clade as *P. subtaeniatus* and *P. orientalis*. The recent work of Trape *et al.* (2019) has, however, demonstrated that the samples associated with *P. sudanensis* in these papers are incorrectly attributed to the species, given their polyphyletic placement relative to the newly acquired samples of *P. sudanensis* from Chad. Trape *et al.* (2019) recovered a polytomy consisting of *P. sudanensis* and *P. sibilans*, with the increased sampling in this study (additional genes and samples: Ethiopian *P. sibilans),* resolving the polytomy. In the BI + ML phylogeny (Fig. 2.3), an Ethiopian clade of *P. sibilans* was recovered as sister to *P. sudanensis* + *P. sibilans*, whilst in the BEAST time-calibrated phylogeny (Fig. 2.4), *P. sudanensis* was recovered as sister to *P. sibilans*. Both relationships were supported by their respective algorithms, casting doubt over the taxonomic status of *P. sudanensis*. Whilst possibly an artefact of high intra-species diversity, because of geographical isolation, the species delimitation analyses in this study did identify the southern and northern clades of *P. sibilans* as putative species. Species delimitation also ratified the validity of *P. sudanensis*, thereby casting doubt on the taxonomical validity of the east African samples referred to as *P.* cf. *sudanensis* in this study. Species delimitation analyses also recognised *P.* cf. *sudanensis* as a distinct taxon, and additional species in both *P. orientalis* and *P. subtaeniatus*. Whilst the latter two species lack robust sampling enough to warrant taxonomic re-evaluation, the status of *P.* cf. *sudanensis* remains clearer. Given their polyphyletic placement, and their sister relationship to *P. orientalis* + *P. subtaeniatus* in the BEAST time-calibrated phylogeny (Fig. 2.4), these samples require recognition as a new species, indigenous to central-eastern Africa. It is thus recommended that a name be erected for *P.* cf. *sudanensis*, to alleviate the confusion associated with this problematic group of snakes.

Lastly, the validity of both *P. rukwae* and *P. afroccidentalis* was ratified by the findings of this study, supporting the recent description of the latter species in Trape *et al.* (2019). Previously a synonym of several taxa within the '*sibilans* complex', the work of Trape *et al.* (2019) resolved many of the discrepancies within the protracted species complex. Species delimitation analyses implemented in this study also recognised a putative taxon within *P. rukwae* but given the lack of robust sampling (only one sample), increased taxon sampling will be required prior to any further investigation of the potential new species.

Conclusion

Taxon sampling is an important yet overlooked aspect of evolutionary studies. The broad scope of this study coupled with robust sampling regimes have facilitated the production of the most comprehensive phylogenetic reconstruction of Psammophiidae to date. Whilst the taxonomical fate of several species within the family remains unknown, this study has resolved several systematic discrepancies within the family. The combination of geometric morphometrics and sophisticated phylogenetics has allowed for more defensible conclusions about the intergeneric structuring within the genus. It must however be noted that many of the samples sourced from GenBank were identified by authors with variable taxonomical expertise. Given this, doubt can be cast on the validity of some of the identifications, especially within problematic species complexes such as the'*sibilans* complex', which have already been the focus of much confusion in the past (Brandstätter, 1995; Hughes, 1999; Trape *et al.*, 2019). This may explain the various instances of paraphyly and polyphyly observed in this thesis. Every effort should thus be made to confirm the identifications of material in future publications, especially in the species listed below.

The use of time-calibrated phylogenetics and robust threshold-based species delimitation analyses has shed light on putative taxa within *Ps. multisquamis, H. nototaenia, P. schokari*, *P. lineatus*, *P. sibilans*, *P. orientalis*, *P. angolensis*, *P. subtaeniatus* and *P. rukwae,* whilst also revealing taxonomic overestimation within the family ('*leightoni* complex', *P.* cf. *occidentalis*). Whilst many of these taxa require extensive sampling to corroborate their taxonomical placement, the broad yet taxon-intensive sampling regime employed in this study has proved useful in tackling problematic taxonomical groups. The following chapters will implement the methodology utilised in this study on *Psammophylax* and *Ps. rhombeatus* to determine the efficacy of the methodology on the genus and species level.

Chapter Three: Systematic Structuring in *Psammophylax* (Fitzinger 1843)[4]

Introduction

In recent years, the number of studies focused on snake systematics has increased due to the improved accessibility to genetic samples and improved genetic analyses. The higher-level relationships of Caenophidia (advanced snakes) have been rigorously examined (Figueroa *et al.*, 2016; Kelly *et al.*, 2003; Lawson *et al.*, 2005; Pyron *et al.*, 2013; Vidal *et al.*, 2007; Vidal & Hedges, 2002; Zaher *et al.*, 2019), allowing for more defensible conclusions about higher-level systematic structuring. With this, lower level taxonomic groups are now being studied in more detail, leading to improved taxonomy and a better understanding of the processes that have led to the diversification of extant snakes, especially in the African region (e.g., Portillo *et al.* 2018)

The superfamily Elapoidea is a large and diverse group of caenophidians, which until recently had been characterised by poorly understood systematic relationships. The work of Vidal *et al.* (2008) and Kelly *et al.* (2011, 2009), and the more recent work of Pyron *et al.* (2013) and Figueroa *et al.* (2016) helped clarify many aspects of the taxonomy of Elapoidea. The recent work of Zaher *et al.* (2019), resulted in the elevation of several subfamilies to family level. One of these newly elevated families is Psammophiidae, the focus of this thesis. Although Kelly *et al.* (2008), and more recently the work of several other authors (Branch *et al.*, 2019; Gonçalves *et al.*, 2018; Ruane *et al.*, 2018; Taft, 2018; Trape *et al.*, 2019), have succeeded in resolving many taxonomic and phylogenetic relationships within Psammophiidae, there is still much that is unknown about the interspecific relationships of many genera within the family. This was highlighted in Chapter Two of this thesis, which recovered substantial sub-structuring in many genera of Psammophiidae, with *Psammophylax* producing some unexpected and interesting results.

[4] This chapter formed the basis of a peer-reviewed publication, but here I have expanded and added some additional analysis and information:

Keates, C., Conradie, W., Greenbaum, E. and Edwards, S. 2019. A snake in the grass: Genetic structuring of the widespread African grass snake (*Psammophylax* Fitzinger 1843), with the description of a new genus and a new species. *Journal of Zoological Systematics and Evolutionary Research*, 57(4): 1039–1066. DOI: 10.1111/jzs.12337

Psammophylax (Fitzinger 1843; family Psammophiidae) is a widespread African snake genus, commonly referred to as 'skaapstekers' ('sheep-stabbers') for the erroneous belief that they commonly bite and kill sheep (Spawls *et al.*, 2002, 2018). To remedy this misinformation, moving forward, effort should be made to replace 'skaapsteker' with 'grass snake' when referring to the animal in the colloquial form. The last systematic review of the genus documented only three species, viz. *Psammophylax rhombeatus*, *Ps. variabilis* and *Ps. tritaeniatus*, with four subspecies (*Ps. r. rhombeatus*, *Ps. r. ocellatus*, *P. v. multisquamis* and *Ps. v. vanoyei*) (Broadley, 1977). Spawls *et al.* (2002) informally treated, based on correspondence with the late Donald Broadley, *Ps. v. multisquamis* as a valid species (S. Spawls pers. comm., 2018). This treatment was followed by subsequent authors (Figueroa *et al.*, 2016; Kelly *et al.*, 2008; Pyron *et al.*, 2013; Wallach *et al.*, 2014), but without a formal species elevation. Largen & Spawls (2010) argued that the taxon should be retained as a subspecies of *Ps. variabilis* pending the results of a phylogenetic analysis. Kelly *et al.* (2008) transferred *Rhamphiophis acutus* and *Rhamphiophis togoensis* (previously *R. a. togoensis*) (Fig. 3.1 A–C) to *Psammophylax* based on genetic similarity and the collective monophyly of the group. The following species and subspecies are recognised in the genus: *Ps. acutus acutus, Ps. a. jappi, Ps. multisquamis, Ps. rhombeatus, Ps. ocellatus, Ps. togoensis, Ps. tritaeniatus tritaeniatus Ps. t. festivus, Ps. t. fitzgeraldi Ps. t. subniger, Ps. variabilis variabilis and Ps. v. vanoyei.*

African grass snakes are small-to-medium sized psammophiids that are found in the moist Savanna and Grassland Biomes, and are often characterised as being terrestrial, diurnal, and active foragers (Alexander & Marais, 2007; Bates *et al.*, 2014; Branch, 1998, 2016; Marais, 2004; Spawls *et al.*, 2001, 2018). Several species of *Psammophylax* display death-feigning and clutch guarding, with the latter behaviour being closely associated with *Ps. rhombeatus* (Bates & Nuttal, 2013; Branch, 1998; Spawls *et al.*, 2018). Body striping is evident in all species, and colouration and pattern differences are the most prominent distinguishing characteristics between the species as they are currently defined (Broadley, 1990; Branch, 1998; Spawls *et al.,* 2002, 2018). The sharply pointed snouts of *Ps. acutus* and *Ps. togoensis* distinguish them from all other members of the genus (Marais, 2004; Segniagbeto *et al.*, 2011; Spawls *et al.*, 2018) and this feature was responsible for their former inclusion in the genus *Rhamphiophis* (beaked snakes).

Figure 3.1**:** A) *Kladirostratus acutus acutus* **comb. nov.** from Angola (Photo: Werner Conradie); B-*Kladirostratus a. acutus* **comb. nov.** from Angola (Photo: Werner Conradie); C) *Psammophylax togoensis* from Nigeria (Photo: Gerald Dunger); D) *Psammophylax variabilis vanoyei* (EBG 2611/UTEP 21868) from Democratic Republic of Congo RC (Photo: Eli Greenbaum); E) *Psammophylax tritaeniatus subniger* (EBG 3006/UTEP 21871) from Democratic Republic of Congo (Photo: Eli Greenbaum); F) *Psammophylax multisquamis* (CMRK363/PEM R23922) from Ethiopia (Photo: Christopher Kelly); G) *Psammophylax multisquamis* from Kenya (Photo: Stephen Spawls); H) *Psammophylax multisquamis* (CMRK 152/PEM R23923) from Kenya (Photo: Christopher Kelly); I) *Psammophylax kellyi* **sp. nov.** (CMRK 328/PEM R23925) from Tanzania (Photo: Christopher Kelly); J) Holotype specimen, *Psammophylax kellyi* **sp. nov.** (CMRK 401/PEM R23926) from Tanzania (Photo: Werner Conradie).

Cryptic species pose a particular challenge for systematics and taxonomy and may result from recently evolved sister species having ambiguous species boundaries because salient morphological differences have not yet accumulated (Florio *et al.*, 2012). Several key instances of cryptic speciation have been highlighted in Elapoidea (Greenbaum *et al.,* 2015; Kelly *et al.,* 2011; Ruane *et al.,* 2018). For example, *Mimophis occultus* (*occultus*–Latin for 'concealed in plain sight') was recently described from northern Madagascar (Ruane *et al.*, 2018), indicating that widespread habitat generalists may be incorrectly described when taking only morphology into account. The taxonomic history of *Psammophylax* suggests that cryptic speciation might be concealing diversity within this genus (Broadley, 1977). This assertion was proved valid by the findings of Chapter Two, that recovered *Ps. multisquamis* as polyphyletic, with little to no morphological distinction between the two clades. The use of rigorous genetic methods, especially with widespread and generalist species that live in close proximity to forests, may uncover diversity previously missed by morphologically orientated taxonomy (Bickford *et al.*, 2007).

Although widespread and abundant, *Psammophylax* remains an understudied genus. Past studies focused on the higher taxonomic levels (Kelly *et al.,* 2008, 2011). Kelly *et al.* (2008) utilised only one representative from each species of *Psammophylax*, as their study focused on the Psammophiidae family. Irrespective of the small sample size, they found enough genetic resolution to transfer *Rhamphiophis acutus* to the genus *Psammophylax*. This was ratified by subsequent studies (Figueroa *et al.*, 2016; Pyron *et al.*, 2013; Zaher *et al.*, 2019). Chapter Two built on these findings, with increased sampling in the genus and revealed substantial genetic structuring, and potential unappreciated diversity. The lack of rigorous genus-specific research, coupled with the possibility of cryptic speciation, makes this genus a viable candidate for a phylogenetic study (Oliver *et al.,* 2009; Böhm *et al.,* 2013; Tolley *et al.,* 2016). Furthermore, Chapter Two revealed substantial morphological variability between genera based on head girth and beak length. Given the presence of pronounced beaks in *P. a. acutus*, geometric morphometrics of the head shape of all *Psammophylax* may reveal taxonomic groups previously missed by conventional taxonomy.

Herein, I investigate the phylogenetic relationships between individuals of *Psammophylax,* including the morphologically disparate *Psammophylax '*[5]*acutus* group'. I sampled from several regions across each species' range and produced a phylogenetic tree using multiple algorithms. I then investigated the level of divergence of each clade within the tree to test for species-level divergences. I also investigated the morphological differences

[5] The '*acutus* group' comprises: *Ps. a. acutus*, *Ps. a. jappi* and *Ps. togoensis.*

between genera in the family Psammophiidae, and differences between species of *Psammophylax*, using both traditional morphological and geometric morphometric techniques.

Methods

Genetic Sampling

The phylogeny of *Psammophylax* was estimated using genetic information from 90 individuals, representing a large part of the genus' distributional range (Fig. 3.2). The study incorporated six of the seven known species (Table S3.1). No tissue samples of *Ps. togoensis* were available and the species was therefore excluded from the study. Tissue samples for the genetic analyses were obtained from Port Elizabeth Museum (PEM), South African National Biodiversity Institute (SANBI; Cape Town), and from scientists and citizen scientists stationed throughout Africa. Tail tips (live specimens) and liver or muscle tissues (preserved specimens) were preserved in ~95% ethanol. Sequences from closely related genera (*Hemirhagerrhis, Psammophis, Mimophis* and *Rhamphiophis*) were obtained from GenBank (https://www.ncbi.nlm.nih.gov/genbank/) and used as outgroups (Table S3.1).

Genetic Laboratory Protocols

Genomic DNA was isolated from tissues with a standard salt extraction method (Bruford *et al.*, 1992) using lysis (Buffer ATL; Qiagen) and elution (Buffer AE; Qiagen) buffers. Standard PCR procedures were utilised to amplify two partial mitochondrial genes (cytochrome b [cytb] and NADH-dehydrogenase subunit 4 [ND4]) and one partial nuclear gene (oocyte maturation factor [c-mos]). PCR amplification was carried out using the primer pairs listed in Table 3.1. Amplification of the selected genes was carried out using 20–50 ng/µl extracted genomic DNA. Each amplification was conducted with a PCR mixture to the total volume of 25 µl containing 12.5 µl TopTaq Mastermix (Qiagen; containing 10x PCR buffer, 1.5 mM $MgCl_2$, 0.2 mM dNTPs, and 0.75 U Taq polymerase), 2 µl forward primer (10 µM), 2 µl reverse primer (10 µM), and 8.5 µl of the genomic DNA and de-nucleated water combined. The cycling profile for gene amplification was as follows: initial denaturing step at 94 °C for 5 min, followed by 35–40 cycles of 94 °C for 30 s, 48–56 °C for 45 s, and 72 °C for 45 s, with a final extension at 72 °C for 8 min. The prepared PCR products were sent to Macrogen Corp. in Amsterdam, Netherlands for sequencing (after purification) with the forward primers only.

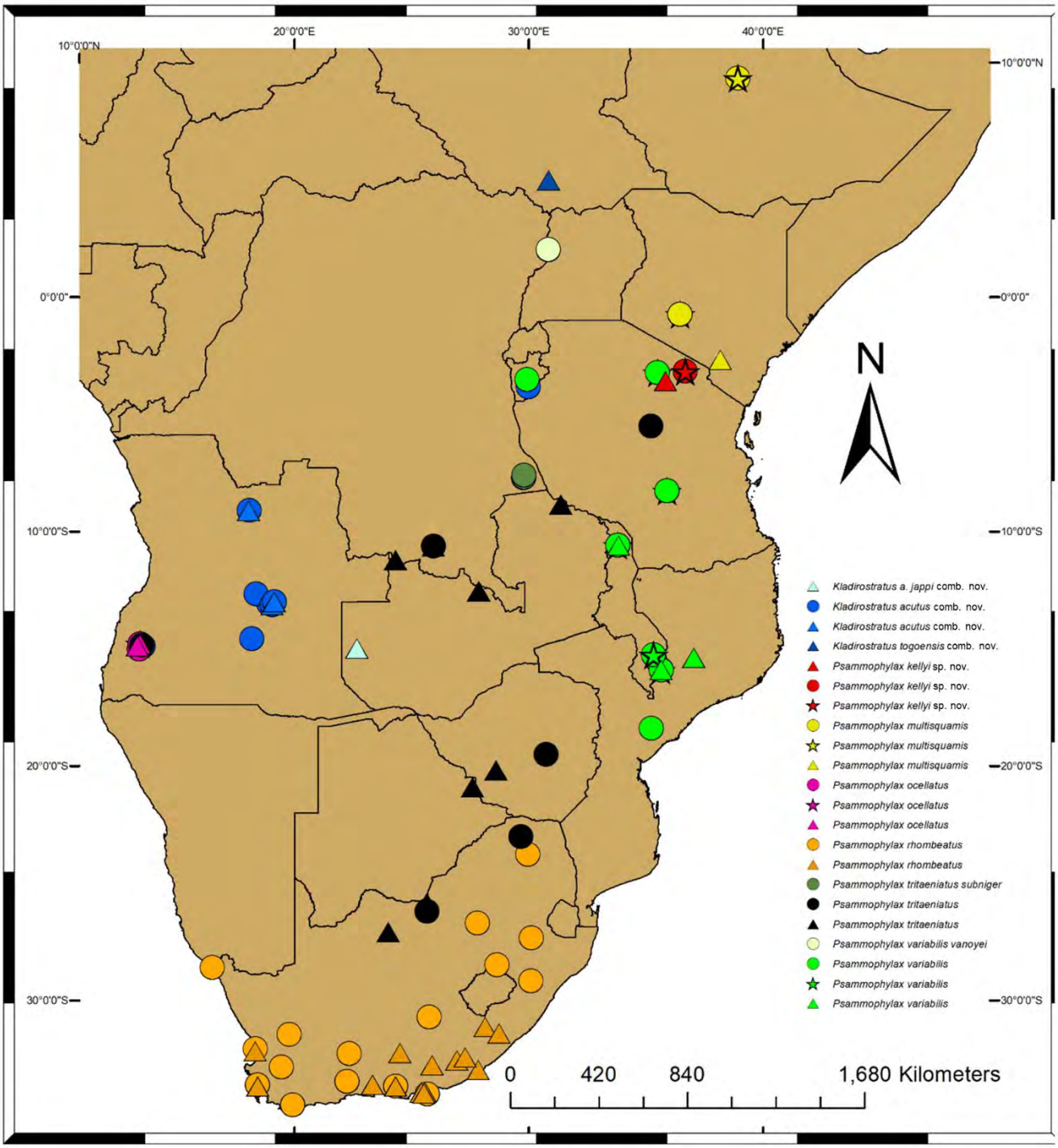

Figure 3.2: Localities of ingroup samples used in this study. Filled circles represent samples used in the genetic analyses, triangles represent samples used in the morphological analyses, and stars represent specimens for which both genetic and morphological samples were available.

Table 3.1: Primers and PCR protocols used to the generate sequences for the study.

Gene	Primer	Source	Annealing Temp (°C)	Cycles
cytb	WWF: 5'—AAAYCAYCGTTGTWATTCAACTAC—3' Cytb-R2: 5'—GGGTGRAAKGGRATTTTATC—3'	Whiting, Bauer, & Sites (2003)	50—52	35
ND4 + LeutRNA	ND4: 5'—TGACTACCAAAAGCTCATGTAGAAGC—3' LeutRNA: 5'—CATTACTTTTACTTGGATTTGCACCA—3'	Arèvalo, Davis, & Sites (1994)	52—56	35
c-mos	S77: 5'—CAT GGACTGGGATCAGTTATG—3' S78: 5'—CCTTGGGTGTGATTTTCT CACCT—3'	Slowinski & Lawson (2002)	48—52	35—40

Sequence Alignment and Gene Partition Congruence Testing

The sequence trace files were checked using BioEdit Sequence Alignment Editor v.7.2.5 (Hall, 1999) and aligned, along with the previously accessioned GenBank sequences, in MEGA v.6.0 (Tamura *et al.*, 2013) using the ClustalW alignment method. Unlike Chapter Two, that omitted LeutRNA, the presence of comparable material in this chapter necessitated the use of LeutRNA in *Dataset 3.1* and *3.2*. The region representing LeutRNA was split from rest of ND4 and treated as a separate locus (non-protein-coding), necessitating the creation of four gene alignments for further analysis. Individual gene trees were constructed in MEGA v. 6.0 using the Maximum Likelihood algorithm, with 100 bootstrap replicates and the GTR+G+I nucleotide substitution model. The Congruence Index (I_{cong}; http://max2.ese.u-psud.fr/icong/index.help.html; de Vienne *et al.,* 2007) was utilised to test for congruence between individual gene trees. All gene-tree combinations were found to be congruent and three datasets were created.

Datasets

Like Chapter Two, to facilitate molecular best practice, different datasets were put together using specific genes, partition schemes, and models of evolution for different analyses. By doing this, I was able to optimize each analysis and ensure the phylogenetic modelling was as robust as possible.

Dataset 3.1 was used for the initial phylogenetic tree and included all available sequences of *Psammophylax*, with a representative sampling from *Ps. rhombeatus*, and was supplemented with several individuals from closely related taxa (Table S3.1). *Dataset 3.1* used the following genes: cytb (91 sequences [sq], 597 base pairs [bp]); ND4 (91 sq, 645 bp); LeutRNA (85 sq, 154 bp); c-mos (48 sq, 552 bp).

Dataset 3.2 was used for multilocus species delimitation and comprised of all the same samples from *Dataset 3.1*, but omitted identical samples and outgroup taxa, resulting in a total dataset of 61 samples (Table S3.1). the nuclear gene, c-mos, was also removed because it is an independently recombining gene and using it in conjunction with single locus species delimitation methods would have invalidated the analyses. *Psammophylax acutus* was removed from the analysis as it was believed the large molecular distance separating *Ps. acutus* from the rest of *Psammophylax* may confound the delimitation results. *Dataset 3.2* used the following genes: cytb (59 sq, 597 bp); ND4 (57 sq, 645 bp); LeutRNA (56 sq, 154 bp).

Dataset 3.3 was used for p-distance analysis and included all available sequences of *Psammophylax* (including *Ps. acutus*) for cytb (187 sq, 582 bp) and ND4 (177 sq, 639 bp), and omitted sequences that contained missing data. *Dataset 3.3* also included sequences from closely related genera within Psammophiidae, for comparison. Given the lack of comparable LeutRNA regions in the outgroup taxa, LeutRNA was omitted from this dataset, to reduce the amount of missing data. The molecular markers and models of evolution utilised in each dataset can be found in Table 3.2.

Table 3.2: Best-fit partitioning schemes and models of evolution for each dataset, according to PartitionFinder 2, with number of sites per partition. Numbers following genes in the subset partition column refer to codon position. NA = Not Applicable.

Dataset	Initial Partition	Subset Partition	Best Model*	Number of Sites
3.1	codon	cytb_1, ND4_1, LeutRNA	HKY+I+G	568
		cytb_2, ND4_2	HKY+I	414
		cytb_3, ND4_3	GTR+G	414
		c-mos_1, c-mos_2	K80 (K2P)	368
		c-mos_3	HKY	184
3.2	gene	cytb, ND4, LeutRNA	TRN+G	1396
3.3	NA	cytb	NA	582
		ND4	NA	639

**MrBayes does not support many of the models implemented in BEAST. In these cases, the best alternative implemented in MrBayes was used. These models are shown in brackets.*

Models of Evolution and Partition Scheme

All gene alignments were tested for saturation using DAMBE v.6.4.67 (Xia, 2013). The protein-coding genes (cytb, ND4, c-mos) were checked for stop codons to ensure they started on the correct reading frame and analysed according to codon position. No saturation was found, enabling the use of gene-partitioned datasets, where necessary. *Dataset 3.1* utilised a codon

partition scheme (codon positions partitioned separately) as it produced better supported topologies using both the Maximum Likelihood (ML) and Bayesian Inference (BI) algorithm. The BEAST algorithm, however, retrieved stronger support using a gene-partitioned dataset (genes partitioned separately), hence its use in *Dataset 3.2*. The best partition schemes and best-fitting models of molecular evolution were selected using PartitionFinder 2 (Lanfear *et al.*, 2016) with the following settings: BIC model selection criterion, BEAST models, linked branches and all partition schemes searched (Table 3.2). For BEAST analysis (*Dataset 3.2*), the gene partitioned dataset was run through jModelTest 2 (Darriba *et al.*, 2012; Guindon & Gascuel, 2003) to determine the optimal gamma shape and invariant site values for the partitions selected by PartitionFinder 2.

Phylogenetic Tree

Dataset 3.1 was used to infer the phylogenetic structuring within *Psammophylax* using BI and ML. Bayesian Inference was carried out using MrBayes v.3.2.2 (Ronquist *et al.,* 2012) on the CIPRES Science Gateway XSEDE online resource (http://www.phylo.org; Miller *et al.* 2010). For MrBayes, four parallel runs of 20 million generations (MCMC analysis) were performed, with trees being sampled every 1000 generations, using uniform priors. BEAGLE was used to speed the process up. The number of generations discarded as burn-in was determined using Tracer v.1.5 (Rambaut & Drummond, 2009). The effective sample size (ESS) was found to be above 200 for all parameters with all runs reaching convergence, indicating that a burn-in of 10% was adequate for the BI tree. Maximum Likelihood analysis was conducted using the GTRGAMMA model in RAXML-HPC v.8.2.12 (Stamatakis, 2014) on the CIPRES Science Gateway. A random starting tree was used and the rapid bootstrapping method. One thousand bootstraps were run, and all other parameters were set to default. All BI and ML trees were viewed and edited in FigTree v.1.4.2 (Rambaut, 2014).

Species Delimitation

To investigate the taxonomical structuring within *Psammophylax*, a combined mitochondrial dataset was created using *Dataset 3.2* (Tables 3.2, S3.1). Bayesian implementation of the Generalized Mixed Yule Coalescent (bGMYC), Automatic Barcode Discovery (ABGD) and Poisson Tree Processes (PTP) were used to test for cryptic taxa within the genus. Although designed for single locus datasets, these species delimitation analyses were implemented on the combined mitochondrial loci (cytb, ND4, LeutRNA) as they have been demonstrated to evolve at similar rates across the mitochondrial genome, thus affording a larger dataset to the analyses. The combined mitochondrial genes thus represent a single locus here.

For bPTP and bGMYC, phylogenetic tree creation, was carried out in BEAST v.2.6.3 (Bouckaert *et al.*, 2019; Drummond & Rambaut, 2007; Suchard & Rambaut, 2009). A gene-partitioned input file (Table 3.2) was input into BEAUti v.2.6.2 (Bouckaert *et al.*, 2019; Drummond & Rambaut, 2007) using the following settings: linked trees, unlinked clock models (relaxed lognormal) and unlinked site models with a Yule prior. The absence of nuclear loci from the dataset resulted in erroneous topologies, and thus several of the intrageneric relationships were constrained using the results from Chapter Two. Three independent analyses of 50 000 000 generations, sampling every 5000 generations, were run through BEAST v.2.6.3. The independent runs were combined in LogCombiner v.2.6.2 (Bouckaert *et al.*, 2019; Drummond & Rambaut, 2007) and a maximum clade credibility tree, with a burn-in of 10% was created in TreeAnnotator v.2.6.2 (Bouckaert *et al.*, 2019; Drummond & Rambaut, 2007). The effective sample size (ESS) was found to be above 200 in Tracer v.1.5 and the final tree was viewed and edited in FigTree v.1.4.2.

Unlike Chapter Two, that only utilised the single tree bGMYC analysis (bgmyc.singlephy; Reid and Carstens, 2012), this chapter utilised both the single tree and the multi-tree method (bgmyc.multiphylo; Reid and Carstens, 2012), to assess the difference between the two. For the single bGMYC method, the maximum clade credibility tree from TreeAnnotator v.2.6.2 was used. For the multi-tree method, one hundred and fifty randomly selected posterior trees, were selected from the BEAST output, using LogCombiner v.2.6.2, and following a burn-in of 10%, 135 trees were analysed. The package bGMYC v.1.0.2 in R studio v.1.1.442 (R Core Team, 2016; Reid & Carstens, 2012) was used with the bgmyc.singlephy and bgmyc.multiphylo functions being used for the single and multi-tree analysis, respectively. The trees from both analyses were subjected to 50 000 MCMC steps, a burn-in of 40 000 steps, and sampling every 100 steps.

Bayesian implementation of the PTP model was conducted via the bPTP server (http://species.h-its.org/ptp/; Zhang *et al.,* 2013) on the maximum clade credibility tree. Lastly, a combined mitochondrial FASTA alignment was created using the sequences from *Dataset 3.2* (Table 3.2, S3.1). The alignment was uploaded onto the ABGD web interface (abgd web (mnhn.fr), web version 10 January 2021), using the following settings: standard p-distance metrics, minimum barcode gap width (1.0), intraspecific divergence minima (0.001) and maxima (0.1). The results from all the threshold analyses were overlaid on the maximum clade credibility tree from TreeAnnotator v.2.6.2.

Pairwise Distance Analysis

Pairwise distance of *Psammophylax* (including *Ps. acutus)* and closely related taxa was carried out using *Dataset 3.3*. Pairwise distance matrices were created for cytb and ND4 (Table 3.2), using MEGA X v.10.1.7 (Kumar *et al.*, 2018) using the following settings: standard uncorrected p-distance model, uniform rates, pairwise deletion and 500 bootstraps. Samples were grouped according to species.

Traditional Morphology

The traditional morphological analyses were mostly based on material in the Port Elizabeth Museum (PEM), which is listed in Table S3.2. Additional data were generated from the publications of Broadley (1971, 1977) and Chirio and Ineich (1991), and from Donald Broadley's unpublished datasheets. The following characters were used to compile the generic and species accounts: dorsal scale rows (counted one head length behind head, at midbody, and one head length anterior to the anal plate), preoculars, postoculars, temporal scale arrangement, upper labials, upper labials entering eye, lower labials, lower labials in contact with 1st sublinguals, ventral scales (Dowling, 1951), and subcaudal scales (counted from anterior cloaca, excluding the terminal spine). The following measurements were recorded: Snout-Vent Length (SVL)–from the tip of the snout to the anterior edge of the cloaca, Tail Length (Tail)–from the tip of tail to posterior edge of the cloaca, Total Length (TL)–combined SVL and Tail Length. Total and tail lengths were measured to the nearest 1 mm using a flexible ruler or a tap measure. The general skull morphology and number of teeth (maxillary, palatine, pterygoid and dentary) are based on the descriptions provided by Broadley (1971, 1977).

Geometric Morphometrics

Geometric morphometric analyses of the external views of the head were performed to investigate the head shape of the genera and constituent species in selected Psammophiidae genera (2–20 individuals per species, totalling 111 individuals). I obtained dorsal and lateral photographs of the heads of specimens at the Port Elizabeth Museum (PEM), Field Museum of Natural History (FMNH), American Museum of Natural History (AMNH), Natural History Museum of Los Angeles County (LACM) and Museum of Comparative Zoology at Harvard University (MCZ) (Table S3.2). We selected the following closely related taxa as defined by Kelly *et al.* (2008) to investigate generic differences: *Psammophis mossambicus*, *Rhamphiophis rostratus*, *Psammophylax rhombeatus* and *Psammophylax acutus*. We also included individuals of all *Psammophylax* species to test for differences in head shape among

species (Table S3.2). The dorsal and lateral profiles (all right-hand-side) of the heads were photographed on grid paper (1 cm x 1 cm) with a digital camera (Canon 600D, resolution 18.0 MP and 100 mm macro lens). Homologous landmarks were placed and digitised on the two views of the heads (Fig. 3.3; TpsUtil v.1.26; Rohlf, 2004b; TpsDig2 v.2.32; Rohlf, 2004a). A Generalized Procrustes Analysis (GPA; Rohlf, 1999; Rohlf and Slice, 1990) was performed during which the landmark configurations were resized, translated and rotated (aligned by principal axis). A covariance matrix was estimated using the symmetrical (dorsal view dataset) or the asymmetrical (lateral view dataset) components. A principal components analysis (PCA) was performed on the covariance matrix to identify which portions of the heads showed the most variation between the different genera (MorphoJ v.1.06d; Klingenberg, 2011). Significant differences between genera with respect to principal components (PC) axes scores were investigated using RStudio v.1.0.136 (R Core Team, 2016), applying the following tests: Analyses of Variance (ANOVAs; package: 'stats', functions: 'anova' and 'lm') and Tukey's Honest Significant Difference (HSD) post-hoc test (package: 'agricolae', function: 'HSD.test', group = F).

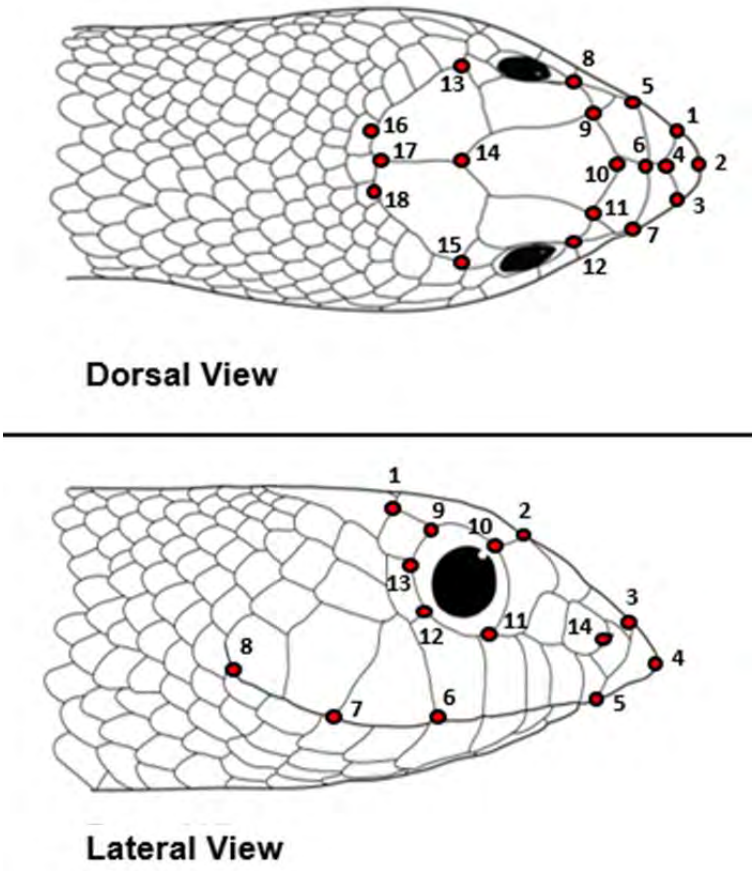

Figure 3.3: The placement of landmarks on photographs of dorsal and lateral aspects of the head for geometric morphometric analysis. Specimen used to render drawing: *Psammophylax a. acutus* (PEM R23450).

Results

Phylogenetic Structuring

The two phylogenetic algorithms found congruent topologies for the concatenated dataset (Fig. 3.4), all supporting the monophyly of *Psammophylax* (100% MLBS, 1.0 BIPP), and all retrieving *Ps. a. acutus* as sister to the other ingroup taxa. Whilst the sister relationship between *Ps. rhombeatus* + *Ps. ocellatus* and *Ps. tritaeniatus* + *Ps. multisquamis* 1 + *Ps. variabilis* was supported by both algorithms, only Bayesian Inference supported the sister relationship *Ps. rhombeatus* and *Ps. ocellatus.* The interspecies relationships among *Ps. tritaeniatus*, *Ps. multisquamis* 1 and *Ps. variabilis* were supported by only Bayesian Inference whereas the monophyly of all the ingroup species (barring *Ps. multisquamis*) was supported by both molecular algorithms. Both topologies supported the polyphyly of *Ps. multisquamis* (*Ps. multisquamis* 1 and *Ps. multisquamis* 2), and the sister relationship between *Ps. multisquamis* 2, and the remainder of the ingroup species (*Ps. ocellatus, Ps. rhombeatus, Ps. tritaeniatus, Ps. multisquamis* 1, and *Ps. variabilis*).

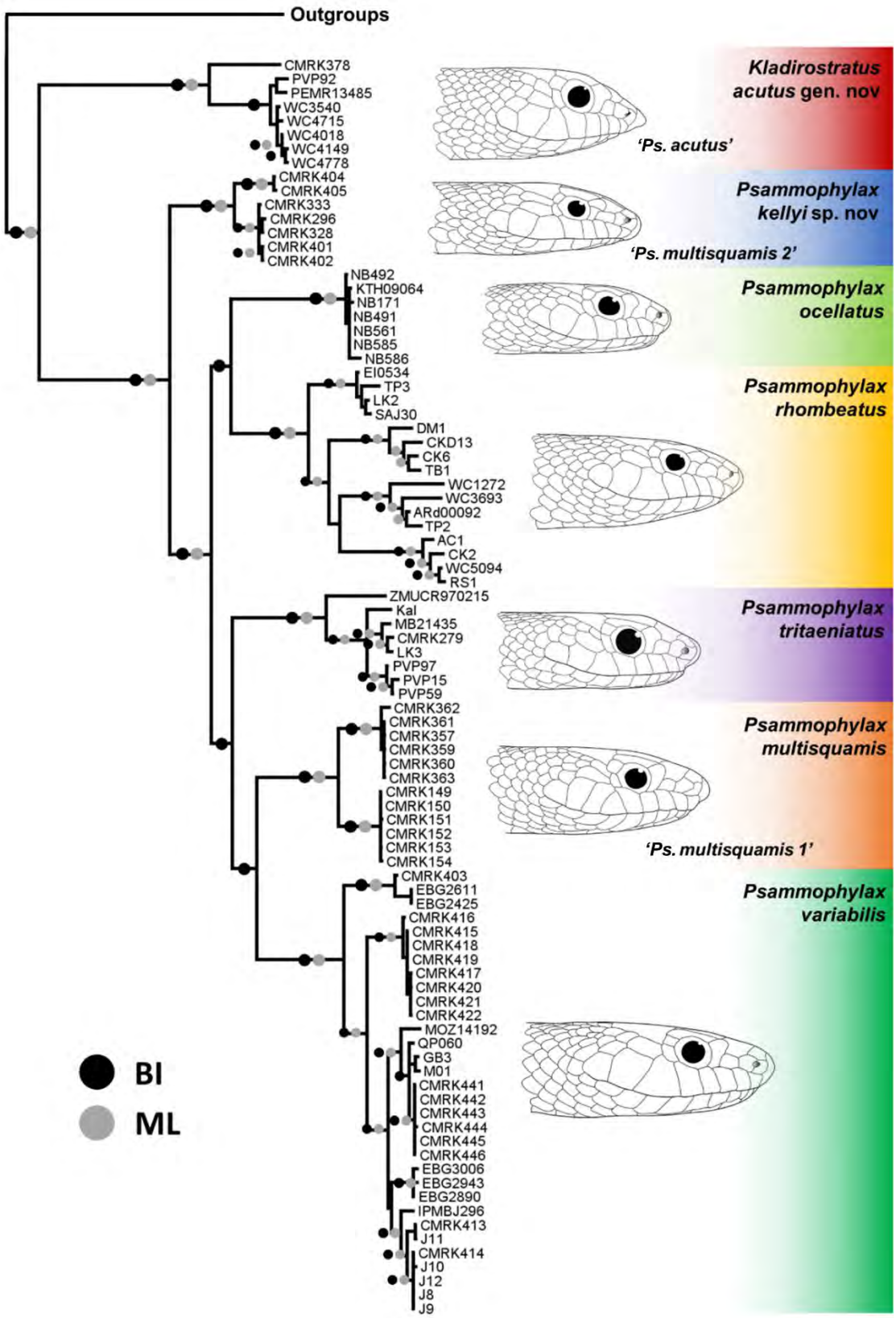

Figure 3.4: Bayesian Inference (BI) tree, with Maximum Likelihood (ML) support overlaid, using *Dataset 3.1,* showing the relationships between species within *Psammophylax*. Circles denote significant support at the nodes. BI posterior probabilities ≥ 0.90 and ML bootstrap values ≥ 75% were considered supported.

Species Delimitation

Results between the species delimitation methods were largely incongruent, with contrasting taxonomic groupings between analyses. The bGMYC outputs were interpreted using two threshold values ($p \geq 0.95$ and $p \geq 0.50$). Firstly, the results from the multi-tree bGMYC method were largely incongruent with the findings of the other methods with bGMYC MT1 ($p \geq 0.95$) recognising only four species, effectively lumping *Ps. rhombeatus* and *Ps. ocellatus,* and *Ps. multisquamis* 1 and *Ps. variabilis*. The second multi-tree bGMYC (bGMYC MT2) ($p \geq 0.5$) recognised 13 species, suggesting an under-appreciation of current taxonomical diversity within the group. The first single tree bGMYC (bGMYC ST1) ($p \geq 0.95$) recognised all currently accepted species and *Ps. multisquamis* 2 as valid taxa whilst bGMYC ST2 ($p \geq 0.5$) recognised 13 species in *Psammophylax*, identical to the findings of bGMYC MT2, recognising all existing species, four species within *Ps. rhombeatus,* two species in *Ps. tritaeniatus,* three species in *Ps. multisquamis* and three species in *Ps. variabilis.* (Fig. 3.5). The PTP and Bayesian implementation (bPTP) of the PTP model recovered the highest number of putative species with 31 and 30 species, respectively (Fig. 3.5). These results are interpreted as an over-estimation, with groupings more likely representative of intraspecific structuring as opposed to potential new species. Both ABGD partitions produced similar results, with the ABGD 1 recognising 12 species, whilst ABGD 2 was slightly more sensitive, identifying the same taxonomical groupings as bGMYC MT2 and bGMYC ST2.

Pairwise Distance Analysis

In terms of pairwise sequence divergences, *Ps. acutus* is divergent from its congeners (Table 3.3). The average interspecific distance between *Ps. acutus* and the other *Psammophylax* species was 12.12 ± 0.55% and 12.69 ± 0.33% for cytb and ND4, respectively. The average interspecies difference separating the polyphyletic *Ps. multisquamis* 2 clade from the rest of the genus (excluding *Ps. acutus*) was 7.77 ± 0.94% and 8.63 ± 0.62% for cytb and ND4, respectively. The average interspecies distance between *Psammophylax* species, excluding *Ps. acutus*, was 8.31 ± 0.91% for cytb and 9.03 ± 0.62% for ND4. By way of comparison, the average interspecies distance between *Hemirhagerrhis kelleri* and the *Psammophylax* species, excluding *Ps. acutus*, was 14.05 ± 0.66% and 14.80 ± 0.70% for cytb and ND4, respectively. The highest intraspecies diversity was observed within *Ps. rhombeatus* (cytb: 5.16%; *ND4*: 5.08%), likely a product of the large sample size afforded to *Ps. rhombeatus*, in comparison to the rest of the genus.

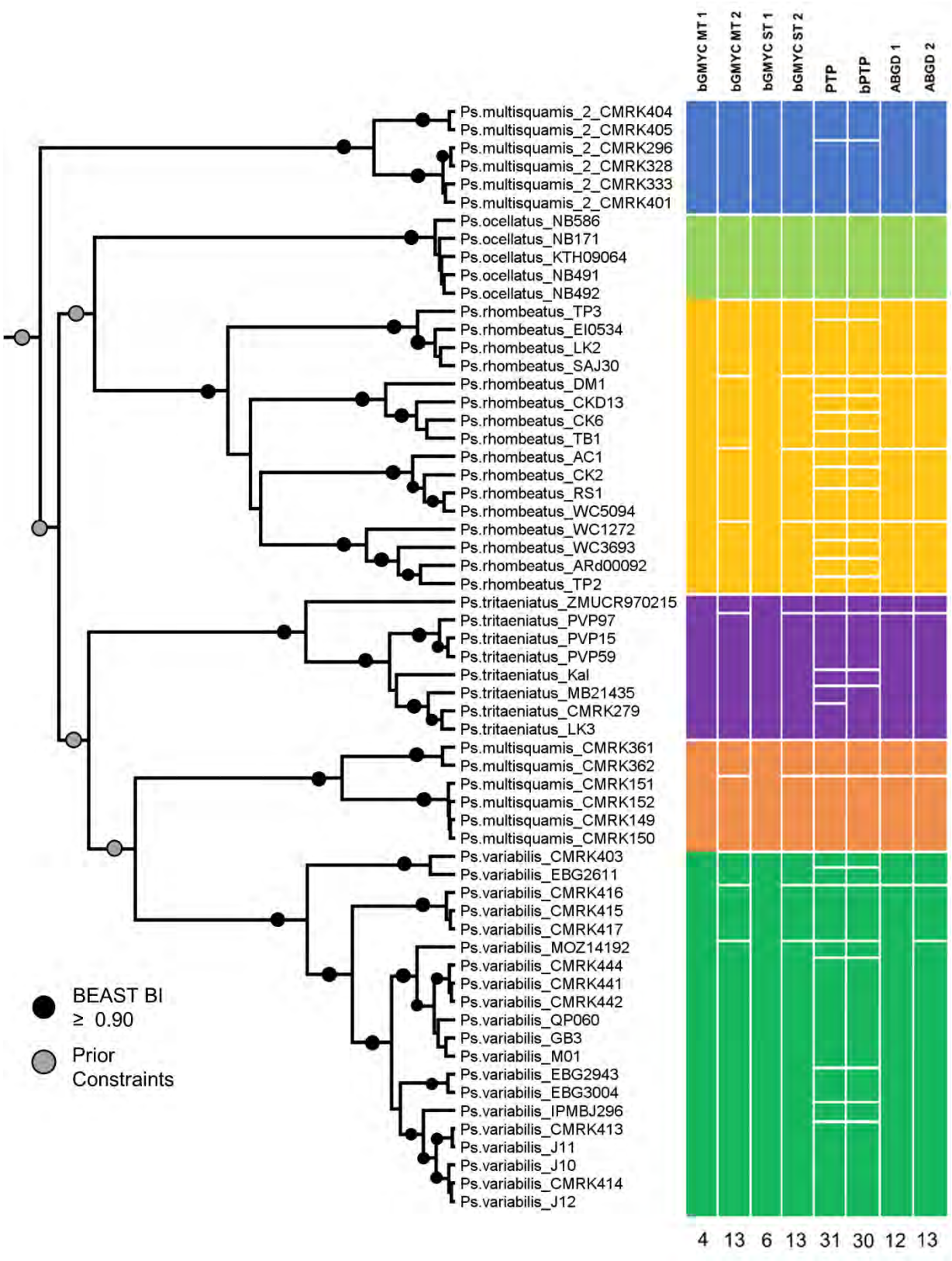

Figure 3.5: Bayesian Inference Beast BI phylogeny of *Psammophylax* derived from *Dataset 3.2*. Black circles denote support and grey circles indicated constrained nodes. Vertical bars denote different species delimitation methods and horizontal white bars show the putative species based on the varying analyses. Size of node circles bear no meaning. MT = multi-tree, ST = Single Tree. bGMYC MT1: ≥ 0.95; bGMYC MT2: ≥ 0.50; bGMYC ST1: ≥ 0.95; bGMYC ST2: ≥ 0.50; ABGD 1: prior maximal distance = 0.012915; ABGD 2: prior maximal distance = 0.007743.

Table 3.3**:** Sequence divergences (uncorrected pairwise distance values) separating species using cytochrome b (cytb) and NADH dehydrogenase subunit 4 (ND4), using *Dataset 3.3*. Numbers in the diagonal (in bold) denote intraspecific divergences, numbers below the diagonal denote interspecific divergences and numbers above the diagonal denote the standard error of the interspecific divergences. Not Available = NA.

	cytb												
		1	2	3	4	5	6	7	8	9	10	11	12
1	*Psammophylax a. acutus*	**1.62**	1.12	1.24	1.19	1.12	1.20	1.18	1.42	1.26	1.40	1.43	1.38
2	*Ps. multisquamis 2 (kellyi)*	11.28	**1.26**	0.92	1.07	0.94	1.03	0.98	1.40	1.27	1.47	1.47	1.39
3	*Ps. multisquamis*	12.39	6.69	**1.69**	0.99	0.89	0.96	0.97	1.38	1.38	1.48	1.48	1.45
4	*Ps. ocellatus*	11.69	6.91	6.98	**0.05**	0.99	1.13	1.11	1.49	1.44	1.55	1.49	1.44
5	*Ps. rhombeatus*	12.40	8.90	8.36	8.93	**5.16**	0.95	0.97	1.30	1.32	1.43	1.38	1.32
6	*Ps. tritaeniatus*	12.79	8.20	7.54	9.18	8.76	**2.03**	1.08	1.40	1.42	1.51	1.43	1.40
7	*Ps. variabilis*	12.14	8.13	8.20	9.29	9.50	9.06	**2.23**	1.42	1.34	1.44	1.48	1.43
8	*Hemirhagerrhis kelleri*	14.70	13.10	13.50	14.86	14.05	14.21	14.58	**0.00**	1.29	1.53	1.42	1.43
9	*Mimophis mahafalensis*	14.52	13.59	14.11	14.29	16.01	16.13	15.68	13.70	**2.23**	1.39	1.48	1.35
10	*Psammophis crucifer*	15.77	16.72	16.40	16.46	18.18	17.81	17.91	16.32	15.16	**1.29**	1.50	1.46
11	*Rhamphiophis rostratus*	16.51	16.88	17.36	17.26	18.54	17.23	18.21	17.08	17.89	16.94	**2.13**	1.35
12	*R. rubropunctatus*	15.61	15.52	15.98	15.63	16.78	16.56	18.20	15.64	15.29	17.10	14.83	**NA**
	ND4												
1	*Ps. a. acutus*	**1.69**	1.27	1.28	1.30	1.16	1.25	1.28	1.34	1.35	1.49	1.43	1.44
2	*Ps. multisquamis 2 (kellyi)*	12.18	**0.94**	0.97	1.08	0.95	1.10	1.08	1.39	1.42	1.50	1.51	1.55
3	*Ps. multisquamis*	12.87	7.88	**1.93**	1.08	0.97	1.09	1.02	1.39	1.39	1.47	1.47	1.54
4	*Ps. ocellatus*	12.79	8.07	9.32	**0.13**	0.99	1.15	1.12	1.41	1.42	1.53	1.49	1.52
5	*Ps. rhombeatus*	12.52	8.81	9.81	8.89	**5.08**	0.98	0.88	1.39	1.32	1.45	1.42	1.49
6	*Ps. tritaeniatus*	12.63	9.16	10.04	9.37	9.71	**2.25**	0.98	1.40	1.37	1.48	1.50	1.56
7	*Ps. variabilis*	13.13	9.21	8.90	9.38	8.40	8.53	**2.22**	1.38	1.37	1.49	1.45	1.52
8	*Hemirhagerrhis kelleri*	14.42	14.04	14.48	14.63	15.95	15.30	14.37	**0.16**	1.42	1.47	1.55	1.42
9	*Mimophis mahafalensis*	14.68	15.93	16.51	16.30	16.13	15.75	16.16	14.57	**1.98**	1.36	1.51	1.52
10	*Psammophis crucifer*	16.47	15.42	17.85	16.72	16.84	16.85	17.07	16.55	14.95	**0.21**	1.48	1.47
11	*Rhamphiophis rostratus*	16.07	17.31	18.01	16.71	16.57	17.27	16.50	18.07	18.01	16.11	**1.75**	1.31
12	*R. rubropunctatus*	17.10	17.40	19.09	18.33	17.94	18.78	17.94	16.35	18.47	15.81	11.99	**NA**

Traditional Morphology

On the basis of skull morphology, dentition, and genetics, *Psammophylax* can be divided into two main groups: a) the '*acutus* group' — shorter skull with the rostral bones in the anterior skull weakly braced by the nasals (with only a single contact between nasal and frontal), high number of dentary teeth (21–24), and acutely pointed snout; and b) the '*Psammophylax'* group — longer skull that lacks the reinforced nasal/frontal bones, lower number of dentary teeth (15–19), and rounded snout (Tables 3.4 and 3.5).

Table 3.4: Summary of measurements and scalation data for species of the new genus and related genera (based partly on Broadley, 1971; 1977; 1983). Not Available = NA.

	Ps. a. acutus	*Ps. a. jappi*	*Ps. togoensis*	*Psammophylax* spp (excluding taxa to left).	*Rhamphiophis* spp.
Midbody scale rows (front-middle-back)	17-17-13	19-17-13	17-17-13	17-17-13	17-17-13
Ventrals + Subcaudals	216–252	249–275	236–259		
Ventrals (males/females)	168–190/155–184	186–201/181–186	173–188/171–179	139–184	148–194
Subcaudals (males/females)	58–67/53–65	71–80/66–70	61–72/63–69	49–84	87–118
Anal scale	divided	divided	divided	divided	divided
Upper labials (touching orbit)	8 (4–5)	8 (4–5)	8 (4–5) [7 (3–4)]	8 (4–5)	8 (5)
Lower labials (touching anterior sublinguals)	9–10 (4–5)	9–10 (4–5)	9–10 (4–5) [11 (4–5)]	8–12 (4–5)	10–11 (5)
Preocular	1 (rarely 2)	1	2 (rarely 1)	1	3
Postocular	2	2 (rarely 3)	2	2	2 (rarely 3 or 4)
Temporals	2+3 (rarely 2+2 or 2+4)	2+3 (rarely 1+2)	1+3, 2+3, 2+4 or 3+4	2+3 (1+2 to 3+4)	2+3 or 3+3
Maxillary teeth	9–11 + II	13 + II	NA	10–12 + II	5–8 + II
Palatine teeth	7	11	NA	9	4–5
Pterygoid teeth	9–18	11	NA	11–23	12–13
Dentary teeth	21–24	22–23	NA	15–19	15–18
Largest male	826 + 155 = 981 mm (RGMC 967)	860 + 217 = 1077 mm (UM 6804)	580 + 130 = 710 mm (S.3509/2)	1200 + 258 + * = 1458 mm (DSP 58)	1104 + 471 = 1575 mm (UM 23818)
Largest female	895 + 160= 1055 mm (Hellmich, 1957)	600 + 177 = 777 mm (FMNH 133045)	605 + 129 = 734 mm (S.4954/3	932 + 265 = 1197 mm (TM 32629)	1070 + 426 = 1496 mm (NMZ 3597)

**truncated*

Table 3.5: Measurements and scalation of *Psammophylax* species (based partly on Broadley, 1977; Branch *et al.* 2019 and this study). Not Available = NA.

	Ps. ocellatus	*Ps. rhombeatus*	*Ps. variabilis*	*Ps. multisquamis* (97 specimens)	*Ps. multisquamis 2* (12 specimens)	*Ps. tritaeniatus*
Midbody scale rows (front-middle-back)	17-17-13	17-17-13	17-17-13	17-17-13	17-17-13	17-17-13
Ventrals	156–183	143–177	149–167	160–184	161–176	139–176
Subcaudals	57–69	60–84	49–61	51–66	53–66	49–69
Anal scale	divided	divided	divided	divided	divided	divided
Upper labials (touching orbit)	8 (4–5)	8 (4–5) [rarely 7,9,10 (3–6)]	8 (4–5)	8 (4–5) [rarely 9 (5–6)]	8 (4–5) [rarely 7 (4)]	8 (4–5) [rarely 7, 9 (3–6)]
Lower labials (touching anterior sublinguals)	10–12 (4–6)	10–11 (4–5) [rarely 9, 12, 13 (6)]	10–11 (5) [rarely 8 ,9, 12 (4,6)]	10–11 (5) [rarely 9, 12 (4, 6)]	11 (5) [rarely 12 (4–6)]	9–11 (4–5) [rarely 8, 12 (6)]
Preocular	1 (rarely 2)	1 (rarely 2)	1 (rarely 2)	1 (rarely 2)	1 (rarely 2)	1 (rarely 2)
Postocular	2 (rarely 2)	2 (rarely 3)	2 (rarely 1 or 3)	2 (rarely 3)	2	2 (rarely 3)
Temporals	2+3 (rarely 2+2, 2+4)	2+3 (rarely 1+2, 1+3, 2+2, 2+4)	1+2, 1+3 (rarely 2+2, 2+3)	2+3 (rarely2+4, 2+1, 1+3)	2+3 (2+4, 2+1, 1+3)	2+3
Maxillary teeth	NA	10–11 + II	10 + II	10–11 + II	NA	10–11 + II
Palatine teeth	NA	9	9 (13 *vanoyei*)	9	NA	9
Pterygoid teeth	NA	11–16	17–23	15	NA	20–22
Dentary teeth	NA	16–18	16	15/17	NA	18–19
Largest male	720 + 155 = 875 mm (MBL 1724)	1200 + 258 = 1458 mm* (DSP 58)	835 + 167 = 1002 mm (TM 16556)	995 + 165 = 1160 mm (FMNH 12513)	480 + 121 = 601 mm (AMNH 50585)	734 + 151 = 885 mm (NMSR 2988)
Largest female	480 + 110 = 590 mm (SAM/ZR 46424)	932 + 265 = 1197 mm (TM 32629)	620 + 149 = 769 mm (IRScNB 9602a)	743 + 149 = 892 mm (PEM R23921)	744 + 168 = 912 mm (PEMR 23924)	700 + 155 = 855 mm (IRScNB 5117c)

**truncated*

Geometric Morphometric Analyses

In the generic-level analyses, the first dorsal PC (DC-PC1) axis contrasted head width, snout length, and parietal scale dorsoventral length, describing 53.5% of total variation, whereas

DC-PC2 contrasted the length of the frontal scale and the length of the snout, contributing 12.9% of the variation (Fig. 3.6). DC-PC3 contributed only 6.3% of total variation, and contrasted width of the mid-snout region (Fig. 3.6). The first lateral PC axis (LC-PC1) contrasted head height and length of the upper labial (lip), and the length of the rostral scale, describing 45.5% of total variation (Fig. 3.7). LC-PC2 described 12.8% of variation, and contrasted the length of the upper labial scales (mouth length) and position of the juncture between the upper labial scales below the eye (landmark 6) (Fig. 3.7). LC-PC3 described only 9.7% of the variation and contrasted posterior head height, as well as overall snout length (Fig. 3.7).

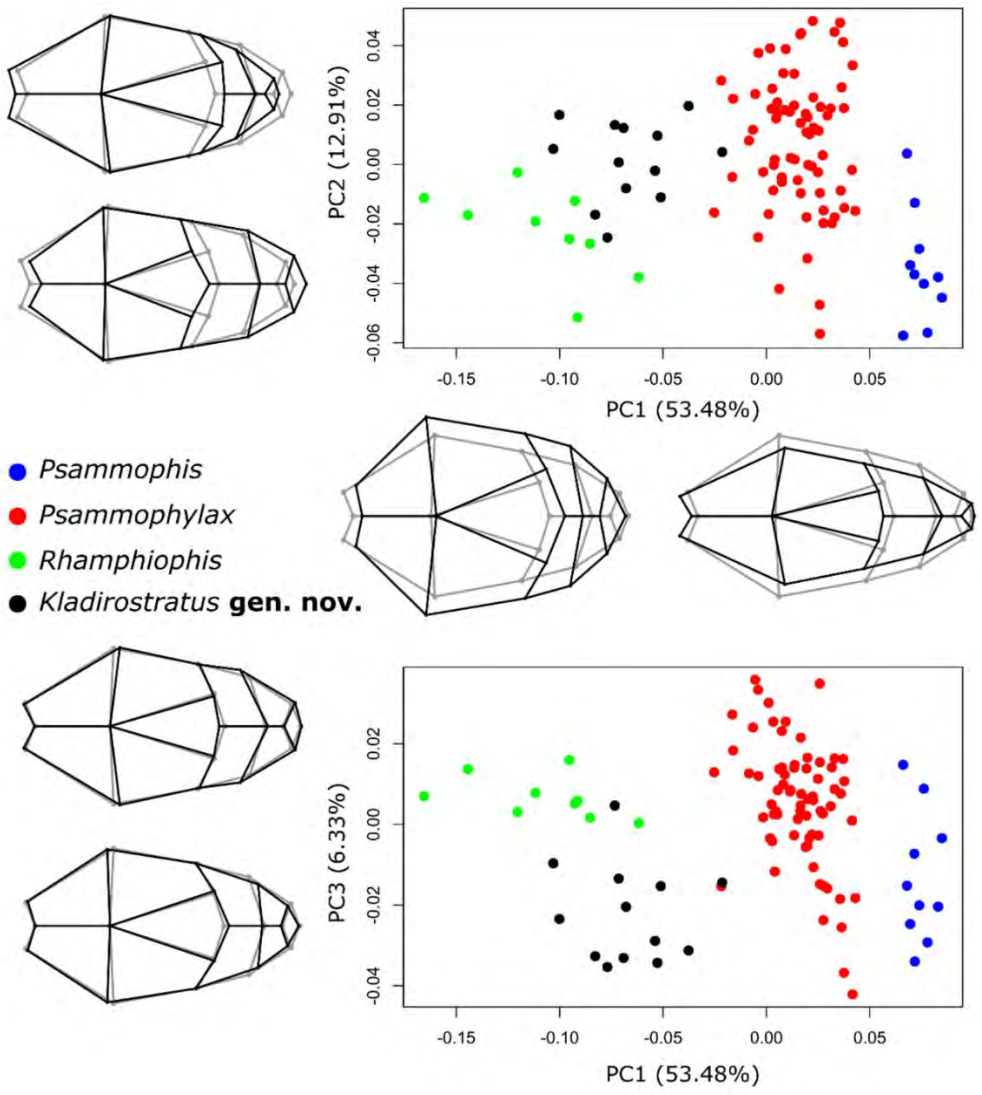

Figure 3.6: Geometric morphometric analyses of the dorsal view of the heads of *Kladirostratus* gen. nov. (members of the *'acutus* group'), *Psammophis, Psammophylax* (excluding members of '*acutus* group') and *Rhamphiophis* (see inset key for colours). Warped outline diagrams (in black lines) to the left and below the scatterplots of the principal component scores for the first three PC axes, represent the shape changes at the positive and negative extremes of each axis. The grey configurations are the mean shapes.

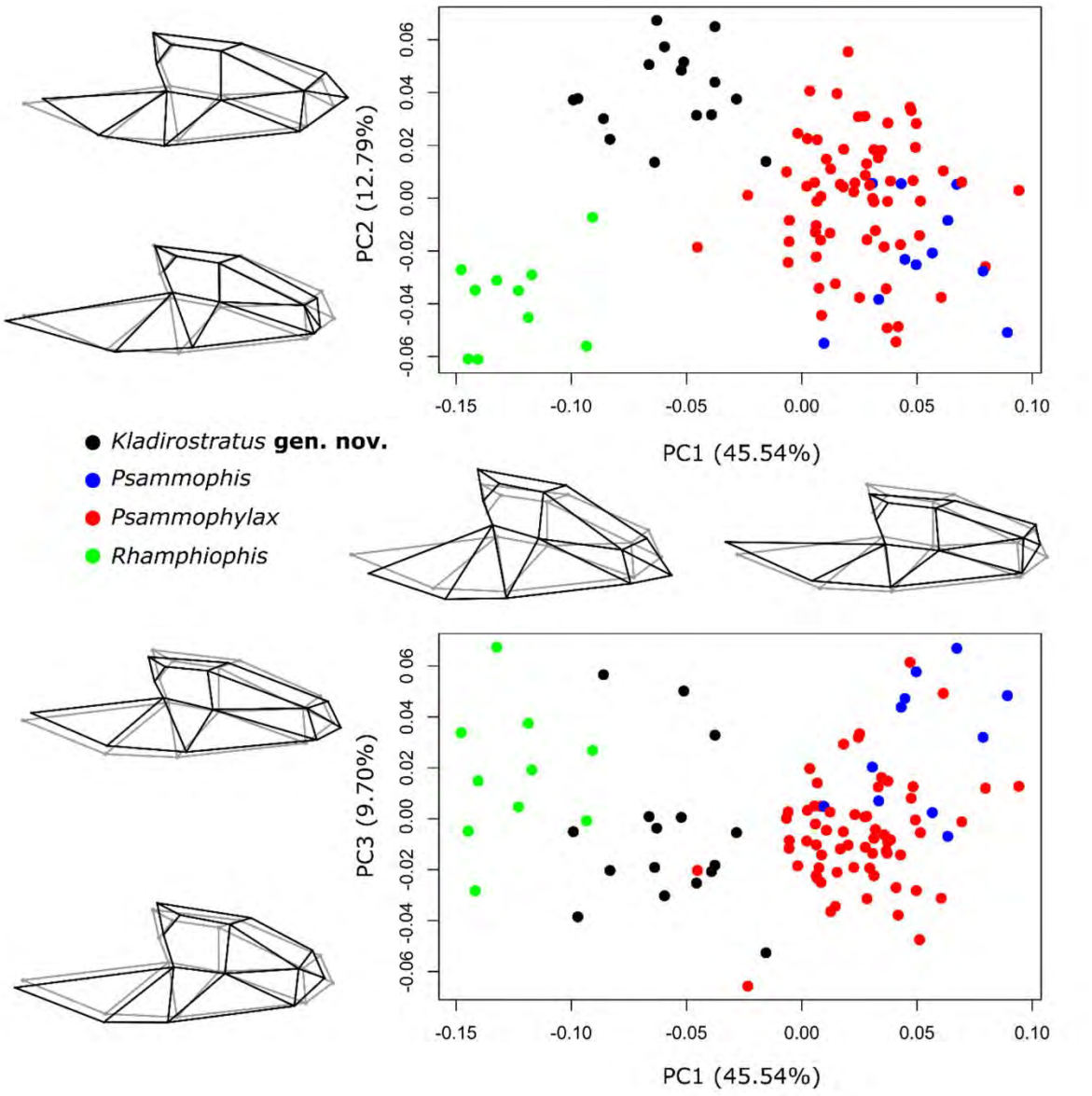

Figure 3.7: Geometric morphometric analyses of the lateral view of the heads of *Kladirostratus* gen. nov. (members of the *'acutus* group'), *Psammophis, Psammophylax* (excluding members of '*acutus* group') and *Rhamphiophis* (see inset key for colours). Warped outline diagrams (black lines) to the left and below the scatterplots of the principal component scores for the first three PC axes represent the shape changes at the positive and negative extremes of each axis. The grey configurations are the mean shapes.

The representatives of the four putative genera investigated (*Psammophylax acutus*, *Psammophis*, *Psammophylax*, and *Rhamphiophis*) all differed significantly from one another in the DC-PC1 (ANOVA: $F_3 = 239.44$, $p < 0.0001$; HSD test: all p-values < 0.0001; Table S3.4) and in the LC-PC1 (ANOVA: $F_3 = 169.02$, $p < 0.0001$; HSD test: all p-values < 0.0001; Table S3.4). *Rhamphiophis* had the widest head, with the shortest, widest snouts (negative DC-PC1 scores; Fig. 3.6) and the highest head, with shortest upper-lip length (negative LC-PC1 scores; Fig. 3.7). *Psammophis* had the narrowest head with a long, narrow snout (positive DC-PC1

scores) and the flattest head, with the narrowest line of upper labial scales (positive LC-PC1 scores; Fig. 3.7). *Psammophylax acutus* was significantly different from *Psammophylax* and *Rhamphiophis* in both the dorsal and lateral views (Table S3.4), with head widths, snout widths, and head heights intermediate between those of the other two genera (Figs 3.6 and 3.7). These genera also differed significantly on the DC-PC2 axis (ANOVA: $F_3 = 15.47$, $p < 0.0001$), but *Ps. acutus* did not differ from *Psammophylax*, nor did *Psammophis* differ from *Rhamphiophis* on this axis (Table S3.4), indicating that *Ps. acutus* had a shorter snout relative to *Rhamphiophis* and *Psammophis*, but had snout lengths and widths similar to those of *Psammophylax* (Fig. 3.6). All genera differed in the LC-PC2 axis (ANOVA: $F_3 = 30.97$, $p < 0.0001$), but *Psammophis* did not differ significantly from *Rhamphiophis* (Table S3.4). This axis showed that, relative to the other genera, *Psammophylax acutus* had a shorter length from the back of the orbital scales (landmark 12) to the joint of the labial scales at the back of the mouth (landmark 8), the sharpest rostral scale, and upper labial scales in a more posterior position (landmark 6). Four of the six comparisons were significant on the DC-PC3 axis, though this axis accounted for a mere 6.3% of the total variation. Finally, on the LC-PC3 axis, there were significant differences between the genera (ANOVA: $F_3 = 9.09$, $p < 0.0001$), corroborating the signal from LC-PC1 showing that *Psammophis* has a significantly flatter head than *Ps. acutus* and *Psammophylax* (Fig. 3.7).

Regarding the interspecific comparisons within *Psammophylax*, the six tentative species (excluding *Ps. acutus*) exhibited no significant differences in head shape on DC-PC2 (ANOVA: $F_5 = 1.41$, $p = 0.23$), LC-PC1 (ANOVA: $F_5 = 1.95$, $p = 0.10$), LC-PC2 (ANOVA: $F_5 = 1.50$, $p = 0.21$), or LC-PC3 (ANOVA: $F_5 = 0.74$, $p = 0.60$). The few significant comparisons on the remaining two PC axes all involved *Ps. tritaeniatus*; DC-PC1 (ANOVA: $F_5 = 4.53$, $p = 0.001$) showed that *Ps. tritaeniatus* differs significantly from *Ps. multisquamis* 2 and *Ps. variabilis* (Table S3.4), and DC-PC3 (ANOVA: $F_5 = 4.18$, $p = 0.003$) showed that *Ps. tritaeniatus* differs significantly from both *Ps. multisquamis* 1 and *Ps. multisquamis* 2 (Table S3.4). Overall, the interspecific morphometric results indicated that *Ps. tritaeniatus* is morphologically distinguished by a shorter upper jaw (because of shorter length of upper labials; negative LC-PC1 scores; Fig. S3.1), a more ventrally oriented positioning of the back of the mouth (landmark 8; positive LC-PC3 scores; Fig. S3.1), and a wider mid-snout and mid-head (positive DC-PC1 scores and negative DC-PC3 scores; Fig. S3.2). *Psammophylax multisquamis* 1 and *Ps. multisquamis* 2 did not differ in head shape in these analyses, but neither did most of the other *Psammophylax* species, indicating that this genus has a conserved head shape.

Taxonomic Changes

Given the phylogenetic results and the morphological distinction between *Psammophylax acutus* and the remaining *Psammophylax* species (see Tables 3.3 and 3.4, and discussions above), I recognise two genera and take this opportunity to describe a new genus for the '*acutus´* group. In addition, although not well-supported by traditional morphology or geometric morphometric analyses, the polyphyly of *Ps. multisquamis* was addressed and *Ps. multisquamis* 2 was described as a new species. The species descriptions from Keates et al. (2019) have been attached below, with minimal alterations (p-distance values changed marginally) to the original text.

Species Descriptions

***Kladirostratus* gen. nov. Conradie, Keates & Edwards 2019**

Proposed common group name: Branch's Beaked Snakes

Type species: *Psammophis acutus* Günther 1888

Etymology: The name *Kladirostratus* is derived from the combination of the Greek word κλάδος (klados) meaning 'branch', and the Latin word 'rostratus' meaning beaked. The name honours Professor William R. Branch (1947–2018), Curator Emeritus of herpetology at Port Elizabeth Museum, in recognition of his many contributions to the field of herpetology of Africa, especially regarding snakes. We benefitted from his generosity as a mentor and he helped shape our careers, for which we are thankful. The name is masculine in gender.

Generic diagnosis: The rostral bones are weakly braced by the nasals, with only a single contact between nasal and frontal (well-developed in *Rhamphiophis* with a double nasal-frontal contact and the prefrontal extensively overlaps the nasal; lacking in *Psammophylax*); higher number of dentary teeth (21–24 versus 15–19 in *Psammophylax* and 15–18 in *Rhamphiophis*); acutely pointed snout (hooked in *Rhamphiophis* and rounded in *Psammophylax*). Average sequence divergence of *Kladirostratus* from *Psammophylax* species was 12.12 ± 0.55% and 12.69 ± 0.33% for cytb and ND4, respectively.

Generic description: Shortened skull with rostral bones weakly braced by the nasals, with only a single contact between nasal and frontal. The maxilla bears 9–13 subequal teeth that increase in size gradually anteriorly, separated by a small diastema from two enlarged grooved fangs on the posterior end of the bone; palatine teeth 7–11; pterygoid 9–18; dentary 21–24. Snout short and acutely pointed, rostral tetrahedral. Eight upper labials with 4th and 5th entering the orbit; 9–10 (rarely 11) lower labials with the first 4–5 in contact with the anterior sublinguals; one or two preoculars, usually separated from the frontal; 2 (rarely 3) postoculars; temporals 2+3 (rarely 1+2, 2+2, 2+4, 1+3, 3+4). Body rounded and smooth; dorsal scales smooth, with single apical pits; 17 scale rows at midbody; total ventrals + subcaudals 216–275; paired

subcaudals 58–80 (males) and 53–71 (females), anal shield divided. Maximum size 1077 mm total length (males) and 1055 mm total length (females). Hemipenis short and smooth. Two longitudinal dorsolateral stripes, one on each side of body extending from the front of the head through the eye to the base of the tail; a thin black ventrolateral stripe is characteristic of *togoensis*.

Members of this genus: *Kladirostratus acutus* (Günther, 1888) **comb. nov**. including the currently recognised subspecies *Kladirostratus a. acutus* and *Kladirostratus a. jappi* (Broadley, 1971); *Kladirostratus togoensis* (Matschie, 1893) **comb. nov**. The latter is provisionally included in this genus based on morphological similarities, but this requires confirmation through molecular phylogenetic analysis**.**

Distribution: *Kladirostratus a. acutus* **comb. nov.** is known from most of Angola through north-western Zambia, southern Democratic Republic of the Congo (DRC) into western Tanzania, northern Malawi, and north to Rwanda (*fide* Broadley, 1971). *Kladirostratus a. jappi* **comb. nov.** is known only from western Zambia and north-eastern Angola (*fide* Broadley, 1971). *Kladirostratus togoensis* **comb. nov.** is known from Ghana, Togo, Central African Republic, northern DRC and western Uganda (*fide* Broadley, 1971; Spawls *et al.* 2018). Occurs at elevations of 450–1800 m.

***Psammophylax kellyi* sp. nov. Conradie, Keates & Edwards 2019**

Fig. 3.1 I & J

Proposed common name: Tanzanian Grass Snake or Tanzanian Skaapsteker

Synonymy*: Psammophylax multisquamis* in part (Boulenger, 1896: 140; Loveridge, 1923: 882; Loveridge, 1932: 84 (Mpwapwa paratypes); Broadley, 1977: 30; Spawls *et al.,* 2002, 2018).

Holotype*:* PEM R23926 (CMRK 401, adult female) collected 17 July 2003, Arusha Region near Oldonyo Sambu, on the foothills of Mount Meru (-3.17° S; 36.68° E, ~1850 m a.s.l.), northern Tanzania. Collected by Christopher R. Kelly.

Paratypes (six specimens): a) PEM R23924 (CMRK 296) collected in 2002 by staff of Meserani Snake Park, Arusha Region; PEM R23925 (CMRK 328) (juvenile) collected 26 April 2003, locality as holotype; PEM R23927 (CMRK 402) collected 18 July 2003, locality as holotype; PEM R23930 (CMRK 333) collected 1 May 2003, near Oldonyo Sambu (-3.15° S; 36.69° E, ~1750 m a.s.l.). b) PEM R23928 (CMRK 404) collected 20 July 2003, Ngorongoro Conservation Area, near Ngorongoro town (-3.23° S; 35.41° E, ~2358 m a.s.l.); PEM R23929 (CMRK 405) collected 21 July 2003, Ngorongoro Conservation Area, Ngorongoro airstrip (-3.22° S; 35.48° E, ~2365 m a.s.l.). All collected by Christopher R. Kelly, except PEM R23924.

Additional material examined: CMRK 297, Arusha Region (head only), same details as PEM R23924.

Etymology. The specific epithet is a patronym in honour of Christopher M. R. Kelly for his considerable contribution to the systematics of the snake family Lamprophiidae.

Diagnosis. Snout rounded (pointed in *Ps. tritaeniatus*), supralabials with dark (usually rust-coloured) spots (immaculate in *Ps. tritaeniatus*), no spots on the nape, sometimes forming longitudinal lines (present in *Ps. rhombeatus* and *Ps. ocellatus*), rostral broader than deep, never separating the internasals (in *Ps. rhombeatus* the rostral is usually as deep as wide and sometimes separating internasals), tail length/total length ratio less than 21% (larger than 21% in *Ps. rhombeatus*), usually two anterior temporals with more than 163 subcaudals (usually one anterior temporal in *Ps. variabilis* with fewer than 163 subcaudals), ventrum light grey or white (dark grey in *Ps. variabilis*). Apparently indistinguishable from southern Kenya *Ps. multisquamis* (Fig. 3.1G and 3.1H) in dorsal colouration—both populations exhibit the pattern illustrated in Broadley (1977: Fig. 7A). Distinguished from Ethiopian *Ps. multisquamis* (Fig. 3.1F), in which the vertebral line is often poorly defined or absent. Scalation and morphometrics (traditional and geometric morphometrics) appear to be unreliable diagnostic tools because of considerable overlap between *Psammophylax* species (Table 3.5). *Psammophylax kellyi* **sp. nov.** (Tanzania) and *Ps. multisquamis* (Kenya/Ethiopia) are allopatric, whilst the Ngorongoro population of *Ps. kellyi* **sp. nov.** is apparently sympatric with *Ps. variabilis* (see PEM R23970/CMRK 403). Average sequence divergence between *Ps. kellyi* **sp. nov.** and other *Psammophylax* species was 7.77 ± 0.94% and 8.63 ± 0.62% for cytb and ND4, respectively.

Description of holotype: Body elongated, robust, tapering gradually to a short tail (tail length 19% of total length, but truncated). Dorsal scales smooth with no apical pits and in 17-17-13 scale rows; 171 ventrals; anal divided; 60+ subcaudals (tail truncated). Narrow pointed head indistinct from the neck and the rest of the body; snout rounded and about half as long as horizontal diameter of orbit (ED/SD = 0.55), rostral clearly visible from above and below, slightly broader than deep (3.5 x 2.6 mm); prenasals pointed anteriorly and postnasals as long as wide; prefrontals as long as wide, which are in broad contact laterally with loreal; frontal pentagonal, longer than wide (6.9 x 3.1 mm), slightly inserting posteriorly between very large parietals; no supraocular; small nasal shield divided by pre- and postnasals, in contact with 1st and 2nd supralabials; loreal as long as wide, in contact with the postnasal, the 2nd and 3rd supralabial below and the prefrontal above, but excluded from orbit by the single preocular, which is well-separated from the frontal; postoculars 2, the lower slightly longer than upper and in contact with 5th and 6th supralabials; temporal arrangement is 2+3 (on left side the upper 1st temporal is divided into two subequal smaller scales); supralabials 8/8, with the 4th and 5th entering the orbit; infralabials 11/11, the first 5 in contact with anterior sublinguals, 1st

infralabials touching each other; two pairs of elongated sublinguals, equal in size; mental small and triangular. Eye medium in size, vertical diameter equal to the distance from orbit to upper lip, and with a round pupil. Size: 685 mm snout-vent length + 161 mm tail length (truncated) = 846+ mm total length. ***Colouration*.** See Fig. 3.1J (holotype, preserved), Fig. 3.1I (paratype, live). In life, the holotype was very similar in colouration to the paratype illustrated in Fig. 3.1. Head is uniform brown above with a few black flecks, darkening posteriorly with the gradual emergence of a dark brown vertebral stripe. Lateral darker brown facial mask extends from nostril, through the eye onto the body; supralabials cream-white with black dorsal edging, and faint grey blotches (rusty orange in life) beginning on the upper half of each scale and extending ventrally to the edge of the mouth. The lateral head patterning (dark brown mask and supralabial pattern) extends seamlessly backwards onto the body. Dorsum striped, with stripes extending to the tail tip and pattern resembling the illustration in Broadley (1977: Fig. 7A). Vertebral scales black with pale cream central vertebral line; paravertebral scale rows russet-brown with each scale black-tipped and scales paler on their lateral edges (especially towards the tail). The vertebral and two paravertebral scale rows form a brown vertebral stripe that extends from the back of the head to the tail tip. The next two lateral scale rows (becoming one on the tail) are beige-tan, forming a pale dorsolateral stripe that extends on each side of the body from the back of the head to the tail tip. The next 3.5 scale rows (becoming 2.5 posteriorly and finally reducing further on the tail) form an extension of the dark brown facial mask that stretches to the tail tip as a brown dorsolateral stripe on each side of the body. The fourth scale row from the vertebral midline forms the dorsal (upper) boundary of this stripe; each scale is black, with a white dorsal edge (pale orange in life). Scales of the fifth and sixth rows are uniform brown, with slightly darker brown posterior edges. The upper half of the seventh scale row forms the lateral (lower) boundary of the dorsolateral stripe; scales in this row are divided linearly into a black upper half (dark brown at the base of each scale) and a white lower half. In life, a thin, diffuse pale orange boundary between black and white gives the effect of an orange lateral edging to the dorsolateral stripe. The eighth scale row (bordering the ventrals) is white, with a grey streak along the midline of each scale (rusty orange in life) forming a grey (rusty orange) lateroventral line along body, just above “ground level”. Ventrum immaculate cream-white coloured with darker lateral blotches (rust-coloured to dull orange-grey in life); throat cream (between infralabials and first ventral scale) with very faint grey speckling (dull orange-grey in life).

Variation. All paratypes agree in general appearance and morphology with the holotype, and variation in scalation is summarised in Table S3.3. PEM R23929 has an extra scale between the frontal and prefrontals. All specimens have very similar dorsal and ventral colouration to the holotype when preserved, and in life (based on specimens seen before preservation). PEM R23928 and PEM R23929 (from Ngorongoro) have distinct faint black spots on infralabials,

sublingual scales and smaller scales between infralabials and first ventral scale. The remaining specimens have only faint speckling on the throat (dull orange-grey in life).

Size. Largest female (PEM R23924) 744 mm snout–vent length + 168 mm tail length = 912 mm total length; largest male (AMNH 50585) 480 + 121 = 601 mm.

Distribution and habitat. Known from only a few localities in northern Tanzania: Tindi (Bogert, 1940), Arusha (Loveridge, 1923), Mpwapwa (Boulenger, 1896), Oldonyo Sambu (Spawls *et al.,* 2018; this study) and Ngorongoro Crater Highlands (this study). Spawls *et al.* (2018) listed some additional localities from the Serengeti in the west to Mt. Kilimanjaro in the east, which we tentatively refer to the new species based on close geographic proximity to our material (Loitokitok, Oldonyo Sambu, Moshi, Chyulu Hills, Mtito Andei and Voi). A specimen from Gabiro (Rwanda) which may be referable to *Ps. kellyi* **sp. nov.** is reportedly uniform grey above and might instead be an atypical *Ps. multisquamis* (Broadley, 1977; de Witte, 1933), but this would need verification. Found in open grassland in the highlands of northern Tanzania above 1700 m a.s.l. (Spawls *et al.,* 2018; this study)

Biology. Three young mice were found in the stomach of the Tindi specimen (Bogert, 1940), and the Arusha specimen had an unidentified skink in its stomach (Loveridge, 1923). One of the paratypes (PEM R23925; CMRK 328) regurgitated the remains of a chameleon after being captured.

Discussion

The phylogeny presented here represents the most comprehensive genetic study of the genus thus far, including all but one of the currently recognised species of *Psammophylax* and several subspecies. Because of small sample sizes, past studies of the genus lacked the support necessary to elucidate interspecific relationships within the genus with confidence (Figueroa *et al.*, 2016; Kelly *et al.*, 2008; Pyron *et al.*, 2013; Zaher *et al.*, 2019). The increased sample size in this study, coupled with gene-specific evolutionary model partitioning, has resulted in a highly supported and robust topology. These analyses have also resolved the polytomy found in Kelly *et al.* (2008) by showing that *Ps. tritaeniatus* is sister to *Ps. multisquamis* + *Ps. variabilis*. Whilst Zaher *et al.* (2019) and Chapter Two (Figs 2.3 and 2.4) recovered similar topological structuring to this chapter, the robust, genus-specific approach of this chapter resulted in the resolution of almost all the intra-generic relationships within *Psammophylax*, with support.

Whilst this chapter retrieved BI support for the sister relationship between *Ps. ocellatus* and *Ps. rhombeatus*, both the phylogenetic tree (Fig. 2.3) and time-calibrated phylogeny (Fig. 2.4) from Chapter Two retrieved support for a sister relationship between *Ps. ocellatus* and

the rest of *Psammophylax* (barring *Ps. kellyi*). Whilst the conflicting findings of Chapter Two and Three conflated my ability to place *Ps. ocellatus* within the genus, they did allow me to disprove the results of Branch *et al.* (2019), given the lack of support for the sister relationship between *Ps. ocellatus* and *Ps. multisquamis* in that paper. My analysis retrieved a substantial amount of sub-structuring within *Ps. rhombeatus,* with four clades (with varying support) being identified both within this chapter and Chapter Two. These findings coupled with the results of the pairwise distance and multilocus species delimitation analyses in this thesis makes the Southern African endemic a viable candidate for a species-specific phylogeographic study. The species is discussed further in Chapter Four.

Kladirostratus [= *Psammophylax*] *a. acutus* **comb. nov.** was recovered as the most divergent species within the genus, a result shared by various past studies (Figueroa *et al.*, 2016; Kelly *et al.*, 2008; Pyron *et al.*, 2013; Zaher *et al.*, 2019). The species was originally considered to be a beaked snake (*Rhamphiophis*) because of its reinforced head and pointed snout, which it uses for digging (Broadley, 1971; Spawls *et al.*, 2002, 2018). However, this trait has since been considered convergent, and therefore homoplasic, because *K. a. acutus* **comb.** forms a sister relationship with *Psammophylax* (Figueroa *et al.*, 2016; Kelly *et al.*, 2008; Zaher *et al.*, 2019) rather than grouping with *Rhamphiophis*. Whilst not at the sequence divergence level of *H. kelleri* and the other outgroup genera, *K. a. acutus* **comb. nov.** is genetically and morphologically distinct from *Psammophylax.* In keeping with the recent work of Broadley *et. al.* (2018), in which separate file snake genera differed by uncorrected cytb p-distances of 8.6% —13.0%, the 12.12% average uncorrected cytb p-distance, separating *K. a. acutus* **comb. nov.** from *Psammophylax,* was considered worthy of genus-level taxonomic recognition.

In addition, this phylogeny suggested that there was a previously unrecognised species of *Psammophylax* among our samples. Increased sampling in eastern Africa resulted in the recovery of *Ps. multisquamis* as polyphyletic, currently including a Tanzanian clade, which is basal within the genus (*Ps. kellyi* **sp. nov.**), and a Kenyan/Ethiopian clade, which is terminal within the genus (*Ps. multisquamis* sensu stricto). These two clades of *Ps. multisquamis* were previously considered geographically distinct (Spawls *et al.*, 2002), but recent findings have shown that the two “populations” are continuous (Spawls *et al.*, 2018).

Geography cannot easily explain the new-found species, as the two clades are not sister to one another and thus are not the product of allopatric speciation. Rather, convergent evolution may be the underlying mechanism explaining the similar morphologies observed in the two species (Gittenberger 2004; Losos 2011). Alternatively, this similarity may be the product of both organisms retaining the morphological characteristics of an ancestral species,

much like salamanders and lizards have retained a similar body plan (Benton, 1997; Revell *et al.*, 2007). Convergent evolution can confound conventional taxonomists because genetically divergent clades can overlap both geographically and morphologically, leading to unappreciated species diversity (Gittenberger, 2004; Losos, 2011).

Mimophis mahfalensis, a widespread Malagasy snake, was recently split into two species based on molecular evidence (Ruane *et al.,* 2018), even though the three distinct colour/pattern forms are known for both species (Ruane *et al.,* 2018). Within *Ps. variabilis, Ps. rhombeatus* and *Ps. multisquamis*, there is substantial intraspecific colour and pattern variation, suggesting that these characters are labile and therefore unsuitable for use in species delineation within *Psammophylax*, much like in *Mimophis* (Broadley, 1977; Ruane *et al.,* 2018; Spawls *et al.,* 2018). Evidenced in Trape *et al.* (2019) and corroborated in Chapter Two of this thesis (Fig. 2.3), specimens of *Psammophis mossambicus* from central Africa also displayed marked pattern polymorphisms, but with little to no genetic difference between morphologically and geographically disparate samples of the same species. This highlights the cryptic nature of variation within Psammophiidae, across the entire distribution of the family.

The use of geometric morphometric analysis successfully distinguished *K. a. acutus* **comb. nov.** from *Psammophylax*, corroborating its position as sister to *Psammophylax.* The analysis could not, however, accurately separate species within *Psammophylax*. Unlike *K. a. acutus* **comb. nov.**, which has an acutely pointed snout, the head structure within *Psammophylax* is a potentially more conservative trait, and it is possible that the morphometric analyses used were not robust enough to tease out subtle differences between the species. The use of different landmarks, a more refined morphological analysis, or alternatively the analysis of different morphological features, may rectify this shortcoming.

East Africa harbours an impressive diversity of herpetofauna, partly because of the complexity of the topographical and climatic features in the region (Spawls *et al.,* 2018). The Great Rift Valley (Greenbaum *et al.*, 2012, 2013, 2015; Portillo *et al.*, 2015) and the Eastern Arc Mountains and associated forest-covered mountain ranges of Tanzania have been the theatre for speciation for several reptile and frog species complexes (Barej *et al.*, 2014; Branch, 1998; Kelly *et al.*, 2008; Loader *et al.*, 2014; Menegon *et al.*, 2009; Portillo *et al.*, 2018; Spawls *et al.*, 2018). Approximately 25–30 million years ago, these mountain ranges uplifted along ancient fault-lines, creating densely forested refuges, which currently harbour high levels of (largely) vicariance-driven endemism and diversity (Roberts *et al.*, 2012). Several species of squamates, including the centipede-eating snake *Aparallactus jacksonii* (Portillo *et al.,* 2018), vipers of the genus *Atheris* (Menegon *et al.*, 2014), and chameleons of the genus

Kinyongia (Hughes *et al.*, 2017; Menegon *et al.*, 2009; Tolley *et al.*, 2011) seem to have speciated because of episodic contact and separation of montane forest in the Eastern Arc Mountains. Unlike forest-dependent species, grassland taxa such as *Psammophylax kellyi* **sp. nov.** might have originated because of the expansion of forests, thereby creating barriers for grassland adapted species. The origins of *Ps. kellyi* **sp. nov.** and the selective pressures that drove its speciation are, however, at best speculative given our current dataset.

The various species delimitation methods revealed substantial genetic structuring within most species of *Psammophylax*. Putative taxa within the genus ranged from four to 31 species, indicating that current taxonomy both severely underestimates and overestimates species diversity. It is hypothesised that much of the interspecies diversity identified in this chapter is confounded intraspecific diversity because of the age of the genus. Whilst the genus split from *K. a. acutus* approximately 10 million years ago (MYA) (Chapter Two: Table 2.4), the genus did not diverge until approximately 5 MYA, with every species within the genus diversifying during the Pleistocene (Chapter Two: Fig. 2.4; Table 2.4). Given that no putative taxa were identified as emerging after the Pliocene, in Psammophiidae (Chapter Two), it is improbable that any of the putative taxa identified in Fig. 3.5 represent novel species given their recent origins. Threshold-based delimitation analyses are based on relativity and given the taxon-specific focus of this chapter, it is likely that much of the intraspecies observed in *Psammophylax* was confounded for interspecies diversity given the lack of comparable species-level divergences within the phylogeny. Irrespective of these assertions, the lack of supporting evidence necessitates the recognition of the putative taxa, from Fig. 3.5, as unconfirmed candidate species (UCS) (Padial *et al.*, 2010). Future studies should thus treat these unconfirmed candidate species as hypothesis that need to be tested (Hillis, 2019). If future studies cannot find evidence enough to warrant taxonomic re-evalauation, the putative taxa, identified here, can be considered deep conspecific lineages (DCL) (Padial *et al*., 2010).

Whilst the taxon-specific focus produced more defensible conclusions about population structuring within the genus, it also highlighted the caveats of threshold-based species delimitation analyses, with the number of samples, choice of loci, and presence of distantly related outgroup taxa having profound effects on species delimitation. For this reason, the multiple species groupings identified across the various species delimitation analyses (Fig. 3.5) are regarded as instances of intraspecies diversity, as opposed to indicators of species-level divergence, in this chapter.

Albeit likely a product of intraspecies divergence, the species-level split between Ngorongoro and Arusha *Ps. kellyi,* as evidenced by PTP and bPTP analysis, is interesting to note, as a similar relationship was found by Medina *et al.* (2016). Their analyses detected two

new cryptic species of *Panaspis* separated by the Great Rift Valley, with one species found in Arusha and the other in Klein's Camp in Serengeti National Park, close to Ngorongoro. Their study (like mine) revealed strong phylogenetic support for cryptic species-level lineages that are grassland and open-habitat adapted, lending credence to the idea that grassland-adapted taxa may have speciated through grassland contraction and isolation. *Psammophylax variabilis* and *Ps. tritaeniatus* have substantially larger ranges than *Ps. kellyi* **sp. nov.** (Spawls *et al.*, 2018), yet neither of them yielded structuring enough to warrant taxonomic re-evaluation. We included two samples (EBG 2611 and EBG 2425) that were morphologically consistent (e.g., two anterior temporals, high number of ventrals) with *Psammophylax variabilis vanoyei* (Fig. 3.1D) from approximately 37 km north-west of the Blukwa type locality in the Lendu Plateau (Laurent, 1956). Unlike *Ps. ocellatus*, which was recently split from *Ps. rhombeatus* and afforded species-level status (Branch *et al.,* 2019), *Ps. v. vanoyei* lacks sufficient genetic differentiation to warrant species-level recognition (Fig. 3.4). It is recommended that this subspecies subsumed into *Ps. variabilis* and henceforth be referred to as a morphotype of this species. Laurent (1956) also described *Ps. tritaeniatus festivus* from the Kundelungu Plateau, and *Ps. tritaeniatus subniger* (Fig. 3.1E) from Kipiri (Marungu Plateau), both of which are located in south-eastern DRC. Broadley (1977) treated the former subspecies as a junior synonym of *Ps. variabilis*, but I lacked topotypic material and could therefore not evaluate its specific status. I further lacked topotypic material of *Psammophylax tritaeniatus fitzgeraldi* (Broadley, 1960) from Mbala, Zambia, and could not assess its specific status, and thus it should remain a junior synonym of *Ps. tritaeniatus*. However, the collection localities of Pepa and Kyalengwe on the Marungu Plateau (yielding samples EBG 2890, EBG 2943, EBG 3006) are approximately the same elevation and only 11–17 km south-west of the Kipiri type locality of *Ps. t. subniger* (see Dowsett & Prigogine, 1974). Voucher specimens of the latter samples are consistent with the morphological diagnosis (e.g., low number of subcaudals) of *Ps. t. subniger* provided by Laurent (1956). The samples attributable to *Ps. t. subniger* were recovered as genetically similar to *Ps. variabilis* in this chapter, thus supporting Broadley's (1977) decision to synonymise *Ps. t. subniger* with *Ps. variabilis*. Because of difficulties associated with fieldwork in eastern DRC (Greenbaum, 2017), it is likely that genetic samples from the above, unsampled topotypic populations will be difficult to obtain for many years, rendering the taxonomic placement of some taxa described by Laurent (1956) as unresolved.

Chapter Four: Phylogeographic Structuring in a Widespread Grass Snake (Lamprophiidae: *Psammophylax rhombeatus*)

Introduction

Sub-Saharan Africa has been a theatre for broad-sweeping climatic and environmental change, with the displacement of woodland/forest habitat towards the end of the Paleogene (66–23 MYA) (Kissling *et al.*, 2012; Linder, 2017). Through the Oligocene and early Miocene, the tropical climate that dominated much of Africa dried, resulting in the contraction of forest and the proliferation of desert habitats, north and south of the newly formed Sahara Desert (Kissling *et al.*, 2012; Linder, 2017). During the late Miocene (10 MYA), open habitats expanded as the levels of precipitation decreased and C4 plant-dominated ecosystems became more widespread. This trend continued through the Plio-Pleistocene (2.8–1.0 MYA) resulting in further open landscape expansion and the contraction of forest/woodland (Kissling *et al.*, 2012; Linder, 2017).

Climatic fluctuations can be catalysts for evolutionary change, promoting diversification and adaptation to new environmental conditions (Barlow *et al.*, 2019; Kulenkampff *et al.*, 2019; Smit *et al.*, 2011; Tolley *et al.*, 2006, 2016). Climatic shifts drive speciation through the creation of vicariant barriers or through the creation of habitat heterogeneity, resulting in diversification (e.g. Bauer, 1999; Wiens, 2004).

In the past 2–3 million years, birds, hominids, and African bovids have spread and diversified, with environmental shifts towards cooler, drier conditions (Branch *et al.*, 2006). Cladogenesis within the *Bitis* subgenus *Calechidna* corresponds with the aridification of southwestern Africa, and associated changes in environmental conditions, resulting in a rich diversity of species within the taxon (Barlow *et al.*, 2019). Much like *Calechidna*, speciation within the southern African elephant shrews (*Elephantulus* sp.) seems to be coincidental with the proliferation of the C4 grasses in the late Miocene, with rocky outcrops, in arid regions being hotspots for diversity (Smit *et al.*, 2011). More specifically, the rapid cooling and concurrent aridification of the last Pleistocene, coupled with multiple local-scale ecological gradients resulted in the creation of a global diversity hotspot in the Cape Floristic Region (CFR) (Broadley, 1990; Pirie *et al.*, 2016; Swart *et al.*, 2009; Tolley *et al.*, 2009). Cicada (*Platypleura stridula* species complex) diversity flourished during the Plio-Pleistocene with the spread of fynbos (open vegetation) (Price *et al.*, 2007). There are ca. 100 species of lizards associated with the CFR, of which, 20% are endemic to the region, with *Agama atra*, several

clades of *Bradypodion, Pedioplanis burchelli* and multiple cordylid species geographically converging in the west (Daniels *et al.*, 2004; Swart *et al.*, 2009; Tolley *et al.*, 2009).

Within southern Africa, recent work has shown a high amount of diversity within the arboreal *Bradypodion* genus (Tolley *et al.*, 2006, 2008, 2009), the rupiculous Gekkonidae (Bauer & Lamb, 2005; Heinicke *et al.*, 2017; Jacobsen *et al.*, 2014; Travers *et al.*, 2014) and the fossorial Acontinae (Busschau *et al.*, 2017; Conradie *et al.*, 2018; Daniels *et al.*, 2002), likely the result of the hyper-specific selection for specific habitats within these taxa. Habitat heterogeneity caused by climatic shifts have resulted in increased herpetological diversity through habitat creation and subsequent isolation. Habitat generalists, and widespread and abundant species, are thus deemed to harbour lower genetic structuring because of their perceived ability to navigate geographical barriers that may otherwise cause vicariant events in other species, thereby reducing their feasibility for large-scale phylogeographic analysis (Branch *et al.*, 2006). Indications, however, suggest that closer inspection of these taxa may reveal unappreciated genetic diversity, especially since widespread taxa are more ecologically pliable, and by association, less morphologically variable.

Convergent evolution can result in animals on independent evolutionary lineages attaining similar morphologies in accordance with similar external selective pressures (Edwards et al., 2012) . This can confound conventional taxonomists, leading to an under-appreciation of species diversity because of a lack of distinguishable morphological characteristics. This was evidenced in Chapter Three, with phylogenetic reconstruction retrieving *Ps. multisquamis* as polyphyletic, with no accompanying morphological differences separating the two clades. Conversely, rapid morphological divergence (divergent evolution) can result in genetically similar taxa acquiring different morphologies in response to contrasting environmental stimuli, confounding morphologically orientated taxonomy. As evidenced in Chapter Two and the work of Taft (2018), members of the '*leightoni* complex' exhibit contrasting colour and patterning, with little associated genetic differentiation. The proliferation of molecular-orientated research in the past two decades has resolved many taxonomical issues, like the ones mentioned above and identified several gaps in our systematic knowledge, previously missed by morpho-centric biologists (Adalsteinsson *et al.*, 2009; Broadley *et al.*, 2018; Busschau *et al.*, 2019, 2020; Conradie *et al.*, 2020; Hallermann *et al.*, 2020; Keates *et al.*, 2019; Oliver *et al.*, 2009; Portillo *et al.*, 2015; Taft, 2018). Thus, the use of molecular phylogenetics on wide-ranging snake species, within southern Africa, represents an integral step in our understanding of African herpetology.

Southern Africa contains over 600 species of reptiles, of which approximately 70% are endemic to the region (Alexander & Marais, 2007; Branch, 1998; Branch et al., 2006). Diversity flourishes in the sub-region, with substantial genetic structure being found, even in large-ranging, generalist snake species (Barlow *et al.*, 2013; Engelbrecht *et al.*, 2019; Kulenkampff *et al.*, 2019; Portillo *et al.*, 2018). Past Plio-Pleistocene climatic oscillations may have driven range fragmentation in currently widespread snake species, with four and five distinct mitochondrial clades found in *Bitis arietans* and *Duberria lutrix*, respectively (Barlow *et al.*, 2013; Kulenkampff *et al.*, 2019). Whilst morphological characteristics may not echo the isolation events of the past, hidden genetic divergences may challenge current taxonomy and lead to taxonomic re-evaluation (Barlow *et al.*, 2013; Engelbrecht *et al.*, 2019).

Psammophylax (Fitzinger 1843) is a widespread, generalist psammophiid genus that is endemic to Africa (Bates *et al.*, 2014; Branch, 2016; Spawls *et al.*, 2002). It has undergone substantial taxonomic shifting as a result of a revived interest in the genus, with recent phylogenetic-oriented analyses supporting the elevation of *Ps. ocellatus* to species level in Angola (Branch et al., 2019), the description of *Ps. kellyi* from Tanzania (Keates *et al.,* 2019), and the description of a new genus (*Kladirostratus*) to house *Ps. a. acutus*, *Ps. a. jappi* and *Ps. togoensis* (Keates *et al.,* 2019). *Psammophylax rhombeatus*, the type species of the genus, is a southern African endemic with high intraspecific morphological variation, even though it has one of the smallest distributions of all *Psammophylax* species. The species is a Southern African endemic and can be in South Africa, Eswatini, Lesotho and Namibia (Branch, 1998). The type locality is south western Western Cape (Broadley, 1977) and Its distribution stretches from southern Namibia, south to the tip of the Cape Peninsula, east along the South Coast, and up into the Lowveld of South Africa (Bates *et al.*, 2014; Branch, 1998, 2016; Marais, 2004).

Interestingly, two varieties have been referred to in the past: *Psammophylax rhombeatus* var. *trilineata* (Boettger, 1883) from ‘Smithfield Transvaal’, and *Psammophylax rhombeatus* var. *biseriata* (Muller, 1892) from ‘Transvaal’ (Fig. 4.1). *Psammophylax rhombeatus* var. *trilineata* was described based on the rostral scale not touching the pre-frontal and several rows of dark spots fusing to form longitudinal ‘spots’. *Psammophylax rhombeatus* var. *biseriata* was described based on the dorsum being uniform grey, having lateral rows of dark spots and the free edges of the ventral scales being adorned with dark ‘half-moons’ (Broadley, 1977). Both varieties have since been sunken into the synonymy of *Psammophylax rhombeatus* (Broadley, 1977). *Psammophis longementalis* (Roux, 1907) was described from ‘Buffelrivier’ (near East London) based on a higher number of ventral scales and a unique scale pattern but has also been synonymised with *Ps. rhombeatus* (Fig. 4.1) (Broadley, 1977).

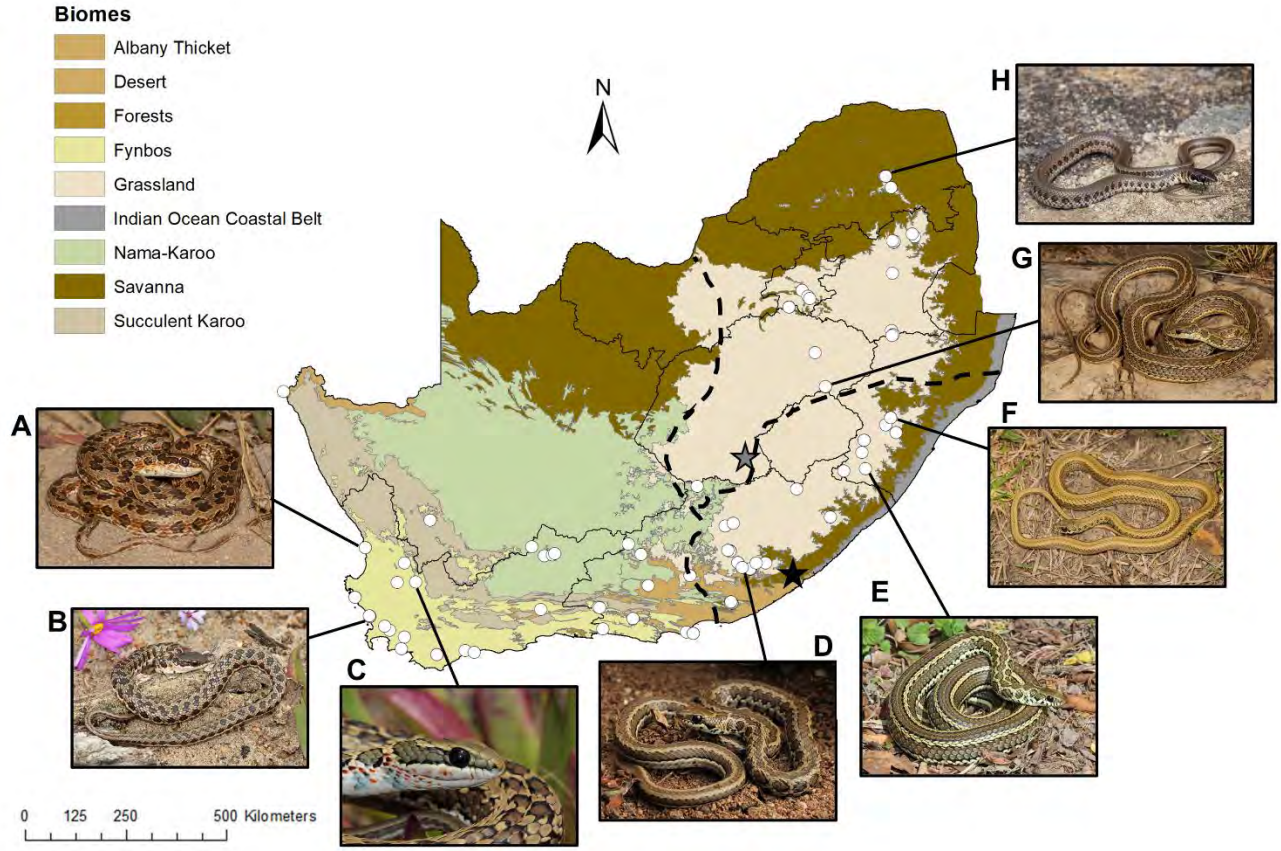

Figure 4.1**:** White dots represent geographical positions of all the genetic samples utilised in the study. Photos (A–H), for a subset of the animals utilised in the study representing the different morphological groups. The dotted line represents the boundary between morphologically distinctive groups, as reported in Broadley (1977) and the 'grey star' and 'black star" symbols represent the approximate type localities of *P. r.* var. *trilineata* and *'P. r.* var. *longmentalis',* respectively. The type locality of *Psammophylax r.* var. *biseriata* cannot be placed on the map because of a lack of accurate locality data. The colours on the map represents the vegetation biomes in South Africa (see inset key). Photos: Chad Keates (A, B, C, D, E), Tyrone Ping (F, G) and Luke Verbugt (H).

According to Broadley (1977), *Psammophylax rhombeatus* consists of three groups (denoted by dotted lines in Fig. 4.1) based on dorsal colour patterns. These include roughly the southern and central Cape (SWSA); northern Eastern Cape, KwaZulu-Natal, and Lesotho (SESA), and Free State, Gauteng, Limpopo, Mpumalanga and western Eswatini (NESA). Populations of SWSA usually show the rhombic pattern (Fig. 4.1 A, B, C) with specimens from western South Africa (WSA) and Little Namaqualand having on average a higher subcaudal scale count (71–84) than other populations (Broadley, 1977). Specimens from WSA also display the rhombic pattern. Populations of SESA display the '*longementalis'* pattern (two yellow dorso-lateral stripes running the length of the body (refer to Broadley, (1977) for description), have a higher ventral scale count (160–177) compared to other populations, and attain a larger than average size. It must, however, be noted that some specimens from the

KwaZulu-Natal Midlands are poorly marked or even uniform (Fig. 4.1 F) (Broadley, 1977). Lastly, the populations of NESA are variable, but usually have three dark stripes, and spots on the side of the neck (Fig. 4.1 G), with some individuals being uniform grey apart from the spots on the neck (Broadley, 1977). Some specimens, especially from Lydenburg in Mpumalanga Province, retain three or four rows of spots anteriorly. Specimens from NESA also have lower average ventral and subcaudal scale counts than individuals from the '*longementalis*' group (SESA) (Broadley, 1977).

Psammophylax rhombeatus is a common, yet understudied species, which exhibits several morphological differences based on geography. Although many of the morphological characteristics (colour and pattern) separating postulated populations (Broadley, 1977) are labile, Chapters Two and Three identified substantial genetic structuring within the species, irrespective of its smaller geographical range (compared to other *Psammophylax* spp.). For this reason, it is the ideal candidate species for a molecular study to test for potential unappreciated diversity. The study also affords me the opportunity to determine whether the molecular make-up of the species is congruent with previous morphological assumptions (according to Broadley 1977). Past morphological findings were supplemented with geometric morphometrics on the dorsal and lateral head shapes of the different populations of *Ps. rhombeatus* to determine whether head shape varies within the species. Using a combination of phylogenetic, phylogeographic, and morphometric analyses, this study aims to create a more robust understanding of the species, through an improved understanding of its genetic diversity, population structure, and evolutionary history.

Methods

Genetic Sampling

The phylogeny of *Ps. rhombeatus* was estimated using genetic information from 103 individuals, representing most of the distributional range of the species. Tissue samples for the genetic analyses were obtained from the South African National Biodiversity Institute (SANBI, Kirstenbosch), Port Elizabeth Museum (PEM, Port Elizabeth), and from scientists and citizen scientists stationed throughout South Africa. Tail tips (live specimens) and liver or muscle tissues (preserved specimens) were preserved in ~95% ethanol. The dataset was supplemented with sequences from four individuals available on GenBank (https://www.ncbi.nlm.nih.gov/genbank/; Table S4.1, Fig. 4.1). Sequences for outgroup taxa were obtained from GenBank and past chapters (Table S4.1).

Genetic Laboratory Protocols

Genomic DNA was isolated from tissues with a standard salt extraction method (Bruford *et al.*, 1992) using lysis (Buffer ATL; Qiagen) and elution (Buffer AE; Qiagen) buffers. Standard PCR procedures were utilised to amplify three partial mitochondrial genes (cytochrome b [cytb], 16S ribosomal ribonucleic acid [16S] and NADH-dehydrogenase subunit 4 [ND4]) and one partial nuclear gene (oocyte maturation factor [c-mos]). PCR amplification was carried out using the primer pairs listed in Table 4.1. Amplifications of the selected genes were carried out using 20–50 ng/µl extracted genomic DNA. Each amplification was conducted with a PCR mixture to the total volume of 25 µl containing 12.5 µl TopTaq Mastermix (Qiagen; containing 10x PCR buffer, 1.5 mM $MgCl_2$, 0.2 mM dNTPs, and 0.75 U Taq polymerase), 2 µl forward primer (10 µM), 2 µl reverse primer (10 µM), and 8.5 µl of the genomic DNA and de-nucleated water combined. The cycling profile for gene amplification was as follows: initial denaturing step at 94°C for 5 min, followed by 35–40 cycles of 94 °C for 30 s, 48–56 °C for 45 s, and 72 °C for 45 s, with a final extension at 72 °C for 8 min (Table 4.1). The prepared PCR products were sent to Macrogen Corp. in Amsterdam, Netherlands for sequencing (after purification) with the forward primers only.

Table 4.1: Primers and PCR protocols used to the generate sequences for the study.

Gene	Primer	Source	Annealing temperature (C°)	Cycles
16S	L2510: 5'—CGCCTGTTTATCAAAAACAT-—3' R1478: 5'—TGACTGCAGAGGGTGACGGGCGGTGTGT—3'	Palumbi (1996)	50-—52	35
cytb	WWF: 5'—AAAYCAYCGTTGTWATTCAACTAC—3' Cytb-R2: 5'—GGGTGRAAKGGRATTTTATC—3'	Whiting, Bauer, & Sites (2003)	50-—52	35
ND4 + LeutRNA	ND4: 5'—TGACTACCAAAAGCTCATGTAGAAGC—3' LeutRNA: 5'—CATTACTTTTACTTG GATTTGCACCA—3'	Arèvalo, Davis, & Sites (1994)	52-—56	35
c-mos	S77: 5'—CAT GGACTGGGATCAGTTATG—3' S78: 5'—CCTTGGGTGTGATTTTCT CACCT—3'	Slowinski & Lawson (2002)	48-—52	35-—40

Sequence Alignment and Gene Partition Congruence Testing

The sequence trace files were checked using BioEdit Sequence Alignment Editor v.7.2.5 (Hall, 1999) and aligned, along with the previously accessioned GenBank sequences, in MEGA v.6.0 (Tamura *et al.*, 2013) using the ClustalW alignment method. The region representing

LeutRNA was split from the genic region of ND4 and treated as a separate locus (non-protein-coding), necessitating the creation of five gene alignments for further analysis. Individual gene trees were constructed in MEGA v.6.0 (Tamura *et al.*, 2013) using the Maximum Likelihood algorithm, with 100 bootstrap replicates and the GTR+G+I nucleotide substitution model. The Congruence Index (I_{cong}; http://max2.ese.u-psud.fr/icong/index.help.html; Vienne, Giraud and Martin, 2007) was utilised to test for congruence between individual gene trees. All gene-tree combinations were found to be congruent and five datasets were created.

Datasets

To facilitate molecular best practice, different datasets were put together using specific genes, partition schemes, and models of evolution for different analyses. By doing this, I was able to optimize each analysis and ensure the phylogenetic modelling was as robust as possible.

Dataset 4.1 was used for initial phylogenetic tree construction (Bayesian Inference (BI) + Maximum Likelihood [ML]) and comprised of all *Ps. rhombeatus* sequences available (Table S4.1) and was supplemented with several individuals from each species of *Psammophylax* (Table S4.1), as outgroups. *Dataset 4.1* used the following genes: 16S (94 sequences [sq], 357 base pairs [bp]); cytb (125 sq, 582 bp); ND4 (117 sq, 639 bp); LeutRNA (115 sq, 168 bp); c-mos (42 sq, 549 bp).

Dataset 4.2 was used for the time-calibrated phylogeny and included a representative sampling from each lineage of *Ps. rhombeatus* (Table S4.1), plus representatives from each species of *Psammophylax*, each genus of Psammophiidae, and several outgroup taxa from Serpentes, that were used to calibrate the analysis (Table S4.1). The 16S and LeutRNA alignments were omitted from the dataset given the lack of comparable material in the outgroup taxa. *Dataset 4.2* used the following genes: cytb (62 sq, 582 bp); ND4 (57 sq, 639 bp); c-mos (52 sq, 549 bp).

Dataset 4.3 was used for species delimitation and comprised of all *Ps. rhombeatus* samples and several samples from each species of *Psammophylax* as outgroups (Table S4.1). *Dataset 4.3* omitted c-mos because it is an independently recombining gene and using it in conjunction with single locus species delimitation methods would have invalidated the analyses. The dataset also omitted identical sequences that would have produced zero branch lengths, and confounded species delimitation. *Dataset 4.2* used the following genes: 16S (90 sq, 357 bp); cytb (114 sq, 582 bp); ND4 (106 sq, 639 bp); LeutRNA (104 sq, 168 bp).

Dataset 4.4 was used for p-distance analyses and included all available sequences of *Psammophylax* for cytb (160sq, 582 bp) and ND4+LeutRNA (152 sq, 792 bp), and omitted sequences that contained missing data (Table S4.1).

Dataset 4.5 was used for population genetic analyses and haplotype network creation and utilised only *Ps. rhombeatus* samples. The 16S and c-mos genes were omitted from the analysis because of the high degree of missing information. All outgroup taxa, and sequences with unknown sites, were omitted from the analyses leaving only *Ps. rhombeatus* sites with a full genetic compliment. The following genes were used: cytb (99 sq, 582 bp); ND4+LeutRNA (90 sq, 808 bp). The models of evolution and molecular markers utilised in each dataset can be found in Table 4.2.

Models of Evolution and Partition Scheme

All gene alignments were tested for saturation using DAMBE v.6.4.67 (Xia, 2013). The protein-coding genes (cytb, ND4, c-mos) were checked for stop codons to ensure they started on the correct reading frame and analysed according to codon position. No saturation was found, enabling the use of gene-partitioned datasets, where necessary. *Dataset 4.1* was partitioned according to codon position and *Dataset 4.2* and *4.3* were partitioned according to gene (reasoning explained in Chapters Two and Three). The best partition schemes and best-fitting models of molecular evolution were selected using PartitionFinder 2 (Lanfear *et al.*, 2016) with the following settings: BIC model selection criterion, Beast models, linked branches, and all partition schemes searched (Table 4.2). For BEAST analysis (*Dataset 4.2* and *4.3*), the gene partitions were run through jModelTest 2 (Darriba *et al.*, 2012; Guindon & Gascuel, 2003) to determine the optimal gamma shape and invariant site values for the partitions selected by PartitionFinder 2.

Table 4.2: Best-fit partitioning schemes and models of evolution for each dataset, according to PartitionFinder 2, with number of sites per partition. Numbers following genes in the subset partition column refer to codon position. NA = Not Applicable.

Dataset	Initial Partition	Subset partition	Best Model*	Number of Sites
4.1	codon	16S	GTR+I+G	357
		cytb_1, ND4_1, LeutRNA	GTR+I+G	575
		cytb_2, ND4_2, c-mos_3	HKY+I	590
		cytb_3, ND4_3	GTR+G	407
		c-mos_1, c-mos_2	JC	366
4.2	gene	cytb, ND4	GTR+I+G	1221
		c-mos	HKY+G	549
4.3	gene	16S	GTR+I+G	357
		cytb, ND4, LeutRNA	TRN+I+G	1389
4.4	NA	cytb	NA	582
		ND4+LeutRNA	NA	792
4.5	NA	cytb	NA	582
		ND4+LeutRNA	NA	808

Phylogenetic Tree

A codon-partitioned dataset (*Dataset 4.1*) was used to infer the phylogenetic structuring within *Ps. rhombeatus* using Bayesian Inference (BI) and Maximum Likelihood (ML). Bayesian Inference was carried out using MrBayes v.3.2.2 (Ronquist *et al.,* 2012) on the CIPRES Science Gateway XSEDE online resource (http://www.phylo.org; Miller *et al.,* 2010). For MrBayes, four parallel runs of 20 million generations (MCMC analysis) were performed, with trees being sampled every 1000 generations, using uniform priors. BEAGLE was used to speed the process up. The number of generations discarded as burn-in was determined using Tracer v.1.5 (Rambaut & Drummond, 2009). The effective sample size (ESS) was found to be above 200 for all parameters with all runs reaching convergence, indicating that a burn-in of 10% was adequate. Maximum Likelihood (ML) analysis was conducted using the GTRGAMMA model in RAXML-HPC v.8.2.12 (Stamatakis, 2014) on the CIPRES Science Gateway. A random starting tree was used and the rapid bootstrapping method. One thousand bootstraps were run, and all other parameters were set to default. All BI and ML trees were viewed and edited in FigTree v.1.4.2 (Rambaut, 2014).

Time-calibrated Phylogeny

Time-calibrated Bayesian Inference (*Dataset 4.2*) was used to estimate the divergence times of the different lineages identified within *Ps. rhombeatus.* A gene-partitioned input file was created in BEAUti v2.6.2 (Bouckaert *et al.*, 2019; Drummond & Rambaut, 2007). Using the

following settings: linked trees, unlinked clock models, and unlinked site models. A relaxed lognormal clock model with a Yule prior was used, along with a similar calibration scheme as Chapter Two (based on Portillo *et al.,* 2018). The tree was constrained with four primary calibration points from Head *et al.* (2016). These were the split between Caenophidia and Booidea (72.1–66 MYA), the split between *Acrochordus* + *Xenodermatidae* and Colubroidea (50.5–72.1 MYA), the divergence of Colubridae and Elapoidea (31–30.8 MYA) and the split between Crotalinae and Viperinae (23.8–20 MYA). All calibrations were constrained with lognormal MRCA priors and set as monophyletic. Means of the age estimates were given in real space and the standard deviations were calculated by working out the standard deviations of the log-transformed range of the fossil calibrations. Three independent analyses of 50 000 000 generations, sampling every 5000, were run through BEAST v.2.6.3 (Bouckaert *et al.*, 2019; Drummond & Rambaut, 2007; Suchard & Rambaut, 2009) on the CIPRES Science Gateway. The independent runs were combined in LogCombiner v.2.6.2 (Bouckaert *et al.*, 2019; Drummond & Rambaut, 2007) and a maximum clade credibility tree, using mean heights, with a burn-in of 10%, was created in TreeAnnotator v.2.6.2 (Bouckaert *et al.*, 2019; Drummond & Rambaut, 2007). The effective sample size (ESS) was found to be above 200 in Tracer v.1.5, and the final trees were viewed and edited in FigTree v.1.4.2.

Species Delimitation

Using a combined mitochondrial dataset (*Dataset 4.3*), Bayesian implementation of the Generalized Mixed Yule Coalescent (bGMYC), Automatic Barcode Discovery (ABGD) and Poisson Tree Processes (PTP) were implemented to determine whether the clades identified in *Ps. rhombeatus* constituted separate species. Although designed for single locus datasets, the species delimitation analyses were implemented on the combined mitochondrial loci as they have been demonstrated to evolve at similar rates, as compared to nuclear genes, thus affording a larger dataset to the analyses (Table 4.2). The combined mitochondrial genes thus represent a single locus here.

Firstly, a combined mitochondrial FASTA alignment was created. The alignment was uploaded onto the ABGD web interface (abgd web (mnhn.fr), web version 10 January 2021) where ABGD infers hypotheses about putative species through the creation of a barcode gap separating intra- and inter-species pairwise distances. The following settings were used: standard p-distance metrics, minimum barcode gap width (1.0), intraspecific divergence minima (0.001) and maxima (0.1).

For bPTP and bGMYC, phylogenetic tree creation was carried out using BEAST v.2.6.3. A gene-partitioned file (Table 4.2) was input into BEAUti v.2.6.2 using the following

settings: linked trees, unlinked clock models, and unlinked site models, with a relaxed lognormal clock and a Yule prior. The absence of nuclear loci from the dataset resulted in erroneous topologies, and thus the relationships among outgroup taxa were constrained using the results from Chapter Two, to ensure that the tree topology remained consistent with prior analyses. Three independent analyses of 50 000 000 generations, sampling every 5000, were run through BEAST v.2.6.3. The independent runs were combined in LogCombiner v.2.6.2 and a maximum clade credibility tree, with a burn-in of 10% was created in TreeAnnotator v.2.6.2. The effective sample size (ESS) was found to be above 200 in Tracer v.1.5 and the final trees were viewed and edited in FigTree v.1.4.2.

Like Chapter Three, the single tree and the multi-tree bGMYC method (bgmyc.singlephy, bgmyc.multiphylo; Reid and Carstens, 2012) were used, to access the difference between the two. For the single bGMYC method, the maximum clade credibility tree from TreeAnnotator v.2.6.2 was used. For the multi-tree method, one hundred and fifty randomly selected posterior trees, were selected from the BEAST output, using LogCombiner v.2.6.2, and following a burn-in of 10%, 135 trees were analysed. The package bGMYC v.1.0.2 in R studio v.1.1.442 (R Core Team, 2016; Reid & Carstens, 2012) was implemented with the bgmyc.singlephy and bgmyc.multiphylo functions being used for the single and multi-tree analysis, respectively.

A traditional GMYC aims to determine when the branching rates within a calibrated tree shift from a Yule to coalescent process, and the Bayesian implementation of the model incorporates more flexibility into the model through the integration of MCMC. Every tree (from both analysis) was subjected to 50 000 MCMC steps, a burn-in of 40 000 steps, and sampling every 100 steps. Bayesian implementation of the PTP model was conducted via the bPTP server (http://species.h-its.org/ptp/; Zhang *et al.,* 2013) on the final maximum clade credibility tree. Unlike bGMYC, that examines time, bPTP differentiates speciation processes among species from the diversification processes within species by examining the substitutions between nodes. The results from all three threshold analyses were overlaid on the maximum clade credibility tree from TreeAnnotator v.2.6.2.

Pairwise Distance and Barcode Gap Analysis

Pairwise distance and barcode analysis of *Psammophylax* was carried out using *Dataset 4.4*. Pairwise distance matrices were created for each gene (Table 4.3), using MEGA X v.10.1.7 (Kumar *et al.*, 2018) and the following settings: standard uncorrected p-distance model, uniform rates, pairwise deletion, and 500 bootstraps. SpeciesIdentifier v.1.8 (Meier *et al.*, 2006) was used to determine whether the clades identified within *Ps. rhombeatus* constitute

species-level divergences through the illustration of the barcode gap within each gene. The intra- and interspecies uncorrected pairwise distances of the cytb and ND4+LeutRNA alignments were created in SpeciesIdentifier and plotted on the same axis (Meier *et al.*, 2006) to determine whether current taxonomy reflects a barcode gap (accurate taxonomy), or an overlap (unappreciated species diversity) (Lefébure *et al.*, 2006).

Haplotype Network & Population Genetics

Population genetic analyses were conducted on two mitochondrial alignments (cytb & ND4+LeutRNA) from *Dataset 4.5*. The genes alignments were partitioned into four groupings based on the clades found in identified in previous analyses, and a median-joining haplotype network (Bandelt *et al.* 1999) was created for each alignment in PopART v.1.7 (http://popart.otago.ac.nz; Leigh and Bryant, 2015). The four groupings were further subdivided into localities and the genetic differentiation between populations was examined using an Analysis of Molecular Variance (AMOVA; Excoffier, Smouse and Quattro, 1992) in Arlequin v.3.5 (Excoffier & Lischer, 2010). Fixation indices were used to estimate the amount of genetic variability between clades (F_{CT}), among localities (F_{ST}), and within localities (F_{SC}). As the field sampling did not focus on acquiring multiple individuals within a single preconceived locality, but rather on collecting samples from the full distribution of the species, samples were grouped into general localities post-collection. This may have partially hampered the reliability of the F_{ST} and F_{SC} statistics as some localities had only one individual assigned to them.

Neutrality tests (Tajima's D and Fu's F_S; Tajima, 1989) were also implemented in Arlequin v.3.5, to determine whether population expansion may have occurred during the evolution of each clade. Finally, mismatch distributions were created for each population by plotting the site differences between each pair of sequences (observed) against the counts determined by the spatial expansion model used (simulated), on the same axis. The similarity of the resulting histograms coupled with the values from the Sum of Squared deviation and Harpending's Raggedness index indicate whether the population refutes or proves the assumptions of the model in question. For this analysis, we used parameters of the spatial expansion, assuming constant deme size, in Arlequin v.3.5, and ran 1000 bootstrap replicates using standard uncorrected pairwise distances, producing a histogram for each population, and for each gene.

Geometric Morphometrics

Geometric morphometric analyses of the external views of the head were performed to investigate the head shape of the clades within *Ps. rhombeatus*. I obtained dorsal and lateral photographs of the heads of specimens at the Port Elizabeth Museum (PEM) and grouped the samples into four clades with each clade including at least 10 individuals (SESA: 48, SWSA: 21, NESA: 9, WSA: 10). The dorsal and lateral profiles of the heads (all right-hand-side) were photographed on grid paper (1 cm x 1 cm) with a digital camera (Canon 6D, resolution 20.2 MP and 100 mm macro lens).

Homologous landmarks were placed and digitized on the two views of the heads (Figure 4.2; TpsUtil v.1.26, Rohlf, 2004b; TpsDig2 v.2.32, Rohlf, 2004a). A Generalized Procrustes Analysis (GPA; Rohlf, 1999; Rohlf and Slice, 1990) was performed during which the landmark configurations were resized, translated and rotated (aligned by principal axis). A covariance matrix was estimated using the symmetrical (dorsal view dataset) or the asymmetrical (lateral view dataset) components. A principal components analysis (PCA) was performed on the covariance matrix to identify which portions of the heads showed the most variation between the different clades (MorphoJ v.1.06d; Klingenberg, 2011).

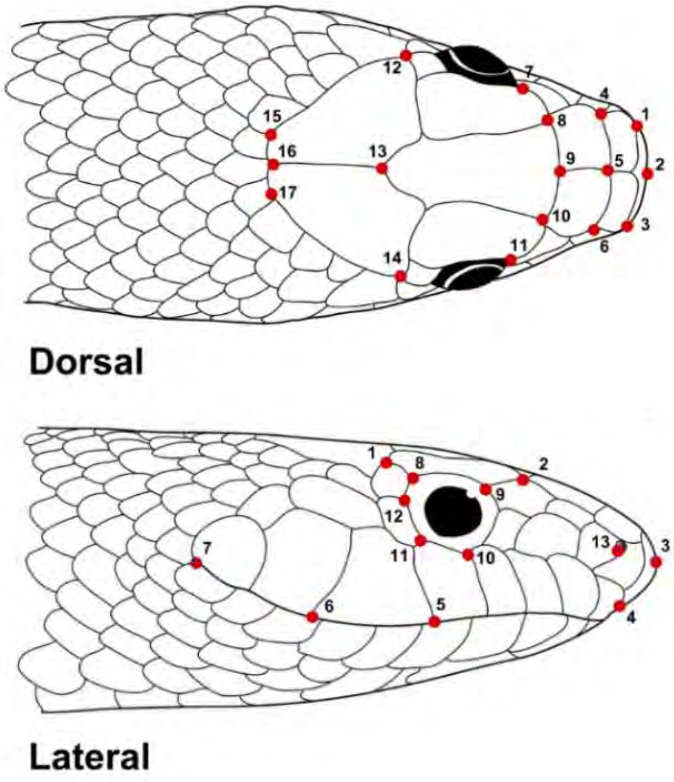

Figure 4.2: The placement of landmarks on photographs of dorsal and lateral aspects of the head of *Psammophylax rhombeatus* for geometric morphometric analysis.

Results

Phylogenetic Structuring

The two phylogenetic algorithms found congruent topologies using the full DNA dataset (*Dataset 4.1*: 2295bp, 103 *Ps. rhombeatus* samples) (Fig. 4.3), both recovering *Ps. rhombeatus* as monophyletic. *Psammophylax ocellatus* was recovered as sister to *Ps. rhombeatus*, with support from the BI algorithm (Fig. 4.3). *Psammophylax rhombeatus* was highly structured with four supported clades (BI > 0.90 PP/ML > 75% BS) being recovered within the species. All four clades represent candidate species and are hereafter referred to as NESA (northeast South Africa), WSA (western South Africa), SWSA (southwest South Africa) and SESA (southeast South Africa) because of their geographical distinctiveness. There is also strong support for intra-clade relationships within *Ps. rhombeatus,* with both algorithms (Fig 4.3) recognising a sister supported relationship between NESA and the rest of *Ps. rhombeatus* and between WSA and SESA + SWSA. Although topologically similar, only BI supported the sister relationship between SESA and SWSA.

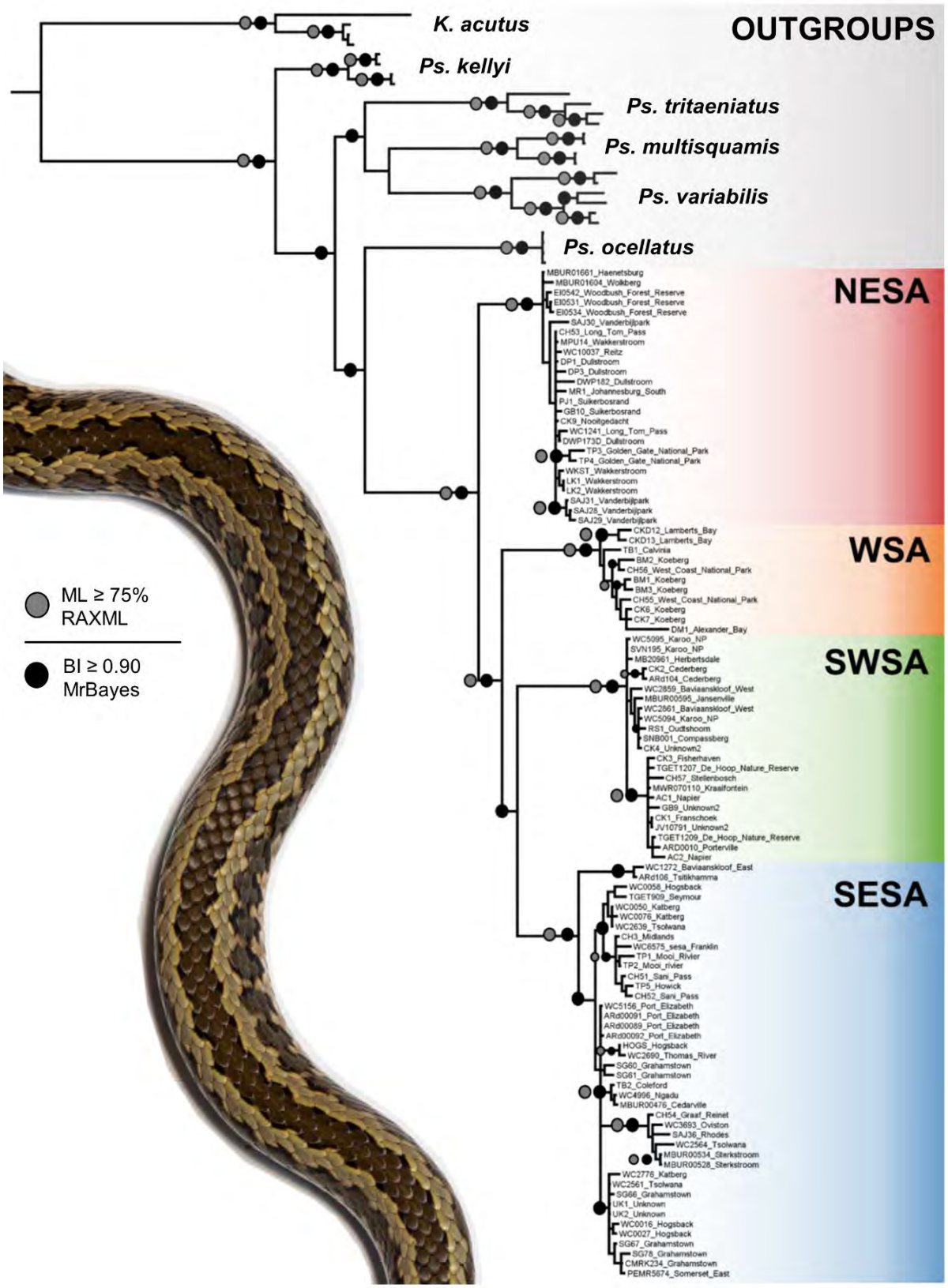

Figure 4.3**:** Bayesian Inference (BI) phylogeny derived from *Dataset 4.1* with Maximum Likelihood (ML) support overlaid, showing the intraspecies relationship within *Psammophylax rhombeatus*. Coloured circles at the nodes denote support of the different algorithms (size of circles have no meaning). NESA= north eastern South Africa, WSA= western South Africa, SWSA= south western South Africa, SESA= south eastern South Africa.

Time-calibrated Phylogeny

Topologies from the time-calibrated BEAST BI analysis (Fig. 4.4) were consistent with the findings of the phylogenetic tree from Fig. 4.3. The lowered support at the nodes, compared to Fig. 4.3, may be an artefact of the decreased number of molecular markers afforded to the analysis due to the lack of comparable data in the outgroup taxa. Dating estimates suggest that *Kladirostratus acutus* split from the rest of *Psammophylax* during the late Miocene, ~10.24 MYA (7.84–12.81 95% Highest Posterior Densities [HPD]) (Fig. 4.4). The split between *Ps. rhombeatus* and *Ps. ocellatus* was recovered during the mid-Pliocene, ~4.10 MYA (3.07–5.15 HPD) (Fig. 4.4), with the diversification within *Ps. rhombeatus* taking place over the late Pliocene through the early Pleistocene. The most basal clade, NESA, diverged from the rest of *Ps. rhombeatus* ~2.58 MYA (1.85–3.32 HPD) (Fig. 4.4), followed soon after by the split of WSA from SESA + SWSA, ~2.24 MYA (1.60–2.92 HPD) (Fig. 4.4) and lastly the split of SWSA from SESA ~1.96 MYA (1.37–2.64 HPD) (Fig. 4.4).

Species Delimitation

Results from the species delimitation methods were largely incongruent, with widely contrasting results within and between the species delimitation analyses (Fig. 4.5) and the p-distance and barcode gap analyses (Fig. 4.6, Table 4.3). The bGMYC output was interpreted using two threshold values ($p \geq 0.95$ and $p \geq 0.50$), against which species could be considered conspecific.

The first threshold from the multi-tree bGMYC method, bGMYC MT1 ($p \geq 0.95$), recognised 6 species, corroborating all existent taxonomy, with no recognised species groupings within *Ps. rhombeatus*. The second threshold from the multi-tree bGMYC method, bGMYC MT2 ($p \geq 0.5$), recognised 12 species, identifying all the *Psammophylax rhombeatus* clades (Fig. 4.3) as potential new species. The SESA clade was further subdivided, with the bGMYC MT2 threshold recognising Tsitsikamma (ARd106) and Baviaanskloof East (WC-1272) as a separate species, independent of the rest of SESA.

The first threshold from the single tree bGMYC method, bGMYC ST1 ($p \geq 0.95$), identified nine species, recognising all currently accepted species and all the *Psammophylax rhombeatus* clades (Fig. 4.3) as potential novel taxa. The second threshold from the single tree bGMYC method, bGMYC ST2 ($p \geq 0.5$), recognised 11 species in *Psammophylax*, and similarly to bGMYC MT2, recognised all *P. rhombeatus* clades as novel taxa, as well as a single putative taxon in both *Ps. variabilis* and *Ps. tritateniatus*. Unlike bGMYC MT2, bGMYC

ST2 did not recognise the SESA subclade, consisting of Tsitsikamma (ARd106) and Baviaanskloof East (WC-1272), as a separate species.

The Maximum Likelihood (PTP) and Bayesian implementation (bPTP) of the PTP model recovered the highest number of putative species with 25 and 58 species, respectively (Fig. 4.5). Bayesian PTP recovered 45 putative species in *Ps. rhombeatus* alone. These results are interpreted as an over-estimation, with groupings more likely representative of intraspecific structuring as opposed to potential new species. Both ABGD partitions produced identical results for *Ps. rhombeatus*, neither of which identified novel species within *Ps. rhombeatus*. They only differed in the number of putative taxa identified within outgroup taxa.

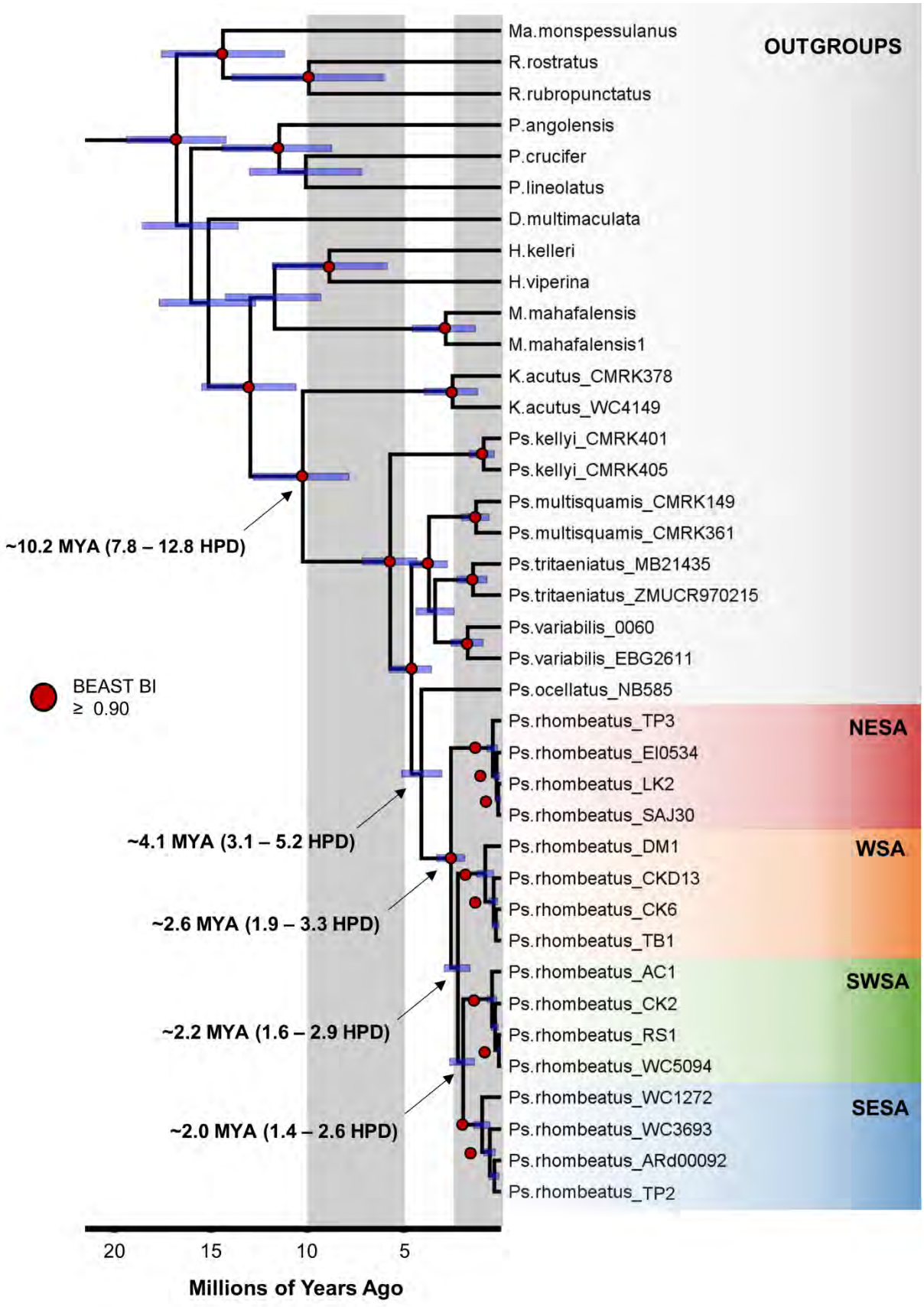

Figure 4.4: Time-calibrated BEAST BI phylogeny derived from *Dataset 4.2*. Blue bars reflect the 95% Highest posterior Distributions of node ages (HPD). Node sizes and vertical grey bars bear no meaning.

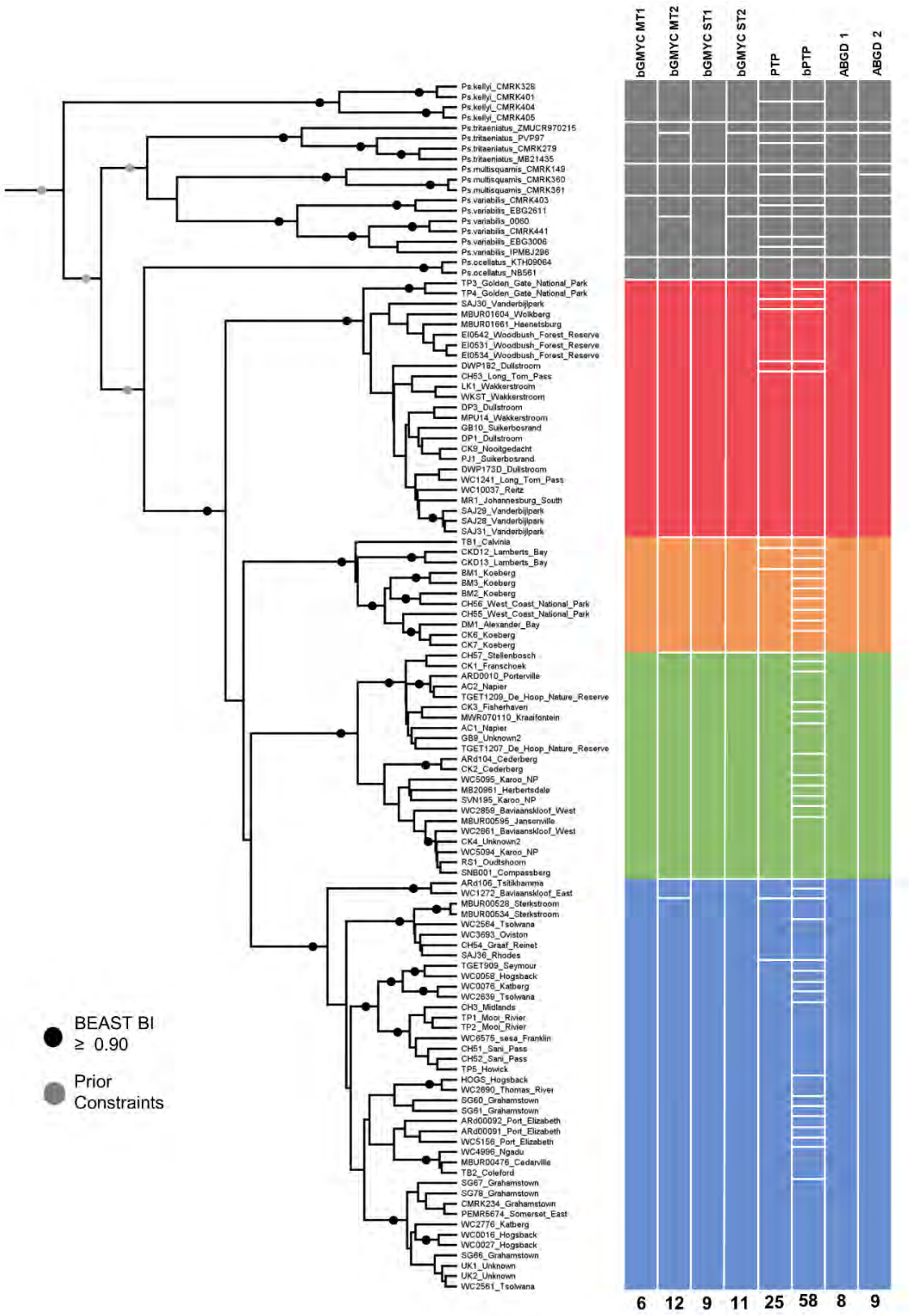

Figure 4.5**:** Bayesian Inference Beast BI phylogeny derived from *Dataset 4.3*. Black circles denote support and grey circles indicated constrained nodes. Vertical bars denote different species delimitation methods and horizontal white bars show the putative species based on the varying analyses. MT = multi-tree, ST = Single Tree. bGMYC MT1: ≥ 0.95; bGMYC MT2: ≥ 0.50; bGMYC ST1: ≥ 0.95; bGMYC ST2: ≥ 0.50; ABGD 1: prior maximal distance = 0.012915; ABGD 2: prior maximal distance = 0.007743.

Pairwise Distance and Barcode Gap Analysis

Results from the p-distance analysis supported the more conservative multilocus species delimitation analyses (bGMYC MT1; ABGD 1), by supporting the existing taxonomy. The average p-distance separating *Ps. rhombeatus* from the rest of *Psammophylax* was 8.69 ± 0.38 and 7.96 ± 0.61 for cytb and ND4+LeutRNA, respectively (Table S4.3), whilst the average distance separating *Psammophylax* species (excluding *Ps. rhombeatus*) was 8.02 ± 0.97 and 8.01 ± 0.70 for cytb and ND4+LeutRNA, respectively (Table S4.3). The average p-distance separating *Ps. rhombeatus* clades from one another was, however, much lower at 6.01 ± 0.75 and 5.11 ± 0.63 for cytb and ND4+LeutRNA, respectively (Table 4.3).

Table 4.3: Sequence divergences (uncorrected pairwise distance values) separating *Ps. rhombeatus* clades from the rest of *Psammophylax* using cytochrome b (cytb) and NADH dehydrogenase subunit 4 + Leucine transfer RNA (ND4+LeutRNA) (*Dataset 4.4*). Numbers in the diagonal (in bold) denote intraspecific divergences, numbers below the diagonal denote interspecific divergences and numbers above the diagonal denote the standard error of the interspecific divergences.

	cytb									
		1	2	3	4	5	6	7	8	9
1	SESA	**1.00**	0.93	0.83	0.85	1.08	1.02	1.09	1.07	1.08
2	SWSA	6.26	**1.00**	1.00	0.88	1.17	1.11	1.24	1.11	1.11
3	NESA	5.10	7.17	**0**	0.88	1.01	1.01	1.09	1.06	1.06
4	WSA	5.33	6.34	5.87	**1.00**	1.11	1.04	1.15	1.10	1.18
5	*Ps. kellyi*	8.41	9.98	7.63	9.38	**1.00**	0.93	1.07	1.03	0.99
6	*Ps. multisquamis*	7.75	9.39	7.63	8.45	6.69	**2.00**	0.99	0.96	0.97
7	*Ps. ocellatus*	8.48	10.29	8.01	8.71	6.91	6.98	**0**	1.13	1.11
8	*Ps. tritaeniatus*	8.26	9.35	8.30	8.72	8.20	7.54	9.18	**2.00**	1.08
9	*Ps. variabilis*	8.82	9.77	8.77	10.53	8.13	8.21	9.30	9.06	**2.00**
	ND4 + LeutRNA									
1	SESA	**1.00**	0.68	0.70	0.80	0.90	0.87	0.91	0.87	0.79
2	SWSA	4.82	**1.00**	0.67	0.80	0.88	0.90	0.89	0.91	0.84
3	NESA	4.39	4.65	**0.00**	0.76	0.94	0.94	0.90	0.97	0.89
4	WSA	5.70	6.03	5.10	**1.00**	0.92	0.95	0.98	0.96	0.81
5	*Ps. kellyi*	7.40	7.95	7.39	8.24	**1.00**	0.82	0.88	0.93	0.86
6	*Ps. multisquamis*	8.17	8.32	8.96	9.23	6.97	**2.00**	0.94	0.90	0.81
7	*Ps. ocellatus*	7.40	7.48	7.41	8.70	6.82	8.43	**0**	0.97	0.87
8	*Ps. tritaeniatus*	8.19	8.77	9.12	9.54	8.33	9.01	8.74	**2.00**	0.82
9	*Ps. variabilis*	6.97	7.75	7.69	7.62	7.94	7.83	8.13	7.92	**2.00**

Barcode gap analysis yielded similar results to the more conservative bGMYC and ABGD analyses with intraspecies variations ranging from 5.5–8.5% (Fig. 4.6A) and 4.5–7.5% (Fig. 4.6C) separating clades of *Ps. rhombeatus* for cytb and ND4+LeutRNA, respectively.

Within cytb (Figure 4A), the highest intraspecies distance (8.4%) separated a sample from SWSA and NESA, whilst in ND4+LeutRNA (Fig. 4.6C), the highest intra species distance (7.07%) separated a SESA and WSA sample.

Within both cytb and ND4+LeutRNA, the highest intra-species distance, barring, *Ps. rhombeatus* separated Congolese and Mozambican *Ps. variabilis* by 5.15% (Fig. 4.6A) and 4.04% (Fig. 4.6C) respectively. *Psammophylax rhombeatus* demonstrated the highest intraspecies variation irrespective of its smaller range, as compared to species like *Ps. tritaeniatus* and *Ps. variabilis*. Within cytb (Fig. 4.6A) and ND4+LeutRNA (Fig. 4.6C), there was a clear overlap between intra- and interspecies variation, indicating potential cryptic diversity.

Psammophylax rhombeatus was split into four clades based on the phylogenetic structuring observed in Figs 4.3 and 4.4. Within both cytb (Fig. 4.6B) and ND4+LeutRNA (Figure 4.6D), the overlap persisted, and no clear barcode gap was observed. With cytb (Fig. 4.6B), intraspecies distance between 4.5–5.5% separated samples of *Ps. variabilis*, whilst in ND4+LeutRNA (Fig. 4.6D), 4–4.5% separated Congolese and South African *Ps. tritaeniatus*, Congolese and Tanzanian *Ps. variabilis* and samples of *Ps. rhombeatus* from Tsitsikamma and Tsolwana, within the SESA clade. The highest intraspecies distance for both genes was observed between *Ps. variabilis* samples, a result replicated in all but two (bGMYC MT1 and bGMYC ST1) of the multilocus species delimitation analyses (Fig. 4.5), indicating potential cryptic diversity within the species.

Interspecies divergences of 4.0–6.5% and 3.5–6.0% were restricted only to the differences between *Ps. rhombeatus* clades in cytb (Fig. 4.6B) and ND4+LeutRNA (Fig. 4.6D), respectively. Whilst the clades remain distinctive from other species of *Psammophylax*, the p-distances separating *Ps. rhombeatus* clades are low in Figs 4.6B and 4.6D, and Table 4.3, meaning that clades cannot be elevated to species level independent of one another. NESA, the most divergent clade of *Ps. rhombeatus*, although genetically distinct from described species of *Psammophylax*, was separated from sister clades of *Ps. rhombeatus* by a p-distance of 6.05 ± 1.05% and 4.71 ± 0.36% in cytb and ND4+LeutRNA, respectively.

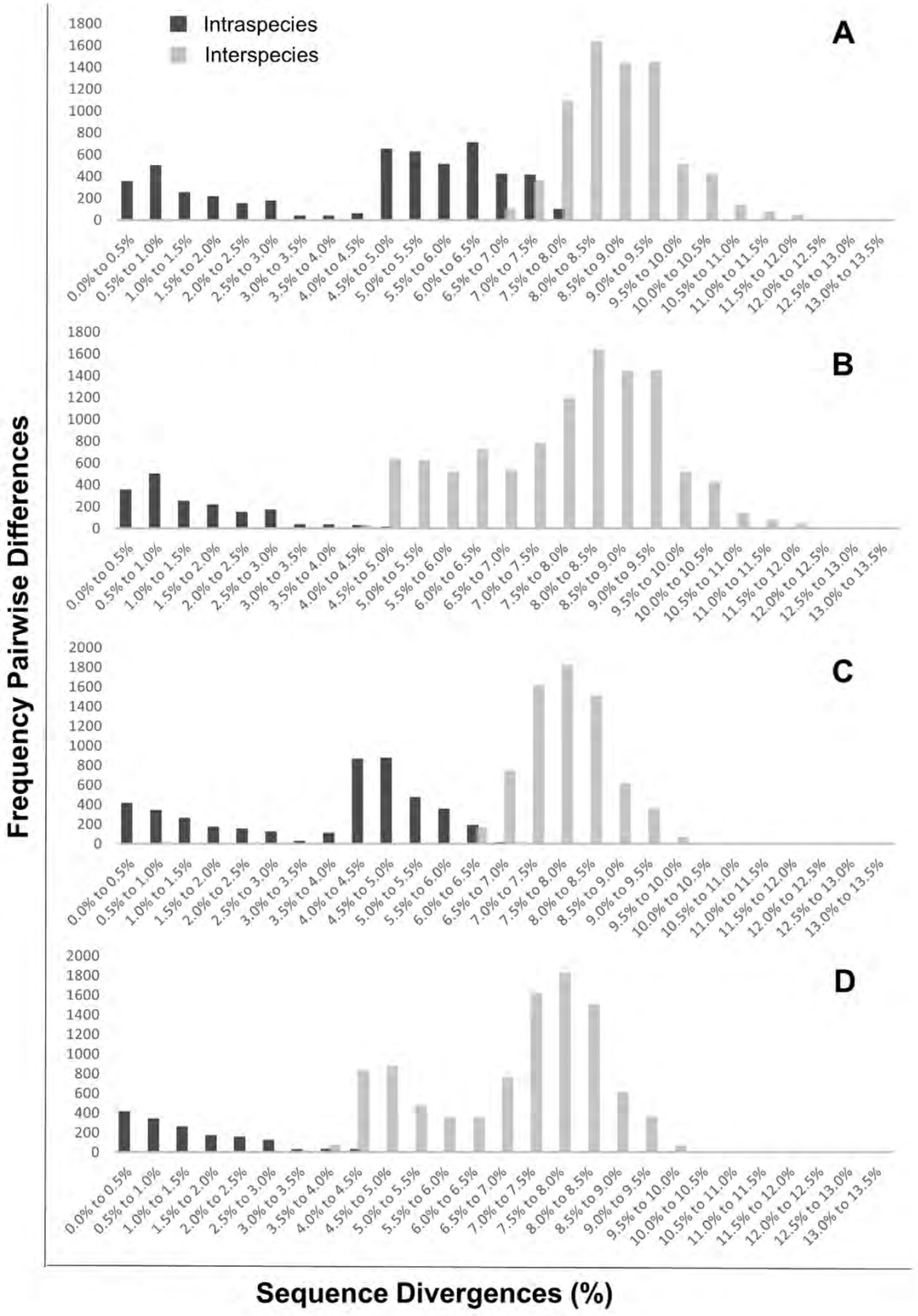

Figure 4.6**:** Uncorrected pairwise distances used to illustrate the barcode gap between intra- and interspecies sequence divergence values in *Psammophylax*, using *Dataset 4.4*. (A) cytb currently accepted taxonomy of *Ps. rhombeatus*; (B) cytb four clades of *Ps. rhombeatus* as separate species; (C) ND4+LeutRNA currently accepted taxonomy of *Ps. rhombeatus*; (D) ND4+LeutRNA four clades of *Ps. rhombeatus* as separate species.

Phylogeographic Structuring

The cytb haplotype alignment was characterised by the presence of 83 parsimony-informative sites, 111 segregating sites and 69 haplotypes (SESA 28, SWSA 17, NESA 13, WSA 11). The ND4+LeutRNA haplotype alignment was characterised by the presence of 113 parsimony-informative sites, 131 segregating sites, and 61 haplotypes (SESA 23, SWSA 16, NESA 13, WSA 9). Both alignments produced highly structured median-joining haplotype networks, both recognising four distinct haplo-clades (Fig. 4.7).

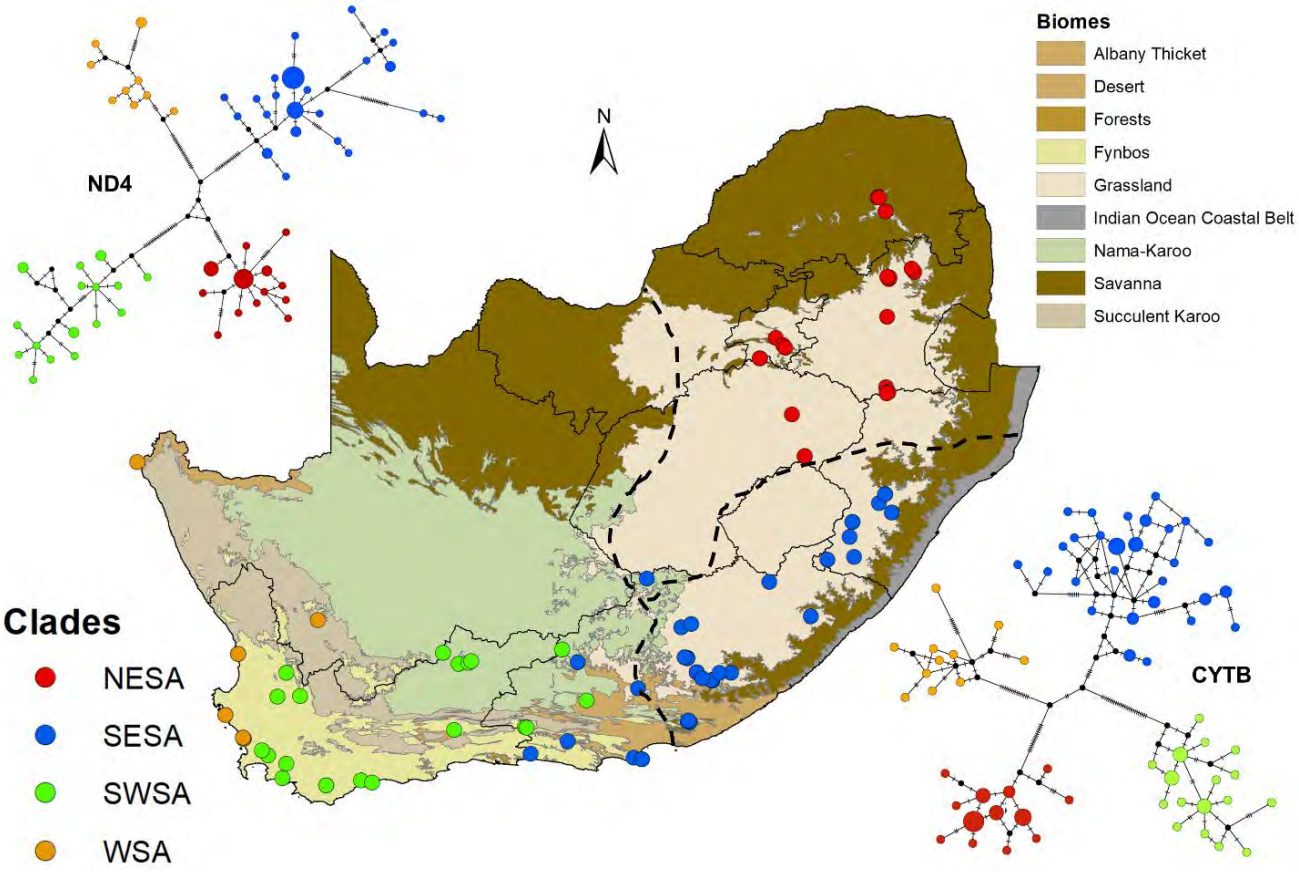

Figure 4.7**:** Distribution of samples use in study with coloured circles denoting their associated clade as identified in Fig. 4.3. On the map, the dotted line represents the boundary between morphologically distinctive groups, as reported in Broadley (1977). Solid lines denote provincial boundaries. Median-joining haplotype networks of cytb and ND4+LeutRNA, from *Dataset 4.5*, have also been overlaid, using an identical colour scheme. On the haplotype networks, the size of a circle is relative to the number of samples sharing that haplotype. Black lines represent mutation steps and black circles represent missing haplotypes.

Overall, most of the genetic variation was found between clades of *Ps. rhombeatus* (cytb: 84.59%, ND4+LeutRNA: 81.71%; Table 4.4), with similar variation partitioned between (cytb: 7.49%, ND4+LeutRNA: 10.58%; Table 4.4) and within (cytb: 7.93%, ND4+LeutRNA: 7.71%; Table 4.5) localities. Low fixation indices indicate evidence for interbreeding among localities, in both cytb (F_{ST} = 0.37–0.54) and ND4+LeutRNA (F_{ST} 0.40–0.57) (barring SWSA clade) (Table 4.4). The only exception was the SWSA clade using ND4+LeutRNA as it registered an F_{ST} value of 0.74 (Table 4.4).

Table 4.4: Hierarchical AMOVA over all sample localities and among the four supported clades in *Ps. rhombeatus* using *Dataset 4.5*. AMOVA on the four supported clades from *Ps. rhombeatus.* All values are statistically significant ($p < 0.05$).

Hierarchical AMOVA						
Source of variation		**Gene**	**DF**	**Variation**	**% Variation**	**Fixation Index**
Among Clades		cytb	3	Va = 14.58	84,59	FCT = 0.85
		ND4+LeutRNA	3	Va = 15.93	81,71	FCT = 0.82
Among Localities		cytb	48	Vb = 1.29	7,49	FST = 0.92
		ND4+LeutRNA	40	Vb = 2.06	10,58	FST = 0.92
Within Localities		cytb	42	Vc = 1.37	7,93	FSC = 0.49
		ND4+LeutRNA	41	Vc = 1.50	7,71	FSC = 0.58
AMOVA						
Clade	**Source of variation**	**Gene**	**DF**	**Variation**	**% Variation**	**Fixation Index**
SESA	Among Localities	cytb	20	Va = 2.02	53,77	FST = 0.54
		ND4+LeutRNA	18	Va = 2.52	56,93	FST = 0.57
	Within Localities	cytb	16	Vb = 1.74	46,23	
		ND4+LeutRNA	17	Vb = 1.91	43,07	
SWSA	Among Localities	cytb	13	Va = 0.71	39,07	FST = 0.39
		ND4+LeutRNA	9	Va = 2.89	73,77	FST = 0.74
	Within Localities	cytb	6	Vb = 1.11	60,93	
		ND4+LeutRNA	6	Vb = 1.03	26,23	
NESA	Among Localities	cytb	11	Va = 0.50	36,91	FST = 0.37
		ND4+LeutRNA	10	Va = 0.72	39,52	FST = 0.40
	Within Localities	cytb	14	Vb = 0.85	63,09	
		ND4+LeutRNA	12	Vb = 1.10	60,48	
WSA	Among Localities	cytb	4	Va = 1.72	48,47	FST = 0.48
		ND4+LeutRNA	3	Va = 2.17	57,02	FST = 0.57
	Within Localities	cytb	6	Vb = 1.83	51,53	
		ND4+LeutRNA	6	Vb = 1.63	42,98	

Excluding ND4+LeutRNA sequences from the SWSA clade, the Fu's F_S index was significantly negative for all clades in both genes, indicating that the clades of *Ps. rhombeatus* have undergone recent expansion, evidenced by the excess alleles detected in the analysis (Table 4.5). Tajima's D index was also negative in all clades across both genes, but only the cytb SWSA, cytb WSA and ND4+LeutRNA NESA groupings carried significance, meaning that the expansion observed here, may be a result of a genetic bottleneck or selective sweep (Table 4.5).

Table 4.5: Population analyses for four supported clades of *Ps. rhombeatus* using *Dataset 4.5.* N = Number of Samples; π = Nucleotide Diversity; F_S = Fu's F_S Statistic; Tajima's D = Tajima's D Statistic; SSD = Sum of Square Distances; RI = Raggedness Index

Clade	Gene	N	π	Fu's F_S	Tajima's D	SSD	RI
SESA	cytb	39	7.12	**-14.58**	-0.73	**0.01**	**0.01**
	ND4+LeutRNA	38	8.21	**-7.26**	-1.27	**0.01**	**0.01**
SWSA	cytb	23	3.51	**-11.34**	**-1.53**	**0.00**	**0.02**
	ND4+LeutRNA	19	7.45	**-6.34**	-0.68	0.04	**0.03**
NESA	cytb	26	2.62	**-5.82**	-1.45	**0.00**	**0.03**
	ND4+LeutRNA	23	3.53	**-4.74**	**-1.89**	**0.01**	**0.04**
WSA	cytb	11	6.36	**-5.92**	**-1.65**	**0.03**	**0.06**
	ND4+LeutRNA	10	6,44	**-2,79**	-0,20	**0,05**	**0,10**

For Fu's Fs and Tajima's D, values in bold indicate rejection of the hypothesis of constant population size ($p < 0.05$). SSD and RI in bold indicate failure to reject the hypothesis of spatial expansion assuming constant deme size ($p > 0.05$).

The potential for a recent genetic bottleneck in cytb SWSA and ND4+LeutRNA NESA is further evidenced by the starburst patterns observed in the haplotype networks in Fig. 4.7. The haplotypes observed in Fig. 4.7 may also be a result of recent spatial expansion, as the observed and expected mismatch frequencies form similar curves when plotted on the same axis (Fig. 4.8). The significant SSD and RI scores show that none, except the bimodal ND4+LeutRNA SWSA, statistically disprove the model of spatial expansion assuming constant deme size (Table 4.5).

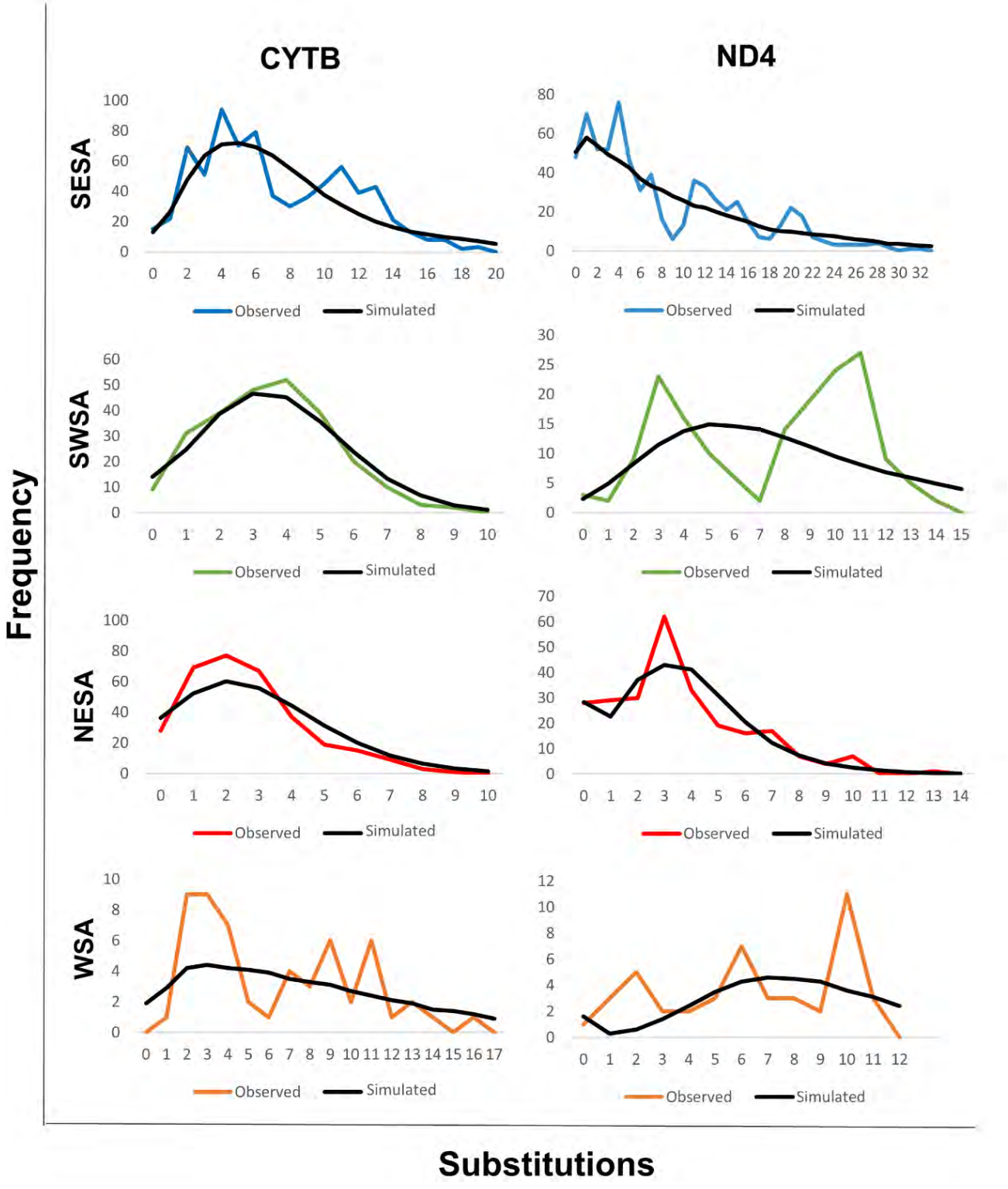

Figure 4.8: Mismatch distributions for each clade of *Ps. rhombeatus* using *Dataset 4.5*. Coloured lines show the observed distribution, and black lines show the distribution simulated under a model of spatial expansion assuming constant deme size.

Geometric Morphometric Analyses

The first dorsal PC (DC-PC1) axis contrasted head width, snout length, and parietal scale width, describing 22.12% of total variation (Fig. 4.9), whereas DC-PC2 contrasted the length of the frontal and internasal scales, width of the posterior of the parietal scale, the width of the head and the sharpness of the snout, contributing 15.52% of the variation (Fig. 4.9). DC-PC3 contributed only 12.9% of total variation, and contrasted width of the mid-snout region and anterio-posterior length of the frontal scale (Fig. 4.9).

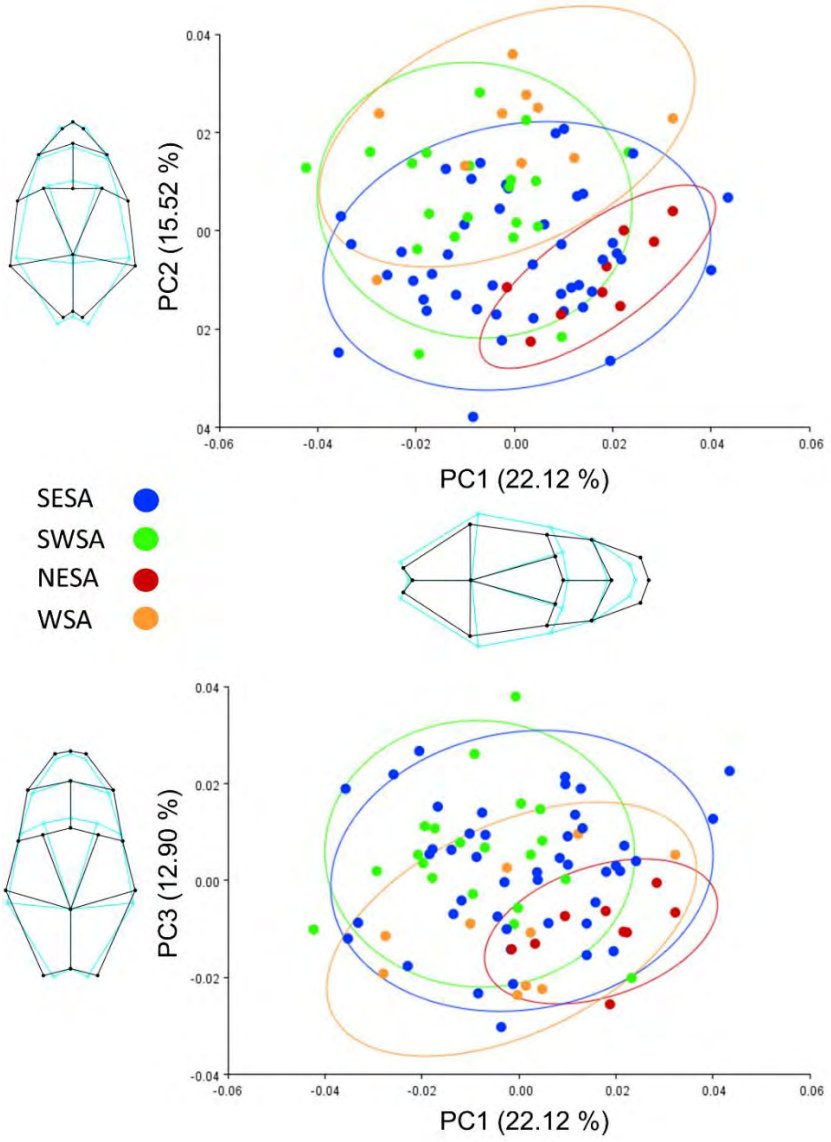

Figure 4.9: Geometric morphometric analyses of the dorsal view of the heads of the four clades within *Psammophylax rhombeatus*. Wireframe diagrams to the left and below the scatterplots of the principal component scores for the first three PC axes, represent the shape changes of each axis. The wireframes showcase the warping of the positive sides of the axes (black lines) from the mean configuration (cyan lines).

The first lateral PC axis (LC-PC1) contrasted head height and length of the upper labial, describing 23.51% of total variation (Fig. 4.10). LC-PC2 described 15.88% of variation and contrasted the width of the upper labial scales (mouth length) (Fig. 4.10). LC-PC3 described only 12.48% of the variation and contrasted posterior head height, and upper labial shape (Fig. 4.10). Representatives of the four clades of *Ps. rhombeatus* did not differ from one another, with substantial overlap in the 90% confidence interval ellipses across all four clades in both the dorsal and lateral views. Further analysis was thus not conducted.

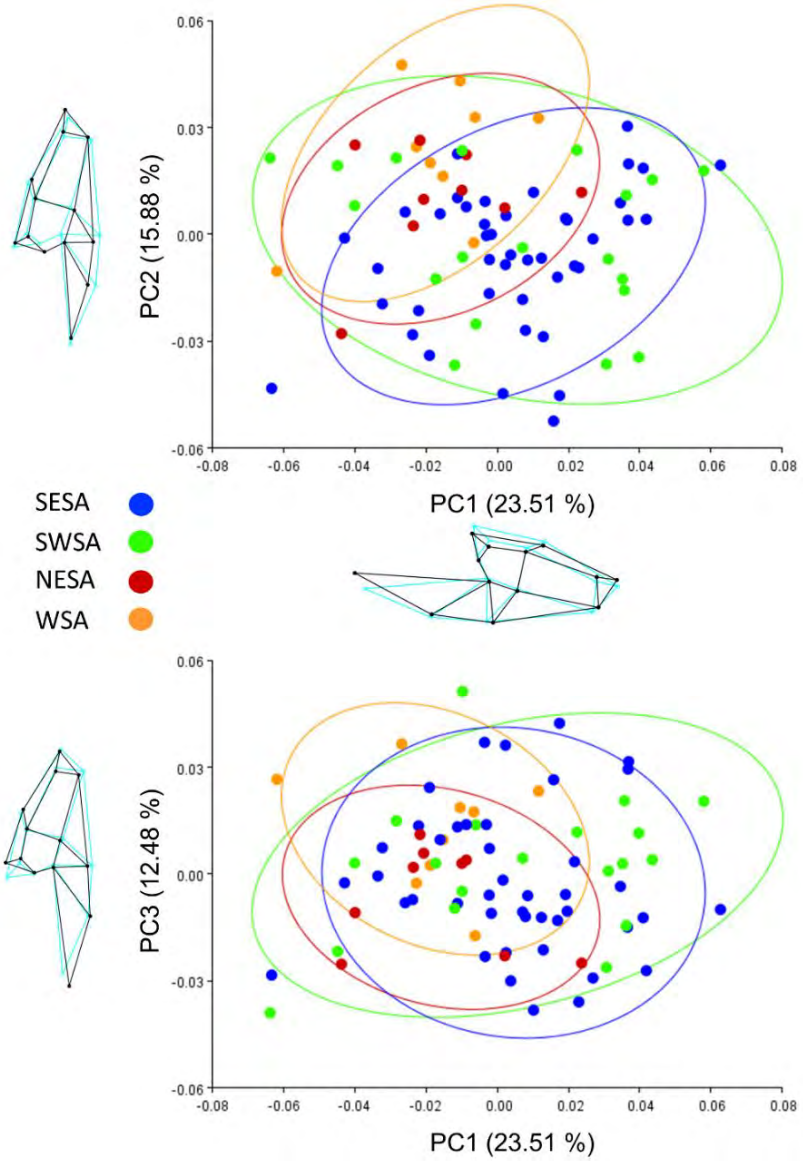

Figure 4.10: Geometric morphometric analyses of the lateral view of the heads of the four clades within *Psammophylax rhombeatus*. Wireframe diagrams to the left and below the scatterplots of the principal component scores for the first three PC axes, represent the shape changes of each axis. The wireframes showcase the warping of the positive sides of the axes (black lines) from the mean configuration (cyan lines).

Discussion

Phylogenetic analysis supported the topology and systematic revisions of previous studies (Keates *et al.*, 2019; Kelly *et al.*, 2008). The large, species-wide sampling afforded to the study uncovered high intraspecies diversity, in the form of four well-supported clades, the taxonomic validity of which were assessed using a combination of threshold- and distance-based analyses. They were used in combination as all species delimitation methods have caveats and pitfalls that can result in incorrect systematic conclusions when used in isolation (Carstens *et al.*, 2013; Flot, 2015; Fontaneto *et al.*, 2015). This can be seen in the implementation of both bPTP and PTP analysis in this study and in Busschau *et al.* (2019) which resulted in an over-estimation of putative taxa, through the recognition of intraspecific diversity as interspecific variation.

Species delimitation is relative and dependent on the taxon upon which natural selection acts, and its associated evolutionary history. Distinctive units can only be elevated to species level based on a shared uniqueness compared to other taxa. The variation in recognised putative taxa between the different species delimitation methods, in this study, highlights the effect that taxon size and type have on the output from these analyses. Furthermore, the results from the single- and multi-tree bGMYC methods varied between this chapter and Chapter Three. This shows the importance of context when interpreting the outputs from species delimitation methods and the need for robust multi-faceted methodologies when making inferences about species boundaries. Whilst several of the species delimitation methods (and varying thresholds) recognised several putative taxa within *Ps. rhombeatus*, the relatively low variation among clades of *Ps. rhombeatus* in this study, combined with the overlap of inter- (*Ps. rhombeatus*) and intraspecies (*Ps. variabilis*) variation in barcode gap analysis, necessitates the recognition of *Ps. rhombeatus* as a single species with four genetically diverse populations. The four clades identified within *Ps. rhombeatus* are not considered separate species, but rather genetically divergent lineages based on the combined findings of the species delimitation analyses and the p-distance and barcode gap analyses. It is important to note the high degree of intraspecies variation within *Ps. rhombeatus,* irrespective of the smaller range of the species, as compared to species like *Ps. tritaeniatus* and *Ps. variabilis,* that span sub-Saharan Africa (Spawls *et al.*, 2018). It must however be noted that all the species delimitation methods in this chapter, and past chapters, omitted nuclear markers, thus making multilocus species delimitation impossible. This was largely a product of a lack of nuclear loci on Genbank. Since the single locus approach omits corroborating evidence from other markers it can argued that the species delimitation used here, although robust, may not represent the most accurate systematic picture. However, for

the interest of this discussion and with the methods used here, I have treated the clades of *Ps. rhombeatus* as representative of intraspecies diversity.

Geometric morphometrics further supported the recognition of *Ps. rhombeatus* as a single species given the lack of morphological difference between the clades. It is, however, interesting to note that the scalation on the head of *Ps. rhombeatus* samples associated with the WSA clade differs from others. In most of the samples examined, snakes associated with the WSA clade had a larger rostral scale, that extended between the internasals, to the anterior of the pre-frontals, giving the tip of the nose a spade-like shape. The rostral scale also extended beyond the internasals, at the tip of the nose. This differed from the other clades (except for several geographically close SWSA samples) that exhibited a smaller rostral scale that did not extend to the anterior of the prefrontals. The rostral scale in the other clades was also found to be wider, more rounded, and did not extend beyond the internasals at the tip of the nose. Whilst neither dorsal nor lateral morphometric analyses could tease apart any differences in head shape between WSA and the other clades (either because of the subtlety of the variation or the inaccuracy of the landmarks used), it is postulated that the shape of the rostral scale confers an advantage for snakes inhabiting softer soils, especially since the clade is restricted to the loose soils of the west coast. The ability to burrow with the modified rostral scale in the alluvial soils of the west coast may afford the animal protection from both the elements and predators, or alternatively may help the snake to locate and prey upon burrowing species of reptiles and amphibians found within the biotype. This can be evidenced by the findings of Cottone and Bauer (2008) that observed *Ps. rhombeatus* from the western coast of South Africa (WSA) using its head and neck to scoop sand out of a burrow in pursuit of an adult *Breviceps namaquensis*. Several members of the SWSA clade also displayed a similar rostral scale shape and given their close geographical proximity to the WSA clade, it is possible that the morphological adaptation is a product of rapid morphological divergence, as a result of an adaptation to post Last Glacial Maximum (LGM) South Africa.

South Africa is the seventeenth most biodiverse country on Earth, playing host to nine biomes and 458 ecosystem types, supporting approximately 407 reptile species, 50% of which are endemic (Bates *et al.*, 2014; Tolley *et al.*, 2019). South Africa also supports three global biodiversity hotspots: the Cape Floristic Region, Succulent Karoo and Maputaland–Pondoland–Albany hotspot, with the interplay between the first two being important to the geographical delineation between the WSA and SWSA clade (Critical Ecosystem Partnership Fund, 2020; Tolley *et al.*, 2009). It is, thus, unsurprising that the largest intraspecific p-distance (ND4+LeutRNA: 8.4%) recorded in *Ps. rhombeatus* was found between a sample from the CFR hotspot (CK2) and the grassland biome (TP3), given the high structural diversity

associated with the different biotypes. This is in stark contrast to *P. schokari*, which exhibits an intraspecific variation of 0.2–7.1% (ND4+LeutRNA) across its entire distribution, that spans two continents (from northern Africa to Pakistan) (Gonçalves *et al.*, 2018).

South Africa's wide range of bioclimates combined with varying geological and topological conditions have produced the high diversity observed currently, supporting the richest diversity of amphisbaenians, cordylids, geckos, and Acontinae in Africa (Bates *et al.*, 2014; Busschau *et al.*, 2017; Jacobsen *et al.*, 2014; Weinell & Bauer, 2018). Snake species richness is low when compared to lizard diversity and this is likely a product of a more generalist, wide-ranging lifestyle in snakes (Bates *et al.*, 2014; Marais, 2004; Spawls *et al.*, 2018). The higher species diversity observed in South African lizards is likely a product of increased habitat specificity, promoting localised adaptation, divergent speciation, and endemism. This can be evidenced by the lowered endemism amongst South African Psammophiidae (14 spp.), with the proposed synonymy of *Psammophis trinasalis* and *Psammphis namibensis* with *Psammophis leightoni* (Taft, 2018).

The habitat-generalist nature of psammophiids likely enables them to navigate vicariant barriers that might otherwise cause speciation in rupiculous lizards (Bauer & Lamb, 2005; Travers *et al.*, 2014) and ambush-hunting snake species (Barlow *et al.*, 2019), allowing intraspecific divergences to accrue in the genome of separate populations without complete isolation. Other widespread members within the family include *Kladirostratus acutus* (Kelly *et al.*, 2008), *Psammophis schokari* (Gonçalves *et al.*, 2018) and *Psammophis mossambicus* (Trape *et al.*, 2019). The geographic exclusivity of the different *Ps. rhombeatus* clades makes them important ecotypes, and potentially morphotypes, based on the work of Broadley (1977).

The geographic positioning of the *Ps. rhombeatus* clades was similar to those proposed by Broadley (1977), who separated the species into three groups based on differing body patterns, and to a lesser extent, scale counts. The geographic split between the SESA and SWSA clade is virtually identical (except for a single SESA sample from southern Free State), whilst the distinction between SESA and SWSA differs in both the complexity and placement of the barrier among populations. The WSA clade identified here was also not attributable to a specific pattern, as SWSA and WSA are combined under the guise of the rhombic pattern in Broadley (1977). Western South African specimens, however, possess a higher subcaudal scale count, making them discernible from their congeners (Broadley, 1977). This highlights the complex interplay between morphology and molecular biology, which seems to be congruent in northern South Africa, and less so in southern and western South Africa.

Incongruent morphological and molecular results are not uncommon in the family, with the recent work of Ruane *et al.* (2018) resulting in the recognition of a new species (*Mimophis occultus*) from northern Madagascar. Interestingly, the three colour forms (striped, unpatterned, and zig-zag), originally thought to be taxonomically informative (Glaw & Vences, 1994; Gunther, 1868), were found in both species irrespective of geography and sex. The same polymorphic forms have been observed in *Psammophis crucifer*, *Psammophis notostictus* and *Psammophis sibilans* (Branch, 1998), *Hemirrhagerhis nototaenia* and *Ps. variabilis* (Spawls *et al.*, 2002), *Ps. schokari* (Kark *et al.*, 1997), and most notably *Ps. rhombeatus* (Fig. 4.1), highlighting the morphological variability of these taxa across heterogeneous environments.

The diversification within *Ps. rhombeatus* coincides with the proliferation of C 4 grasses in the late Pliocene/early Pleistocene (Hewitt, 2004b). This shift was once believed to have facilitated the shift from forested to open habitats, driving speciation, but new evidence suggests that C 3 grasses displaced C 4 grasses in the Miocene, with C 4 grasses emerging later (Edwards et al., 2010; Quade et al., 1989). Given this, the habitat topology would have remained similar for *Ps. rhombeatus* through the vegetative shift, meaning the grasses probably had little bearing on the diversification of the species. Mammalian diversity, however, increased post-C4 expansion as the change in grass brought with it changes to the food web, that in turn, sustained large ungulates. Similar patterns of diversification are seen in *Bitis arietans* (Barlow *et al.*, 2013), *Psammophis schokari* (Gonçalves *et al.*, 2018), and several other psammophiids from Chapter Two, which diversified approximately 1–5 MYA. Much like *B. arietans*, *Ps. rhombeatus* exhibits a high degree of phylogeographic structuring, unlike mammals that generally exhibit high levels of genetic diversity (Lorenzen *et al.*, 2012). This suggests that southern Africa represented a large, stable, refugial area for mammals (Lorenzen *et al.*, 2010, 2012).

Unlike East Africa, which experienced fluctuating humidity regimes, causing episodic forest expansion and contraction, South African humidity levels remained relatively stable. This supports the stable refugial hypothesis for mammals as open landscapes would have persisted through the Pliocene, Pleistocene, and into current day (Maslin *et al.*, 2012). Amid a stable, open-habitat South Africa, climatic factors such as temperature and rainfall varied greatly during glacial cycles. Mean temperature varied as much as 5 °C between the Last Glacial Maxima (LGM) and the inter-glacials (current day) (Kulongoski & Hilton, 2004). The distribution of reptiles is strongly dependent on temperature and rainfall (Ward, 2009). In Barlow *et al.* (2013), reduced winter temperatures and, to a lesser extent, reduced precipitation were postulated as the driving factors that resulted in refugial populations of *B. arietans*, that

expanded post LGM. Given the similarity in the population structure within *Ps. rhombeatus* and *B. arietans*, it is possible that the highly structured genetic clades retrieved within *Ps. rhombeatus* are a product of the same abiotic factors that resulted in the current phylogeographic structuring within *B. arietans.*

Psammophylax rhombeatus is a widespread habitat-generalist that can be found throughout South Africa, absent only from the arid interior (Broadley, 1977), an environment that was proposed as unsuitable during the LGM, just 21 000 years ago (Barlow *et al.*, 2013). *Psammophylax rhombeatus* also shares a relatively similar population structure to *B. arietans* (Barlow *et al.*, 2013), with similar contact zones between genetically diverse clades (WSA + SWSA and NESA +SESA). The high mean rainfall region of the CFR is of particular interest as it dissects the WSA and SWSA clades of both species, almost identically (Barlow *et al.*, 2013; Tolley *et al.*, 2009). This same region has also been observed as an important biogeographic barrier separating genetically diverse clades of *Agama atra*, *Bradypodion* spp. and *Pedioplanis burchelli* (Tolley *et al.*, 2009) and populations of *Cordylus cordylus* (Diedericks & Daniels, 2014).

The similarity of the population structuring within *Ps. rhombeatus* coupled with the biogeographic analysis (in this thesis), supporting recent expansion, either spatially or demographically, gives support to the hypothesis that clade structure in this study may be the result of ancient refugial isolation (potentially LGM induced). Post-refugial expansion is thus proposed as a possible explanation for the population structuring observed in *Ps. rhombeatus*. Future research can be geared towards modelling the distribution of *Ps. rhombeatus* throughout the Last Glacial Maxima to determine whether the assumptions of this paper are supported.

Although highly structured, this species lacks the support necessary to warrant taxonomic re-evaluation, under the guise of the Unified Species Concept. Barring this, the clades identified within this chapter harbour substantial genetic diversity, with intraspecies variation comparable with that of cross-continental species such as *Ps. tritaeniatus* and *Ps. variabilis*. Given the comparably smaller distribution of *Ps. rhombeatus*, these findings highlight the substantial effect that South Africa's past and present biogeography and climate have had on the structuring within the species. Much like *B. arietans*, the clades identified within this study represent evolutionary significant units, and whilst species status cannot be afforded to them, conservation authorities should endeavour to safeguard each clade, and in doing so preserve their ecological future.

Chapter Five: General Conclusion

This study represents the most comprehensive evolutionary study of the family Psammophiidae to date. Using sophisticated phylogenetics, comprehensive taxon sampling and geometric morphometric techniques, the findings from this thesis allow me to make inferences about the taxonomy, and by extension, the evolutionary history of the family, across multiple levels of organismal biology. The taxon-specific focus that predicated this thesis allowed me to determine the best methodology, and suite of analysis necessary, to accurately capture the species diversity within Psammophiidae.

Using a combination of accessioned and newly sequenced material, Chapter Two produced a comprehensive phylogenetic reconstruction of the family. Barring *Kladirostratus togoensis*, *Psammophis pulcher* and several of the Asiatic *Psammophis*, the phylogeny contained all recognised species of the family. The results from the phylogenetic component of Chapter Two showed improved systematic structuring, through the resolution of previously unsupported relationships at both the genus and species level. Threshold-based species delimitation uncovered several putative taxa within *Psammophis*; a feat made possible by the acquisition of multiple samples from novel localities throughout Africa. Whilst phylogenetic reconstruction did not recover novel taxa in the other groups, the robust taxon-sampling afforded to this study ratified, and in some cases improved, upon the findings of past papers focusing on genera such as *Malpolon*, *Rhagerhis,* and *Mimophis* (Carranza *et al.*, 2006; Ruane *et al.*, 2018). Whilst the placement of *Dipsina* remains unresolved, time-calibrated phylogenetics shed light on the potential evolutionary history of the family. Lastly, geometric morphometrics of head shape highlighted the variation in head shape between genera, with ecology postulated as a potential driver of 'beakedness' in several members of the family.

The methodology from Chapter Two when applied to the generic level (Chapter Three) improved the resolution of several intrageneric relationships within *Psammophylax*, when compared to the findings of the past chapter. The phylogenetic methods championed in Chapter Two, also revealed genetic diversity enough to warrant the recognition of a cryptic species and a novel genus, when applied to Chapter Three. Geometric morphometrics supported the recognition of *Psammophylax acutus* as a novel genus (now *Kladirostratus*)*,* and in so doing supported the findings of Chapter Two that postulated that variation in head shape ('beakedness') may represent an ecological adaptation. Geometric morphometrics (of head shape) were, however, not useful in teasing apart species within *Psammophylax*.

Chapter Four uncovered substantial phylogeographic sub-structuring within *Ps. rhombeatus*, and with the exception of the *P. schokari* phylogeographic study (Gonçalves *et*

al., 2018), represented the most comprehensive phylogenetic study of a single psammophiid. By focussing on the species level, arguably the lowest form of recognised taxonomic structuring, I was able to determine the difference between intra- and interspecies variation among populations and through this, determine whether the methods championed in previous chapters were effective at the lowest taxonomic rank. The phylogeographic structuring within *Ps. rhombeatus*, similar to that of *Bitis arietans* (Barlow *et al.*, 2013), irrespective of the contrasting ecology and behaviour of the snake, has provided valuable insights into the potential phylogeographic structuring of other members of the family.

Knowledge Gaps in Psammophiidae

The research from this thesis builds on the enormous body of work available for African snakes, and more specifically, Christopher Kelly's PhD thesis (Kelly, 2005). Whilst most of his thesis focused on the phylogenetics of advanced snakes, his last chapter (Chapter Four) dealt with Psammophiinae. His work identified seven gaps in our knowledge of the family; gaps that have been addressed by the completion of this thesis, and by several other authors over the past decade.

Psammophylax Taxonomy

The chequered taxonomical structuring within *Psammophylax,* identified in Kelly (2005), was explored and discussed in Chapters Three and Four of this thesis. Increased taxon sampling within *Psammophylax*, coupled with the inclusion of *Ps. ocellatus,* allowed me to address the the knowledge gap within the genus. In Chapter Three, I recovered a cryptic species within *Ps. multisquamis*, resulting in the description of *Psammophylax kellyi* **sp. nov.** from Tanzania. The robust taxon sampling afforded to Chapter Three also facilitated the resolution of all the intrageneric relationships within the family, corroborating the species-level status of all described species. The sub-specific status of *Ps. v. vanoyei and Ps. t. subniger* was also addressed in this thesis, and found wanting, with shallow structuring in both subspecies resulting in the synonymisation of these taxa with *Ps. variabilis*. Additionally, Chapter Three and four highlighted substantial phylogenetic sub-structuring within the genus, with *Ps. rhombeatus* exhibiting the highest intraspecific variation, irrespective of its comparably smaller distribution. The findings discussed above were published recently in Keates *et al.* (2019)

The 'acutus' Problem

Previously a member of *Rhamphiophis*, *K. acutus* was recovered as sister to *Psammophylax* in Kelly (2005) and the many publications that followed (Figueroa et al., 2016; Kelly et al.,

2008; Zaher et al., 2019). These findings were ratified by the multiple phylogenetic analyses implemented across all three data chapters of this thesis. The incorporation of west African *K. a. acutus* strengthened this assertion and the use of distance-based analysis and geometric morphometrics (on head shape) provided strong support for the separation of the species from the rest of *Psammophylax*. Based on both molecular and morphological evidence *K. a. acutus, K. a. jappi, and K. togoensis* were moved into a new genus, termed *Kladirostratus*, in honour of the late Professor Bill Branch. The genus description published recently by Keates *et al.* (2019)

Cryptic Speciation in Mimophis

Christopher Kelly uncovered substantial genetic structuring within *Mimophis* during his thesis (Kelly, 2005), and subsequent publication (Kelly *et al.*, 2008), and developed the hypothesis, based on limited sampling, that the high intraspecific diversity found within the monotypic genus may represent unappreciated species diversity. This was confirmed by Ruane *et al.* (2018), with the description of *Mimophis occultus* from northern MadagascarThe latter was made possible by the inclusion of a more complete taxon sampling regime and species-specific phylogenetic testing. Although morphologically indistinct, the new species can be distinguished from *M. mahafalensis* on phylogenetic and geographic grounds. The inclusion of newly sequenced samples of *M. occultus* in Chapter Two of this thesis allowed me to corroborate the results of Ruane *et al.* (2018), and in doing so, support the original hypothesis of Kelly (2005).

The 'leightoni Complex'

The '*leightoni* complex' was a large, protracted taxonomical problem until the recent study of (Taft, 2018). *Psammophis l. leightoni*, *P. l. namibensis* and *P. l. trinasalis* were elevated to species level by Broadley (2002) based on ecological and morphological differences. in Kelly (2005), *P. leightoni* and *P. namibensis* were shown to harbour low levels of genetic diversity with preliminary results indicating that the two species were synonymous. The species complex was investigated by Taft (2018) and through the incorporation of never-before-sequenced *P. trinasalis* samples and improved taxon sampling, the findings of Kelly (2005) were recovered similarily. Based on the findings of Taft (2018), doubt was cast on the original ecological and morphological assertions made by Broadley (2002) and all three species will likely be synonymised, pending the publication of the results from Taft (2018). I improved on the taxon sampling of the complex to incorporate an additional Namibian *P. namibensis* sample, as this clade was retrieved as sister to the entire '*leightoni* complex' in Taft (2018). My results produced similar results, but with a different taxonomical conclusion. It was

however concluded that no taxonomical assertions would be made, based on the findings of this thesis alone, given the the more robust methodology employed in Taft (2018).

The 'sibilans Complex'

The '*sibilans* complex' is among the most protracted and problematic species complexes in African herpetology (Broadley, 1963; Hughes, 1999; Trape *et al.*, 2019). Our understanding of the group has improved gradually over the past century through the efforts of many morphological taxonomists (such as: Loveridge, 1940; Broadley, 1963, 2002; Brandstätter, 1995; Hughes, 1999; Hughes & Wade, 2004). Kelly (2005) built on these findings with comprehensive genetic analysis. This was improved upon by Trape *et al.* (2019), with taxon-specific genetic and morphological analysis, which resulted in the recognition of a new species, *P. afroccidentalis*, from west Africa. In addition to improving molecular taxon sampling within the *'sibilans* complex', Trape *et al.* (2019) also improved on the descriptions of all the species and clarified their distributions with updated geographic sampling. In Chapter Two of this thesis, a representative sampling from Trape *et al.* (2019), Kelly *et al.* (2008) and various other papers was included. The findings from this thesis corroborate the newly described species from Trape *et al.* (2019), with strong support. Through the use of a larger molecular compliment, Chapter Two also improved on the findings of all past papers, with stronger nodal support and more pronounced genetic structuring (Kelly *et al.*, 2008; Trape *et al.*, 2019; Zaher *et al.*, 2019). Whilst the group remains problematic, evidenced by the lack of support at several nodes, the phylogenetic reconstruction in Chapter Two represents a step forward in our understanding of the problematic complex.

Taxon sampling

This thesis built on Kelly (2005) through the incorporation of a vastly greater dataset for Psammophiidae. The recent taxon-specific studies of Carranza *et al.* (2006), Gonçalves *et al.* (2018), Taft (2018), Ruane *et al.* (2018) and Trape *et al.* (2019) afforded novel sampling to many species with this thesis filling in the gaps with representative sampling from under sampled taxa (especially from south-western Angola). This thesis also added two never-before-sequenced animals (*P. zambiensis* and *H. nototaenia*). The result was the recognition of several potential new species in Chapter Two and the recognition and the description of both a new genus and species in Chapter Three. Whilst *Ps. rhombeatus* lacked the structuring necessary to warrant taxonomic re-evaluation, the comprehensive sampling afforded to Chapter Four highlighted the enormous potential for phylogeographic studies within the family. Variable taxon sampling was at the centre of this thesis. By incorporating multiple taxon-specific datasets into a larger family level study, this study was afforded the robustness to

resolve many of the unsupported relationships identified in other studies. The complete dataset of Chapter Two resolved several of the intergeneric relationships within Psammophiidae whilst still retaining the robustness necessary to tease apart potential new taxa in enigmatic species such as *H. nototaenia*, *P. angolensis* and *P. lineatus*. In Chapter Three, the focus was narrowed to the genus level, with a larger sampling afforded to each species. Whilst the topology of *Psammophylax* was retrieved similarly to Chapter Two, it was retrieved with greater support. In Chapter Four, the focus was once again narrowed, but this time, to the species level. The larger dataset afforded to *Ps. rhombeatus* once again resolved several of the topological arrangements of Chapter Two and Three, with increased support. Species delimitation analyses employed in Chapters Three and Four also retrieved contrasting numbers of putative taxa. Although not a focus of this thesis, the variation in results between all three chapters highlights the enormous effect that dataset size and composition can have on phylogenetic results. With molecular biology becoming increasingly more prevalent in taxonomic studies, this is something that should be considered by scientists, especially when interpretating species delimitation results and making recommendations about potential new taxa.

Disparity Between Node Dates

One of the biggest caveats of Kelly (2005) was the disparity between equivalent node dates between chapters. When estimating the mean age of the crown node of Psammophiidae, Kelly (2005) recovered the radiation in the early Oligocene (~33.5 MYA) and early Eocene (~48.2 MYA), in Chapters Three and Four, respectively. In this thesis however, the radiation of the family was recovered ~17.97 MYA and ~16.77 MYA in Chapters Two and Four, respectively. The crown node was thus retrieved in the same epoch, around the same time period (Early Miocene) in this thesis. Kelly (2005) postulated that the discrepancy may be a product of biased taxon sampling, with his chapters utilising vastly different sampling regimes. Whilst species composition of ingroup taxa varied between the two chapters in this thesis, the outgroup taxa remained the same, thus producing similar node age estimates between the two time-calibrated phylogenies. These findings support the conclusions of Kelly (2005) and highlight the variable effect that species representation and taxon sampling has on molecular biology. Evolutionary biologists should be wary of these potential discrepancies when drawing parallels between studies that utilise contrasting time-calibrated phylogenies, as the inferences could be wrong.

Future directions

Chapter Two: Psammophiidae

Whilst this thesis was afforded the most comprehensive sampling of the family possible, several species are yet to be sequenced. Future studies should thus endeavour to include *Psammophis pulcher*, *P. indochinensis*, *P. leithi* and *P. longifrons*, as their phylogenetic placement may resolve the unsupported relationships that remain within the family. The Asiatic whip snakes are of particular interest given their sister relationship with the rest of *Psammophis*. The acquisition of novel Asiatic *Psammophis* samples in future studies will be critical to the phylogenetic resolution of the group, to determine the validity of '*Taphrometopon'*. The robust taxonomic sampling afforded to Chapter Two resulted in the recognition of several potential new taxa (*H. nototaenia, P. schokari*, *P. lineatus*, *P. sibilans*, *P. orientalis*, *P. angolensis*, *P. subtaeniatus* and *P. rukwae).* Future studies should investigate these taxa, in detail, to determine whether the groupings identified here represent novel species or instances of intraspecies variation.

Chapter Three: Psammophylax

Biological material for *Kladirostratus a. togoensis* and *K. a. jappi* were not available, so going forward, material for both taxa should be sought and sequenced to determine their phylogenetic placement. *Kladirostratus togoensis* (previously *Ps. a. togoensis*) was recently elevated to species level based on labile morphological characteristics identified in Segniagbeto *et al.* (2011). Future research should thus endeavour to assess the species status of both *K. togoensis* and *K. a. jappi.* Whilst most species were well sampled, *Ps. tritaeniatus* remains relatively under-represented in this thesis, and the acquisition of novel samples from the full distributional extent of this species may reveal unappreciated diversity. As alluded to in chapter three, future systematic work on the group could test the viability of the putatitve taxa identified by the species delimitation analyses using a hypothesis testing framework. Through the use of additional nuclear loci and multilocus species delimitation, future work may recognise taxa, labelled as unconfirmed candidate species here.

Chapter Four: Psammophylax rhombeatus

Whilst this study captured virtually the entire extent of *Ps. rhombeatus*, samples from Namibia were not available. This area represents an interesting biogeographical component of the distribution of the species, especially since it is separated from South Africa by the Orange River, a a potential vicariant barrier for the snake. Whilst *P. trinasalis* and *P. notostictus* show

little molecular variation between populations distributed north and south of the Orange River, *P. namibensis* shows substantial variation, making it a point of interest for future work on *Ps. rhombeatus* (Taft, 2018). Whilst not possible for this thesis, given the logistical constraints arising from the global pandemic, resulting work on the species should include an ancestral state reconstruction to determine, with confidence, whether the colour and pattern forms identified by Broadley (1977) are attributable to the molecular clades identified in Chapter Four. Lastly, future research on the group could treat the four clades of *Ps. rhombeatus* as unconfirmed candidate species and test their viability for species level status using a hypothesis testing framework.

Epilogue

I began this research with the belief that systematic sorting was convoluted and error-prone, a product of humanity's perpetual over-simplification of the evolutionary process. Unfortunately, nature cannot be ordered, especially by only one species concept in isolation. In this thesis, I thus endeavoured to remedy this perceived failing through the application of multiple species concepts. Psammophiidae was chosen given its protracted taxonomical history and abundance of biological material across multiple systematic levels. Whilst my findings shed light on countless instances of over- and under-appreciated diversity, thereby facilitating improvements to our understanding of the group, it also highlighted the incredible fuzziness of the evolutionary process, through the lens of a single family. Whilst our understanding of evolutionary history continually improves with the advent of improving systematic methods, our refined findings cannot reconcile the ephemeral, intercalated, and messy nature of 'species'. Species are essentially cross-sections through evolutionary time, with scientists dictating their existence simply by where they decide to draw the line. Whilst problematic, systematic assignment should remain a prevalent part of the scientific endeavour. I believe; however, a restructuring is in order. To this end, the Unified Concept of Species should be adopted, because not only does this result in the most accurate taxonomy possible, but it also highlights the evolutionary and ecological significance of the animal in question, allowing us to make more educated decisions about wildlife, and in doing so, protect nature for generations to come.

References

Adalsteinsson, S. A., Branch, W. R., Trape, S., Vitt, L. J., & Hedges, S. B. (2009). Molecular phylogeny, classification, and biogeography of snakes of the family Leptotyphlopidae (Reptilia, Squamata). *Zootaxa*, *2244*, 1–50. https://doi.org/10.11646/zootaxa.2244.1.1

Agapow, P. M., Bininda-Emonds, O. R. P., Crandall, K. A., Gittleman, J. L., Mace, G. M., Marshall, J. C., & Purvis, A. (2004). The impact of species concept on biodiversity studies. *Quarterly Review of Biology*, *79*(2), 161–179. https://doi.org/10.1086/383542

Alexander, G. J., & Marais, J. (2007). *A Guide to the Reptiles of Southern Africa*. STRUIK Nature.

Arevalo, E., Davis, S. K., & Sites Jr, J. W. (1994). Mitochondrial DNA sequence divergence and phylogenetic relationships among eight chromosome races of the *Sceloporus grammicus* complex (Phrynosomatidae) in central Mexico. *Systematic Biology*, *43*(3), 387-418.

Armstrong, R. A., & Mcgehee, R. (1980). Competitive exclusion. *The American Naturalist*, *115*(2), 151–170.

Bandelt, H-J., Forster, P., & Rohl, A. (1999). Median-joining networks for inferring intraspecific phylogenies. *Molecular Biology and Evolution*, *16*(1), 37–48.

Barej, M. F., Rödel, M. O., Loader, S. P., Menegon, M., Gonwouo, N. L., Penner, J., Gvoždík, V., Günther, R., Bell, R. C., Nagel, P., & Schmitz, A. (2014). Light shines through the spindrift - Phylogeny of African torrent frogs (Amphibia, Anura, Petropedetidae). *Molecular Phylogenetics and Evolution*, *71*(1), 261–273. https://doi.org/10.1016/j.ympev.2013.11.001

Barlow, A., Baker, K., Hendry, C. R., Peppin, L., Hendry, C. R., Peppin, L., Phelps, T., Tolley, K. A., Wuster, C. E., & Wuster, W. (2013). Phylogeography of the widespread African puff adder (*Bitis arietans*) reveals multiple Pleistocene refugia in southern Africa. *Molecular Ecology*, *22*, 1134–1157. https://doi.org/10.1111/mec.12157

Barlow, A., Wüster, W., Kelly, C. M. R., Branch, W. R., Phelps, T., & Tolley, K. A. (2019). Ancient habitat shifts and organismal diversification are decoupled in the African viper genus Bitis (Serpentes : Viperidae). *Journal of Biogeography*, 1–15. https://doi.org/10.1111/jbi.13578

Bates, M. F., Branch, W. R., Bauer, A. M., Burger, M., Marais, J., Alexander, G. J., & de Villiers, M. S. (Eds.). (2014). *Atlas and Red List of the Reptiles of South Africa, Lesotho*

and Swaziland. Suricata 1. SANBI. https://doi.org/10.1017/CBO9781107415324.004

Bates, M. F., & Nuttal, R. (2013). A case of death-feigning in the striped grass snake *Psammophylax tritaeniatus* (Günther), with a review on the occurrence of this phenomenon in southern and eastern African snakes. *African Herp News*, *60*(60), 5–9.

Bauer, A. M. (1999). Evolutionary scenarios in the *Pachydactylus* Group geckos of southern Africa : new hypotheses. *African Journal of Herpetology*, *48*(1&2), 53–62. https://doi.org/10.1080/21564574.1999.9651072

Bauer, A. M., & Lamb, T. (2005). Phylogenetic Relationships of southern African geckos in the *Pachydactylus* Group (Squamata : Gekkonidae). *African Journal of Herpetology*, *54*(2), 105–129. https://doi.org/10.1080/21564574.2005.9635525

Baum, D. (1998). Individuality and the existence of species through time. *Systematic Biology*, *47*, 641–653.

Bazzaz, F. A. (1975). Plant species diversity in old-field successional ecosystems in southern Illinois. *Ecology*, *56*(2), 485–488.

Benton, M. J. (1997). *Vertebrate Palaeontology* (2nd ed.). Chapman & Hall.

Bickford, D., Lohman, D. J., Sodhi, N. S., Ng, P. K. L., Meier, R., Winker, K., Ingram, K. K., & Das, I. (2007). Cryptic species as a window on diversity and conservation. *Trends in Ecology and Evolution*, *22*(3), 148–155. https://doi.org/10.1016/j.tree.2006.11.004

Bogert, C. M. (1940). Herpetological results of the Vernay Angola expedition. *Bulletin of the American Museum of Natural History*, *77*, 1–107.

Böhm, M., Collen, B., Baillie, J. E. M., Bowles, P., Chanson, J., Cox, N., Hammerson, G., Hoffmann, M., Livingstone, S. R., Ram, M., Rhodin, A. G. J., Stuart, S. N., van Dijk, P. P., Young, B. E., Afuang, L. E., Aghasyan, A., García, A., Aguilar, C., Ajtic, R., … Zug, G. (2013). The conservation status of the world's reptiles. *Biological Conservation*, *157*, 372–385. https://doi.org/10.1016/j.biocon.2012.07.015

Böhme, W., & de Pury, S. (2011). A note on the generic allocation of *Coluber moilensis* Reuss, 1834 (Serpentes: Psammophiidae). *Salamandra*, *47*(2), 120–123.

Bouckaert, R., Vaughan, T. G., Barido-Sottani, J., Duchêne, S., Fourment, M., Gavryushkina, A., Heled, J., Jones, G., Kűhnert, D., Maio, N. De, Matschiner, M., Fábio Mendes, K., Műller, N. F., Ogilvie, H. A., Plessis, L. du, Popinga, A., Rambaut, A., Rasmussen, D., Siveroni, I., … Drummond, A. J. (2019). BEAST 2.5: An advanced software platform for Bayesian evolutionary analysis. *Plos Computational Biology*, 1–

28.

Boulenger, G. A. (1896). *Catalogue of the Snakes in the British Museum (Natural History). Volume III, containing the Colubridae (Opisthoglyphae and Proteroglyphae), Amblycephalidae, and Viperidae*. British Museum (Natural History).

Bourgeois, M. (1968). Contribution à la morphologie comparée du crâne des Ophidiens de l'Afrique Centrale. *Publications de l'Université Officielle Du Congo*, *18*, 1–293.

Branch, W. R. (1998). *Snakes and other Reptiles of Southern Africa*. STRUIK Nature.

Branch, W. R. (2016). *Pocket Guide: Snakes and Other Reptiles of Southern Africa*. STRUIK Nature.

Branch, W. R., Baptista, N., Keates, C., & Edwards, S. (2019). Rediscovery, taxonomic status, and phylogenetic relationships of two rare and endemic snakes (Serpentes: Psammophiinae) from the southwestern Angolan plateau. *Zootaxa*, *4590*(3), 342–366. https://doi.org/10.11646/zootaxa.4590.3.2

Branch, W. R., Tolley, K. A., Cunningham, M., Bauer, A. M., Alexander, G., Harrison, J. A., Turner, A. A., & Bates, M. F. (2006). *SANBI Biodiversity Series 5: A plan for phylogenetic studies of southern African reptiles* (Issue Biodiversity Series 5).

Brandstätter, F. (1995). *Eine Revision der Gattung Psammophis mit Berücksichtigung der Schwestergattungen innerhalb der Tribus Psammophiini (Colubridae: Lycodontinae).* Mathematik und Naturwissenschaften, Universität des Saarlandes, Saarbrücken.

Brandt, J. F. (1838). Note sur quatre nouvelles espéces de serpents de la coÎte occidentale de la mer Caspicane et de la Parse septentrionale découventes par M. Kareline. *Bulletin Science, Academy Imperial Science St. Petersberg*, 3(16), 241—244.

Brito, D. (2010). Overcoming the Linnean shortfall: Data deficiency and biological survey priorities. *Basic and Applied Ecology*, *11*(8), 709–713. https://doi.org/10.1016/j.baae.2010.09.007

Broadley, D. G. (1963). *Psammophis sibilans* (Linnaeus, 1758) – A taxonomic dustbin. *Herpetological Association of Rhodesia*, *20*(1), 5–7.

Broadley, D. G. (1966). A review of the African Stripebellied Sand snakes of the genus *Psammophis*. *Arnoldia, Rhodesia*, *2*(36), 1–9.

Broadley, D. G. (1971). A review of *Rhamphiophis acutus* (Günther) with the description of a new subspecies from Zambia (Serpentes: Colubridae). *Arnoldia*, *5*, 1–8.

Broadley, D. G. (1977). A revision of the African Snakes of the Genus *Psammophylax* Fitzinger (Colubridae). *Occasional Papers of the National Museums and Monuments of Rhodesia*, *6*(1), 1–44.

Broadley, D. G. (1983). *FitzSimons' Snakes of Southern Africa*. Delta Books.

Broadley, D. G. (1990). *FitzSimons' Snakes of Southern Africa* (Revised Ed). Donker Publishers.

Broadley, D. G. (1997). A review of *Hemirhagerrhis viperina* (Bocage) (Serpentes: Colubridae), a rupicolous Psammophine snake. *Madoqua*, *19*(2), 161–169.

Broadley, D. G. (2002). A review of the species of *Psammophis* Boie found south of latitude 12° S (Serpentes: Psammophiinae). *African Journal of Herpetology*, *51*(2), 83–119. https://doi.org/10.1080/21564574.2002.9635466

Broadley, D. G., Tolley, K. A., Conradie, W., Wishart, S., Trape, J.-F., Burger, M., Kusamba, C., Zassi-Boulou, A.-G., & Greenbaum, E. (2018). A phylogeny and genus-level revision of the African file snakes *Gonionotophis* Boulenger (Squamata : Lamprophiidae). *African Journal of Herpetology*, *67*(1), 43–60. https://doi.org/10.1080/21564574.2018.1423578

Bromham, L., Woolfit, M., Lee, M. S. Y., & Rambaut, A. (2002). Testing the relationship between morphological and molecular rates of change along phylogenies. *Evolution*, *56*(10), 1921–1930. https://doi.org/10.1111/j.0014-3820.2002.tb00118.x

Brown, W. M., George, M., & Wilson, A. C. (1979). Rapid evolution of animal mitochondrial DNA. *Proceedings of the National Academy of Sciences of the United States of America*, *76*(4), 1967–1971. https://doi.org/10.1073/pnas.76.4.1967

Bruford, M. W., Hanotte, M., Brookfield, J. F. Y., & Burke, T. (1992). Single Locus and Multilocus DNA Fingerprint. In *Molecular Genetic Analysis of Populations: A Practical Approach* (pp. 225–270). IRL Press.

Burns, K. J., Hackett, S. J., & Klein, N. K. (2002). Phylogenetic relationships and morphological diversity in Darwin's finches and their relatives. *Evolution*, *56*(6), 1240–1252.

Busschau, T. (2019). *Phylogeographic patterning of three co-distributed forest-dwelling reptile species along the east coast of South Africa*. Stellenbosch University.

Busschau, T., Conradie, W., & Daniels, S. R. (2019). Evidence for cryptic diversification in a rupicolous forest-dwelling gecko (Gekkonidae: *Afroedura pondolia*) from a biodiversity

hotspot. *Molecular Phylogenetics and Evolution*, *139*. https://doi.org/10.1016/j.ympev.2019.106549

Busschau, T., Conradie, W., & Daniels, S. R. (2020). One species hides many: Molecular and morphological evidence for cryptic speciation in a thread snake (Leptotyphlopidae: *Leptotyphlops sylvicolus* Broadley & Wallach, 1997). *Journal of Zoological Systematics and Evolutionary Research*, *May*, 1–27. https://doi.org/10.1111/jzs.12401

Busschau, T., Conradie, W., Jordaan, A., & Daniels, S. R. (2017). Unmasking evolutionary diversity among two closely related South African legless skink species (Acontinae: *Acontias*) using molecular data. *Zoology*, *121*, 72–82. https://doi.org/10.1016/j.zool.2016.11.005

Cadle, J. E. (1994). The colubrid radiation in Africa (Serpentes: Colubridae): phylogenetic relationships and evolutionary patterns based on immunological data. *Zoological Journal of the Linnaean Society*, *110*, 103–140.

Carranza, S., Arnold, E. N., & Pleguezuelos, J. M. (2006). Phylogeny, biogeography, and evolution of two Mediterranean snakes, *Malpolon monspessulanus* and *Hemorrhois hippocrepis* (Squamata, Colubridae), using mtDNA sequences. *Molecular Phylogenetics and Evolution*, *40*(2), 532–546. https://doi.org/10.1016/j.ympev.2006.03.028

Carstens, B. C., Pelletier, T. A., Reid, N. M., & Satler, J. D. (2013). How to fail at species delimitation. *Molecular Ecology*, *22*, 4369–4383. https://doi.org/10.1111/mec.12413

Chippaux, J. P., & Jackson, K. (2019). *Snakes of Central and Western Africa*. JHU Press.

Chirio, L., & Ineich, I. (1991). Les genres *Rhamphiophis* Peters, 1854 et *Dipsina*, Jan, 1863 (Serpentes, Colubridae): revue des taxons reconnus et descripyion d'une espèce nouvelle. *Bulletin Du Museum National d'histoire Naturelle, Paris, 4e Sèr. A*, *13*, 217–235.

Conradie, W., Busschau, T., & Edwards, S. (2018). Two new species of *Acontias* (Acontinae, Scincidae) from the Mpumalanga Highveld escarpment of South Africa. *Zootaxa*, *4429*(1), 89–106. https://doi.org/10.11646/zootaxa.4429.1.3

Conradie, W., Deepak, V., Keates, C., & Gower, D. J. (2020). Kissing cousins: a review of the African genus *Limnophis* Günther, 1865 (Colubridae: Natricinae), with the description of a new species from north-eastern Angola. *African Journal of Herpetology*, *69*(1), 1–29. https://doi.org/10.1080/21564574.2020.1782483

Cottone, A. M., & Bauer, A. M. (2008). Prey excavation by *Psammophylax rhombeatus rhombeatus* (Colubridae: Psammophiinae) from South Africa. *Herpetological Bulletin*, *103*, 11–15.

Critical Ecosystem Partnership Fund. (2020). *Explore the Biodiversity Hotspots*. https://www.cepf.net/our-work/biodiversity-hotspots

Cureton, J. C., & Broughton, R. E. (2014). Rapid morphological divergence of a stream fish in response to changes in water flow. *Biology Letters*, *10*(6), 8–11. https://doi.org/10.1098/rsbl.2014.0352

Daniels, S. R., Heideman, N., Hendricks, M., & Willson, B. (2002). A molecular phylogeny for the South African limbless lizard taxa of the subfamily Acontinae (Sauria : Scincidae) with special emphasis on relationships within *Acontias*. *Molecular Phylogenetics and Evolution*, *24*, 315–323.

Daniels, S. R., Mouton, le F. N., & Du Toit, D. A. (2004). Molecular data suggest that melanistic ectotherms at the south-western tip of Africa are the products of Miocene climatic events: evidence from Cordylid lizards. *Journal of Zoology*, *263*, 373–383. https://doi.org/10.1017/S0952836904005424

Darriba, D., Taboada, G. L., Doallo, R., & Posada, D. (2012). jModelTest 2: more models, new heuristics and parallel computing. *Nature Methods*, *9*(8), 772. https://doi.org/10.1038/nmeth.2109

Darwin, C. (1859). *On The Origin of Species by Means of Natural Selection, or the Preservation of Favoured Races in the Struggle for Life*. John Murray. https://doi.org/10.1525/aa.1959.61.1.02a00760

Dellicour, S., & Flot, J. F. (2015). Delimiting species-poor data sets using single molecular markers: a study of barcode gaps, haplowebs and GMYC. *Systematic Biology*, *64*(6), 900-908.

Dellicour, S., & Flot, J. F. (2018). The hitchhiker's guide to single-locus species delimitation. *Molecular Ecology Resources*, *18*(6), 1234-1246.

Dawson, T. P., Jackson, S. T., House, J. I., Prentice, I. C., & Mace, G. M. (2011). Beyond predictions: Biodiversity conservation in a changing climate. *Science*, *332*(6025), 53–58. https://doi.org/10.1126/science.332.6030.664-b

De Queiroz, K. (1998). The General Lineage Concept of Species, Species Criteria, and the Process of Speciation. In D. Howard & S. Berlocher (Eds.), *Endless Forms: Species*

and Speciation (pp. 57–75). Oxford University Press.

De Queiroz, K. (1999). The General Lineage Concept of Species and the Defining Properties of the Species Category. In Wilson RA (Ed.), *New Interdisciplinary Essays* (pp. 49–89). MIT Press.

De Queiroz, K. (2005). Different species problems and their resolution. *BioEssays*, *27*(12), 1263–1269. https://doi.org/10.1002/bies.20325

De Queiroz, K. (2007). Species concepts and species delimitation. *Systematic Biology*, *56*(6), 879–886. https://doi.org/10.1080/10635150701701083

de Witte, G. F. (1933). Batraciens et Reptiles recueillis par M. L. Burgeon au Ruwenzori, au Kivu et au Tanganika. *Revue De Zoologie Et De Botanique Africaines*, *24*, 111–123.

Diedericks, G., & Daniels, S. R. (2014). Ain't no mountain high enough, ain't no valley low enough? Phylogeography of the rupicolous Cape girdled lizard (*Cordylus cordylus*) reveals a generalist pattern. *Molecular Phylogenetics and Evolution*, *71*(1), 234–248. https://doi.org/10.1016/j.ympev.2013.10.015

Domergue, C. A. (1969). Clé simplifié pour la détermination sur le terrain des serpents communs de Madagascar. *Bulletin Académie Malgache*, *45*(2), 13–26.

Dowling, H. G., & Duellman, W. E. (1978). *Systematic Herpetology: A Synopsis of Families and Higher Categories*. HISS Publications.

Drummond, A. J., & Rambaut, A. (2007). BEAST: Bayesian evolutionary analysis by sampling trees. *BMC Evolutionary Biology*, *7*(214), 1–8. https://doi.org/10.1186/1471-2148-7-214

Dupuis, J. R., Roe, A. D., & Sperling, F. A. (2012). Multi-locus species delimitation in closely related animals and fungi: one marker is not enough. *Molecular ecology*, *21*(18), 4422-4436.

Edgar, R. C. (2004). MUSCLE: multiple sequence alignment with high accuracy and high throughput. *Nucleic Acids Research*, *32*(5), 1792–1797.

Edwards, E. J., Osborne, C. P., Strömberg, C. A. E., Smith, S. A., & Consortium, C. G. (2010). The origins of C 4 grasslands: Integrating evolutionary and ecosystem science. *Science*, *328*, 587–592.

Edwards, S., Vanhooydonck, B., Herrel, A., Measey, G. J., & Tolley, K. A. (2012). Convergent evolution associated with habitat decouples phenotype from phylogeny in a clade of lizards. *PLoS ONE*, *7*(12). https://doi.org/10.1371/journal.pone.0051636

Endler, J. (1989). Conceptual and Other Problems in Speciation. In J. Endler & D. Otte (Eds.), *Speciation and its Consequences* (pp. 625–648). Sinauer Associates.

Engelbrecht, H. M., Branch, W. R., Greenbaum, E., Alexander, G. J., Jackson, K., Burger, M., Conradie, W., Kusamba, C., Zassi-boulou, A., & Tolley, K. A. (2019). Diversifying into the branches : Species boundaries in African green and bush snakes, *Philothamnus* (Serpentes : Colubridae). *Molecular Phylogenetics and Evolution*, *130*, 357–365. https://doi.org/10.1016/j.ympev.2018.10.023

Excoffier, L., & Lischer, H. E. L. (2010). Arlequin suite ver 3.5 : a new series of programs to perform population genetics analyses under Linux and Windows. *Molecular Ecology Resources*, *10*, 564–567. https://doi.org/10.1111/j.1755-0998.2010.02847.x

Excoffier, L., Smouse, P. E., & Quattro, J. M. (1992). Analysis of molecular variance inferred from metric distances among DNA haplotypes: Application to human mitochondrial DNA restriction data. *Genetics*, *131*(2), 479–491. https://doi.org/10.5962/bhl.title.86657

Figueroa, A., McKelvy, A. D., Grismer, L. L., Bell, C. D., & Lailvaux, S. P. (2016). A species-level phylogeny of extant snakes with description of a new colubrid subfamily and genus. *PLoS ONE*, *11*(9). https://doi.org/10.1371/journal.pone.0161070

Florio, A. M., Ingram, C. M., Rakotondravony, H. A., Louis, E. E., & Raxworthy, C. J. (2012). Detecting cryptic speciation in the widespread and morphologically conservative carpet chameleon (*Furcifer lateralis*) of Madagascar. *Journal of Evolutionary Biology*, *25*(7), 1399–1414. https://doi.org/10.1111/j.1420-9101.2012.02528.x

Flot, J. (2015). Species delimitation’s coming of age. *Systematic Biology*, *64*(6), 897–899. https://doi.org/10.1093/sysbio/syv071

Flot, J. F., Couloux, A., & Tillier, S. (2010). Haplowebs as a graphical tool for delimiting species: a revival of Doyle's" field for recombination" approach and its application to the coral genus Pocillopora in Clipperton. *BMC Evolutionary Biology*, *10*(1), 1-14.

Fontaneto, D., Flot, J., & Tang, C. Q. (2015). Guidelines for DNA taxonomy, with a focus on the meiofauna. *Marine Biodiversity*, *45*, 433–451. https://doi.org/10.1007/s12526-015-0319-7

Foote, A. D. (2018). Sympatric speciation in the genomic era. *Trends in Ecology and Evolution*, *33*(2), 85–95. https://doi.org/10.1016/j.tree.2017.11.003

Funk, D. J., Nosil, P., & Etges, W. J. (2006). Ecological divergence exhibits consistently positive associations with reproductive isolation across disparate taxa. *Proceedings of*

the National Academy of Sciences of the United States of America, *103*(9), 3209–3213. https://doi.org/10.1073/pnas.0508653103

Gaston, K. J. (2010). Valuing common species. *Science*, *327*(5962), 154–155. https://doi.org/10.1126/science.1182818

Geniez, P., Cluchier, A., & De Haan, C. . (2006). A multivariate analysis of the morphology of the colubrid snake *Malpolon monspessulanus* in Morocco and Western Sahara: biogeographic and systematic implications. *Salamandra*, *42*, 65–82.

Ghiselin, M. (2001). *Species Concepts. In: Encyclopedia of Life Sciences*. Wiley.

Gittenberger, E. (2004). Radiation and adaptation, evolutionary biology and semantics. *Organisms Diversity and Evolution*, *4*(3), 135–136. https://doi.org/10.1016/j.ode.2004.04.002

Glaw, F., & Vences, M. (1994). *Amphibians and Reptiles of Madagascar* (2nd ed.). Verlag.

Glaw, F., & Vences, M. (2007). *Amphibians and Reptiles of Madagascar* (3rd ed.). Verlag.

Gonçalves, D. V., Martínez-Freiría, F., Crochet, P.-A., Geniez, P., Carranza, S., & Brito, J. C. (2018). The role of climatic cycles and trans-Saharan migration corridors in species diversification: Biogeography of *Psammophis schokari* group in North Africa. *Molecular Phylogenetics and Evolution*, *118*, 64–74. https://doi.org/10.1016/j.ympev.2017.09.009

Gravlund, P. (2001). Radiation within the advanced snakes (Caenophidia) with special emphasis on African opistoglyph colubrids, based on mitochondrial sequence data. *Biological Journal of the Linnean Society*, *72*(1), 99–114. https://doi.org/10.1006/bijl.2000.0495

Greenbaum, E. (2017). *Emerald Labyrinth: a Scientist's Adventures in the Jungles of the Congo*. NH: ForeEdge.

Greenbaum, E., Portillo, F., Jackson, K., & Kusamba, C. (2015). A phylogeny of Central African *Boaedon* (Serpentes: Lamprophiidae), with the description of a new cryptic species from the Albertine Rift. *African Journal of Herpetology*, *64*(1), 18–38. https://doi.org/10.1080/21564574.2014.996189

Greenbaum, E., Sinsch, U., Lehr, E., Valdez, F., & Kusamba, C. (2013). Phylogeography of the reed frog *Hyperolius castaneus* (Anura: Hyperoliidae) from the Albertine Rift of Central Africa: Implications for taxonomy, biogeography and conservation. *Zootaxa*, *3731*(4), 473–494. https://doi.org/10.11646/zootaxa.3731.4.3

Greenbaum, E., Tolley, K. A., Joma, A., & Kusamba, C. (2012). A new species of chameleon

(Sauria: Chamaeleonidae: *Kinyongia*) from the northern Albertine Rift , Central Africa. *Herpetologica*, *68*(1), 60–75.

Guindon, S., & Gascuel, O. (2003). A simple, fast, and accurate algorithm to estimate large phylogenies by Maximum Likelihood. *Systematic Biology*, *52*(5), 696–704. https://doi.org/10.1080/10635150390235520

Gűnther, A. (1868). Sixth account of new species of snakes in the collection of the British Museum. *Annals and Magazine of Natural History*, *1*, 413–529

Hall, T. A. (1999). BioEdit, a user-friendly biological sequence alignment editor and analysis program for Windows 95/98/NT. *Nucleic Acids Symposium Series*, *41*, 95–98. https://doi.org/citeulike-article-id:691774

Hallermann, J., Ceríaco, L. M. P., Schmitz, A., Ernst, R., Conradie, W., Verburgt, L., Marques, M. P., & Bauer, A. M. (2020). A review of the Angolan House snakes, genus *Boaedon* Duméril, Bibron and Duméril (1854) (Serpentes: Lamprophiidae), with description of three new species in the *Boaedon fuliginosus* (Boie, 1827) species complex. *African Journal of Herpetology*, *69*(1), 1–50. https://doi.org/10.1080/21564574.2020.1777470

Harrington, S. M., De Haan, J. M., Shapiro, L., & Ruane, S. (2018). Habits and characteristics of arboreal snakes worldwide: Arboreality constrains body size but does not affect lineage diversification. *Biological Journal of the Linnean Society*, *125*(1), 61–71. https://doi.org/10.1093/BIOLINNEAN/BLY097

Head, J. J., Mahlow, K., & Müller, J. (2016). Fossil calibration dates for molecular phylogenetic analysis of snakes 2 : Caenophidia, Colubroidea, Elapoidea, Colubridae. *Palaeontologia Electronica*, 1–21.

Heinicke, M. P., Turk, D., & Bauer, A. M. (2017). Molecular phylogeny reveals strong biogeographic signal and two new species in a Cape Biodiversity Hotspot endemic mini-radiation, the pygmy geckos (Gekkonidae: *Goggia*). *Zootaxa*, *4312*(3), 449–470. https://doi.org/10.11646/zootaxa.4312.3.3

Hewitt, G. M. (2004a). Genetic consequences of climatic oscillations in the Quaternary. *Philosophical Transactions of the Royal Society of London. Series B: Biological Sciences*, *359*(1442), 183–195. https://doi.org/10.1098/rstb.2003.1388

Hewitt, G. M. (2004b). The structure of biodiversity–insights from molecular phylogeography. *Frontiers in Zoology*, *1*(4), 1–16. https://doi.org/10.1186/1742-9994-1-4

Hey, J. (2001). *Genes, Categories, and Species. The Evolutionary and Cognitive Causes of the Species Problem*. Oxford University Press.

Hey, J., Waples, R., Arnold, M., Butlin, R., & Harrison, R. (2003). Understanding and confronting species uncertainty in biology and conservation. *Trends in Ecology and Evolution*, *18*, 597–603.

Hillis, D. M. (2019). Species delimitation in herpetology. *Journal of Herpetology*, *53*(1), 3-12.

Hughes, B. (1999). Critical review of a revision of *Psammophis* (Linnaeus 1758) (Serpentes, Reptilia) by Frank Brandstätter. *African Journal of Herpetology*, *48*, 63–70.

Hughes, B., & Wade, E. O. (2002). On the African leopard whip snake, *Psammophis leopardinus* Bocage, 1887 (Serpentes, Colubridae), with the description of a new species from Zambia. *Bulletin of the Natural History Museum: Zoology Series*, *68*(2), 75–81.

Hughes, B., & Wade, E. O. (2004). Is Psammophis *sibilans occidentalis* Werner, 1919 a junior synonym of *Psammophis phillipsi* (Hallowell, 1844)? *Herpetozoa*, *16*(3/4), 127–132.

Hughes, D. F., Kusamba, C., Behangana, M., & Greenbaum, E. (2017). Integrative taxonomy of the Central African forest chameleon, *Kinyongia adolfifriderici* (Sauria: Chamaeleonidae), reveals underestimated species diversity in the Albertine Rift. *Zoological Journal of the Linnean Society*, *181*(2), 400–438. https://doi.org/10.1093/zoolinnean/zlx005

Hull, D. L. (1965). The effect of essentialism on taxonomy–two thousand years of stasis (I). *The British Journal for the Philosophy of Science*, *15*(60), 314–326.

Ineich, I., Girard, F., Ping, T., Reynes, J., & Weinstein, S. A. (2021). Two case reports of local envenoming by the Spotted grass snake, *Psammophylax rhombeatus* (Linnæus, 1758)(Serpentes, Psammophiidae). *Toxicon*, *195*, 24-28.

Jacobsen, N. H. G., Kuhn, A. L., Jackman, T. R., & Bauer, A. M. (2014). A phylogenetic analysis of the southern African gecko genus *Afroedura* Loveridge (Squamata: Gekkonidae), with the description of nine new species from Limpopo and Mpumalanga provinces of South Africa. *Zootaxa*, *3846*(4), 451–501. https://doi.org/10.11646/zootaxa.3846.4.1

Kark, S., Warburg, I., & Werner, Y. L. (1997). Polymorphism in the snake *Psammophis schokari* on both sides of the desert edge in Israel and Sinai. *Journal of Arid*

Environments, *37*, 513–527.

Keates, C., Conradie, W., Greenbaum, E., & Edwards, S. (2019). A snake in the grass: Genetic structuring of the widespread African grass snake (*Psammophylax* Fitzinger 1843), with the description of a new genus and a new species. *Journal of Zoological Systematics and Evolutionary Research*, *57*(4), 1039–1066. https://doi.org/10.1111/jzs.12337

Kelly, C. M. R. (2005). *Systematics and Phylogeography of Advanced Snakes: Global Phylogenetics and Focus on Some African Endemics*. Oxford University.

Kelly, C. M. R., Barker, N. P., & Villet, M. H. (2003). Phylogenetics of advanced snakes (Caenophidia) based on four mitochondrial genes. *Systematic Biology*, *52*(4), 439–459. https://doi.org/10.1080/10635150390218132

Kelly, C. M. R., Barker, N. P., Villet, M. H., & Broadley, D. G. (2009). Phylogeny, biogeography and classification of the snake superfamily Elapoidea: a rapid radiation in the late Eocene. *Cladistics*, *25*, 38–63. https://doi.org/10.1111/j.1096-0031.2008.00237.x

Kelly, C. M. R., Barker, N. P., Villet, M. H., Broadley, D. G., & Branch, W. R. (2008). The snake family Psammophiidae (Reptilia: Serpentes): Phylogenetics and species delimitation in the African sand snakes (*Psammophis* Boie, 1825) and allied genera. *Molecular Phylogenetics and Evolution*, *47*(3), 1045–1060. https://doi.org/10.1016/j.ympev.2008.03.025

Kelly, C. M. R., Branch, W. R., Broadley, D. G., Barker, N. P., & Villet, M. H. (2011). Molecular systematics of the African snake family Lamprophiidae Fitzinger, 1843 (Serpentes: Elapoidea), with particular focus on the genera *Lamprophis* Fitzinger 1843 and *Mehelya* Csiki 1903. *Molecular Phylogenetics and Evolution*, *58*(3), 415–426. https://doi.org/10.1016/j.ympev.2010.11.010

Kissling, W. D., Eiserhardt, W. L., Baker, W. J., Borchsenius, F., Couvreur, T. L. P., Balslev, H., & Svenning, J. C. (2012). Cenozoic imprints on the phylogenetic structure of palm species assemblages worldwide. *Proceedings of the National Academy of Sciences of the United States of America*, *109*(19), 7379–7384. https://doi.org/10.1073/pnas.1120467109

Klingenberg, C. P. (2011). MorphoJ: An integrated software package for geometric morphometrics. *Molecular Ecology Resources*, *11*(2), 353–357. https://doi.org/10.1111/j.1755-0998.2010.02924.x

Kornfield, I., & Smith, P. F. (2000). African cichlid fishes: model systems for evolutionary biology. *Annual Review of Ecology, Evolution, and Systematics*, *31*(2000), 163–182.

Kulenkampff, K., Zyl, F. Van, Klaus, S., & Daniels, S. R. (2019). Molecular evidence for cryptic species in the common slug eating snake *Duberria lutrix lutrix* (Squamata , Lamprophiidae) from South Africa. *Zookeys*, *838*, 133–154. https://doi.org/10.3897/zookeys.838.32022

Kulongoski, J. T., & Hilton, D. R. (2004). Climate variability in the Botswana Kalahari from the late Pleistocene to the present day. *Geophysical Research Letters*, *31*, 1–5. https://doi.org/10.1029/2003GL019238

Kumar, S., Stecher, G., Li, M., Knyaz, C., & Tamura, K. (2018). MEGA X : Molecular Evolutionary Genetics Analysis across computing platforms. *Molecular Biology and Evolution*, *35*(6), 1547–1549. https://doi.org/10.1093/molbev/msy096

Lanfear, R., Frandsen, P. B., Wright, A. M., Senfeld, T., & Calcott, B. (2016). PartitionFinder 2 : New methods for selecting partitioned models of evolution for molecular and morphological phylogenetic analyses. *Molecular Biology and Evolution*, *34*(3), 772–773. https://doi.org/10.1093/molbev/msw260

Largen, M. J., & Spawls, S. (2010). *Amphibians and Reptiles of Ethiopia and Eritrea*. Edition Chimaira.

Laurent, R. F. (1956). *Contribution a l'herpetologie de la region des grands lacs de l'Afrique centrale: I. Généralités. II. Cheloniens. III. Ophidiens*, 48. 1–390.

Lawson, R., Slowinski, J. B., Crother, B. I., & Burbrink, F. T. (2005). Phylogeny of the Colubroidea (Serpentes): New evidence from mitochondrial and nuclear genes. *Molecular Phylogenetics and Evolution*, *37*(2), 581–601. https://doi.org/10.1016/j.ympev.2005.07.016

Lefébure, T., Douady, C. J., Gouy, M., & Gibert, J. (2006). Relationship between morphological taxonomy and molecular divergence within Crustacea: Proposal of a molecular threshold to help species delimitation. *Molecular Phylogenetics and Evolution*, *40*, 435–447. https://doi.org/10.1016/j.ympev.2006.03.014

Leigh, J. W., & Bryant, D. (2015). POPART : A full-feature software for haplotype network construction. *Methods in Ecology and Evolution*, *6*, 1110–1116. https://doi.org/10.1111/2041-210X.12410

Linder, H. P. (2017). East African Cenozoic vegetation history. *Evolutionary Anthropology*,

26(6), 300–312. https://doi.org/10.1002/evan.21570

Loader, S. P., Sara Ceccarelli, F., Menegon, M., Howell, K. M., Kassahun, R., Mengistu, A. A., Saber, S. A., Gebresenbet, F., de Sá, R., Davenport, T. R. B., Larson, J. G., Müller, H., Wilkinson, M., & Gower, D. J. (2014). Persistence and stability of Eastern Afromontane forests: Evidence from *brevicipitid* frogs. *Journal of Biogeography*, *41*(9), 1781–1792. https://doi.org/10.1111/jbi.12331

Lorenzen, E. D., Heller, R., & Siegismund, H. R. (2012). Comparative phylogeography of African savannah ungulates. *Molecular Ecology*, *21*, 3656–3670. https://doi.org/10.1111/j.1365-294X.2012.05650.x

Lorenzen, E. D., Masembe, C., Arctander, P., & Siegismund, H. R. (2010). A long-standing Pleistocene refugium in southern Africa and a mosaic of refugia in East Africa : insights from mtDNA and the common eland antelope. *Journal of Biogeography*, *37*, 571–581. https://doi.org/10.1111/j.1365-2699.2009.02207.x

Losos, J. B. (2011). Convergence, adaptation, and constraint. *Evolution*, *65*(7), 1827–1840. https://doi.org/10.1111/j.1558-5646.2011.01289.x

Loveridge, A. (1923). Notes on East African snakes, collected 1918-1923. *Proceedings of the Zoological Society of London*, *93*, 871–897.

Loveridge, A. (1932). New opisthoglyphous snakes of the genera *Crotaphopeltis* and *Trimerorhinus* from Angola and Kenya colony. *Proceedings of the Biological Society of Washington*, *45*, 83–86.

Loveridge, A. (1940). Revision of the African snakes of the genera *Dromophis* and *Psammophis*. *Bulletin of the Museum of Comparative Zoology*, *87*(1), 1–69.

Mangiacotti, M., Limongi, L., Sannolo, M., Sacchi, R., Zuffi, M. A. L., & Scali, S. (2014). Head shape variation in eastern and western Montpellier snakes. *Acta Herpetologica*, *9*(2), 167–177. https://doi.org/10.13128/Acta

Marais, J. (2004). *A Complete Guide to the Snakes of Southern Africa*. STRUIK Nature.

Maslin, M. A., Pancost, R. D., Wilson, K. E., Lewis, J., & Trauth, M. H. (2012). Three and half million year history of moisture availability of South West Africa: Evidence from ODP site 1085 biomarker records. *Palaeogeography, Palaeoclimatology, Palaeoecology*, *317–318*, 41–47. https://doi.org/10.1016/j.palaeo.2011.12.009

Mayden, R. L. (1997). A Hierarchy of Species Concepts: the Denouement in the Saga of the Species Problem. In M. Claridge, H. Dawah, & M. Wilson (Eds.), *Species: The Units of*

Biodiversity (pp. 381–424). Chapman & Hall.

Mayden, R. L. (1999). Consilience and a hierarchy of species concepts: Advances toward closure on the species puzzle. *Journal of Nematology*, *31*(2), 95–116.

Mayden, R. L. (2002). On biological species, species concepts and individuation in the natural world. *Fish and Fisheries*, *3*(3), 171–196. https://doi.org/10.1046/j.1467-2979.2002.00086.x

Mayden, R. L. (2013). Species, Trees, Characters, and Concepts: Ongoing Issues, Diverse Ideologies, and a Time for Reflection and Change. In I. Pavlinov (Ed.), *The Species Problem–Ongoing Issues* (pp. 171–191). InTech.

Mayr, E. (1942). *Systematics and the Origin of Species from the Viewpoint of a Zoologist*. Columbia University Press.

Mayr, E. (1963). *Animal Species and Evolution*. Harvard University Press.

McKane, R. B., Johnson, L. C., Shaver, G. R., Nadelhoffer, K. J., Rastetter, E. B., Fry, B., Giblin, A. E., Kielland, K., Kwlatkowski, B. L., Laundre, J. A., & Murray, G. (2002). Resource-based niches provide a basis for plant species diversity and dominance in arctic tundra. *Nature*, *415*(6867), 68–71. https://doi.org/10.1038/415068a

Medina, M. F., Bauer, A. M., Branch, W. R., Schmitz, A., Conradie, W., Nagy, Z. T., Hibbitts, T. J., Ernst, R., Portik, D. M., Nielsen, S. V., Colston, T. J., Kusamba, C., Behangana, M., Rödel, M. O., & Greenbaum, E. (2016). Molecular phylogeny of *Panaspis* and *Afroablepharus* skinks (Squamata: Scincidae) in the savannas of sub-Saharan Africa. *Molecular Phylogenetics and Evolution*, *100*, 409–423. https://doi.org/10.1016/j.ympev.2016.04.026

Meier, R., Shiyang, K., Vaidya, G., & Ng, P. K. L. (2006). DNA barcoding and taxonomy in *Diptera* : A tale of high intraspecific variability and low identification success. *Systematic Biology*, *55*(5), 715–728. https://doi.org/10.1080/10635150600969864

Menegon, M., Loader, S. P., Marsden, S. J., Branch, W. R., Davenport, T. R. B., & Ursenbacher, S. (2014). The genus *Atheris* (Serpentes: Viperidae) in East Africa: Phylogeny and the role of rifting and climate in shaping the current pattern of species diversity. *Molecular Phylogenetics and Evolution*, *79*(1), 12–22. https://doi.org/10.1016/j.ympev.2014.06.007

Menegon, M., Tolley, K. A., Jones, T., Rovero, F., Marshall, A. R., & Tilbury, C. R. (2009). A new species of chameleon (Sauria: Chamaeleonidae: *Kinyongia*) from the Magombera

forest and the Udzungwa Mountains National Park, Tanzania. *African Journal Of Herpetology*, *58*(2), 59–70.

Miller, M. A., Pfeiffer, W., & Schwartz, T. (2010). Creating the CIPRES Science Gateway for Inference of Large Phylogenetic Trees. *Gateway Computing Environments Workshop*, 1–8.

Nagy, Z. T., Joger, U., Wink, M., Glaw, F., & Vences, M. (2003). Multiple colonization of Madagascar and Socotra by colubrid snakes: Evidence from nuclear and mitochondrial gene phylogenies. *Proceedings of the Royal Society of London. Series B: Biological Sciences*, *270*(1533), 2613–2621. https://doi.org/10.1098/rspb.2003.2547

Nagy, Z. T., Sonet, G., Glaw, F., & Vences, M. (2012). First large-scale DNA barcoding assessment of reptiles in the biodiversity hotspot of Madagascar, based on newly designed COI primers. *PLoS ONE*, *7*(3). https://doi.org/10.1371/journal.pone.0034506

Needham, R. (1975). Polythetic classification: Convergence and consequences. *Royal Anthropological Institute of Great Britain and Ireland*, *10*(3), 349–369.

Nowak, E. M., Theimer, T. C., & Schuett, G. W. (2008). Functional and numerical responses of predators: Where do vipers fit in the traditional paradigms? *Biological Reviews*, *83*(4), 601–620. https://doi.org/10.1111/j.1469-185X.2008.00056.x

Oliver, P. M., Adams, M., Lee, M. S. Y., Hutchinson, M. N., & Doughty, P. (2009). Cryptic diversity in vertebrates: Molecular data double estimates of species diversity in a radiation of Australian lizards (*Diplodactylus*, Gekkota). *Proceedings of the Royal Society B: Biological Sciences*, *276*, 2001–2007. https://doi.org/10.1098/rspb.2008.1881

Padial, J. M. (2006). Commented distributional list of the reptiles of Mauritania (West Africa). *Graellsia*, *62*(2), 159–178. https://doi.org/10.3989/graellsia.2006.v62.i2.64

Padial, J. M., Miralles, A., De la Riva, I., & Vences, M. (2010). The integrative future of taxonomy. *Frontiers in Zoology*, *7*(1), 1-14.

Palumbi, S. R. (1996). What can molecular genetics contribute to marine biogeography? An urchin's tale. *Journal of Experimental Marine Biology and Ecology*, *203*(1), 75-92.

Pigliucci, M. (2003). Species as family resemblance concepts: The (dis-)solution of the species problem? *BioEssays*, *25*(6), 596–602. https://doi.org/10.1002/bies.10284

Pinto, G., Mahler, D. L., Harmon, L. J., & Losos, J. B. (2008). Testing the island effect in adaptive radiation: Rates and patterns of morphological diversification in Caribbean and

mainland *Anolis* lizards. *Proceedings of the Royal Society B: Biological Sciences*, *275*(1652), 2749–2757. https://doi.org/10.1098/rspb.2008.0686

Pirie, M. D., Oliver, E. G. H., Kuppler, A. M. De, Gehrke, B., Maitre, N. C. Le, Kandziora, M., & Bellstedt, D. U. (2016). The biodiversity hotspot as evolutionary hot-bed: Spectacular radiation of *Erica* in the Cape Floristic Region. *BMC Evolutionary Biology*, *16*(190). https://doi.org/10.1186/s12862-016-0764-3

Pons, J., Barraclough, T. G., Gomez-Zurita, J., Cardoso, A., Duran, D. P., Hazell, S., ... & Vogler, A. P. (2006). Sequence-based species delimitation for the DNA taxonomy of undescribed insects. *Systematic Biology*, *55*(4), 595-609.

Portillo, F., Branch, W. R., Conradie, W., Rödel, M. O., Penner, J., Barej, M. F., Kusamba, C., Muninga, W. M., Aristote, M. M., Bauer, A. M., Trape, J.-F., Nagy, Z. T., Carlino, P., Pauwels, O. S. G. G., Menegon, M., Burger, M., Mazuch, T., Jackson, K., Hughes, D. F., … Zassi-Boulou, A. G. (2018). Phylogeny and biogeography of the African burrowing snake subfamily Aparallactinae (Squamata: Lamprophiidae). *Molecular Phylogenetics and Evolution*, *127*, 288–303. https://doi.org/10.1016/j.ympev.2018.03.019

Portillo, F., Greenbaum, E., Menegon, M., Kusamba, C., & Maximilian Dehling, J. (2015). Phylogeography and species boundaries of *Leptopelis* (Anura: Arthroleptidae) from the Albertine Rift. *Molecular Phylogenetics and Evolution*, *82*, 75–86. https://doi.org/10.1016/j.ympev.2014.09.024

Price, B. W., Barker, P., & Villet, M. H. (2007). Patterns and processes underlying evolutionary significant units in the *Platypleura stridula* L . species complex (Hemiptera : Cicadidae) in the Cape Floristic Region , South Africa. *Molecular Ecology*, *16*, 2574–2588. https://doi.org/10.1111/j.1365-294X.2007.03328.x

Puillandre, N., Lambert, A., Brouillet, S., & ACHAZ, G. (2012). ABGD, Automatic Barcode Gap Discovery for primary species delimitation. *Molecular ecology*, *21*(8), 1864-1877.

Pyron, R. A., Burbrink, F. T., & Wiens, J. (2013). A phylogeny and revised classification of Squamata, including 4161 species of lizards and snakes. *BMC Evolutionary Biology*, *13*(93). https://doi.org/10.1186/1471-2148-13-93

Quade, J., Cerling, T. E., & Bowman, J. R. (1989). Development of Asian Monsoon revealed by marked ecological shift during the latest Miocene in northern Pakistan. *Nature*, *342*, 163–166. https://doi.org/10.1038/342163a0

R Core Team. (2016). *R: A language and environment for statistical computing.* R

Foundation for Statistical Computing.

Rainey, P. B., & Travisano, M. (1998). Adaptive radiation in a heterogeneous environment. *Nature*, *394*, 69–72. https://doi.org/10.1038/27900

Rambaut, A. (2014). *Figtree: Tree drawing tool* (1.4.2). Institute of Evoltionary Biology, University of Edinburgh.

Rambaut, A., & Drummond, A. J. (2009). *Tracer: MCMC trace analysis package* (1.5). Institute of Evolutionary Biology, University of Edinburgh.

Rato, C., Brito, J. C., Carretero, M. A., Larbes, S., Shacham, B., Harris, D. J., Brito, J. C., Carretero, M. A., Larbes, S., Shacham, B., Rato, C., Brito, J. C., Carretero, M. A., Larbes, S., Shacham, B., & Harris, D. J. (2015). Phylogeography and genetic diversity of *Psammophis schokari* (Serpentes) in North Africa based on mitochondrial DNA sequences. *African Zoology*, *42*(1), 112–117. https://doi.org/10.1080/15627020.2007.11407383

Reid, N. M., & Carstens, B. C. (2012). Phylogenetic estimation error can decrease the accuracy of species delimitation: A Bayesian implementation of the general mixed Yule-coalescent model. *BMC Evolutionary Biology*, *12*(196), 1–11.

Renoult, J. P., Geniez, P., Bacquet, P., Benoit, L., & Crochet, P. A. (2009). Morphology and nuclear markers reveal extensive mitochondrial introgressions in the Iberian Wall Lizard species complex. *Molecular Ecology*, *18*(20), 4298–4315. https://doi.org/10.1111/j.1365-294X.2009.04351.x

Revell, L. J., Johnson, M. A., Schulte, J. A., Kolbe, J. J., & Losos, J. B. (2007). A phylogenetic test for adaptive convergence in rock-dwelling lizards. *Evolution*, *61*(12), 2898–2912. https://doi.org/10.1111/j.1558-5646.2007.00225.x

Roberts, E. M., Stevens, N. J., O'Connor, P. M., Dirks, P. H. G. M., Gottfried, M. D., Clyde, W. C., Armstrong, R. A., Kemp, A. I. S., & Hemming, S. (2012). Initiation of the western branch of the East African Rift coeval with the eastern branch. *Nature Geoscience*, *5*(4), 289–294.

Rohlf, F. J. (1999). Shape statistics: Procrustes superimpositions and tangeant places. *Journal of Classification*, *16*, 197–223. https://doi.org/10.1093/hmg/ddn214

Rohlf, F. J. (2004a). *TpsDig2: Digitize coordinates of landmarks and capture outlines*. Department of Ecology and Evolution, State University of New York at Stony Brook.

Rohlf, F. J. (2004b). *TpsUtil, file utility program* (1.26). Department of Ecology and Evolution,

State University of New York at Stony Brook.

Rohlf, F. J., & Slice, D. (1990). Extensions of the procrustes method for the optimal superimposition of landmarks. *Systematic Zoology*, *39*(1), 40–59. https://doi.org/10.2307/2992207

Ronquist, F., Teslenko, M., Van Der Mark, P., Ayres, D. L., Darling, A., Höhna, S., Larget, B., Liu, L., Suchard, M. A., & Huelsenbeck, J. P. (2012). MrBayes 3.2: Efficient Bayesian phylogenetic inference and model choice across a large model space. *Software for Systematic and Evolution*, *61*(3), 539–542. https://doi.org/10.1093/sysbio/sys029

Ruane, S., Myers, E. A., Lo, K., Yuen, S., Welt, R. S., Juman, M., Futterman, I., Nussbaum, R. A., Schneider, G., Burbrink, F. T., & Raxworthy, C. J. (2018). Unrecognized species diversity and new insights into colour pattern polymorphism within the widespread Malagasy snake *Mimophis* (Serpentes: Lamprophiidae). *Systematics and Biodiversity*, *16*(3), 229–244. https://doi.org/10.1080/14772000.2017.1375046

Ruthven, A. G. (1908). Variations and genetic relationships of the garter-snakes. *Bulletin of the United States National Museum, 61*, 1-201.

Schluter, D. (2000). *The Ecology of Adaptive Radiation*. Oxford University Press.

Schlüter, U. (2006). Sandliebhaber - die psammophilen Nattern Nordafrikas. *Reptilia (Münster)*, *11*(4), 72–80.

Scott, P., & Rines, R. (1975). Naming the Loch Ness monster. *Nature*, *258*, 466–468.

Segniagbeto, G. H., Trape, J.-F., David, P., Ohler, A., Dubois, A., & Glitho, I. A. (2011). The snake fauna of Togo: systematics, distribution and biogeography, with remarks on selected taxonomic problems. *BioOne*, *33*(3), 325–360. https://doi.org/10.5252/z2011n3a4.KEY

Sites, J. W., & Marshall, J. C. (2003). Delimiting species: A Renaissance issue in systematic biology. *Trends in Ecology and Evolution*, *18*(9), 462–470. https://doi.org/10.1016/S0169-5347(03)00184-8

Sites, J. W., & Marshall, J. C. (2004). Operational criteria for delimiting species. *Annual Review of Ecology, Evolution, and Systematics*, *35*, 199–227. https://doi.org/10.1146/annurev.ecolsys.35.112202.130128

Slowinski, J. B., & Lawson, R. (2002). Snake phylogeny: evidence from nuclear and mitochondrial genes. *Molecular Phylogenetics and Evolution*, *24*(2), 194-202.

Smit, H. A., Jansen van Vuuren, B., O' Brien, P. C. M., Ferguson-Smith, M., Yang, F., & Robinson, T. J. (2011). Phylogenetic relationships of elephant-shrews (*Afrotheria*, Macroscelididae). *Journal of Zoology*, *284*(2003), 133–143. https://doi.org/10.1111/j.1469-7998.2011.00790.x

Spawls, S., Howell, K., Drewes, R. C., & Ashe, J. (2002). *A Field Guide to the Reptiles of East Africa* (1st ed.). UK: Academic Press.

Spawls, S., Howell, K., Drewes, R. C., Ashe, J., Duff-Mackey, A., & Hinkel, H. (2001). *A Field Guide to the Reptiles of East Africa. Kenya, Tanzania, Uganda, Rwanda and Burundi*. Princeton University press.

Spawls, S., Howell, K., Hinkel, H., & Menegon, M. (2018). *A Field Guide to East African Reptiles* (2nd ed.). Bloomsbury Publishing.

Stamatakis, A. (2014). RAxML version 8 : a tool for phylogenetic analysis and post-analysis of large phylogenies. *Bioinformatics*, *30*(9), 1312–1313. https://doi.org/10.1093/bioinformatics/btu033

Steehouder, T. (2020). *(Self-) rubbing behaviour of psammophiine (or psammophiid) snakes*. Psammophis.nl

Suchard, M. A., & Rambaut, A. (2009). Many-core algorithms for statistical phylogenetics. *Bioinformatics*, *25*(11), 1370–1376. https://doi.org/10.1093/bioinformatics/btp244

Swart, B. L., Tolley, K. A., & Matthee, C. A. (2009). Climate change drives speciation in the southern rock agama (*Agama atra*) in the Cape Floristic Region, South Africa. *Journal of Biogeography*, *36*, 78–87. https://doi.org/10.1111/j.1365-2699.2008.01988.x

Taft, J. M. (2018). *Phylogenetic assessment and historical biogeography of the Psammophis leightoni complex*. University of Western Cape.

Tamura, K., Stecher, G., Peterson, D., Filipski, A., & Kumar, S. (2013). MEGA6: Molecular Evolutionary Genetics Analysis Version 6.0. *Molecular Biology and Evolution*, *30*(12), 2725–2729. https://doi.org/10.1093/molbev/mst197

Taylor, E. B., Darveau, C. A., & Schulte, P. M. (2013). Setting conservation priorities in a widespread species: Phylogeographic and physiological variation in the lake chub, *Couesius plumbeus* (Pisces: Cyprinidae). *Diversity*, *5*(2), 149–165. https://doi.org/10.3390/d5020149

Tews, J., Brose, U., Grimm, B., Tielborger, K., Wichmann, M. C., Schwager, M., & Jeltsch, F. (2004). Animal species diversity driven by habitat heterogeneity/diversity: The

importance of keystone structures. *Journal of Biogeography*, *31*, 79–92.

Tolley, K. A., Alexander, G. J., Branch, W. R., Bowles, P., & Maritz, B. (2016). Conservation status and threats for African reptiles. *Biological Conservation*, *204*, 63–71. https://doi.org/10.1016/j.biocon.2016.04.006

Tolley, K. A., Burger, M., Turner, A. A., & Matthee, C. A. (2006). Biogeographic patterns and phylogeography of dwarf chameleons (*Bradypodion*) in an African biodiversity hotspot. *Molceular Ecology*, *15*, 781–793. https://doi.org/10.1111/j.1365-294X.2006.02836.x

Tolley, K. A., Chase, B. M., & Forest, F. (2008). Speciation and radiations track climate transitions since the Miocene Climatic Optimum : a case study of southern African chameleons. *Journal of Biogeography*, *35*, 1402–1414. https://doi.org/10.1111/j.1365-2699.2008.01889.x

Tolley, K. A., Makhokha, J. S., Houniet, D. T., Swart, B. L., & Matthee, C. A. (2009). The potential for predicted climate shifts to impact genetic landscapes of lizards in the South African Cape Floristic Region. *Molecular Phylogenetics and Evolution*, *51*(1), 120–130. https://doi.org/10.1016/j.ympev.2008.11.017

Tolley, K. A., Tilbury, C. R., Measey, G. J., Menegon, M., Branch, W. R., & Matthee, C. A. (2011). Ancient forest fragmentation or recent radiation? Testing refugial speciation models in chameleons within an African biodiversity hotspot. *Journal of Biogeography*, *38*(9), 1748–1760. https://doi.org/10.1111/j.1365-2699.2011.02529.x

Tolley, K. A., Weeber, J., Maritz, B., Verburgt, L., Bates, M. F., Conradie, W., Hofmeyr, M. D., Turner, A. A., da Silva, J. M., & Alexander, G. J. (2019). No safe haven: Protection levels show imperilled South African reptiles not sufficiently safe-guarded despite low average extinction risk. *Biological Conservation*, *233*(February), 61–72. https://doi.org/10.1016/j.biocon.2019.02.006

Torres-Pérez, F., Méndez, M. A., Benavides, E., Moreno, R. A., Lamborot, M., Palma, R. E., & Ortiz, J. C. (2009). Systematics and evolutionary relationships of the mountain lizard *Liolaemus monticola* (Liolaemini): How morphological and molecular evidence contributes to reveal hidden species diversity. *Biological Journal of the Linnean Society*, *96*(3), 635–650. https://doi.org/10.1111/j.1095-8312.2008.01140.x

Trape, J.-F., Crochet, P.-A., Broadley, D. G., Sourouille, P., Mané, Y., Burger, M., Böhme, W., Saleh, M., Karan, A., Lanza, B., & Mediannikov, O. (2019). On the *Psammophis sibilans* group (Serpentes, Lamprophiidae, Psammophiinae) north of 12°S, with the description of a new species from West Africa. *Bonn Zoological Bulletin*, *68*(1), 61–91.

Trape, J.-F., & Mane, Y. (2006). *Guide des serpents d'Afrique occidentale. Savane et desert. [Senegal, Gambia, Mauritiania, Mali,Burkina Faso, Niger]*. IRD Editions.

Travers, S. L., Jackman, T. R., & Bauer, A. M. (2014). A molecular phylogeny of Afromontane dwarf geckos (*Lygodactylus*) reveals a single radiation and increased species diversity in a South African montane center of endemism. *Molecular Phylogenetics and Evolution*, *80*, 31–42. https://doi.org/10.1016/j.ympev.2014.07.017

Trombulak, S. C., Omland, K. S., Robinson, J. A., Lusk, J. J., Fleischner, T. L., Brown, G., & Domroese, M. (2004). Principles of conservation biology: Recommended guidelines for conservation literacy from the education committee of the society for conservation biology. *Conservation Biology*, *18*(5), 1180–1190.

Uetz, P., Freed, P., & Hosek, J. (2020). *The Reptile Database*. The Reptile Database. http://www.reptile-database.org/

Vawter, L., & Brown, W. M. (1986). Nuclear and mitochondrial dna comparisons reveal extreme rate variation in the molecular clock. *American Association for the Advancement of Science*, *234*(4773), 194–196.

Via, S. (2001). Sympatric speciation in animals: the ugly duckling grows up. *TRENDS in Ecology & Evolution*, *16*(7), 381–390.

Vidal, N., & Hedges, S. B. (2002). Higher-level relationships of snakes inferred from four nuclear and mitochondrial genes. *Comptes Rendus - Biologies*, *325*(9), 977–985. https://doi.org/10.1016/S1631-0691(02)01510-X

Vidal, N., Branch, W. R., Pauwels, O. S. G., Hedges, S. B., Broadley, D. G., Wink, M., Cruaud, C., Joger, U., & Nagy, Z. T. (2008). Dissecting the major African snake radiation: A molecular phylogeny of the Lamprophiidae Fitzinger (Serpentes, Caenophidia). *Zootaxa*, *66*(1945), 51–66. https://doi.org/10.11646/zootaxa.1945.1.3

Vidal, N., Delmas, A. S., David, P., Cruaud, C., Couloux, A., & Hedges, S. B. (2007). The phylogeny and classification of caenophidian snakes inferred from seven nuclear protein-coding genes. *Comptes Rendus - Biologies*, *330*(2), 182–187. https://doi.org/10.1016/j.crvi.2006.10.001

Vienne, D. M. De, Giraud, T., & Martin, O. C. (2007). A congruence index for testing topological similarity between trees. *Bioinformatics*, *23*(23), 3119–3124. https://doi.org/10.1093/bioinformatics/btm500

Wallach, V., Williams, K. L., & Boundy, J. (2014). *Snakes of the World: A Catalogue of Living*

and Extinct Species. CRC Press.

Ward, D. (2009). *The Biology of Deserts*. Oxford University Press.

Weinell, L., & Bauer, A. M. (2018). Phylogeography of the widely distributed African skink *Trachylepis varia* species complex. *Molecular Phylogentics and Evolution*, *120*, 103–117. https://doi.org/10.1016/j.ympev.2017.11.014

Weinstein, S. A., White, J., Keyler, D. E., & Warrell, D. A. (2013). Non-front-fanged colubroid snakes: A current evidence-based analysis of medical significance. *Toxicon*, *69*, 103–113. https://doi.org/10.1016/j.toxicon.2013.02.003

Whiting, A. S., Bauer, A. M., & Sites Jr, J. W. (2003). Phylogenetic relationships and limb loss in sub-Saharan African scincine lizards (Squamata: Scincidae). *Molecular Phylogenetics and Evolution*, *29*(3), 582-598.

Wiens, J. J. (2004). Speciation and ecology revisited: Phylogenetic niche conservatism and the origin of species. *Evolution*, *58*(1), 193–197.

Wiley, E., & Mayden, R. (2000). The Evolutionary Species Concept. In Q. Wheeler & R. Meier (Eds.), *Species Concepts and Phylogenetic Theory–A Debate* (pp. 70–89). Columbia University Press.

Williams, M. B. (1992). Species: current usages. *Keywords in Evolutionary Biology*, 318–323.

Wittgenstein, L. (1953). *Philosophical Investigations*. Macmillan.

Xia, X. (2013). DAMBE5: A comprehensive software package for data analysis in molecular biology and evolution. *Molecular Biology and Evolution*, *30*(7), 1720–1728. https://doi.org/10.1093/molbev/mst064

Zachos, F. E. (2016). *Species Concepts in Biology: Historical Development, Theoretical Foundations and Practical Relevance*. Springer. https://doi.org/10.1007/978-3-319-44966-1

Zaher, H. (1999). Hemipenial morphology of the south american xenodontine snakes, with a proposal for a monophyletic xenodontinae and a reappraisal of colubroid hemipenes. *Bulletin of the American Museum of Natural History*, *240*. https://doi.org/10.1016/s1098-3015(11)72087-3

Zaher, H., Murphy, R. W., Arredondo, J. C., Graboski, R., Machado-Filho, P. R., Mahlow, K., Montingelli, G. G., Quadros, A. B., Orlov, N. L., Wilkinson, M., Zhang, Y. P., & Grazziotin, F. G. (2019). Large-scale molecular phylogeny, morphology, divergence-

time estimation, and the fossil record of advanced caenophidian snakes (Squamata: Serpentes). *PLoS ONE*, *14*(5), 1–82. https://doi.org/10.1371/journal.pone.0217959

Zhang, J., Kapli, P., Pavlidis, P., & Stamatakis, A. (2013). A general species delimitation method with applications to phylogenetic placements. *Bioinformatics*, *29*(22), 2869–2876. https://doi.org/10.1093/bioinformatics/btt499

Zhao, Y., Yi, Z., Warren, A., & Song, W. B. (2018). Species delimitation for the molecular taxonomy and ecology of the widely distributed microbial eukaryote genus *euplotes* (Alveolata, Ciliophora). *Proceedings of the Royal Society B: Biological Sciences*, *285*(1871). https://doi.org/10.1098/rspb.2017.2159

Appendices

Appendix A: Chapter Two

Tables

Table S2.1**:** List of specimens used for genetic analyses, and the GenBank Accession Numbers for each gene marker (cytb = cytochrome b; ND4 = NADH dehydrogenase subunit 4; c-mos = oocyte maturation factor; RAG2 = recombination activating gene 2). Dataset (2.) denotes which specimens were present in which dataset, specific to Chapter Two.

Species	Field Number	Museum Number	Locality		Coordinates		Dataset (2.*)	Genbank Accession Numbers				
			Region	Country	Lat	Long		cytb	ND4	c-mos	16S	RAG2
Dipsina												
D. multimaculata	CMRK 62			Namibia			1,4	DQ486370	DQ486209	NA	NA	NA
D. multimaculata	TM 84514	TM 84514	Namaqualand	South Africa	-29.02	18.09	1,4	DQ486357	DQ486332	DQ486181	NA	NA
D. multimaculata	WB1		Groblershoop	South Africa			1,2,4	TBA	TBA	TBA	TBA	NA
D. multimaculata	WB2			Central Namibia			1,2,4	TBA	TBA	TBA	TBA	NA
D. multimaculata	CKD26		Port Nolloth	South Africa	-29.26	16.91	1,2,4	TBA	TBA	TBA	TBA	NA
D. multimaculata	KF 330	PEM R24595	Road south of Kleinsee, Northern Cape	South Africa	-29.82	17.12	1	NA	TBA	TBA	TBA	NA
Hemirhagerrhis												
H. hildebrandtii	CMRK 319		Arusha Region	Tanzania			1,2	DQ486418	DQ486255	NA	NA	NA
H. kelleri	CMRK 396			Tanzania			1,4	DQ486434	DQ486271	NA	NA	NA
H. kelleri	CMRK 78	PEM R21447	Arusha district	Tanzania	-3.17	36.68	1,2,4	DQ486372	DQ486211	NA	NA	NA
H. kelleri	CMRK 400	PEM R22889	Kingori	Tanzania	-3.28	36.98	1,4	DQ486436	DQ486272	NA	NA	NA
H. kelleri	CMRK 77	PEM R21446	Kingori	Tanzania	-3.28	36.98	1,2,4	DQ486335	DQ486311	DQ486159	NA	NA
H. notonaenia	PEM R09700	PEM R09700	70 km S.S.E. Dodoma	Tanzania			1,2	FJ404311	FJ404337	FJ387214	FJ404214	FJ404409
H. notonaenia	WC-2660	NA	Quirmbas NP	Mozambique	-12.14	40.43	1,2,4	TBA	TBA	TBA	TBA	NA
H. viperina	Kelly 2008_1		Kaokoveld	Namibia			1,4	AY235725	NA	NA	NA	NA
H. viperina	CAS AMB5989		Okangwati	Namibia	-17.07	13.27	1,2,4	DQ486453	DQ486289	NA	NA	NA

H. viperina	PVP 101	PEM R22061	Near Quilengues	Angola	-14.05	14.08	1,2,4	TBA	TBA	TBA	TBA	NA
Malpolon												
Ma. i. insignitus	E2509.14		Tozeur city	Jordan			1	DQ451886	NA	NA	NA	NA
Ma. i. insignitus	E2509.13		Tabarka T31-20	Tunisia			1	DQ451885	NA	NA	NA	NA
Ma. i. insignitus	E14053.4		El Cairo	Egypt			1,2	DQ451887	NA	NA	NA	NA
Ma. i. insignitus	E14053.3		Vrysoulles	Egyypt			1	DQ451884	NA	NA	NA	NA
Ma. i. insignitus	IPMB S89		Tasan	Jordan			1,2,4	AY612033	NA	AY611942	AY611851	NA
Ma. i. insignitus	ROM 44298						1,2	KX694879	NA	KX694786	KX694653	NA
Ma. i. fuscus	E14053.5	NHMC 80.3.24.10	Khíos (Chios) Island	Greece			1	DQ451883	NA	NA	NA	NA
Ma. i. fuscus	E14053.8	NHMC 80.3.24.7	Prefecture of Evritania	Greece			1	DQ451882	NA	NA	NA	NA
Ma. i. fuscus	E14053.6	NHMC 80.3.24.4	Kimih island of Eyvoia	Greece			1,2	DQ451880	NA	NA	NA	NA
Ma. i. fuscus	E14053.7	NHMC 80.3.24.6	Kletoria Lake, Peloponnisios	Greece			1	DQ451881	NA	NA	NA	NA
Ma. i. fuscus	HLMD RA2606		Polidrassi	Greece			1,2,4	AY188029	FJ404320	AY187990	AY188068	FJ404390
Ma. m. monspessulanus	E2509.18		Ras el Ma	Morocco			1	DQ451903	NA	NA	NA	NA
Ma. m. monspessulanus	E9124.2		N. of Chrea	Algeria			1	DQ451919	NA	NA	NA	NA
Ma. m. monspessulanus	E14053.12		Sevilla	Spain			1	DQ451921	NA	NA	NA	NA
Ma. m. monspessulanus	MVZ 186256			Spain			1,2,4	AY058965	AY058989	AY058936	NA	NA
Ma. m. monspessulanus	MM020286M			Portugal	41.78	8.18	1	KY762178	NA	KY762082	NA	NA
Mimophis												
M. mahfalensis	PEM2		Tulear District	Madagascar			1,2,4	DQ486461	DQ486297	NA	NA	NA
M. mahfalensis	Mim mad/ZSM 397/2000		Mount Ibity	Madagascar			1,4	AY188031	NA	AY187992	AY188070	
M. mahfalensis	24 str		Mount Ibity	Madagascar			1,4	DQ486440	DQ486276	NA	NA	NA
M. mahfalensis	Mim mah/HLMD J68		Kirindy	Madagascar			1,2,4	AY188032	FJ404321	AY187993	AY188071	FJ404391
M. mahfalensis	FMNH259984		Ambohitantley Reserve, Ankazobe, Antananaviro	Madagascar	-18.68	47.32	1	NA	NA	MF795220	NA	MF795289
M. occultus	23		Mont des Francais	Madagascar			1,2,4	DQ486363	DQ486202	NA	NA	NA
M. occultus	RAN68828		Tsiambara Forest, Mahajanga	Madagascar	-15.91	45.99	1	NA	NA	MF795237	NA	MF795276
M. occultus	RAN68124		Tsiombikibo Forest Antsakoamanery, Mahajanga, Mahajanga	Madagascar	-16.02	45.60	1,2	NA	NA	MF795236	NA	MF795275

M. occultus	RAX9641		Ambohibola Forest, Tsaratanana Town	Madagascar	-16.63	47.42	1	NA	NA	MF795255	NA	MF795282
Psammophis												
P. aegyptius	BEV.T4801			Egypt	25.04	33.77	1,2,3,4	MG002976	MG003042	MG002911	NA	MG003097
P. aegyptius	BEV.10372			Egypt	24.36	35.29	1,3,4	MG002975	MG003041	MG002910	NA	NA
P. aegyptius	BEV.11350			Egypt	22.35	31.61	1,3,4	MG002972	MG003038	MG002907	NA	NA
P. aegyptius	BEV.6557			Niger	20.54	8.99	1,3	NA	MG003036	MG002905	NA	NA
P. aegyptius	BEV.8964			Egypt	22.75	35.79	1,3,4	MG002969	MG003034	MG002903	NA	NA
P. aegyptius	JCB00341		Bilma Oasis	Niger	18.69	12.92	1,2,3,4	MG002988	EF128026	MG002922	NA	MG003108
P. aegyptius	JCB00340		Dirkou Oasis	Niger	18.98	12.90	1,3,4	MG002987	EF128025	MG002921	NA	NA
P. afroccidentalis	ZFMK 77036		Bohicon	Benin	7.18	2.07	1,3,4	MH997973	MK032683	NA	NA	NA
P. afroccidentalis	IRD 370.N		Toundi Farkia	Niger	14.03	1.53	1,3	NA	MK032663	NA	NA	NA
P. afroccidentalis	IRD TR.4173		Pâ	Burkina Faso	11.53	3.30	1,2,3,4	MH997961	MK032677	NA	MK005718	NA
P. afroccidentalis	IRD TR.4167		Dar Salam	Senegal	13.20	13.10	1,4	MH997960	NA	NA	MK005717	NA
P. afroccidentalis	IRD 328.CI		Niagnon	Ivory Coast	9.52	6.43	1	NA	MK032660	NA	NA	NA
P. afroccidentalis	IRD 115.M		Doussoudiana	Mali	11.15	7.80	1	NA	MK032642	NA	NA	NA
P. afroccidentalis	IRD TR.4177		near Tiva	Guinea	10.27	14.18	1,3,4	MH997962	MK032671	NA	MK005719	NA
P. afroccidentalis	IRD 5001.G		near Sangaredi	Guinea	11.17	13.83	1,3,4	MH997954	MK032665	NA	MK005711	NA
P. afroccidentalis	IRD TR.4501		near Matmata	Mauritiania	17.85	12.15	1,3,4	MH997965	MK032674	NA	MK005721	NA
P. afroccidentalis	IRD 2808.N		Mao	Chad	14.13	15.30	1	MK005683	NA	NA	MK005708	NA
P. afroccidentalis	D421		Fada N'Gourma-Bogande	Burkina Faso	12.22	0.30	1,3	NA	EF128028	NA	NA	NA
P. afroccidentalis	D432		Fama, Segou Bamako	Mali	12.77	7.20	1,3	NA	EF128029	NA	NA	NA
P. afroccidentalis	Vidal 2008_3			Niger			1,2,3,4	FJ404316	FJ404325	FJ404228	FJ404219	FJ404397
P. afroccidentalis	WB4			Senegal			1,3,4	TBA	TBA	NA	TBA	NA
P. afroccidentalis	MNHN			Senegal	13.98	-14.57	1,3,4	DQ486452	DQ486288	NA	NA	NA
P. angolensis	CMRK 263	PEM R22894	Kazungula	Botswana	-17.84	25.23	1,2,3,4	DQ486410	DQ486248	DQ486189	NA	NA
P. angolensis	CMRK 283	PEM R22895	Kabwe	Zambia	-14.48	28.26	1,3,4	DQ486416	DQ486254	NA	NA	NA
P. angolensis	CMRK 392	PEM R22896	Usa River	Tanzania	-3.37	36.85	1,3,4	DQ486433	DQ486270	NA	NA	NA
P. angolensis	CMRK 447	PEM R22897	Kasane	Botswana	-17.82	24.86	1,3,4	DQ486439	DQ486275	NA	NA	NA
P. angolensis	CT 643	PEM R22781	Fungurume, grounds of the Mother & Child clinic	DRC	-10.62	26.31	1,2,3,4	TBA	TBA	NA	TBA	NA
P. angolensis	NIMB 158	PEM R21806	Lapalala	South Africa			1,4	TBA	NA	NA	TBA	NA

P. ansorgii	NB 560		Tundavala, Huila Province	Angola	-14.81	13.40	1,2,3,4	LS992123	LS992132	LS992108	NA	NA
P. ansorgii	NB 600		Tundavala, Huila Province	Angola	-14.82	13.42	1,2,3,4	LS992127	LS992130	LS992112	NA	NA
P. biseriatus	CMRK 169	PEM R21467	Arusha	Tanzania	-3.37	36.68	1,2,3,4	DQ486389	DQ486228	NA	NA	NA
P. biseriatus	CMRK 397			Tanzania			1,4	DQ486435	NA	NA	NA	NA
P. biseriatus	BK10724		Watamu	Kenya	-3.35	40.07	1,2,3,4	DQ486448	DQ486284	NA	NA	NA
P. brevirostris	CMRK 186	PEM R21473	Marondera	Zimbabwe	-18.18	31.51	1,2,3,4	DQ486395	DQ486234	NA	NA	NA
P. brevirostris	CMRK 237	PEM R25094	Hole in the Wall	South Africa	-32.03	29.11	1,3,4	DQ486402	DQ486241	NA	NA	NA
P. brevirostris	CMRK 238	PEM R22898	Hole in the wall	South Africa	-32.03	29.11	1,3,4	DQ486403	DQ486242	NA	NA	NA
P. brevirostris	CMRK 277	PEM R22899	Naboomspruit	South Africa	-24.36	28.83	1,2,3,4	DQ486412	DQ486250	NA	NA	NA
P. brevirostris	TM 83922	TM 83922	Cullinan mine	South Africa	-25.68	28.52	1,3,4	DQ486470	DQ486306	NA	NA	NA
P. brevirostris	WB15		Mkuze Game Reserve	South Africa	-27.64	32.16	1,3,4	TBA	TBA	NA	TBA	NA
P. condanarus	CAS:HERP:205003		Ayeyarwady Div	Myanmar			1,2,3,4	AF471075	AY058987	AF471104	NA	NA
P. crucifer	CMRK 19	PEM R22905	Somerset East	South Africa	-32.72	25.58	1,3,4	DQ486360	DQ486199	NA	NA	NA
P. crucifer	CMRK 70	PEM R21444	Jeffrey's Bay	South Africa	-33.94	24.99	1,3,4	DQ486334	DQ486310	DQ486158	NA	NA
P. crucifer	CMRK 203	PEM R21479	Nyanga National Park	Zimbabwe	-18.24	32.77	1,2,3,4	DQ486397	DQ486236	DQ486188	NA	NA
P. crucifer	CMRK 214	PEM R21482	Nyanga National Park	Zimbabwe	-18.30	32.71	1,3,4	DQ486398	DQ486237	NA	NA	NA
P. crucifer	CMRK 222	PEM R21464	Nyanga National Park	Zimbabwe	-18.21	32.79	1,3,4	DQ486399	DQ486238	NA	NA	NA
P. crucifer	Kelly 2008_2		De Hoop Nature Reserve	South Africa	-34.43	20.48	1,3,4	DQ486466	DQ486302	NA	NA	NA
P. crucifer	CK10		St Francis Bay	South Africa	-34.16	24.82	1,3,4	TBA	TBA	TBA	TBA	NA
P. crucifer	WC-6656	PEM R24866	Ongeluksnek NR, Trap 1	South Africa	-30.33	28.36	1,2,3,4	TBA	TBA	TBA	TBA	NA
P. crucifer	WC-DNA-0184	PEM R19322	Sneeuberge, Farm Zuurfontein (Nieu-Bethesda)	South Africa	-31.72	24.67	1,3,4	TBA	TBA	NA	TBA	NA
P. crucifer	WC-DNA-0031	PEM R18996	Rocky ridge, Amatola Forestry Company Hogsback	South Africa	-32.58	26.95	1,3,4	TBA	TBA	TBA	TBA	NA
P. crucifer	CKD28	CKD28		South Africa			1,3,4	TBA	TBA	TBA	TBA	NA
P. crucifer	WB3						1,2,4	TBA	NA	NA	NA	NA
P. elegans	D434		Didieni, Bamako Kayes	Mali	13.73	8.02	1,3	NA	EF128027	NA	NA	NA
P. elegans	Chir03		La Tapoa	Niger	12.05	2.26	1,3	NA	EU526862	NA	NA	NA
P. elegans	IRD TR.4504		35 km E Rosso	Mauritiana	16.55	15.52	1,2,4	MH997966	MK032675	NA	MK005722	NA
P. elegans	ROM_23333						1	NA	NA	KX694791	KX694659	NA

P. elegans	IRD:222.CI		Drekro	Ivory Coast	7.00	5.28	1,3,4	MH997943	MK005728	NA	NA	NA
P. e. univittatus	IRD 2761		Bon Amdaoud	Chad	10.68	19.47	1,2,4	MK005679	MK032659	NA	MK005707	NA
P. jallae	CMRK 256	PEM R22906	Kazungula	Botswana	-17.95	25.23	1,2,3,4	DQ486409	DQ486247	NA	NA	NA
P. jallae	WC-4572	PEM R23523	west of Cuanavale River source	Angola	-13.01	18.82	1,2,3,4	TBA	TBA	TBA	TBA	NA
P. leightoni	ARD0025		Church Haven, Langebaan	South Africa	-33.16	18.04	1,3	TBA	TBA	TBA	NA	NA
P. leightoni	WP1601JM		Koeberg Nature Reserve	South Africa	-33.65	18.44	1,2,4	TBA	TBA	TBA	NA	NA
P. leightoni	ATDHKPL1		Draaihoek	South Africa	-32.61	18.33	1,3,4	TBA	TBA	TBA	NA	NA
P. leightoni	ATTKPL1		Tweekuilen	South Africa	na	na	1,3,4	TBA	TBA	TBA	NA	NA
P. leightoni	KTH05-03		Redelinghuys	South Africa	-32.44	18.58	1	TBA	TBA	TBA	NA	NA
P. leightoni	TM 83620	TM 83620	Piketberg	South Africa	-32.90	18.77	1,2,3,4	DQ486467	DQ486303	DQ486197	NA	NA
P. leopardinus	CAS214727		Grootberg Pass	Namibia	-19.87	14.07	1,2,3,4	DQ486462	DQ486298	NA	NA	NA
P. leopardinus	CAS214763		Opuwo	Namibia	-18.47	13.80	1,2,3,4	DQ486456	DQ486292	NA	NA	NA
P. lineatus	CMRK 379	PEM R22907	Bujumbura	Burundi	-3.35	29.29	1,2,3,4	DQ486426	DQ486263	NA	NA	NA
P. lineatus	CMRK 383		Bujumbura	Burundi	-3.21	29.39	1,3,4	DQ486428	DQ486265	NA	NA	NA
P. lineatus	Kelly 2008_3		Bello Tonga	Benin	12.05	3.21	1,3	NA	EU526861	NA	NA	NA
P. lineatus	Vidal 2008_1						1,2,3,4	FJ404313	FJ404354	FJ404256	FJ404216	FJ404426
P. lineatus	IRD 2120.N		Baïbokoum	Chad	7.73	15.68	1,3,4	MH997938	MK032649	NA	MK005695	NA
P. lineolatus	CAS179682		Nephtezavodsk	Turkmenistan	39.25	63.18	1,2,3,4	DQ486450	DQ486286	DQ486195	NA	NA
P. lineolatus	IPMB J261			Uzbekistan			1,4	AY612004	NA	AY611913	AY611821	NA
P. lineolatus	IPMB28601/HLMD J76		Charyn Canyon	Kasakhstan			1,2,4	AY188034	NA	AY187995	AY188073	FJ404392
P. mossambicus	IRD 2224.N		Baïbokoum	Chad	7.73	15.68	1,2,3,4	MH997944	MK032653	NA	MK005700	NA
P. mossambicus	IRD 2238.N		Baïbokoum	Chad	7.73	15.68	1,3,4	MH997947	MK032656	NA	MK005702	NA
P. mossambicus	IRD TR.4579		Foumbam	Cameroon	5.72	10.92	1,3,4	MH997967	MK032676	NA	MK005723	NA
P. mossambicus	ZFMK 88703		Luambe Nat. Park	Zambia	-12.33	32.25	1,3,4	MH997976	MK032686	NA	NA	NA
P. mossambicus	ZFMK 88502		Ikelenge Nchila	Zambia	-11.23	24.27	1,4	MH997974	MK032684	NA	NA	NA
P. mossambicus	IRD TR.4366.LC		Gamba	Gabon	-2.72	10.02	1,3,4	MH997963	MK032672	NA	MK005720	NA
P. mossambicus	MBUR 08242		Hinda	Republic of Congo	-4.53	12.07	1	MK005685	NA	NA	MK005725	NA
P. mossambicus	MBUR 03143		Lake Fony	Republic of Congo	-4.48	11.77	1	MK005684	NA	NA	MK005724	NA
P. mossambicus	PEM R05679	PEM R05679	Tanga	Tanzania	-5.16	38.98	1,3,4	DQ486359	DQ486198	NA	NA	NA

P. mossambicus	CMRK 81	PEM R21450	Kingori	Tanzania	-3.28	36.98	1,3,4	DQ486373	DQ486212	NA	NA	NA
P. mossambicus	CMRK 125	PEM R21461	Nyagatare	Rwanda	-1.36	30.35	1,3,4	DQ486383	DQ486222	DQ486185	NA	NA
P. mossambicus	CMRK 126	PEM R21462	Nyagatare	Rwanda	-1.29	30.23	1,3,4	DQ486384	DQ486223	NA	NA	NA
P. mossambicus	CMRK 175	PEM R21470	Mikumi Nature Park	Tanzania	-7.35	37.08	1,3,4	DQ486392	DQ486231	NA	NA	NA
P. mossambicus	CMRK 231	PEM R22908	Sodwana Bay	South Africa	-27.69	32.37	1,3,4	DQ486400	DQ486239	NA	NA	NA
P. mossambicus	CMRK 268	PEM R22909	Pandamatenga	Botswana	-18.64	25.63	1,3,4	DQ486411	DQ486249	NA	NA	NA
P. mossambicus	CMRK 376	PEM R22910	Butare	Rwanda	-2.69	29.71	1,3,4	DQ486423	DQ486260	NA	NA	NA
P. mossambicus	Kelly 2008_4		Maun	Botswana	-19.98	23.42	1,3,4	DQ486442	DQ486278	NA	NA	NA
P. mossambicus	BK10357		Makuyu	Kenya	-0.90	37.18	1,3,4	DQ486447	DQ486283	NA	NA	NA
P. mossambicus	PEM R13258	PEM R13258	Moebase	Mozambique	-17.06	38.69	1,3,4	DQ486457	DQ486293	NA	NA	NA
P. mossambicus	TM 83688	TM 83688	Palaborwa	South Africa	-23.95	31.12	1,3,4	DQ486468	DQ486304	NA	NA	NA
P. mossambicus	WC-4831	PEM R23448	Cuando River Source Trap 3	Angola	-13.00	19.14	1,3,4	TBA	TBA	NA	TBA	NA
P. mossambicus	WC-4067	PEM R23286	Cuanavale River Source	Angola	-13.09	18.89	1,3,4	TBA	TBA	NA	TBA	NA
P. mossambicus	WC12-A142	PEM R20024	4 km from Village Kassenge to Cuchi River	Angola	-12.54	16.68	1,3,4	TBA	TBA	NA	TBA	NA
P. mossambicus	WB13		Maunga River	Mozambique			1,3,4	TBA	TBA	NA	TBA	NA
P. mossambicus	WB16		Mkuze	South Africa	-27.64	32.16	1,4	TBA	NA	NA	TBA	NA
P. mossambicus	PEM R15488	PEMR 15488	Zambezi Delta	Mozambique			1,2,3,4	FJ404314	FJ404322	FJ404224	FJ404217	FJ404393
P. mossambicus	MM1	MM1					1,3,4	TBA	TBA	NA	TBA	NA
P. mossambicus	PVP 055		10km north of Cusse	Angola			1,3,4	TBA	TBA	NA	NA	NA
P. mossambicus	LN10/11	PEM R22047	Farm in Kikuxi, near Luanda	Angola	-9.06	13.35	1,2,3,4	TBA	TBA	TBA	TBA	NA
P. mossambicus	WB14		Kalundula	Angola			1,3,4	TBA	TBA	NA	TBA	NA
P. mossambicus	WB17		Dande	Angola			1,3,4	TBA	TBA	NA	TBA	NA
P. mossambicus	PEM R05451	PEM R05451	Loango Nature Park	Gabon	-2.36	9.64	1,3,4	DQ486454	DQ486290	AY611970	AY611879	FJ404395
P. namibensis	PEM R15811	PEM R15811	Farm Augrabies Wes, 3km West of Fifteenmile Mountain	South Africa	-29.24	17.09	1,3,4	DQ486455	DQ486291	NA	NA	NA
P. namibensis	TGET569		Port Nolloth	South Africa	-29.28	16.97	1,2,3,4	TBA	TBA	TBA	NA	NA
P. namibensis	1819		Port Nolloth	South Africa	na	na	1,3,4	TBA	TBA	TBA	NA	NA
P. namibensis	LHU01	PEM R18131	Langer Heinrich Mine	Namibia	-22.81	15.37	1,2,3	TBA	TBA	TBA	NA	NA
P. namibensis	WB11	PEM R17296	Sossusvlei Mountain Lodge	Namibia	-24.84	15.25	1,3,4	TBA	TBA	TBA	TBA	NA
P. namibensis	CKD27		Port Nolloth	South Africa	-29.26	16.91	1,3,4	TBA	TBA	NA	TBA	NA

P. notostictus	PEM R05682	PEM R05682	Mountain Zebra NP	South Africa	-31.70	25.27	1,3,4	DQ486366	DQ486205	DQ486182	NA	NA
P. notostictus	PEM R05660	PEM R05660	Grahamstown	South Africa	-33.30	26.51	1,3,4	DQ486362	DQ486201	NA	NA	NA
P. notostictus	PEM R05669	PEM R05669	Mountain Zebra NP	South Africa	-31.70	25.27	1,3,4	DQ486367	DQ486206	NA	NA	NA
P. notostictus	PEM R05670	PEM R05670	Mountain Zebra NP	South Africa	-32,22	258	1,3,4	DQ486368	DQ486207	NA	NA	NA
P. notostictus	PEM	PEM R12435	Port Nolloth	South Africa	-29.25	16.87	1,3,4	DQ486463	DQ486299	NA	NA	NA
P. notostictus	EI_0291		Beaufort West	South Africa	-32.68	22.68	1,2,3,4	TBA	TBA	TBA	NA	NA
P. notostictus	EI_0351		Hardap Region	Namibia	-24.18	15.98	1,4	TBA	TBA	TBA	NA	NA
P. notostictus	FP037		Northern Cape	South Africa	-31.34	22.29	1,3	TBA	TBA	TBA	NA	NA
P. notostictus	NCP16-70		Springbok	South Africa	-29.66	17.89	1,3,4	TBA	TBA	TBA	NA	NA
P. notostictus	WW2562		West Coast NP	South Africa	-33.15	18.02	1,4	TBA	TBA	TBA	NA	NA
P. notostictus	WP1605JM		Koeberg Nature Reserve	South Africa	-33.63	18.44	1,4	TBA	TBA	TBA	NA	NA
P. notostictus	WB5		near Molteno	Northern Cape			1,3,4	TBA	TBA	TBA	TBA	NA
P. notostictus	CKD22		Koingnaas	South Africa	-30.19	17.28	1,3,4	TBA	TBA	TBA	TBA	NA
P. notostictus	CKD23		Koingnaas	South Africa	-30.19	17.28	1,2,3,4	TBA	TBA	TBA	TBA	NA
P. notostictus	WB8	PEM R18171	Farm Trompfontein, Steytlerville	South Africa	-33.56	24.47	1,3,4	TBA	TBA	TBA	TBA	NA
P. cf. notostictus	ANG 0257	PEM R21671	55 km N on road to Lucira from Lubango-Namibe road	Angola	-14.68	12.53	1,2,3,4	TBA	TBA	NA	TBA	NA
P. orientalis	CMRK 171	PEM R21468	Nguru Mountains	Tanzania	-5.43	37.45	1,3,4	DQ486390	DQ486229	NA	NA	NA
P. orientalis	CMRK 172	PEM R21469	Nguru Mountains	Tanzania	-5.43	37.45	1,3,4	DQ486391	DQ486230	NA	NA	NA
P. orientalis	CMRK 177	PEM R21471	Udzungwa Nature Park	Tanzania	-7.58	36.36	1,2,3,4	DQ486393	DQ486232	NA	NA	NA
P. orientalis	CMRK 187	PEM R21474	Gorongosa	Mozambique	-18.18	34.11	1,3,4	DQ486396	DQ486235	NA	NA	NA
P. orientalis	PEM R15622	PEM R15622	Moma	Mozambique	-16.76	39.22	1,3,4	DQ486459	DQ486295	NA	NA	NA
P. orientalis	PEM R16132	PEM R16132	Nyassa	Mozambique	-12.07	37.57	1,2,4	FJ404315	NA	FJ404225	FJ404218	FJ404394
P. orientalis	WB9	PEM R13233	Moebase	Mozambique	-17.06	38.74	1,4	TBA	NA	NA	TBA	NA
P. orientalis	MO1	MO1					1,3,4	TBA	TBA	TBA	TBA	NA
P. orientalis	MO2	MO2					1,3,4	TBA	TBA	NA	NA	NA
P. occidentalis	CMRK 71	PEM R21445	Serenje	Zambia	-12.76	30.93	1,2,3,4	DQ486371	DQ486210	NA	NA	NA
P. occidentalis	CMRK 377	PEM R22900	Kizuka	Burundi	-3.90	29.39	1,2,3,4	DQ486424	DQ486261	NA	NA	NA
P. occidentalis	CMRK 381	PEM R22901	Bubanza	Burundi	-3.06	29.43	1,3,4	DQ486427	DQ486264	NA	NA	NA
P. phillipsii	IRD 358.T		Djiguengué	Togo	8.08	0.63	1,2,4	MK005680	MK032661	NA	MK005709	NA

P. phillipsii	IRD 10.T		Sodo	Togo	7.32	0.80	1	MK005686	NA	NA	NA	NA
P. phillipsii	IRD 44.T		Kpalimé	Togo	6.90	0.62	1,4	MH997953	MK032664	NA	NA	NA
P. phillipsii	IRD 5002.G		Kindia	Guinea	10.05	12.85	1,3,4	MH997955	MK032666	NA	MK005712	NA
P. phillipsii	IRD 5004.G		Kissidougou	Guinea	9.23	10.05	1,2,3,4	MH997957	MK032668	NA	MK005713	NA
P. phillipsii	IRD TR.4609		Ziéla	Guinea	7.72	8.35	1,4	MK005681	NA	NA	MK005715	NA
P. phillipsii	IRD TR.4610		Païa	Guinea	8.02	9.03	1,4	MK005682	NA	NA	MK005716	NA
P. praeornatus	Vidal 2008_2			Ghana			1,2	NA	FJ404355	FJ387216	NA	FJ404427
P. praeornatus	Kelly 2008_5		Nienie	Benin	11.36	2.21	1,3	NA	EU526860	NA	NA	NA
P. praeornatus	IRD 9193.S		Senegal	Fafakourou	13.07	14.55	1,2,3,4	MH997959	MK032670	NA	NA	NA
P. punctulatus trivirgatus	CMRK 167	PEM R21465	Lolkisale	Tanzania	-3.77	36.42	1,2,3,4	DQ486387	DQ486226	DQ486186	NA	NA
P. p. trivirgatus	CMRK 168	PEM R21466		Kenya			1,3,4	DQ486388	DQ486227	NA	NA	NA
P. p. trivirgatus	CMRK 391	PEM R22912	Arusha	Tanzania			1,3,4	DQ486432	DQ486269	NA	NA	NA
P. p. trivirgatus	BK10476		Watamu	Kenya	-3.35	40.02	1,2,3,4	DQ486445	DQ486281	NA	NA	NA
P. rukwae	BK10620		Kakuyuni	Kenya	-3.22	40.00	1,2,3,4	DQ486446	DQ486282	NA	NA	NA
P. rukwae	BK10358		Lake Baringo	Kenya	0.47	35.97	1,3,4	DQ486443	DQ486279	NA	NA	NA
P. rukwae	CMRK 83	PEM R21452	Kondoa Region	Tanzania	-4.90	35.78	1,3,4	DQ486375	DQ486214	NA	NA	NA
P. rukwae	CMRK 85	PEM R21454	Kondoa Region	Tanzania	-4.90	35.78	1,3,4	DQ486376	DQ486215	NA	NA	NA
P. rukwae	MBUR 08343		Kutaworke	Ethiopia	10.60	34.40	1,2,3,4	MH997968	MK032678	NA	MK005726	NA
P. rukwae	IRD 2759.N		Kieke	Chad	10.55	19.80	1,3,4	MH997951	MK032658	NA	MK005706	NA
P. rukwae	IRD 2020.N		Baïbokoum	Chad	7.73	15.68	1,3,4	MH997931	MK032646	NA	MK005692	NA
P. rukwae	IRD 2002.N		N'Djaména	Chad	12.07	15.12	1,3,4	MH997930	MK032645	NA	MK005691	NA
P. rukwae	IRD 1949.N		Bon Amdaoud	Chad	10.68	19.47	1,3,4	MH997937	MK032644	NA	NA	NA
P. rukwae	IRD 1888.N		Mahargal	Chad	12.12	21.37	1,3,4	MH997936	MK032643	NA	MK005689	NA
P. schokari	BEV.12013			Morocco	32.49	-5.94	1,3,4	MG002979	MG003045	MG002914	NA	NA
P. schokari	JCB9186			Morocco	21.88	-15.57	1,3,4	MG003025	MG003077	MG002955	NA	MG003142
P. schokari	JCB9781			Mauritania	18.35	-9.17	1,3,4	MG003028	MG003080	MG002958	NA	NA
P. schokari	RIM129			Mauritania	21.38	-12.98	1,3,4	MG002984	MG003050	MG002918	NA	NA
P. schokari	BEV.8963			Egypt	30.91	29.42	1,3,4	MG002971	MG003037	MG002906	NA	NA
P. schokari	BEV.T2460			Kuwait	28.58	48.07	1,3,4	MG002973	MG003039	MG002908	NA	NA
P. schokari	HDB5246			Tunisia	34.30	8.36	1,3,4	MG002964	MG003030	MG002899	NA	NA

P. schokari	JCB915			Algeria	35.00	6.03	1,3,4	MG003000	EF128020	MG002934	NA	NA
P. schokari	HDB2213			Israel	29.88	35.05	1,2,3,4	MG002963	MG003029	MG002898	NA	MG003084
P. schokari	KP29			Tunisia	34.50	9.50	1,3,4	DQ486441	DQ486277	DQ486194	NA	NA
P. schokari	NHMC 80.3.45.2			Syria	34.36	38.17	1,3,4	MG002968	MG003033	MG002902	NA	NA
P. schokari	CN356			Oman	23.16	57.42	1,2,3,4	MG002980	MG003046	MG002915	NA	NA
P. schokari	IR 035			Iran	35.11	50.90	1,3,4	MG002982	MG003048	NA	NA	NA
P. schokari	IPMB 28602		Bou Hedma	Tunisia			1,2,3,4	AY612034	FJ404324	AY611943	AY611852	FJ404396
P. sibilans	CMRK 352	PEM R22902	Keriyo Hamlet	Ethiopia	9.40	38.65	1,3,4	DQ486419	DQ486256	NA	NA	NA
P. sibilans	CMRK 358	PEM R22903	Keriyo Hamlet	Ethiopia	9.40	38.65	1,3,4	DQ486420	DQ486257	NA	NA	NA
P. sibilans	CMRK 364	PEM R22904	Keriyo Hamlet	Ethiopia	9.40	38.65	1,3,4	DQ486422	DQ486259	NA	NA	NA
P. sibilans	Kelly 2008_6		Derba	Ethiopia	9.40	38.67	1,2,3,4	DQ486449	DQ486285	NA	NA	NA
P. sibilans	MBUR08588		near Kutaworke	Ethiopia	10.58	34.35	1,3,4	MH997970	MK032680	NA	NA	NA
P. sibilans	BEV T.4799		near Edfu	Egypt	25.02	32.97	1,3,4	MH997935	MK032641	NA	MK005727	NA
P. sibilans	AUZC R.143973		Faiyum	Egypt	29.42	30.90	1,2,3,4	MH997934	MK032640	NA	MK005688	NA
P. sibilans	AUZC R.143972		Faiyum	Egypt	29.42	30.90	1,3,4	MH997928	MK032639	NA	MK005687	NA
P. subtaeniatus	CMRK 249	PEM R22913	Kazungula	Botswana	-17.96	25.23	1,4	DQ486408	NA	NA	NA	NA
P. subtaeniatus	CMRK 282	PEM R22914	Kariba	Zimbabwe	-16.52	28.80	1,4	DQ486415	DQ486253	NA	NA	NA
P. subtaeniatus	NMZB		Kwekwe	Zimbabwe	-18.92	29.82	1,4	DQ486358	NA	NA	NA	NA
P. subtaeniatus	WB7		Blouberg	South Africa			1,2,3,4	TBA	TBA	NA	TBA	NA
P. subtaeiniatus	WB18		Mkuze	South Africa	-27.64	32.16	1,3,4	TBA	TBA	NA	TBA	NA
P. subtaeiniatus	ANG-424	PEM R20506	Camp site 6 km west of Sashae	Angola	-17.57	23.23	1,4	TBA	TBA	NA	NA	NA
P. subtaeiniatus	X2	NA	Chiawa	Zambia	-15.89	28.90	1,2,3,4	TBA	TBA	NA	TBA	NA
P. subtaeiniatus	WB20			Mozambique			1,4	TBA	TBA	NA	TBA	NA
P. species	TP28431			Somalia			1,3,4	FJ404317	FJ404326	FJ387217	FJ404220	FJ404398
P. sudanensis	CMRK 91	PEM R21460	Kingori	Tanzania	-3.28	36.98	1,2,3,4	DQ486382	DQ486221	DQ486184	NA	NA
P. sudanensis	CMRK 334	PEM R22915	Loitokitok	Kenya	-2.84	37.52	1,3	NA	DQ486307	NA	NA	NA
P. sudanensis	CMRK 385	PEM R22916	Athi River	Kenya	-1.45	36.98	1,3,4	DQ486429	DQ486266	NA	NA	NA
P. sudanensis	CMRK 386	PEM R22917	Athi River	Kenya	-1.45	36.98	1,2,3,4	DQ486430	DQ486267	NA	NA	NA
P. sudanensis	CMRK 390	PEM R22918	Namanga	Tanzania	-2.87	36.72	1,3,4	DQ486431	DQ486268	NA	NA	NA
P. sudanensis	BK10603		Tsavo Nature Park	Kenya	-2.98	38.47	1,3,4	DQ486444	DQ486280	NA	NA	NA

P. sudanensis	IRD 2231.N		Baïbokoum	Chad	7.73	15.68	1,3,4	MH997946	MK032655	NA	NA	NA
P. sudanensis	IRD 2283.N		Baïbokoum	Chad	7.73	15.68	1,2,3,4	MH997949	MK032657	NA	MK005704	NA
P. tanganicus	CMRK 86	PEM R21455	Dodoma region	Tanzania			1,3,4	DQ486377	DQ486216	NA	NA	NA
P. tanganicus	CMRK 87	PEM R21456	Dodoma region	Tanzania			1,2,3,4	DQ486378	DQ486217	DQ486183	NA	NA
P. tanganicus	CMRK 88	PEM R21457	Dodoma region	Tanzania			1,3,4	DQ486379	DQ486218	NA	NA	NA
P. tanganicus	CMRK 90	PEM R21459	Arusha Region	Tanzania			1,2,3,4	DQ486381	DQ486220	NA	NA	NA
P. trigrammus	CAS 214751	CAS 214751	Sesfontein	Namibia	-19.17	13.57	1,2,3,4	DQ486458	DQ486294	DQ486196	NA	NA
P. trigrammus	TM 83873	TM 83873	Brandberg	Namibia	-21.13	14.58	1,3,4	DQ486469	DQ486305	NA	NA	NA
P. trigrammus	F1/LHU14	PEM R18133	Top of Schiefferberg, Langer Heinrich Uranium Mine	Namibia	-22.83	15.32	1,3,4	TBA	TBA	TBA	TBA	NA
P. trinasalis	GNR 002		Goegap Nat. Pk.	South Africa	-29.70	17.93	1,2,3	TBA	TBA	TBA	NA	NA
P. trinasalis	ARD00028		20.5 km from Onseepkans road, on Skitskop road, Northern Cape	South Africa	-28.83	19.51	1,3,4	TBA	TBA	TBA	NA	NA
P. trinasalis	EI_0028		Tsawisis	Namibia	-26.18	18.16	1	NA	TBA	TBA	NA	NA
P. trinasalis	KTH583		Northern Cape	South Africa	-30.08	18.31	1,3,4	TBA	TBA	TBA	NA	NA
P. trinasalis	RSP144		Northern Cape	South Africa	-28.57	24.20	1,4	TBA	TBA	TBA	NA	NA
P. trinasalis	WC-3012		Bethulie	South Africa	-30.46	25.95	1,2,3,4	TBA	TBA	TBA	NA	NA
P. trinasalis	WC-3798		Karoo NP	South Africa	-31,74	22,19	1,3	TBA	TBA	TBA	NA	NA
P. trinasalis	WC-DNA-991	PEM R20505	23km West of Orapa mine on A300	Botswana	-21.29	25.15	1,3	TBA	TBA	TBA	NA	NA
P. trinasalis	KF192	PEM R24353	24km W of Van Zylsrus	South Africa	-26.96	21.86	1,4	NA	NA	TBA	TBA	NA
P. zambiensis	WC-4829	PEM R23433	Cuando River Source Trap 2	Angola	-13.00	19.13	1,2,3,4	TBA	TBA	NA	TBA	NA
P. zambiensis	WC-4746	PEM R23475	Quembo Trap 1	Angola	-13.14	19.04	1,3,4	TBA	TBA	NA	TBA	NA
P. zambiensis	WC-4012	PEM R23287	Cuanavale River Source	Angola	-13.09	18.89	1,3,4	TBA	TBA	NA	TBA	NA
P. zambiensis	PVP 070	PEM R22074	Lubango, Portuguese School	Angola	-14,93	136	1,2,3	NA	TBA	TBA	NA	NA
Psammophylax												
Ps. acutus	WC-3540	PEM R21485	Luissingua River	Angola	−14.60	18.17	1,2,4	LR213493	LR213550	LR213470	NA	NA
Ps. acutus	WC-4018	PEM R23288	Cuanavale River Source	Angola	−13.09	18.09	1,4	LR213494	LR213551	LR213471	NA	NA
Ps. acutus	WC-4149	PEM R23315	Cuito River Source	Angola	−12.66	18.35	1,4	LR213495	LR213552	LR213472	NA	NA
Ps. acutus	PEMR13485	PEM R13485	Luzamba	Angola	−9.12	18.06	1,4	DQ486464	DQ486300	NA	NA	NA

Ps. acutus	CMRK 378		Gitaba	Burundi	−3.85	29.98	1,2,4	DQ486425	DQ486262	DQ486192	NA	NA
Ps. multisquamis	CMRK 328	PEM R23925	Arusha	Tanzania	−3.17	36.68	1,2,4	LR213511	LR213568	NA	NA	NA
Ps. multisquamis	CMRK 401	PEM R23926	Arusha	Tanzania	−3.17	36.68	1,4	LR213517	LR213575	NA	NA	NA
Ps. multisquamis	CMRK 405	PEM R23929	Ngorongoro	Tanzania	−3.22	35.48	1,2,4	LR213520	LR213578	NA	NA	NA
Ps. multisquamis	CMRK 404	PEM R23928	Ngorongoro	Tanzania	−3.23	35.41	1,4	DQ486437 /LR213503	DQ486273	NA	NA	NA
Ps. multisquamis	CMRK 149		Naivasha	Kenya	−0.74	36.45	1,2,4	LR213507	LR213561	NA	NA	NA
Ps. multisquamis	CMRK 150		Naivasha	Kenya	−0.74	36.45	1,4	LR213508	LR213562	NA	NA	NA
Ps. multisquamis	CMRK 360	PEM R23920	Ethiopian Plateau	Ethiopia	9.33	38.92	1,4	LR213514	LR213572	NA	NA	NA
Ps. multisquamis	CMRK 361	PEM R22919	Ethiopian Plateau	Ethiopia	9.33	38.92	1,2,4	DQ486421	DQ486258	DQ486191	NA	NA
Ps. ocellatus	KTH09-064	PEM R17986	Zootecnica, Humpata	Angola	−15.03	13.37	1,2,4	LR213506	LR213560	LR213479	NA	NA
Ps. ocellatus	NB 491		Tundavala	Angola	−14.81	13.40	1,4	LS992121	LS992136	LS992106	NA	NA
Ps. ocellatus	NB 561	PEM R16270	Tundavala	Angola	−14.81	13.40	1,4	LS992124	LS992133	LS992109	NA	NA
Ps. ocellatus	NB 585		Tundavala	Angola	−14.81	13.40	1,2,4	LS992125	LS992128	LS992110	NA	NA
Ps. rhombeatus	WC-1272	PEM R20527	Baviaanskloof East	EC	-33.68	24.31	1,4	TBA	TBA	NA	NA	NA
Ps. rhombeatus	TP2		Mooi Rivier	KZN	-29.19	30.08	1,4	TBA	TBA	TBA	TBA	NA
Ps. rhombeatus	CK2		Cederberg	WC	-32.86	19.44	1,4	TBA	TBA	TBA	TBA	NA
Ps. rhombeatus	AC1		Napier	WC	-34.48	19.92	1,2,4	TBA	TBA	TBA	TBA	NA
Ps. rhombeatus	EI0534		Woodbush Forest Reserve	LIM	-23.80	29.95	1,4	TBA	TBA	TBA	TBA	NA
Ps. rhombeatus	TP3		Golden Gate National Park	FS	-28.51	28.63	1,4	TBA	TBA	TBA	TBA	NA
Ps. rhombeatus	Ck6		Koeberg	WC	-33.62	18.41	1,2,4	TBA	TBA	TBA	TBA	NA
Ps. rhombeatus	DM1		Alexander Bay	NC	-28.61	16.49	1,4	TBA	NA	TBA	TBA	NA
Ps. rhombeatus	PEM R09727	PEM R9727	Suikerbosrand Nature Reserve	South Africa	26.51	28.25	1,2,4	FJ404312	FJ404327	FJ387215	FJ404215	FJ404399
Ps. tritaeniatus	MB 21435	PEM R21083	Gelukspan	South Africa	−26.22	25.66	1,2,4	LR213499	LR213556	LR213476	NA	NA
Ps. tritaeniatus	PVP 97		Huambo	Angola	-12.72	15.77	1,4	LR213502	LR213557	LR213478	NA	NA
Ps. tritaeniatus	ZMUC R970215	ZMUC R970215	Manyoni	Tanzania	−5.52	35.21	1,2,4	DQ486451	DQ486287	NA	NA	NA
Ps. tritaeniatus	CMRK 279	PEM R22921	Mvuma	Zimbabwe	−19.53	30.73	1,4	DQ486414	DQ486252	DQ486190	NA	NA
Ps. tritaeniatus	Kal	PEM R17451	Kalakundi Fragment	DRC	−10.64	25.93	1,4	LR213541	LR213599	NA	NA	NA
Ps. tritaeniatus	LK3		Limpopo	South Africa	−23.03	29.66	1,4	LR213542	LR213600	NA	NA	NA
Ps. variabilis	EBG 3006	UTEP 21871	Marungu Plateau	DRC	−7.72	29.76	1,2,4	LR213486	LR213543	LR213463	NA	NA

Ps. variabilis	EBG 2611	UTEP 21868	Lendu Plateau	DRC	2.01	30.84	1,2,4	LR213489	LR213546	LR213466	NA	NA
Ps. variabilis	MOZ14-0192	PEM R21186	Mount Namuli	Mozambique	−15.39	37.05	1,4	LR213491	LR213548	LR213468	NA	NA
Ps. variabilis	CMRK 403	PEM R23970	Crater Highlands	Tanzania	−3.23	35.48	1,4	LR213519	LR213577	LR213481	NA	NA
Ps. variabilis	CMRK 414	PEM R23969	Udzungwa Mountains	Tanzania	−8.28	35.90	1,4	LR213521	LR213579	NA	NA	NA
Ps. variabilis	QP060	PEM R18522	Mulanje Massif	Malawi	−15.9	35.65	1,2,4	LR213492	LR213549	LR213469	NA	NA
Ps. variabilis	CMRK 441	PEM R23962	Zomba Plateau	Malawi	−15.28	35.32	1,4	DQ486438	DQ486274	DQ486193	NA	NA
Ps. variabilis	CMRK 419		Nyika Plateau	Malawi	−10.6	33.80	1,4	LR213526	LR213584	NA	NA	NA
Ps. variabilis	IPMBJ296		Gishubi	Burundi	−3.52	29.91	1,4	AY612046	FJ404328	AY611955	AY611864	EF144107
Ps. variabilis	WB6	PEM R21936	Mt Namuli	Mozambique	-15,4	37,05	1,4	NA	TBA	TBA	TBA	NA
Rhamphiophis												
R. oxyrhynchus	MNHN 1990.4336		Dielmo, close to Toubakouta, 15 km from The Gambia border	Senegal			1,2	NA	NA	AF544710	FJ404213	FJ404400
R. oxyrhynchus	ROM 21917						1,2	JQ598953	NA	KX694825	KX694664	NA
R. rostratus	CMRK 80	PEM R21449	Dodoma Region	Tanzania	-6.18	35.75	1,2,4	DQ486336	DQ486312	NA	NA	NA
R. rostratus	CMRK 185	PEM R21472	Bubye River	Zimbabwe	-21.70	30.51	1,4	DQ486394	DQ486233	DQ486187	NA	NA
R. rostratus	FN 1400/IPMB J408	PEM R13209	N. Moebase Village	N. Mozambique	-16.98	38.73	1,4	AY612079	FJ404329	AY611988	AY611897	FJ404401
R. rostratus	W19/WC-DNA-1185	NA	Tenge camp, east of Revubo River	Mozambique	-15.72	33.78	1,2,4	TBA	TBA	TBA	TBA	NA
R. rostratus	X1	NA	Chiawa	Zambia	-15.89	28.90	1,4	TBA	TBA	NA	NA	NA
R. rubropunctatus	CMRK 303		Kilimanjaro Airport	Tanzania	-3.43	37.07	1,2,4	DQ486417	NA	NA	NA	NA
R. rubropunctatus	Vidal 2008_4						1,2,4	FJ404310	FJ404330	FJ404232	NA	FJ404402
Rhagerhis												
Rh. moilensis	HLMD			Tunisia			1,2,4	DQ486333	DQ486309	DQ486157	NA	NA
Rh. moilensis	E1110.16						1,2	AY643397	NA	NA	AY643355	NA
Rh. moilensis	ISOLATE 28			Saudi Arabia			1	NA	NA	NA	HQ267802	NA
Outgroups												
Lycophidion capense	PEM R13512	PEM R13512	Port Elizabeth	South Africa	-33,97	25,6	1	AY612075	FJ404376	AY611984	AY611893	FJ404450
Lycodonomorphus rufulus	PEM R08042	PEM R08042	Sherwood, Port Elizabeth	South Africa	-33,97	25,6	1	FJ404299	FJ404374	FJ387200	FJ404199	FJ404448
Lycodonomorphus rufulus	CMRK 236	PEM R22892	Hole in the wall	South Africa	-32,03	29,12	2	HQ207111	HQ207153	HQ207076	NA	NA
Lamprophis guttatus	AMB 6058		N.E. Cape	South Africa			1	AY612072	FJ404366	AY611981	AY611890	FJ404439

Amphlorhinus multimaculatus	PEM R05490	PEM R05490	Mpur forest	South Africa	-30,28	29,58	1	AY612062	FJ404346	AY611971	AY611880	FJ404418
Amplorhinus multimaculatus	CMRK 208	PEM R21480	Nyanga National Park	Zimbabwe	-18,26	32,74	2	DQ486340	DQ486316	DQ486164	NA	NA
Duberrix lutrix	PEM 5411	PEM R24797	Coega Salt Works, Port Elizabeth	South Africa	-33,8	25,7	1	FJ404305	FJ404356	FJ387207	FJ404207	FJ404428
Boa constrictor							2	AF471036	NA	AF471115	NA	NA
Boa constrictor sabogae	NE6.9						2	KF576747	KF576715	NA	NA	NA
Acrochordus granulatus							2	AF217841	U49296	AF471124	NA	NA
Acrochordus arafurae	MZB3342						2	NA	HM234056	HM234059	NA	NA
Agkistrodon piscivorus							2	AF471074	AF156578	AF471096	NA	NA
Atheris nitschei							2	AF471070	AY223618	AF471125	NA	NA
Crotalus viridis							2	AF471066	AF194157	AF471135	NA	NA
Diadophis punctatus							2	AF471094	AF258910	AF471122	NA	NA
Hypsiglena torquata							2	AF471038	U49309	AF471159	NA	NA
Natrix natrix							2	AY873710	AF471059	AF471121	NA	NA
Thamnophis sirtalis infernalis							2	AF402929	AF420196	DQ902094	NA	NA
Dendroaspis polylepis							2	AF217832	AY058974	AY058928	NA	NA
Naja kaouthia							2	AF217835	AY058982	AY058938	NA	NA
Naja annulata							2	AF217829	AY058970	AY058925	NA	NA
Oxyrhabdium leporinum							2	AF471029	NA	DQ112081	NA	NA
Gonionotophis brussauxi	IRSNB16266						2	AY612043	FJ404358	AY611952	NA	NA
Boaedon fuliginosus							2	FJ404302	FJ404364	AF544686	NA	NA
Atractaspis bibronii	MCZ-R 184500						2	MK621603	MK621545	MK621667	NA	NA
Atractaspis congica	WRB 633	PEM R20856	Kwanda power plant, Soyo	Angola	-6.13	12.33	2	MK621587	MK621529	MK621651	NA	NA
Aparallactus capensis	MCZ-R 184501						2	MG746890	MG776004	MG775887	NA	NA
Leioheterodon modestus							2	AY058967	AY058978	AY058933	NA	NA
Prosymna ruspolii							2	DQ486347	DQ486323	DQ486171	NA	NA
Prosymna visseri							2	AY188033	NA	AY187994	NA	NA

Table S2.2: List of samples used in the morphometric analyses. X's denote whether a photographs was available for the dorsal and/or lateral view.

Field Number	Museum Number	Locality		Coordinates		Morphometric Photographs	
		Region	Country	Lat	Long	Dorsal	Lateral
D. multimaculata							
	PEMR3508	Kwaggaskop Farm, North of Vanrhynsdorp	South Africa			X	X
	PEMR4331	Molteno Pass, Karoo National Park	South Africa	-32.23	22.58	X	X
	PEMR4447	Along railway line 8-10km South of Beaufort West	South Africa			X	X
	PEMR4836	20km From Aus Luderitz	Namibia			X	X
	PEMR7256	Swellendam	South Africa			X	X
	PEMR7257	Richtersveldt National Park (Namaqualand)	South Africa			X	X
	PEMR16742	Near Springbok	South Africa	-29.60	18.00	X	X
	PEMR16999	Farm Eselkopvlakte, NWW of Loeriesfontein at trap 1-6	South Africa	-30.94	19.02	X	X
JM 01088	PEMR17635	Port Nolloth Cemetry	South Africa	-29.24	16.87	X	X
WC-0506	PEMR18386	Koppies at Telkom Tower, Groot-Graafwater	South Africa	-31.25	18.52	X	X
H. kelleri							
CMRK 78	PEMR21447	Arusha district.	Tanzania	-3.17	36.68	X	
	PEMR9700	70km SSE Dodoma	Tanzania	-6.90	36.04	X	X
H. nototania							
	PEMR24569	Nyala Lodge, Lengwe National Park	Malawi	-16.22	34.78	X	X
P. mossambicus							
CMRK 71	PEM R21445					X	X
	PEM R12069	KwaZulu-Natal	South Africa	-27.05	32.43	X	X
	PEM R12070	KwaZulu-Natal	South Africa	-27.05	32.43	X	X
	PEM R13203	Moebase Village	Mozambique	-16.98	38.73	X	X
	PEM R13258	Moebase Village	Mozambique			X	X
	PEM R13301	Moebase Village	Mozambique			X	X
	PEM R15486	Marromeu	Mozambique	-18.38	35.88	X	X
	PEM R15487	Malinga Pansi	Mozambique	-18.68	36.10	X	X
	PEM R17178	Chingola, Oppenheimer drive	Zambia	-12.54	27.86		X
Z08	PEM R18884	Kalumbila Mine	Zambia	-12.24	25.34	X	X

						X	X
Ps. variabilis							
CMRK 413	PEM R22922	Undzungwa Mountains	Tanzania	-8.28	35.90	X	X
CMRK 414	PEM R23969	Undzungwa Mountains	Tanzania	-8.28	35.90	X	
CMRK 416	PEM R23955	Nyika plateau	Malawi	-10.60	33.80		X
CMRK 441	PEM R23962	Zomba Plateau	Malawi	-15.28	35.32	X	X
CMRK 442	PEM R23963	Zomba Plateau	Malawi	-15.28	35.32	X	X
CMRK 444	PEM R23965	Zomba Plateau	Malawi	-15.28	35.32	X	X
CMRK 445	PEM R23966	Zomba Plateau	Malawi	-15.28	35.32	X	X
CMRK 446	PEM R23967	Zomba Plateau	Malawi	-15.28	35.32	X	X
CMRK M01	PEM R23968	Mulajne Massif	Malawi	-15.92	35.63	X	X
	PEM R12591	Nyika Plateau	Malawi	-10.61	33.83	X	X
	PEM R12604	Trausherbler	Malawi			X	X
	PEM R21939	Mt Namuli	Mozambique	-15.39	37.05	X	X
WC-3287/MOZ14-192	PEM R21186	Mt Namuli	Mozambique	-15.39	37.05	X	X
WC-0210	PEM R18522	Mulajne Massif	Malawi	-15.90	35.65	X	X
R. rostratus							
	PEM R934	Komatiepoort, Mpumalanga	South Africa	-25.44	31.94	X	X
	PEM R935	Komatiepoort, Mpumalanga	South Africa	-25.44	31.94	X	
	PEM R936	Musina	South Africa	-22.39	30.06	X	X
	PEM R1154		Tanzania			X	X
	PEM R6433	Nkhotakota Village	Malawi	-12.93	34.28	X	X
	PEM R7265	Farm Uitenpas, Messina	South Africa	-22.28	30.07		X
	PEM R13209	Moebase Village	Mozambique	-16.98	38.73	X	X
	PEM R13216	Moebase Village	Mozambique	-17.05	38.80	X	X
	PEM R13225	Namagure Village	Mozambique	-16.96	38.69	X	X
	PEM R13312	Moebase Village	Mozambique	-16.98	38.73	X	X
P. crucifer							
WC-5542	PEMR23112	Plains of Camdeboo, hike up saddle	South Africa	-32.54	25.22	X	X
WC-5488	PEMR23110	Alstonfield, point site	South Africa	-32.89	26.00	X	X

WC-5043	PEMR22570	Mpofu Nature Reserve	South Africa	-32.61	26.58	X	X
						X	X
	PEMR24866	Ongeluksnek NR, trap 1	South Africa	-30.33	28.36	X	X
	PEMR24848	Ongeluksnek NR, enroute to Bush Camp	South Africa	-30.30	28.37	X	X
No. 677	PEMR1609	Swartberg Pass (Oudtshoorn)	South Africa			X	X
	PEMR6603	10,7km East of Swartberg Pass (Prince Albert)	South Africa	-33.33	22.10	X	
	PEMR16385	5km N Blaawbergstrand	South Africa	-33.74	18.44	X	
		Honeydew	South Africa			X	X
CMRK 203	PEMR21479	Nyanga National Park.	Zimbabwe	-18.24	32.77	X	X
	PEMR16403	Monk's Cowl	South Africa	-29.06	29.40	X	X
CMRK 214	PEMR21482	Nyanga National Park.	Zimbabwe	-18.30	32.71	X	X

Table S2.3: Results of the HSD post-hoc tests for the principal component analyses (PC) for the dorsal (DC) and lateral (LC) view of the heads. The difference values (diff.) and the p-values (p-value) are shown. Significance ($p \leq 0.05$) is indicated with bold font.

Genera	DC-PC1		DC-PC2		DC-PC3		LC-PC1		LC-PC2		LC-PC3	
	diff.	p-value	diff.	p-value	diff.	p-value	diff.	p-value	diff.	p-value	diff.	p-value
Hemirhagerrhis - Dipsina	**0.052**	**0.003**	**-0.048**	**0.004**	**0.054**	**0.000**	**0.101**	**0.000**	-0.001	1.000	0.001	1.000
Psammophis - Dipsina	**0.096**	**0.000**	**0.026**	**0.041**	**0.048**	**0.000**	**0.107**	**0.000**	**-0.056**	**0.000**	**-0.036**	**0.001**
Psammophylax - Dipsina	**0.047**	**0.000**	**-0.042**	**0.000**	**0.019**	**0.000**	**0.086**	**0.000**	**-0.068**	**0.000**	0.009	0.867
Rhamphiophis - Dipsina	**-0.089**	**0.000**	-0.015	0.535	**0.052**	**0.000**	**-0.068**	**0.000**	**-0.096**	**0.000**	-0.017	0.443
P. crucifer - Dipsina	**0.083**	**0.000**	**-0.052**	**0.000**	**0.040**	**0.000**	**0.113**	**0.000**	**-0.081**	**0.000**	0.015	0.518
Psammophis - Hemirhagerrhis	**0.045**	**0.014**	**0.074**	**0.000**	-0.006	0.913	0.005	1.000	**-0.056**	**0.016**	-0.037	0.151
Psammophylax - Hemirhagerrhis	-0.004	0.999	0.007	0.995	**-0.035**	**0.000**	-0.015	0.964	**-0.067**	**0.002**	0.008	0.995
Rhamphiophis - Hemirhagerrhis	**-0.141**	**0.000**	0.034	0.093	-0.002	0.999	**-0.170**	**0.000**	**-0.095**	**0.000**	-0.018	0.844
P. crucifer - Hemirhagerrhis	0.031	0.153	-0.004	1.000	-0.014	0.203	0.012	0.989	**-0.080**	**0.000**	0.013	0.947
Psammophylax - Psammophis	**-0.049**	**0.000**	**-0.068**	**0.000**	**-0.029**	**0.000**	-0.021	0.342	-0.011	0.794	**0.045**	**0.000**
Rhamphiophis - Psammophis	**-0.186**	**0.000**	**-0.040**	**0.000**	0.004	0.943	**-0.175**	**0.000**	**-0.039**	**0.002**	0.019	0.264
P. crucifer - Psammophis	-0.014	0.592	**-0.078**	**0.000**	-0.008	0.379	0.007	0.989	-0.025	0.084	**0.051**	**0.000**
Rhamphiophis - Psammophylax	**-0.137**	**0.000**	**0.027**	**0.015**	**0.033**	**0.000**	**-0.154**	**0.000**	**-0.028**	**0.042**	**-0.026**	**0.040**
P. crucifer - Psammophylax	**0.036**	**0.000**	-0.010	0.736	**0.021**	**0.000**	0.027	0.100	-0.014	0.616	0.006	0.982
P. crucifer - Rhamphiophis	**0.172**	**0.000**	**-0.038**	**0.000**	-0.012	0.054	**0.182**	**0.000**	0.014	0.674	**0.032**	**0.010**

Appendix B: Chapter Three

Figures

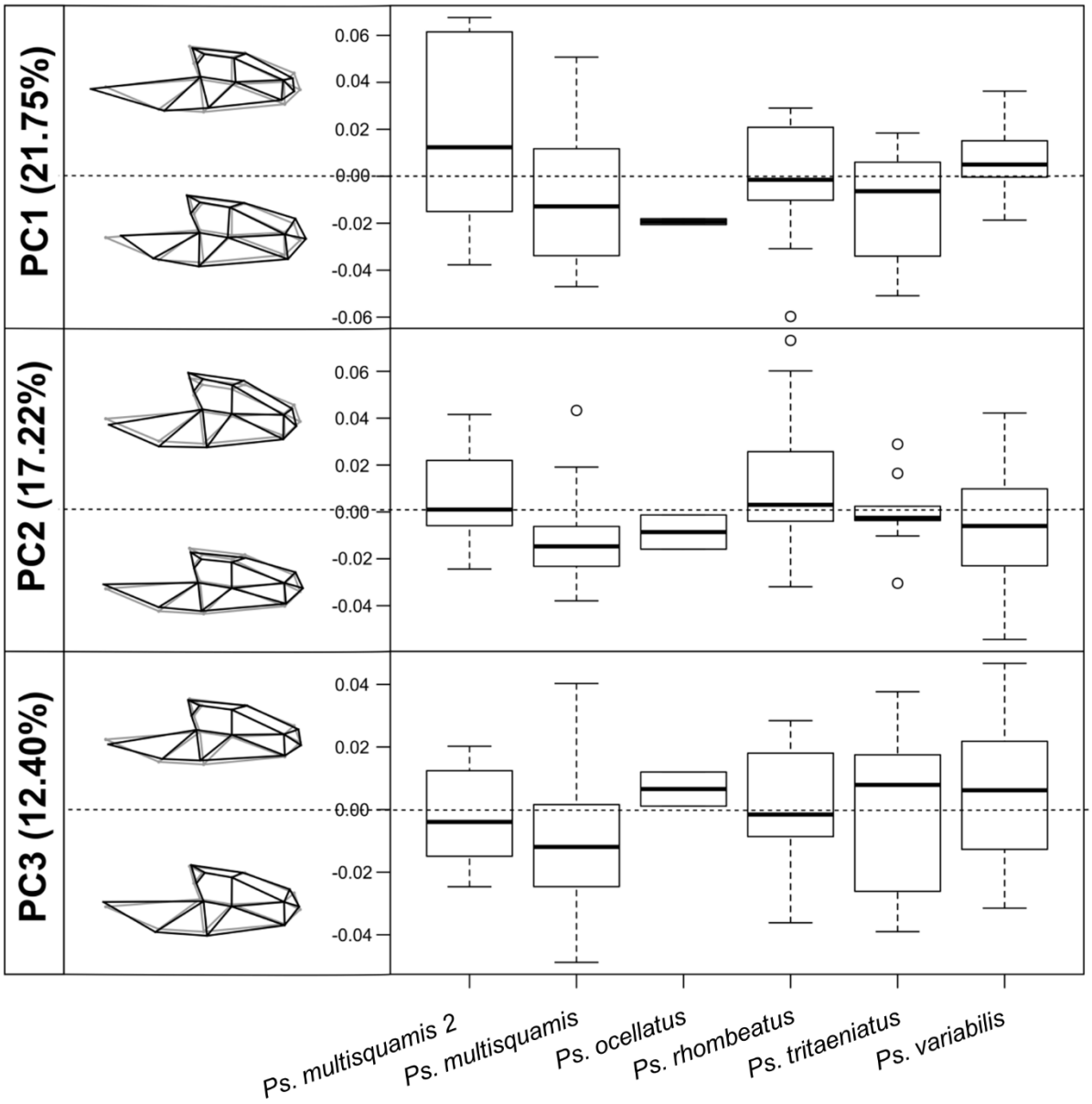

Figure S3.1: Geometric morphometric analyses of the lateral view of the heads of *Psammophylax*. Warped outline diagrams to the left of the boxplots of the principal component scores for the first three PC axes represent the shape changes at the positive and negative extremes of each axis. Boxplots show the median values (thick central line), upper and lower quartiles (box edges), and the highest and lowest values (error bars), excluding the outliers (circles).

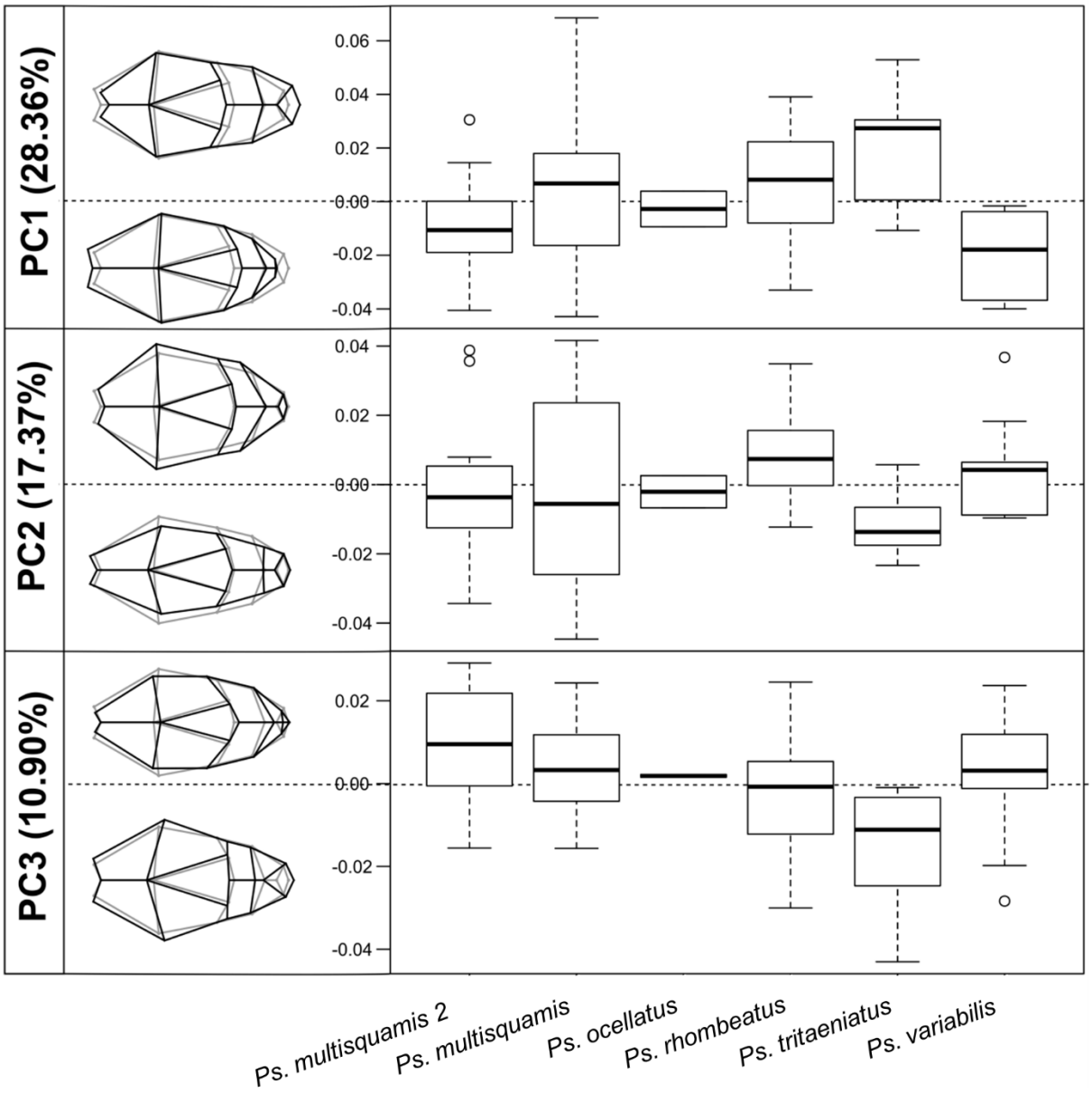

Figure S3.2: Geometric morphometric analyses of the dorsal view of the heads of *Psammophylax*. Warped outline diagrams to the left of the boxplots of the principal component scores for the first three PC axes represent the shape changes at the positive and negative extremes of each axis. Boxplots show the median values (thick central line), upper and lower quartiles (box edges), and the highest and lowest values (error bars), excluding the outliers (circles).

Tables

Table S3.1**:** List of specimens used for genetic analyses, and the GenBank Accession Numbers for each gene marker (cytb = cytochrome b; ND4+LeutRNA = NADH dehydrogenase subunit 4 + Leucine transfer RNA; c-mos = oocyte maturation factor). Collections abbreviations: WC = Werner Conradie, PEM = Port Elizabeth Museum, PVP = Pedro Vaz Pinto, CMRK = Christopher Kelly, NB = Ninda Baptista, UTEP = University of Texas at El Paso Biodiversity Collections, ZMUC = Zoological Museum University of Copenhagen. Dataset (3.) denotes which specimens were present in which dataset, specific to Chapter Three. Not Available = NA.

Field Number	Museum Number	Locality		Coordinates		Dataset (3.)	Genbank Accession Numbers		
		Region	Country	Lat	Long		cytb	ND4+LeutRNA	c-mos
Ingroups									
Kladirostratus a. acutus **comb. nov.** (*Psammophylax acutus acutus*)									
WC-3540	PEM R21485	Luissinga River	Angola	-14.6	18.17	1,3	LR213493	LR213550	LR213470
WC-4018	PEM R23288	Cuanavale River Source	Angola	-13.09	18.89	1,3	LR213494	LR213551	LR213471
WC-4149	PEM R23315	Cuito River Source	Angola	-12.66	18.35	1,3	LR213495	LR213552	LR213472
WC-4715	PEM R23476	Kembo River Source	Angola	-13.14	19.04	1,3	LR213496	LR213553	LR213473
WC-4778	PEM R23449	Cuando River Source	Angola	-13,00	19.14	1,3	LR213497	LR213554	LR213474
PVP 92		20km S. of Lucas	Angola	-11.07	16.17	1,3	LR213498	LR213555	LR213475
PEM R13485	PEM R13485	Luzamba	Angola	-9.12	18.06	1,3	DQ486464	DQ486300	NA
CMRK 378		Gitaba	Burundi	-3.85	29.98	1,3	DQ486425	DQ486262	DQ486192
Psammophylax kellyi **sp. nov.** (*Psammophylax multisquamis 2*)									
CMRK 296	PEM R23924	Arusha	Tanzania	-3.17	36.68	1,2,3	LR213510	LR213567	NA
CMRK 328	PEM R23925	Arusha	Tanzania	-3.17	36.68	1,2,3	LR213511	LR213568	NA
CMRK 333	PEM R23930	Arusha	Tanzania	-3.15	36.69	1,2	NA	LR213569	NA
CMRK 401	PEM R23926	Arusha	Tanzania	-3.17	36.68	1,2,3	LR213517	LR213575	NA
CMRK 402	PEM R23927	Arusha	Tanzania	-3.17	36.68	1,3	LR213518	LR213576	NA
CMRK 405	PEM R23929	Ngorongoro	Tanzania	-3.22	35.48	1,2,3	LR213520	LR213578	NA
CMRK 404	PEM R23928	Ngorongoro	Tanzania	-3.23	35.41	1,2,3	DQ486437/ LR213503	DQ486273	NA
Psammophylax multisquamis									
CMRK 149		Naivasha	Kenya	-0.74	36.45	1,2,3	LR213507	LR213561	NA
CMRK 150		Naivasha	Kenya	-0.74	36.45	1,2,3	LR213508	LR213562	NA
CMRK 151		Naivasha	Kenya	-0.74	36.45	1,2	NA	LR213563	NA

CMRK 152	PEM R23923	Naivasha	Kenya	-0.74	36.45	1,2,3	LR213509	LR213564	NA
CMRK 153		Naivasha	Kenya	-0.74	36.45	1	NA	LR213565	LR213480
CMRK 154		Naivasha	Kenya	-0.74	36.45	1	NA	LR213566	NA
CMRK 357	PEM R22903	Ethiopian Plateau	Ethiopia	9.33	38.92	1,3	LR213512	LR213570	NA
CMRK 359	PEM R23844	Ethiopian Plateau	Ethiopia	9.33	38.92	1,3	LR213513	LR213571	NA
CMRK 360	PEM R23920	Ethiopian Plateau	Ethiopia	9.33	38.92	1,3	LR213514	LR213572	NA
CMRK 362	PEM R23921	Ethiopian Plateau	Ethiopia	9.33	38.92	1,2,3	LR213515	LR213573	NA
CMRK 363	PEM R23922	Ethiopian Plateau	Ethiopia	9.33	38.92	1,3	LR213516	LR213574	NA
CMRK 361	PEM R22919	Ethiopian Plateau	Ethiopia	9.33	38.92	1,2,3	DQ486421	DQ486258	DQ486191
Psammophylax ocellatus									
KTH09-064	PEM R17986	Zootecnica. Humpata	Angola	-15.03	13.37	1,2,3	LR213506	LR213560	LR213479
NB 171		Tundavala	Angola	-14.82	13.4	1,2,3	LS992120	LS992135	LS992105
NB 491		Tundavala	Angola	-14.81	13.4	1,2,3	LS992121	LS992136	LS992106
NB 492		Tundavala	Angola	-14.81	13.4	1,2,3	LS992122	LS992131	LS992107
NB 561	PEM R16270	Tundavala	Angola	-14.81	13.4	1,3	LS992124	LS992133	LS992109
NB 585		Tundavala	Angola	-14.81	13.4	1,3	LS992125	LS992128	LS992110
NB 586		Tundavala	Angola	-14.81	13.4	1,2,3	LS992126	LS992129	LS992111
Psammophylax rhombeatus									
WC-3693	PEM R21883	Oviston	RSA	-30.73	25.75	1,2,3	TBA	TBA	TBA
WC-1272	PEM R20527	Baviaanskloof East	RSA	-33.68	24.31	1,2,3	TBA	TBA	NA
ARD00092		Port Elizabeth	RSA	-34.01	25.66	1,2,3	TBA	TBA	TBA
TP2		Mooi Rivier	RSA	-29.19	30.08	1,2,3	TBA	TBA	TBA
WC-5094	PEM R22610	Karoo NP	RSA	-32.28	22.33	1,2,3	LS992116	LS992137	LS992103
CK2		Cederberg	RSA	-32.86	19.44	1,2,3	TBA	TBA	TBA
RS1		Oudtshoorn	RSA	-33.48	22.24	1,2,3	TBA	TBA	TBA
AC1		Napier	RSA	-34.48	19.92	1,2,3	TBA	TBA	TBA
LK2		Wakkerstroom	RSA	-27.36	30.11	1,2,3	TBA	TBA	TBA
EI_0534		Woodbush Forest Reserve	RSA	-23.80	29.95	1,2,3	TBA	TBA	TBA
SAJ30		Vanderbijlpark	RSA	-26.72	27.81	1,2,3	TBA	TBA	TBA
TP3		Golden Gate National Park	RSA	-28.51	28.63	1,2,3	TBA	TBA	TBA
Ck6		Koeberg	RSA	-33.62	18.41	1,2,3	TBA	TBA	TBA
DM1		Alexander Bay	RSA	-28.61	16.49	1,2,3	TBA	NA	TBA
TB1		Calvinia	RSA	-31.48	19.77	1,2,3	TBA	TBA	NA
CKD13		Lamberts Bay	RSA	-32.09	18.32	1,2,3	TBA	TBA	TBA

Psammophylax tritaeniatus									
MB 21435		Gelukspan	RSA	-26.22	25.66	1,2,3	LR213499	LR213556	LR213476
PVP 15	PEM R22075	Lubango	Angola	-14.87	13.48	1,2,3	LR213500	NA	NA
PVP 59	PEM R22076	Lubango	Angola	-14.87	13.48	1,2,3	LR213501	NA	LR213477
PVP 97		Huambo	Angola	-12.73	15.78	1,2,3	LR213502	LR213557	LR213478
ZMUC R970215	ZMUC R970215	Manyoni	Tanzania	-5.52	35.21	1,2,3	DQ486451	DQ486287	NA
CMRK 279	PEM R22921	Mvuma	Zimbabwe	-19.53	30.73	1,2,3	DQ486414	DQ486252	DQ486190
Kal		Kalakundi Fragment	DRC	-10.64	25.93	1,2,3	LR213541	LR213599	NA
LK3		Limpopo	RSA	-23.03	29.66	1,2,3	LR213542	LR213600	NA
Psammophylax variabilis									
EBG 3006	UTEP 21871	Marungu Plateau	DRC	-7.72	29.76	1,2,3	LR213486	LR213543	LR213463
EBG 2943	UTEP 21870	Marungu Plateau	DRC	-7.71	29.78	1,2,3	LR213487	LR213544	LR213464
EBG 2890	UTEP 21869	Marungu Plateau	DRC	-7.62	29.79	1,3	LR213488	LR213545	LR213465
EBG 2611	UTEP 21868	Lendu Plateau	DRC	2.01	30.84	1,2,3	LR213489	LR213546	LR213466
EBG 2425	UTEP 21867	Lendu Plateau	DRC	2.01	30.83	1,3	LR213490	LR213547	LR213467
MOZ14-192	PEM R21186	Mount muli	Mozambique	-15.39	37.05	1,2,3	LR213491	LR213548	LR213468
IPMBJ296		Gishubi	Burundi	-3.52	29.91	1,2,3	NA	FJ404328	AF544709
CMRK 413	PEM R22922	Udzungwa Mountains	Tanzania	-8.28	35.9	1,2,3	EU526863	EU526859	NA
CMRK 403	PEM R23970	Crater Highlands	Tanzania	-3.23	35.48	1,2,3	LR213519	LR213577	LR213481
CMRK 414	PEM R23969	Udzungwa Mountains	Tanzania	-8.28	35.9	1,2,3	LR213521	LR213579	NA
J10		Udzungwa Mountains	Tanzania	-8.28	35.9	1,2,3	LR213535	LR213593	NA
J11		Udzungwa Mountains	Tanzania	-8.28	35.9	1,2,3	LR213536	LR213594	NA
J12		Udzungwa Mountains	Tanzania	-8.28	35.9	1,2,3	LR213537	LR213595	NA
J8		Udzungwa Mountains	Tanzania	-8.28	35.9	1,3	LR213538	LR213596	NA
J9		Udzungwa Mountains	Tanzania	-8.28	35.9	1,3	LR213539	LR213597	NA
QP060	PEM R18522	Mulanje Massif	Malawi	-15.9	35.65	1,2,3	LR213492	LR213549	LR213469
M01	PEM R23968	Mulanje Massif	Malawi	-15.92	35.63	1,2,3	LR213540	LR213598	NA
GB3		Mulanje Massif	Malawi	-15.92	35.65	1,2	AY235724	NA	NA
CMRK 415	PEM R23954	Nyika Plateau	Malawi	-10.6	33.8	1,2,3	LR213522	LR213580	NA
CMRK 416	PEM R23955	Nyika Plateau	Malawi	-10.6	33.8	1,2,3	LR213523	LR213581	NA
CMRK 417	PEM R23956	Nyika Plateau	Malawi	-10.6	33.8	1,2,3	LR213524	LR213582	NA
CMRK 418	PEM R23957	Nyika Plateau	Malawi	-10.6	33.8	1,3	LR213525	LR213583	NA
CMRK 419	PEM R23958	Nyika Plateau	Malawi	-10.6	33.8	1,3	LR213526	LR213584	NA
CMRK 420	PEM R23959	Nyika Plateau	Malawi	-10.6	33.8	1,3	LR213527	LR213585	NA

CMRK 421	PEM R23960	Nyika Plateau	Malawi	-10.6	33.8	1,3	LR213528	LR213586	NA
CMRK 422	PEM R23961	Nyika Plateau	Malawi	-10.6	33.8	1,3	LR213529	LR213587	NA
CMRK 441	PEM R23962	Zomba Plateau	Malawi	-15.28	35.32	1,2,3	DQ486438	DQ486274	DQ486193
CMRK 442	PEM R23963	Zomba Plateau	Malawi	-15.28	35.32	1,2,3	LR213530	LR213588	NA
CMRK 443	PEM R23964	Zomba Plateau	Malawi	-15.28	35.32	1,3	LR213531	LR213589	NA
CMRK 444	PEM R23965	Zomba Plateau	Malawi	-15.28	35.32	1,2,3	LR213532	LR213590	NA
CMRK 445	PEM R23966	Zomba Plateau	Malawi	-15.28	35.32	1,3	LR213533	LR213591	NA
CMRK 446	PEM R23967	Zomba Plateau	Malawi	-15.28	35.32	1,3	LR213534	LR213592	NA
Outgroups									
Hemirhagerrhis kelleri									
CMRK396		Tanzania				3	DQ486434	DQ486271	
CMRK78	PEM R21447	Arusha district	Tanzania	-3.17	36.68	3	DQ486372	DQ486211	
CMRK400	PEM R22889	Kingori	Tanzania	-3.28	36.98	3	DQ486436	DQ486272	
CMRK77	PEM R21446	Kingori	Tanzania	-3.28	36.98	1,3	DQ486335	DQ486311	DQ486159
Hemirhagerrhis viperina									
CAS(AMB5989)		Okangwati	Namibia	−17.07	13.27	1	DQ486453	DQ486289	
Mimophis mahafalensis									
PEM2		Tulear District	Madagascar			3	DQ486461	DQ486297	
Mim_mad/ZSM 397/2000		Mount Ibity	Madagascar			3	AY188031		AY187992
24_str		Mount Ibity	Madagascar			3	DQ486440	DQ486276	
Mim_mah/ HLMD J68		Kirindy	Madagascar			3	AY188032	FJ404321	AY187993
Mimophis occultus									
23		Mont. des Francais	Madagascar			1	DQ486363	DQ486202	AY187993
Psammophis crucifer									
CMRK19	PEM R22905	Somerset East	RSA	-32.72	25.58	3	DQ486360	DQ486199	
CMRK70	PEM R21444	Jeffrey's Bay	RSA	-33.94	24.99	1,3	DQ486334	DQ486310	DQ486158
CMRK203	PEM R21479	Nyanga	Zimbabwe	-18.24	32.77	3	DQ486397	DQ486236	DQ486188
CMRK214	PEM R21482	Nyanga National Park	Zimbabwe	-18.30	32.71	3	DQ486398	DQ486237	
Rhamphiophis rostratus									
CMRK80	PEM R21449	Dodoma Region	Tanzania	-6.18	35.75	3	DQ486336	DQ486312	
CMRK185	PEM R21472	Bubye River	Zimbabwe	-21.70	30.51	1,3	DQ486394	DQ486233	DQ486187
FN 1400/IPMB J408	PEM R13209	Northern Moebase Village	N.Mozambique	-16.98	38.73	3	AY612079	FJ404329	AY611988

W19/WC-DNA-1185	Tenge campe. east of Revubo River	Mozambique	-15.72	33.78	3	TBA	TBA	TBA
Rhamphiophis rubropunctatus								
CMRK303	Kilimanjaro Airport	Tanzania	-3.43	37.07	3	DQ486417		
Vidal2008_4					3	FJ404310	FJ404330	FJ404232

Table S3. 2**:** List of Specimens used in the morphometric analyses. The X's refer to samples used in the family (intergeneric comparisons) and genus (interspecific comparisons) analyses, with the lateral (LC) and dorsal (DC) view of the head. The phylogeny column (In Phyl. Tree) denotes samples used in the phylogenetic tree (Fig. 3.4), and subsequent molecular analyses. Collection abbreviations: PEM = Port Elizabeth Museum, CMRK = Christopher Kelly, FMNH = Field Museum of Natural History, AMNH = American Museum of Natural History, LACM = Natural History Museum of Los Angeles County and MCZ = Museum of Comparative Zoology. Not Available = NA.

Museum Number	Locality		Coordinates		Family		Genus		In Phyl. Tree
	Region	Country	Lat	Long	DC	LC	DC	LC	
Ingroup									
Kladirostratus a. acutus **comb. nov.** (*Psammophylax acutus acutus*)									
PEM R6161	Sakeji, North-Western	Zambia	-11.23	24.32	X	X			
PEM R6154	Sakeji, North-Western	Zambia	-11.23	24.32	X	X			
PEM R6158	Sakeji, North-Western	Zambia	-11.23	24.32	X	X			
PEM R6160	Sakeji, North-Western	Zambia	-11.23	24.32	X	X			
PEM R6159	Sakeji, North-Western	Zambia	-11.23	24.32	X	X			
PEM R6163	Sakeji, North-Western	Zambia	-11.23	24.32	X	X			
PEM R6164	Sakeji, North-Western	Zambia	-11.23	24.32	X	X			
PEM R6156	Sakeji, North-Western	Zambia	-11.23	24.32	X	X			
PEM R6165	Sakeji, North-Western	Zambia	-11.23	24.32	X	X			
PEM R6166	Sakeji, North-Western	Zambia	-11.23	24.32	X	X			
PEM R13485	Cvabgo River	Angola	-9.12	18.05		X			
PEM R23459	Kembo River source	Angola	-13.14	19.05	X	X			
PEM R23435	Cuando River source	Angola	-13.00	19.14	X	X			
PEM R23450	Cuando River source	Angola	-13.00	19.14	X	X			
Kladirostratus a. jappi **comb. nov**. (*Psammophylax acutus jappi*)									
FMNH 133045	Kalabo	Zambia	-14.99	22.67	X	X			
FMNH 134243	Kalabo	Zambia	-14.99	22.67	X	X			
Kladirostratus togoensis **comb. nov.** (*Psammophylax acutus togoensis*)									
FMNH 58328	Equatoria	Sudan	4.98	30.85	X				
Psammophylax kellyi **sp. nov.** (*Psammophylax multisquamis 2*)									
PEM R23924	Arusha	Tanzania	-3.17	36.68	X	X	X	X	X
CMRK 297	Arusha	Tanzania	-3.17	36.68	X	X	X	X	
PEM R23930	Arusha	Tanzania	-3.15	36.69	X	X	X	X	X
PEM R23926	Arusha	Tanzania	-3.17	36.68	X	X	X	X	X
PEM R23927	Arusha	Tanzania	-3.17	36.68	X	X	X	X	X
PEM R23928	Ngorongoro	Tanzania	-3.23	35.41	X	X	X		X
PEM R23929	Ngorongoro	Tanzania	-3.22	35.48	X	X	X	X	X
LACM 35664	East Side	Tanzania	-3.58	35.83	X	X	X	X	
AMNH R50585	NA	Tanzania	NA	NA	X	X	X	X	
AMNH R60037	NA	Tanzania	NA	NA	X	X	X	X	
FMNH 35303	NA	Tanzania	NA	NA	X	X	X	X	
Psammophylax multisquamis									
PEM R23844	Ethiopian Plateau	Ethiopia	9.33	38.92	X	X	X	X	X
ADDIT5	NA	NA	NA	NA	X	X	X	X	
PEM R23923	Kenyan Rift	Kenya	-0.74	36.45	X	X	X	X	X
PEM R22919	Ethiopian Plateau	Ethiopia	9.33	38.92	X	X	X	X	X

PEM R23921	Ethiopian Plateau	Ethiopia	9.33	38.92	X	X	X	X	X
PEM R23922	Ethiopian Plateau	Ethiopia	9.33	38.92	X	X	X	X	X
PEM R23920	Ethiopian Plateau	Ethiopia	9.33	38.92	X	X	X	X	X
PEM R23844	Ethiopian Plateau	Ethiopia	9.33	38.92	X	X	X	X	
AMNH R16898	NA	Kenya	NA	NA	X	X	X	X	
AMNH R16899	NA	Kenya	NA	NA	X	X	X	X	
AMNH R37894	NA	Ethiopia	NA	NA	X	X	X	X	
AMNH R37895	NA	Ethiopia	NA	NA	X	X	X	X	
AMNH R88619	Nyeri	Kenya	NA	NA	X	X	X	X	
FMNH 58339	Rift Valley	Kenya	NA	NA	X	X		X	
FMNH 79148	NA	Kenya	NA	NA	X	X	X	X	
FMNH 79150	NA	Kenya	NA	NA	X	X	X	X	
FMNH 79151	NA	Kenya	NA	NA	X	X	X	X	
MCZ R29430	Lake Nawaska	Kenya	NA	NA	X	X	X	X	
MCZ R29431	Guaro Nyiro	Kenya	NA	NA		X		X	
MCZ R29432	Makueni	Kenya	-2.68	38.17	X	X	X	X	
Psammophylax ocellatus									
PEM R16270	Tundavala	Angola	-14.81	13.40	X	X	X	X	X
PEM R17986	Zootecnica, Humpata	Angola	-14.91	13.30	X	X	X		
Psammophylax rhombeatus									
PEM R6505	Cookhouse, Eastern Cape	RSA	-32.77	25.87	X	X	X	X	
PEM R6798	Port Elizabeth, Eastern Cape	RSA	-33.90	25.56	X	X	X	X	
PEM R7051	Maclear, Eastern Cape	RSA	-31.13	28.13	X	X	X	X	
PEM R7287	East London, Eastern Cape	RSA	-32.97	27.83	X	X	X		
PEM R7721	Graaf-Reinett, Eastern Cape	RSA	-32.25	24.50	X	X		X	
PEM R7770	Port Elizabeth, Eastern Cape	RSA	-33.93	25.42	X	X	X	X	
PEM R12909	Koudow, Western Cape	RSA	-33.60	23.33	X	X	X	X	
PEM R16387	East London, Eastern Cape	RSA	-33.68	18.44	X	X	X	X	
PEM R17275	Lamberts Bay, Western Cape	RSA	-32.17	18.32	X	X			
PEM R19012	Hogsback, Eastern Cape	RSA	-32.57	26.93	X	X	X	X	
PEM R20527	Baviaanskloof, Eastern Cape	RSA	-33.68	24.31	X	X	X	X	
PEM R20533	Baviaanskloof, Eastern Cape	RSA	-33.68	24.31	X	X	X	X	
PEM R21098	Thomas River, Eastern Cape	RSA	-32.44	27.29	X	X	X	X	
PEM R22664	Nquadu, Eastern Cape	RSA	-31.41	28.73	X	X	X	X	
PEM R22808	Port Elizabeth, Eastern Cape	RSA	-33.98	25.51	X	X	X	X	
Psammophylax tritaeniatus									
PEM R1333	Bulawayo Hillside	Zimbabwe	20.20	28.60	X	X	X	X	
PEM R1980	Mbala Abercorn	Zambia	-8.85	31.36	X	X	X	X	
PEM R4116	Mafikeng, North West	RSA	-25.85	25.64	X	X	X	X	
PEM R6149	Sakeji, North-Western	Zambia	-11.23	24.32	X	X	X		
PEM R6150	Sakeji, North-Western	Zambia	-11.23	24.32	X	X	X		
PEM R6151	Sakeji, North-Western	Zambia	-11.23	24.32	X	X	X	X	

PEM R7133	Chingola Oppenheimer dr	Zambia	-12.57	27.88	X	X	X	X	
PEM R17203	Chingola	Zambia	-12.54	27.86	X	X	X	X	
PEM R17451	Kalakundi, Katanga	DRC	-10.64	25.93	X	X	X	X	
PEM R18276	Rhamokgwabne	Botswana	-20.92	27.61		X		X	
PEM R21083	Lykso, North West	RSA	-27.09	24.01	X	X	X	X	
Psammophylax variabilis									
PEM R22922	Udzungwa Mountains	Tanzania	-8.28	35.90	X	X	X	X	X
PEM R23969	Udzungwa Mountains	Tanzania	-8.28	35.90	X	X	X	X	X
PEM R23955	Nyika plateau	Malawi	-10.60	33.80	X	X	X	X	X
PEM R23962	Zomba Plateau	Malawi	-15.28	35.32	X	X	X	X	X
PEM R23963	Zomba Plateau	Malawi	-15.28	35.32	X	X	X	X	X
PEM R23965	Zomba Plateau	Malawi	-15.28	35.32	X	X	X	X	X
PEM R23966	Zomba Plateau	Malawi	-15.28	35.32	X	X	X	X	X
PEM R23967	Zomba Plateau	Malawi	-15.28	35.32	X	X	X	X	X
PEM R23968	Mulajne Massif	Malawi	-15.92	35.63	X	X	X	X	X
PEM R12591	Nyika Plateau	Malawi	-10.61	33.83	X	X		X	
PEM R12604	Trausherbler	Malawi	NA	NA	X	X	X		
PEM R21939	Mt Namuli	Mozambique	-15.39	37.05	X	X	X	X	
PEM R21186	Mt Namuli	Mozambique	-15.39	37.05	X	X	X	X	
PEM R18522	Mulanje Massif	Malawi	-15.90	35.65	X	X	X	X	
Outgroups									
Psammophis mossambicus									
PEM R21445	Mpika	Zambia	-11.83	31.44	X	X			
PEM R12069	Tembe Elephant Park, KwaZulu-Natal	RSA	-27.05	32.43	X	X			
PEM R12070	Tembe Elephant Park, KwaZulu-Natal	RSA	-27.05	32.43	X	X			
PEM R13203	Moebase Village	Mozambique	-16.98	38.73	X	X			
PEM R13258	Moebase Village	Mozambique	-16.98	38.73	X	X			
PEM R13301	Moebase Village	Mozambique	-16.98	38.73	X	X			
PEM R15486	Marromeu	Mozambique	-18.38	35.88	X	X			
PEM R15487	Malinga Pansi	Mozambique	-18.68	36.10	X	X			
PEM R17178	Chingola, Oppenheimer dr	Zambia	-12.54	27.86	X	X			
PEM R18884	Kalumbila Mine	Zambia	-12.24	25.34	X	X			
Rhamphiophis rostratus									
PEM R934	Komatiepoort, Mpumalanga	RSA	-25.44	31.94	X	X			
PEM R935	Komatiepoort, Mpumalanga	RSA	-25.44	31.94	X	X			
PEM R936	Musina, Limpopo	RSA	-22.39	30.06	X	X			
PEM R1154	NA	Tanzania	NA	NA	X	X			
PEM R6433	Nkhotakota Village	Malawi	-12.93	34.28	X	X			
PEM R7265	Farm Uitenpas, Limpopo	RSA	-22.28	30.07		X			
PEM R13209	Moebase Village	Mozambique	-16.98	38.73	X	X			
PEM R13216	Moebase Village	Mozambique	-17.05	38.80	X	X			
PEM R13225	Namagure Village	Mozambique	-16.96	38.69	X	X			
PEM R13312	Moebase Village	Mozambique	-16.98	38.73	X	X			

Table S3.3: Measurements and scalation data of *Psammophylax kellyi* **sp. nov.** SVL - snout-vent length, PEM - Port Elizabeth Museum, AMNH - American Museum of Natural History, UMMZ - University of Michigan Museum of Zoology. Not Available = NA.

Museum number	PEM R23926	PEM R23927	PEM R23928	PEM R23924	PEM R23925	PEM R23930	PEM R23929	CMRK297	AMNH 50585	AMNH 60037	Boulenger 1896:140	UMMZ 61233
Type status	Holotype	Paratype	Paratype	Paratype	Paratype	Paratype	paratype	Additional	Additional	Additional	Additional	Additional
Locality	Arusha	Arusha	Ngorongoro	Arusha	Arusha	Oldonyo Sambu	Ngorongoro	Arusha	Tindi	"Northern Tanganyika"	Mpwapwa	Arusha
Sex	Female	Female	Female	Female	Juvenile	Female	NA	NA	Male	Female	Female	Female
Midbody scale rows	17–17–13	17–17–13	17–17–13	17–17–13	17–17–13	17–17–13	17–17–13	17–17–13	NA	17–17–13	NA	17–17–13
Ventrals	171	173	172	171	176	169	170	NA	161	164	165	174
Subcaudals	60	64	63	63	NA	60	65	NA	61	58+	66	62
Anal scale	D	D	D	D	D	D	D	D	D	D	NA	D
Upper labials (touching orbit)	8 (4-5)	8 (4-5)	8 (4-5)	8 (4-5)	8 (4-5)	8 (4-5)	8 (4-5)	8 (4-5)	8 (4-5)	8 (4-5)	NA	8 (4-5)
Lower labials (touching anterior sublinguals)	11(5)	11(5)	11(4/5)	11(5)	11(5)	12/11(6/5)	11(5)	11(5)	12 (6)	11 (5)	NA	11(5)
Preocular	1	1	2	1	1	1	1	1	1	1	NA	1
Postocular	2	2	2	2	2	2	2	2	2	2	NA	2
Temporals	2+3	2+1/2+3	2+3	2+3/2+2	2+3/1+3	2+3	2+3	2+3	2+3	2+4	NA	2+3
SVL Length (mm)	685	626	520	744	237	433	273	NA	480	615	NA	590
Tail Length (mm)	161	137	131	168	58	102	62	NA	121	142	NA	133
Total Length (mm)	846	763	651	912	295	535	335	NA	601	757	NA	723

Table S3.4: Results of the HSD post-hoc tests for the principal component analyses (PC) for the dorsal (DC) and lateral (LC) view of the heads. The difference values (diff.) and the p-values (p-value) are shown. Significance ($P \leq 0.05$) is indicated with bold font.

	DC-PC1		DC-PC2		DC-PC3		LC-PC1		LC-PC2		LC-PC3	
	diff.	p-value	diff.	p-value	diff.	p-value	diff.	p-value	diff.	p-value	diff.	p-value
Genera												
Kladirostratus – Psammophis	**-0.141**	**0.000**	**0.036**	**0.001**	-0.009	0.461	**-0.109**	**0.000**	**0.061**	**0.000**	**-0.036**	**0.001**
Kladirostratus – Psammophylax	**-0.082**	**0.000**	-0.006	0.773	**-0.027**	**0.000**	**-0.083**	**0.000**	**0.040**	**0.000**	0.000	1.000
Kladirostratus – Rhamphiophis	**0.041**	**0.000**	**0.024**	**0.047**	**-0.029**	**0.000**	**0.067**	**0.000**	**0.079**	**0.000**	-0.023	0.081
Psammophis – Psammophylax	**0.059**	**0.000**	**-0.042**	**0.000**	**-0.018**	**0.002**	**0.027**	**0.004**	**-0.021**	**0.024**	**0.036**	**0.000**
Psammophis – Rhamphiophis	**0.182**	**0.000**	-0.012	0.607	**-0.020**	**0.021**	**0.177**	**0.000**	0.018	0.272	0.012	0.632
Psammophylax – Rhamphiophis	**0.123**	**0.000**	**0.030**	**0.001**	-0.002	0.990	**0.150**	**0.000**	**0.038**	**0.000**	**-0.023**	**0.026**
***Psammophylax* species**												
kellyi – multisquamis	-0.013	0.622	0.002	1.000	0.006	0.860	0.024	0.321	0.015	0.706	0.007	0.976
kellyi – ocellatus	-0.006	0.999	0.002	1.000	0.008	0.972	0.036	0.520	0.014	0.976	-0.009	0.993
kellyi – rhombeatus	-0.015	0.557	-0.010	0.812	0.014	0.150	0.019	0.542	-0.007	0.984	-0.005	0.990
kellyi – tritaeniatus	**-0.030**	**0.030**	0.010	0.796	**0.025**	**0.001**	0.031	0.138	0.006	0.996	-0.003	1.000
kellyi – variabilis	0.011	0.831	-0.004	0.993	0.009	0.605	0.009	0.969	0.012	0.810	-0.008	0.946
multisquamis – ocellatus	0.007	0.998	-0.001	1.000	0.002	1.000	0.012	0.993	-0.001	1.000	-0.016	0.921
multisquamis – rhombeatus	-0.002	1.000	-0.012	0.576	0.008	0.681	-0.006	0.995	-0.022	0.223	-0.012	0.701
multisquamis – tritaeniatus	-0.016	0.439	0.008	0.889	**0.019**	**0.013**	0.007	0.993	-0.009	0.952	-0.010	0.912
multisquamis – variabilis	0.024	0.056	-0.006	0.943	0.003	0.994	-0.016	0.689	-0.003	1.000	-0.015	0.511
ocellatus – rhombeatus	-0.009	0.995	-0.011	0.973	0.006	0.995	-0.017	0.954	-0.021	0.867	0.004	1.000
ocellatus – tritaeniatus	-0.024	0.732	0.009	0.990	0.017	0.598	-0.005	1.000	-0.008	0.998	0.006	0.999
ocellatus – variabilis	0.017	0.919	-0.006	0.999	0.001	1.000	-0.027	0.755	-0.002	1.000	0.001	1.000
rhombeatus – tritaeniatus	-0.015	0.592	0.020	0.144	0.012	0.354	0.012	0.879	0.012	0.830	0.002	1.000
rhombeatus – variabilis	0.025	0.051	0.005	0.982	-0.005	0.947	-0.010	0.911	0.019	0.277	-0.003	1.000
tritaeniatus – variabilis	**0.040**	**0.001**	-0.015	0.450	-0.016	0.066	-0.022	0.367	0.007	0.986	-0.005	0.993

Table S3. 5: List of relevant material examined in this study for the new species description (AMNH, American Museum of Natural History; CMRK, Christopher Kelly; FMNH, Field Museum of Natural History; LACM, Natural History Museum of Los Angeles County; MCZ, Museum of Comparative Zoology; PEM, Port Elizabeth Museum; UMMZ, University of Michigan Museum of Zoology; NMSR, National Museum Southern Rhodesia; BM, Natural History Museum London; RGMC, Royal Museum of Central Africa; SMF, Senckenberg Museum; USNM, National Museum of Natural History; Smithsonian Institution).

Species	Number of Samples	Sample Information
Psammophylax kellyi sp. nov.	12	*AMNH 50585, Tindi, Tanzania; *AMNH 60037, "Northern Tanganyika", Tanzania; *UMMZ 61233, Arusha, Tanzania; PEM R23926 (CMRK 401), Arusha Region near Oldonyo Sambu, Tanzania; PEM R23924 (CMRK 296) Meserani Snake Park, Arusha Region, Tanzania; PEM R23925 (CMRK 328), Arusha Region near Oldonyo Sambu, Tanzania; PEM R23927 (CMRK 402), Arusha Region near Oldonyo Sambu, Tanzania; PEM R23930 (CMRK 333), near Oldonyo Sambu, Tanzania; PEM R23928, Ngorongoro Conservation Area, near Ngorongoro town, Tanzania; PEM R23929 (CMRK 405), Ngorongoro Conservation Area, Ngorongoro airstrip, Tanzania; CMRK 297, Meserani Snake Park, Arusha Region, Tanzania.
Psammophylax multisquamis	72	*NMSR 3348, Sotik, Guaso Njiro, Kenya; *BM 1963.444-455, Laitokitok, Kenya; *RGMC 21907, Nairobi, Kenya; *SMF 41300, Nairobi, Kenya; *SMF 43817, Nairobi, Kenya; *MCZ 18213, Nairobi (Parklands), Kenya; *MCZ 17976, Loita Plains, Mau Escarpment @ 7000ft S. Masai Reserve, Kenya; *MCZ 29429, Juja Farm Kapiti Plains, Kenya; *MCZ 29430, Lake Nawasha, Kenya; *MCZ 29431, (G)uaso Nyiro; *MCZ 29432, Mtito Andei; *MCZ 34926, Molo; *AMNH 88619, 8ml NE Bellevue, S Laikipia Forest, Nyeri Dist. (7100 ft); *AMNH 16898-16899, Nairobi; *USNM 40893, Juja Farm, Kenya; *USNM 40901-40902, Lake Naivasha, Kenya; *USNM 41516, Lake Naivasha, Kenya; *USNM 41517-41518, Lake Naivasha, Kenya; *USNM 41672-41673, Lake Naivasha, Kenya; *USNM 40968, Nairobi, Kenya; *USNM 40997, Sotik, Guaso Njiro, Kenya; *MCZ 48413-48415, South Kinangop Plateau, Kenya; *FMNH 2258, Naivasha (or Kijabe?), Kenya; *FMNH 2262, Athi River, Kenya; *FMNH 2271, Voi, Kenya; *FMNH 2393, Molo, Kenya; *FMNH 79148, Mugaga, Kikuyu, Kenya; *AMNH 37894, Albasso Platea, Arussi (2700m), Ethiopia; *AMNH 37895, Addis Ababa (6000ft), Ethiopia; *BM 1973.3182-3183, Debra Markos, Gojjam (2500m), Ethiopia; *FMNH 12513, Near Allata, Lidama (2500m), Ethiopia; *FMNH 12525, Near Lajo, Webbe Shibeli River, Ethiopia; PEM R23844 (CMRK 357), Ethiopian plateau; Ethiopia; PEM R22919 (CMRK 361), Ethiopian plateau; Ethiopia; PEM R23920 (CMRK 360), Ethiopian plateau; Ethiopia; PEM R23922 (CMRK 363), Ethiopian plateau; Ethiopia; PEM R23921 (CMRK 362), Ethiopian plateau; Ethiopia; PEM R23923 (CMRK 152), Kenyan Rift, Kenya; *MNHN 1905.195.6, Toullo (2000m), Kenya; *BM 1952.1.2.34-.36, Spring Valley Farm, 15mls N of Gilgil (8000ft) , Kenya; *BM 1960.1.6.41, Ngong near Nairobi (7000') , Kenya; *BM 1950.1.2.68, 4mls SW of Rutundu, Mt Kenya (11000ft) , Kenya; *BM 1902.12.13.87, Rambuti, Ethiopia; *BM 1901.1.3.5, Kijabi; *BM 1901.1.3.11, Ongotta (Nairowa) , Kenya; *BM 1901.1.3.12, Ongotta (Gwelil) , Kenya; *BM 1909.11.15.1, Nairobi, Kenya; *BM 1912.6.6.15, Addis Ababa (2500m), Ethiopia; *BM 1934.10.1.1, Nairobi, Kenya; *BM 1910.10.31.10, Nairobi; *BM 96.3.27.17, "Uganda" (FJ Jackson) i.e. Uganda Railway, Uganda; *BM 1913.2.24.20, "Abyssinia", Ethiopia; *BM 98.12.27.21, Mau Ravine (7500ft), Kenya.

* indicates material examined by the late Donald Broadley.

Appendix C: Chapter Four

Tables

Table S4.1: List of specimens used for genetic analyses, and the GenBank Accession Numbers for each gene marker (16S = 16S ribosomal nucleic acid; cytb = cytochrome b; ND4+LeutRNA = NADH dehydrogenase subunit 4 + Leucine transfer RNA; c-mos = oocyte maturation factor). Dataset (4.) denotes which specimens were present in which dataset, specific to Chapter Four.

Species	Field Number	Museum Number	Locality		Coordinates		Clade	Dataset (4.)	GenBank Accession Numbers			
			Locality	Province	Lat	Long			16S	cytb	ND4+ LeutRNA	c-mos
Ingroup												
Ps. rhombeatus	WC-3693	PEM R21883	Oviston	EC	-30.73	25.75	SESA	1,2,3,4,5	TBA	TBA	TBA	TBA
Ps. rhombeatus	WC-DNA-0016		Hogsback	EC	-32.58	26.95	SESA	1,3,4,5	TBA	TBA	TBA	NA
Ps. rhombeatus	WC-DNA-0027		Hogsback	EC	-32.58	26.95	SESA	1,3,4,5	TBA	TBA	TBA	NA
Ps. rhombeatus	WC-DNA-0058	PEM R19012	Hogsback	EC	-32.57	26.93	SESA	1,3,4,5	TBA	TBA	TBA	NA
Ps. rhombeatus	HOGS		Hogsback	EC	-32.44	27.07	SESA	1,3,4,5	TBA	TBA	TBA	TBA
Ps. rhombeatus	WC-DNA-0050	PEM R19006	Katberg	EC	-32.43	26.66	SESA	1,4,5	TBA	TBA	TBA	NA
Ps. rhombeatus	WC-DNA-0076		Katberg	EC	-32.43	26.66	SESA	1,3,4,5	TBA	TBA	TBA	NA
Ps. rhombeatus	WC-2776	PEM R21282	Katberg	EC	-32.43	26.66	SESA	1,3,4,5	TBA	TBA	TBA	NA
Ps. rhombeatus	WC-DNA-1272	PEM R20527	Baviaanskloof East	EC	-33.68	24.31	SESA	1,2,3,4,5	NA	TBA	TBA	NA
Ps. rhombeatus	WC-2639	PEM R20720	Tsolwana	EC	-32.17	26.48	SESA	1,3,4,5	TBA	TBA	TBA	NA
Ps. rhombeatus	WC-2561	PEM R20718	Tsolwana	EC	-32.18	26.49	SESA	1,3,4,5	TBA	TBA	TBA	NA
Ps. rhombeatus	WC-2564	PEM R20719	Tsolwana	EC	-32.16	26.44	SESA	1,3,4,5	TBA	TBA	TBA	NA
Ps. rhombeatus	WC-2690	PEM R21098	Thomas River	EC	-32.44	27.29	SESA	1,3,4,5	TBA	TBA	TBA	NA
Ps. rhombeatus	WC-4996	PEM R22664	Ngadu	EC	-31.41	28.73	SESA	1,3,4,5	TBA	TBA	NA	NA
Ps. rhombeatus	WC-5156	PEM R22808	Port Elizabeth	EC	-33.98	25.51	SESA	1,3,4,5	TBA	NA	TBA	NA
Ps. rhombeatus	ARd00091		Port Elizabeth	EC	-34.01	25.66	SESA	1,3,4,5	TBA	TBA	TBA	NA
Ps. rhombeatus	ARd00089		Port Elizabeth	EC	-34.01	25.66	SESA	1,4,5	TBA	TBA	TBA	NA
Ps. rhombeatus	ARD00092		Port Elizabeth	EC	-34.01	25.66	SESA	1,2,3,4,5	TBA	TBA	TBA	TBA
Ps. rhombeatus	SG60		Grahamstown	EC	-33.32	26.51	SESA	1,3,4,5	TBA	TBA	TBA	NA
Ps. rhombeatus	SG61		Grahamstown	EC	-33.32	26.51	SESA	1,3,4,5	TBA	TBA	TBA	NA

Ps. rhombeatus	SG66		Grahamstown	EC	-33.33	26.53	SESA	1,3,4,5	TBA	TBA	TBA	NA
Ps. rhombeatus	SG67		Grahamstown	EC	-33.33	26.53	SESA	1,3,4,5	TBA	TBA	TBA	NA
Ps. rhombeatus	SG78		Grahamstown	EC	-33.33	26.50	SESA	1,3,4,5	TBA	NA	TBA	TBA
Ps. rhombeatus	CMRK234	PEM R22920	Grahamstown	EC	-33.30	26.51	SESA	1,3,4,5	NA	DQ486342	DQ486318	DQ486166
Ps. rhombeatus	CH3		Midlands	KZN	-29.35	29.98	SESA	1,3,4,5	TBA	TBA	TBA	NA
Ps. rhombeatus	ARD106		tsitsikamma	WC	-33.91	23.64	SESA	1,3,4,5	TBA	TBA	TBA	NA
Ps. rhombeatus	TP1		Mooi River	KZN	-29.19	30.08	SESA	1,3,4,5	TBA	TBA	TBA	NA
Ps. rhombeatus	TP2		Mooi River	KZN	-29.19	30.08	SESA	1,2,3,4,5	TBA	TBA	TBA	TBA
Ps. rhombeatus	TGE T9-09		Seymour	EC	-32.54	26.76	SESA	1,3,4,5	TBA	TBA	TBA	NA
Ps. rhombeatus	SAJ36		Rhodes	EC	-30.79	27.98	SESA	1,3,4,5	TBA	TBA	TBA	NA
Ps. rhombeatus	TB2		Coleford	EC	-29.97	29.44	SESA	1,3,4,5	TBA	TBA	TBA	TBA
Ps. rhombeatus	CH54		Graaff Reinet	EC	-32.25	24.50	SESA	1,3,4,5	TBA	TBA	TBA	NA
Ps. rhombeatus	MBUR 00534	PEM R24897	Sterkstroom	EC	-31.61	26.38	SESA	1,3,4,5	TBA	TBA	TBA	NA
Ps. rhombeatus	MBUR 00528		Sterkstroom	EC	-31.55	26.56	SESA	1,3,4,5	TBA	TBA	TBA	NA
Ps. rhombeatus	PEM R5674		Somerset East	EC	-32.72	25.59	SESA	1,3,4,5	NA	DQ486361	DQ486200	NA
Ps. rhombeatus	WC-6575	PEM 024322	Franklin	KZN	-30.33	29.52	SESA	1,3,4	TBA	NA	NA	NA
Ps. rhombeatus	TP5		Howick	KZN	-29.53	30.21	SESA	1,3,4,5	TBA	TBA	NA	NA
Ps. rhombeatus	CH51		Sani Pass	KZN	-29.70	29.49	SESA	1,3,4,5	TBA	TBA	TBA	NA
Ps. rhombeatus	CH52		Sani Pass	KZN	-29.70	29.49	SESA	1,3,4,5	TBA	TBA	TBA	NA
Ps. rhombeatus	MBUR 00476		Cedarville	EC	-30.38	29.04	SESA	1,3,4,5	TBA	TBA	TBA	TBA
Ps. rhombeatus	UK1		Unknown	EC			SESA	1,3,4,5	TBA	TBA	TBA	NA
Ps. rhombeatus	UK2		Unknown	EC			SESA	1,3,4,5	TBA	TBA	TBA	NA
Ps. rhombeatus	WC-2861	PEM R21254	Baviaanskloof West	EC	-33.42	23.54	SWSA	1,3,4,5	TBA	TBA	TBA	NA
Ps. rhombeatus	WC-2859	PEM R21253	Baviaanskloof West	EC	-33.43	23.57	SWSA	1,3,4,5	NA	TBA	TBA	NA
Ps. rhombeatus	WC-5094	PEM R22610	Karoo NP	WC	-32.28	22.33	SWSA	1,2,3,4,5	NA	LS992116	LS992137	LS992103
Ps. rhombeatus	WC-5095	PEM R22611	Karoo NP	WC	-32.26	22.51	SWSA	1,3,4,5	TBA	TBA	TBA	NA
Ps. rhombeatus	SVN-195	PEM R18833	Karoo NP	WC	-32.23	22.56	SWSA	1,3,4,5	TBA	LR213504	LR213558	NA
Ps. rhombeatus	CK1		Franschoek	WC	-34.09	19.19	SWSA	1,3,4,5	TBA	TBA	TBA	NA
Ps. rhombeatus	CK2		Cederberg	WC	-32.86	19.44	SWSA	1,2,3,4,5	TBA	TBA	TBA	TBA
Ps. rhombeatus	ARD104		Cederberg	WC	-32.44	19.19	SWSA	1,3,4,5	TBA	TBA	TBA	NA
Ps. rhombeatus	CK3		Fisherhaven	WC	-34.36	19.12	SWSA	1,3,4,5	TBA	TBA	NA	NA
Ps. rhombeatus	RS1		Oudtshoorn	WC	-33.48	22.24	SWSA	1,2,3,4,5	TBA	TBA	TBA	TBA
Ps. rhombeatus	TGET12-09		De Hoop Nature reserve	WC	-34.39	20.55	SWSA	1,3,4,5	TBA	TBA	TBA	NA

Ps. rhombeatus	TGET12-07		De Hoop Nature reserve	WC	-34.44	20.75	SWSA	1,3,4,5	NA	TBA	TBA	NA
Ps. rhombeatus	CH57		Stellenbosch	WC	-33.94	18.87	SWSA	1,3,4,5	TBA	TBA	TBA	NA
Ps. rhombeatus	MWR 070110		Kraaifontein	WC	-33.85	18.75	SWSA	1,3,4,5	TBA	TBA	NA	NA
Ps. rhombeatus	MBUR 00595		Jansenville	EC	-32.94	24.65	SWSA	1,3,4,5	TBA	LR213505	LR213559	NA
Ps. rhombeatus	ARd0010		Porterville	WC	-32.87	19.04	SWSA	1,3,4,5	TBA	TBA	TBA	NA
Ps. rhombeatus	SNB-001		Compassberg	EC	-32.02	24.22	SWSA	1,3,4,5	TBA	TBA	NA	NA
Ps. rhombeatus	MB20961		Herbertsdale	WC	-32.08	22.05	SWSA	1,3,4,5	TBA	TBA	NA	NA
Ps. rhombeatus	AC1		Napier	WC	-34.48	19.92	SWSA	1,2,3,4,5	TBA	TBA	TBA	TBA
Ps. rhombeatus	AC2		Napier	WC	-34.48	19.92	SWSA	1,3,4,5	NA	TBA	TBA	TBA
Ps. rhombeatus	CK4		Unknown	WC			SWSA	1,3,4,5	TBA	TBA	TBA	NA
Ps. rhombeatus	JV10791		Unknown	WC			SWSA	1,4,5	TBA	TBA	TBA	NA
Ps. rhombeatus	GB9		Unknown	WC			SWSA	1,3,4,5	NA	DQ486465	DQ486301	NA
Ps. rhombeatus	WC-1241	PEM R19434	Long Tom Pass	MPU	-25.15	30.62	NESA	1,3,4,5	TBA	LS992116	LS992137	NA
Ps. rhombeatus	CH53		Long Tom Pass	MPU	-25.09	30.56	NESA	1,3,4,5	TBA	TBA	TBA	NA
Ps. rhombeatus	MPU14-001		Wakkerstroom	MPU	-27.25	30.11	NESA	1,3,4,5	TBA	TBA	TBA	NA
Ps. rhombeatus	WKST		Wakkerstroom	MPU	-27.34	30.13	NESA	1,3,4,5	TBA	TBA	TBA	NA
Ps. rhombeatus	LK1		Wakkerstroom	MPU	-27.34	30.14	NESA	1,3,4,5	TBA	TBA	TBA	NA
Ps. rhombeatus	LK2		Wakkerstroom	MPU	-27.36	30.11	NESA	1,4,5	TBA	TBA	TBA	TBA
Ps. rhombeatus	WC-10-037	PEM R19180	Reitz	FS	-27.74	28.39	NESA	1,3,4,5	TBA	TBA	TBA	NA
Ps. rhombeatus	EI_0531		Woodbush Forest Reserve	LIM	-23.79	29.97	NESA	1,3,4,5	TBA	TBA	TBA	NA
Ps. rhombeatus	EI_0534		Woodbush Forest Reserve	LIM	-23.80	29.95	NESA	1,2,3,4,5	TBA	TBA	TBA	TBA
Ps. rhombeatus	EI_0542		Woodbush Forest Reserve	LIM	-23.80	29.98	NESA	1,3,4,5	TBA	TBA	TBA	NA
Ps. rhombeatus	DP1		Verloren vallei	MPU	-25.28	30.16	NESA	1,3,4,5	TBA	TBA	TBA	NA
Ps. rhombeatus	DWP 173D		Verloren vallei	MPU	-25.29	30.15	NESA	1,3,4,5	TBA	TBA	TBA	NA
Ps. rhombeatus	DP3		Verloren vallei	MPU	-25.26	30.16	NESA	1,3,4,5	TBA	TBA	TBA	NA
Ps. rhombeatus	DWP 182		Steenkampsberg	MPU	-25.24	30.12	NESA	1,3,4,5	TBA	TBA	TBA	NA
Ps. rhombeatus	SAJ28		Vanderbijlpark	GP	-26.72	27.81	NESA	1,3,4,5	TBA	TBA	TBA	NA
Ps. rhombeatus	SAJ29		Vanderbijlpark	GP	-26.72	27.81	NESA	1,3,4,5	TBA	TBA	TBA	NA
Ps. rhombeatus	SAJ30		Vanderbijlpark	GP	-26.72	27.81	NESA	1,2,3,4,5	TBA	TBA	TBA	TBA
Ps. rhombeatus	SAJ31		Vanderbijlpark	GP	-26.72	27.81	NESA	1,3,4,5	TBA	TBA	TBA	NA
Ps. rhombeatus	MR1		Johannesburg South	GP	-26.36	28.10	NESA	1,3,4,5	TBA	TBA	TBA	NA

Ps. rhombeatus	MBUR 01661		Haenetsburg	LIM	-24.06	30.09	NESA	1,3,4,5	TBA	TBA	TBA	NA
Ps. rhombeatus	MBUR 01604		Wolkberg	LIM	-24.06	30.09	NESA	1,3,4,5	TBA	TBA	NA	NA
Ps. rhombeatus	PJ1		Suikerbosrand	GP	-26.48	28.23	NESA	1,3,4,5	TBA	TBA	TBA	TBA
Ps. rhombeatus	GB10		Suikerbosrand	GP	-26.53	28.27	NESA	1,3,4,5	FJ404215	FJ404312	FJ404327	FJ404230/ FJ387215
Ps. rhombeatus	CK9		Nooitgedacht	MPU	-25.97	30.12	NESA	1,3,4,5	TBA	TBA	TBA	TBA
Ps. rhombeatus	TP3		Golden Gate National Park	FS	-28.51	28.63	NESA	1,2,3,4,5	TBA	TBA	TBA	TBA
Ps. rhombeatus	TP4		Golden Gate National Park	FS	-28.50	28.62	NESA	1,3,4,5	TBA	TBA	NA	NA
Ps. rhombeatus	BM1		Koeberg	WC	-33.64	18.42	WSA	1,3,4,5	LS992118	LS992139	TBA	LS992104
Ps. rhombeatus	BM2		Koeberg	WC	-33.64	18.42	WSA	1,3,4,5	TBA	TBA	TBA	NA
Ps. rhombeatus	BM3		Koeberg	WC	-33.64	18.42	WSA	1,3,4,5	TBA	TBA	TBA	NA
Ps. rhombeatus	Ck6		Koeberg	WC	-33.62	18.41	WSA	1,2,3,4,5	TBA	TBA	TBA	TBA
Ps. rhombeatus	CK7		Koeberg	WC	-33.62	18.41	WSA	1,3,4,5	TBA	TBA	TBA	TBA
Ps. rhombeatus	DM1		Alexander Bay	NC	-28.61	16.49	WSA	1,2,3,4,5	TBA	TBA	NA	TBA
Ps. rhombeatus	TB1		Calvinia	NC	-31.48	19.77	WSA	1,2,3,4,5	TBA	TBA	TBA	NA
Ps. rhombeatus	CKD12		Lamberts Bay	WC	-32.09	18.32	WSA	1,3,4,5	TBA	TBA	TBA	NA
Ps. rhombeatus	CKD13		Lamberts Bay	WC	-32.09	18.32	WSA	1,2,3,4,5	TBA	TBA	TBA	TBA
Ps. rhombeatus	CH55		West Coast National Park	WC	-33.21	18.09	WSA	1,3,4,5	TBA	TBA	TBA	NA
Ps. rhombeatus	CH56		West Coast National Park	WC	-33.21	18.09	WSA	1,3,4,5	TBA	TBA	TBA	NA
Outgroups												
Ps. kellyi	CMRK 296	PEM R23924						4	NA	LR213510	LR213567	NA
Ps. kellyi	CMRK 328	PEM R23925						1,3,4	NA	LR213511	LR213568	NA
Ps. kellyi	CMRK 333	PEM R23930						4	NA	NA	LR213569	NA
Ps. kellyi	CMRK 401	PEM R23926						1,2,3,4	NA	LR213517	LR213575	NA
Ps. kellyi	CMRK 402	PEM R23927						4	NA	LR213518	LR213576	NA
Ps. kellyi	CMRK 405	PEM R23929						1,2,3,4	NA	LR213520	LR213578	NA
Ps. kellyi	CMRK 404	PEM R23928						1,3,4	NA	DQ48643/LR213503	DQ486273	NA
Ps. multisquamis	CMRK 149							1,2,3,4	NA	LR213507	LR213561	NA
Ps. multisquamis	CMRK 150							1,4	NA	LR213508	LR213562	NA
Ps. multisquamis	CMRK 151							4	NA	NA	LR213563	NA
Ps. multisquamis	CMRK 152	PEM R23923						4	NA	LR213509	LR213564	NA

Ps. multisquamis	CMRK 153		4	NA	NA	LR213565	LR213480
Ps. multisquamis	CMRK 154		4	NA	NA	LR213566	NA
Ps. multisquamis	CMRK 357	PEM R22903	4	NA	LR213512	LR213570	NA
Ps. multisquamis	CMRK 359	PEM R23844	4	NA	LR213513	LR213571	NA
Ps. multisquamis	CMRK 360	PEM R23920	1,3,4	NA	LR213514	LR213572	NA
Ps. multisquamis	CMRK 362	PEM R23921	4	NA	LR213515	LR213573	NA
Ps. multisquamis	CMRK 363	PEM R23922	4	NA	LR213516	LR213574	NA
Ps. multisquamis	CMRK 361	PEM R22919	1,2,3,4	NA	DQ486421	DQ486258	DQ486191
Ps. ocellatus	KTH09-064	PEM R17986	1,3,4	NA	LR213506	LR213560	LR213479
Ps. ocellatus	NB 171		4	NA	LS992120	LS992135	LS992105
Ps. ocellatus	NB 491		1,4	NA	LS992121	LS992136	LS992106
Ps. ocellatus	NB 492		4	NA	LS992122	LS992131	LS992107
Ps. ocellatus	NB 561	PEM R16270	1,3,4	NA	LS992124	LS992133	LS992109
Ps. ocellatus	NB 585		1,2,4	NA	LS992125	LS992128	LS992110
Ps. ocellatus	NB 586		4	NA	LS992126	LS992129	LS992111
Ps. tritaeniatus	MB 21435		1,2,3	NA	LR213499	LR213556	LR213476
Ps. tritaeniatus	PVP 15	PEM R22075	4	NA	LR213500	NA	NA
Ps. tritaeniatus	PVP 59	PEM R22076	4	NA	LR213501	NA	LR213477
Ps. tritaeniatus	PVP 97		1,3	NA	LR213502	LR213557	LR213478
Ps. tritaeniatus	ZMUC R970215	ZMUC R970215	1,2,3	NA	DQ486451	DQ486287	NA
Ps. tritaeniatus	CMRK 279	PEM R22921	1,3	NA	DQ486414	DQ486252	DQ486190
Ps. tritaeniatus	Kal		4	NA	LR213541	LR213599	NA
Ps. tritaeniatus	LK3		4	NA	LR213542	LR213600	NA
Ps. variabilis	EBG 3006	UTEP 21871	1,3,4	NA	LR213486	LR213543	LR213463
Ps. variabilis	EBG 2943	UTEP 21870	4	NA	LR213487	LR213544	LR213464
Ps. variabilis	EBG 2890	UTEP 21869	4	NA	LR213488	LR213545	LR213465
Ps. variabilis	EBG 2611	UTEP 21868	1,2,3,4	NA	LR213489	LR213546	LR213466
Ps. variabilis	EBG 2425	UTEP 21867	4	NA	LR213490	LR213547	LR213467
Ps. variabilis	MOZ14-192	PEM R21186	4	NA	LR213491	LR213548	LR213468
Ps. variabilis	IPMBJ296		1,3,4	NA	NA	FJ404328	AF544709
Ps. variabilis	CMRK 413	PEM R22922	4	NA	EU526863	EU526859	NA
Ps. variabilis	CMRK 403	PEM R23970	1,3,4	NA	LR213519	LR213577	LR213481
Ps. variabilis	CMRK 414	PEM R23969	4	NA	LR213521	LR213579	NA
Ps. variabilis	J10		4	NA	LR213535	LR213593	NA

Ps. variabilis	J11		4	NA	LR213536	LR213594	NA
Ps. variabilis	J12		4	NA	LR213537	LR213595	NA
Ps. variabilis	J8		4	NA	LR213538	LR213596	NA
Ps. variabilis	J9		4	NA	LR213539	LR213597	NA
Ps. variabilis	QP060	PEM R18522	1,2,3,4	NA	LR213492	LR213549	LR213469
Ps. variabilis	M01	PEM R23968	4	NA	LR213540	LR213598	NA
Ps. variabilis	GB3		4	NA	AY235724	NA	NA
Ps. variabilis	CMRK 415	PEM R23954	4	NA	LR213522	LR213580	NA
Ps. variabilis	CMRK 416	PEM R23955	4	NA	LR213523	LR213581	NA
Ps. variabilis	CMRK 417	PEM R23956	4	NA	LR213524	LR213582	NA
Ps. variabilis	CMRK 418	PEM R23957	4	NA	LR213525	LR213583	NA
Ps. variabilis	CMRK 419	PEM R23958	4	NA	LR213526	LR213584	NA
Ps. variabilis	CMRK 420	PEM R23959	4	NA	LR213527	LR213585	NA
Ps. variabilis	CMRK 421	PEM R23960	4	NA	LR213528	LR213586	NA
Ps. variabilis	CMRK 422	PEM R23961	4	NA	LR213529	LR213587	NA
Ps. variabilis	CMRK 441	PEM R23962	1,3,4	NA	DQ486438	DQ486274	DQ486193
Ps. variabilis	CMRK 442	PEM R23963	4	NA	LR213530	LR213588	NA
Ps. variabilis	CMRK 443	PEM R23964	4	NA	LR213531	LR213589	NA
Ps. variabilis	CMRK 444	PEM R23965	4	NA	LR213532	LR213590	NA
Ps. variabilis	CMRK 445	PEM R23966	4	NA	LR213533	LR213591	NA
Ps. variabilis	CMRK 446	PEM R23967	4	NA	LR213534	LR213592	NA
K. acutus	WC-3540	PEM R21485	1,4	NA	LR213493	LR213550	LR213470
K. acutus	WC-4018	PEM R23288	1,4	NA	LR213494	LR213551	LR213471
K. acutus	WC-4149	PEM R23315	1,2,4	NA	LR213495	LR213552	LR213472
K. acutus	WC-4715	PEM R23476	4	NA	LR213496	LR213553	LR213473
K. acutus	WC-4778	PEM R23449	4	NA	LR213497	LR213554	LR213474
K. acutus	PVP 92		4	NA	LR213498	LR213555	LR213475
K. acutus	PEM R13485	PEM R13485	4	NA	DQ486464	DQ486300	NA
K. acutus	CMRK 378		1,2,4	NA	DQ486425	DQ486262	DQ486192
Boa constrictor			2	NA	AF471036	NA	AF471115
Boa constrictor sabogae	NE6.9		2	NA	KF576747	KF576715	NA
Acrochordus granulatus			2	NA	AF217841	U49296	AF471124

Acrochordus arafurae	MZB3342		2	NA	NA	HM234056	HM234059
Agkistrodon piscivorus			2	NA	AF471074	AF156578	AF471096
Atheris nitschei			2	NA	AF471070	AY223618	AF471125
Crotalus viridis			2	NA	AF471066	AF194157	AF471135
Diadophis punctatus			2	NA	AF471094	AF258910	AF471122
Hypsiglena torquata			2	NA	AF471038	U49309	AF471159
Natrix natrix			2	NA	AY873710	AF471059	AF471121
Thamnophis sirtalis infernalis			2	NA	AF402929	AF420196	DQ902094
Dendroaspis polylepis			2	NA	AF217832	AY058974	AY058928
Naja kaouthia			2	NA	AF217835	AY058982	AY058938
Naja annulata			2	NA	AF217829	AY058970	AY058925
Oxyrhabdium leporinum			2	NA	AF471029	NA	DQ112081
Gonionotophis brussauxi	IRSNB16266		2	NA	AY612043	FJ404358	AY611952
Lycodonomorphus rufulus	PEM R22892	CMRK 236	2	NA	HQ207111	HQ207153	HQ207076
Lamprophis fuliginosus			2	NA	FJ404302	FJ404364	AF544686
Atractaspis bibronii	MCZ-R 184500		2	NA	MK621603	MK621545	MK621667
Atractaspis congica	633	PEM R20856	2	NA	MK621587	MK621529	MK621651
Aparallactus capensis	MCZ-R 184501		2	NA	MG746890	MG776004	MG775887
Leioheterodon modestus			2	NA	AY058967	AY058978	AY058933
Amplorhinus multimaculatus	CMRK 208	PEM 021480	2	NA	DQ486340	DQ486316	DQ486164
Prosymna ruspolii			2	NA	DQ486347	DQ486323	DQ486171
Prosymna visseri			2	NA	AY188033	NA	AY187994
Malpolon monspessulanus			2	NA	AY058965	AY058989	AY058936
Rhamphiophis rostratus	CMRK 185	PEM R021472	2	NA	DQ486394	DQ486233	DQ486187

Rhamphiophis rubropunctatus	CMRK 303		2	NA	DQ486417	NA	NA
Dipsina multimaculata	TM84514		2	NA	DQ486357	DQ486332	DQ486181
Hemirhagerrhis kelleri	CMRK 77	PEM R21446	2	NA	DQ486335	DQ486311	DQ486159
Hemirhagerrhis viperina	AMB5989		2	NA	DQ486453	DQ486289	NA
Mimophis mahafalensis			2	NA	DQ486363	DQ486202	NA
Mimophis mahafalensis			2	NA	AY188032	AF544662	AY187993
Psammophis angolensis	CMRK 263	PEM R22894	2	NA	DQ486410	DQ486248	DQ486189
Psammophis crucifer	CMRK 203	PEM R21479	2	NA	DQ486397	DQ486236	DQ486188
Psammophis lineolatus	CAS179682		2	NA	DQ486450	DQ486286	DQ486195

Table S4.2: List of Specimens used in the morphometric analyses. X's denote whether a photograph was available for the dorsal and/or lateral view.

Museum Number	Region		Coordinates		Clade	Morphometric Photographs	
	Locality	Province/Country	Lat	Long		Dorsal	Lateral
PEM R00954	Melmoth	KZN	-28.58	31.39	SESA		X
PEM R00957	Port Elizabeth	EC	-33.96	25.43	SESA	X	X
PEM R00958	Berlin	EC	-32.88	27.58	SESA	X	X
PEM R00939	Pietermaritzburg	KZN	-29.63	30.36	SESA	X	X
PEM R00028	5 miles West of East London	EC	-33.09	27.75	SESA	X	X
PEM R01120	Swart River	EC	-34.04	24.86	SESA	X	
PEM R01121	3km East of Mushmane	EC	-33.96	25.43	SESA	X	
PEM R01448	Walmer Drive Inn, Port Elizabeth	EC	-33.97	25.61	SESA	X	X
PEM R02592	Barkly East	EC	-30.96	27.60	SESA	X	X
PEM R03465	6km to Addo from Coega turning	EC	-33.40	25.46	SESA	X	X
PEM R04033	Keiskammahoek	EC	-32.69	27.14	SESA	X	X
PEM R04062	King William's Town	EC	-32.88	27.45	SESA		X
PEM R04120	King William's Town	EC	-32.70	27.57	SESA	X	
PEM R07721	Valley of Desolation	EC	-32.26	24.50	SESA	X	X
PEM R07751	Doornkloof Nature Reserve	NC	-30.34	24.96	SESA	X	X
PEM R07770	Greenbushes, Port Elizabeth	EC	-33.93	25.42	SESA	X	
PEM R07897	Borva	EC	-31.43	28.06	SESA	X	X
PEM R07916	Rosetta	KZN	-29.31	29.99	SESA	X	X
PEM R07929	Bedford	EC	-32.70	26.07	SESA	X	X
PEM R14915	Koedoeskop Farm, Noorsveld	EC	-32.98	25.18	SESA	X	X
PEM R06505	Adelaide road	EC	-32.77	25.87	SESA	X	X
PEM R06798	Algoa Park, Port Elizabeth	EC	-33.90	25.56	SESA	X	X
PEM R07051	Prentjiesberg	EC	-31.13	28.13	SESA	X	X
PEM R07287	Amalinda Fish Station, East London	EC	-32.97	27.83	SESA	X	X
PEM R11791	Indwe	EC	-31.45	27.30	SESA	X	X
PEM R12258	Devil's Bellows, Katberg Pass	EC	-32.53	26.65	SESA	X	X
PEM R11455	45km north northwest of Cradock	EC	-31.79	25.43	SESA	X	X
PEM R11457	Bathurst	EC	-33.51	26.83	SESA	X	X
PEM R08795	Oviston Nature Reserve	EC	-30.75	25.74	SESA	X	
PEM R09343	Langkloof Forest Kammiesbos	EC	-33.90	24.14	SESA	X	X
PEM R16393	11km east of Underberg	KZN	-29.82	29.51	SESA	X	X
PEM R16400	11km east of Underberg	KZN	-29.82	29.51	SESA	X	X
PEM R19012	Hogsback	EC	-32.57	26.93	SESA	X	X
PEM R20527	Akkerdal track onto Grasnek (Baviaanskloof)	EC	-33.68	24.31	SESA		X
PEM R20533	Akkerdal track onto Grasnek (Baviaanskloof)	EC	-33.68	24.31	SESA	X	X
PEM R21098	Junction of Little and Big Thomas	EC	-32.44	27.29	SESA	X	X
PEM R21254	Welbedacht	EC	-33.42	23.54	SESA	X	X
PEM R21282	Devil's Bellows, Katberg Pass	EC	-32.43	26.66	SESA	X	X
PEM R22664	Nqadu Forest	EC	-31.41	28.73	SESA	X	X
PEM R22808	Lorraine, Port Elizabeth	EC	-33.98	25.51	SESA	X	X

PEM R23115	Alstonfield	EC	-32.91	26.07	SESA	X	X
PEM R23693	Tarkastad, Modderfontein	EC	-31.86	26.16	SESA	X	X
PEM R23795	Colesberg, Rietfontein	NC	-30.92	25.04	SESA	X	X
PEM R23796	Colesberg, Rietfontein	NC	-30.92	25.04	SESA	X	X
PEM R23818	Venterstad	EC	-30.96	25.74	SESA	X	X
PEM R24322	Mpur Forestry, Franklin	KZN	-30.33	29.52	SESA	X	X
PEM R24862	Ongeluksnek NR, staff village	EC	-30.33	28.35	SESA	X	X
PEM R24897	unnamed road Avilion, near Sterkstroom	EC	-31.61	26.38	SESA	X	X
PEM R18718	Olifants Bos, Cape Point	WC	-34.25	18.38	SWSA	X	X
PEM R18833	Moltenopass, 10km from Beaufort-West	WC	-32.21	22.56	SWSA	X	X
PEM R07937	Gansbaai	WC	-34.58	19.35	SWSA	X	X
PEM R08626	6km South of Calitzdorp.	WC	-33.57	21.70	SWSA	X	X
PEM R11085	Kammanassieberge	WC	-33.61	22.61	SWSA		X
PEM R11104	Gamka Mountain Reserve	WC	-33.69	21.96	SWSA	X	X
PEM R11472	Baviaanskloof	EC	-33.58	24.15	SWSA	X	X
PEM R12909	Kareedouw, Outeniquaberg	WC	-33.60	23.33	SWSA	X	X
PEM R13717	Groot Swartberg, Matjiesvlei	WC	-33.36	21.62	SWSA	X	X
PEM R04765	Karoo National Park	WC	-32.36	22.54	SWSA	X	X
PEM R04949	George	WC	-33.99	22.43	SWSA	X	X
PEM R04950	George	WC	-33.99	22.43	SWSA	X	X
PEM R06097	Anysberg Nature Reserve,	WC	-33.46	20.59	SWSA	X	X
PEM R-000938	Prince Albert	WC	-33.23	22.03	SWSA	X	X
PEM R-007331	Gamka Poort Nature Reserve	WC	-33.69	21.92	SWSA	X	X
PEM R03442	9km West of Willowmore	EC	-33.37	23.44	SWSA	X	X
PEM R03453	Rondevlei	WC	-33.99	22.71	SWSA	X	
PEM R23603	Klavervlei, Karoo National Park	WC	-32.13	22.35	SWSA	X	X
PEM R23611	Karoo National Park	WC	-32.27	22.49	SWSA	X	X
PEM R20321	Karoo Botanic Garden	WC	-33.61	19.45	SWSA	X	
PEM R00947	Stellenbosch	WC	-33.95	18.86	SWSA	X	X
PEM R00941	Lothair	MPU	-26.38	30.43	NESA	X	X
PEM R00942	Lothair	MPU	-26.38	30.43	NESA	X	X
PEM R00943	Lothair	MPU	-26.38	30.43	NESA	X	X
PEM R00944	Lothair	MPU	-26.38	30.43	NESA	X	X
PEM R00946	Lothair	MPU	-26.38	30.43	NESA	X	X
PEM R01117	Mbabane	Swaziland	-26.30	31.13	NESA	X	X
PEM R01118	Lothair	MPU	-26.38	30.43	NESA	X	X
PEM R04874	Malolotsha National Reserve	Swaziland	-26.14	31.11	NESA	X	X
PEM R20669	Driefontein road (Volksrust)	MPU	-27.31	30.20	NESA	X	X
PEM R16387	Koeberg Nature Reserve	WC	-33.68	18.44	WSA	X	X
PEM R17268	7km S of Lambert's Bay	WC	-32.17	18.32	WSA	X	X
PEM R17269	7km S of Lambert's Bay	WC	-32.17	18.32	WSA	X	X
PEM R17270	7km S of Lambert's Bay	WC	-32.17	18.32	WSA	X	X
PEM R17271	7km S of Lambert's Bay	WC	-32.17	18.32	WSA	X	X
PEM R17272	7km S of Lambert's Bay	WC	-32.17	18.32	WSA	X	X
PEM R17273	7km S of Lambert's Bay	WC	-32.17	18.32	WSA	X	X
PEM R17274	7km S of Lambert's Bay	WC	-32.17	18.32	WSA	X	X
PEM R17275	7km S of Lambert's Bay	WC	-32.17	18.32	WSA	X	X

PEM R01895	Graafwater, Lamberts Bay	WC	-32.15	18.60	WSA	X
PEM R01895	Graafwater, Lamberts Bay	WC	-32.15	18.60	WSA	X

Table S4.3: Sequence divergences (uncorrected pairwise distance values) separating *Psammophylax* species from each other another using cytochrome b (cyt b) and NADH dehydrogenase subunit 4 + LeutRNA transfer RNA (ND4+LeutRNA) (*Dataset 4.4*). Numbers in the diagonal (in bold) denote intraspecific divergences, numbers below the diagonal denote interspecific divergences and numbers above the diagonal denote the standard error of the interspecific divergences.

	cytb						
		1	2	3	4	5	6
1	*Ps. kellyi*	**1.00**	0.93	1.02	0.96	0.99	1.02
2	*Ps. multisquamis*	6.69	**2.00**	0.96	0.89	0.97	0.97
3	*Ps. ocellatus*	6.91	6.98	**0**	0.96	1.11	1.13
4	*Ps. rhombeatus*	8.68	8.18	8.80	**5.00**	0.95	0.97
5	*Ps. tritaeniatus*	8.20	7.54	9.18	8.57	**2.00**	1.02
6	*Ps. variabilis*	8.13	8.21	9.30	9.22	9.06	**2.00**
	ND4 + LeutRNA						
1	*Ps. kellyi*	**1.00**	0.84	0.85	0.80	0.87	0.89
2	*Ps. multisquamis*	6.97	**2.00**	0.95	0.81	0.86	0.81
3	*Ps. ocellatus*	6.82	8.43	**0**	0.83	0.90	0.91
4	*Ps. rhombeatus*	7.61	8.52	7.56	**4.00**	0.83	0.78
5	*Ps. tritaeniatus*	8.33	9.01	8.74	8.70	**2.00**	0.85
6	*Ps. variabilis*	7.94	7.83	8.13	7.39	7.92	**2.00**